

This file is part of the following work:

Crook, Kevin Alexander (2020) *Assessing the functional roles of rays in coastal sandflats*. PhD Thesis, James Cook University.

Access to this file is available from:

<https://doi.org/10.25903/rq54%2D5813>

Copyright © 2020 Kevin Alexander Crook.

The author has certified to JCU that they have made a reasonable effort to gain permission and acknowledge the owners of any third party copyright material included in this document. If you believe that this is not the case, please email

researchonline@jcu.edu.au

ASSESSING THE FUNCTIONAL ROLES OF RAYS IN COASTAL SANDFLATS

by

Kevin Alexander Crook (BSc hons, MSc)

Submitted in fulfillment of the requirements for the Degree of
Doctor of Philosophy

College of Science and Engineering
James Cook University

September 2020

Acknowledgements

First and foremost, this thesis is dedicated to my wife Leigh. Thank you for the incredible sacrifice you made; moving to the other side of the world, far away from friends and family, so I could pursue my dream. Your unwavering love, support, and confidence were my rock, and I could not have done this without you. Thanks for sharing in this amazing adventure with me for the past 4 years! Also, to our immediate families for making the journey down under to see us!

To my supervisors, Adam Barnett, Marcus Sheaves, and Katya Abrantes, thank you for your support and guidance throughout my PhD. I appreciate your trust and the autonomy you gave me to take the project and run with it. To Adam, thanks for always picking up the phone when I needed advice and for the quick turnaround on manuscript drafts, particularly in the last month of my thesis.

To my lab mates, thanks for being my sounding board when I needed to talk things out and for all your friendship, advice, and support along the way. Special thanks to Michael Bradley and Cesar Herrera for our lunchtime chats, it was usually the best part of my day. Thanks also to all the JCU students who volunteered to help me catch and track stingrays at Lucinda. I know the work was not as glamorous as it sounded, so thank you for all your hard work and patience during long field days traipsing across the Lucinda sandflat. To Claudia Trave, thanks for drawing up some marine critters at the last minute when I had a vision for a conceptual diagram. It looks great!

A big thank you to the SeaWorld Research and Rescue Foundation, Save Our Seas Foundation, and Holsworth Wildlife Research Endowment for funding the project. Thanks also to Jeremy Vanderwal for covering the cost of my remote pilot license. I did not know at the start of my PhD how much I would end up using drones, but the pilot license really helped me take the project to new heights! To Glen Ewels and Greg Suosaari at JCU boating and diving, thank you for getting me the right gear for the job. I probably would have been fine in my kayak though right?...

Finally, thank you to my BSc. Hons and MSc supervisor, Gail Davoren, for nurturing my passion for research and setting me on the path to becoming a scientist. You have been, and continue to be, a great mentor, friend, and role model.

Statement of Contributions of Others

Nature of Assistance	Contribution	Contributor
Intellectual support	Supervisors Study design Theoretical background Editorial assistance Permits and animal ethics	Dr. Adam Barnett Prof. Marcus Sheaves Dr. Katya Abrantes
	Statistical support	Dr. Ross Dwyer, UQ Dr. Vinay Udyawer, AIMS
Financial support	Stipend/Tuition Waiver	James Cook University
	Research Funding	SeaWorld Research and Rescue Foundation Save Our Seas Foundation Holsworth Wildlife Research Endowment
	Drone training	Prof. Jeremy Vanderwal
Project Infrastructure	Field equipment	JCU boating and diving Glen Ewels Greg Suosaari Dr. Adam Barnett Prof. Marcus Sheaves JCU advanced analytical centre Dr. Shane Askew Dr. Kevin Blake
	Drone training	NQUAV/FlyFreely Ashley Walker
Other Contributions	Illustrations	Dr. Claudia Trave

Abstract

Knowledge of the functional roles of animals is crucial for understanding ecosystem function. Functional roles can be assessed by directly linking individual phenotypes with ecosystem processes or services and assessment requires a trait-based approach that includes all facets of animal ecology with the potential to impact ecosystem performance and function. Rays (superorder Batoidea) are often the most abundant large predators in intertidal sandflats; however, there is a general lack of information about the functional roles of rays in these habitats. Additionally, rays have been identified as a priority group for conservation because their large body size and affinity for coastal habitats make them vulnerable to fishing pressure, making it critical to establish their ecological importance. The aim of this study was to assess the functional roles of rays in coastal sandflats and establish the level of functional redundancy/complementarity among sympatric species. Specifically, I examined individual and species-specific behaviours and resource use to directly link behaviour with function. Acoustic tracking revealed that juvenile rays restricted habitat use to within the sandflat boundary, used similar activity spaces, and performed daily tidal migrations. Direct observation of rays using drones identified intertidal areas as key foraging habitats and daily movements between intertidal foraging areas and subtidal resting areas suggests rays function as energetic links between the two. Although overall habitat use was similar among species, foraging habitats were segregated on a fine scale. *Himantura australis* foraged intensely in a small core area whereas *Pastinachus ater* foraged less often but over a broader sandflat area. Quantification of pit sizes revealed that pit size was strongly linked to feeding behaviour. Excavation feeding was the most disruptive behaviour and accounted for 58–67 % of sediment turnover despite occurring in only 22–31 % of feeding events. *Pastinachus ater* individuals favoured non-disruptive feeding which was the only feeding type that did not make feeding pits. Consequently, *P. ater* had lower bioturbation rates than *H. australis* which favoured more disruptive feeding behaviours and made three times as many feeding pits. Isotopic niche sizes of *H. australis* and *P. ater* reflected their differences in foraging behaviour. *Pastinachus ater* occupied the largest niche space which is consistent with foraging over a broad area whereas *H. australis* occupied less niche space, consistent with more specialized foraging in a specific area. Overall, the integration of acoustic telemetry, drone tracking, and stable isotope datasets revealed that, despite contributing to the same broad ecological roles, the magnitude and spatial scale of those roles differed between species. Consequently, the functional roles of rays are not equal, but are complementary and are driven by species-specific foraging behaviours. In particular, the repeated and intense foraging in a concentrated area by *H. australis* suggests a significant bioturbation and ecosystem engineering impact whereas lower foraging rates over a broader area for *P. ater* suggests a broader nutrient

deposition footprint. Although stable isotope analysis revealed that rays were positioned at similar trophic levels to teleost carnivores, rays occupied unique niche space. Furthermore, bioturbation and ecosystem engineering roles are also unique among sandflat predators as teleost carnivores lack the excavation capability of rays. Consequently, rays are keystone species on coastal sandflats and conservation of ray populations is critical for maintaining ecosystem function.

Table of Contents

Acknowledgements.....	i
Statement of Contributions of Others	ii
Abstract.....	iii
List of Tables	vii
List of Figures	viii
Chapter 1: Introduction	1
Study Site Description	4
Chapter 2: Eye in the sky: Drone observations identify foraging habitat partitioning among sympatric stingrays	7
Introduction	8
Methods.....	9
Results.....	13
Discussion.....	25
Chapter 3: All rays are not created equal: Species-specific foraging behaviours define the functional roles of sympatric stingrays.	30
Introduction	31
Methods.....	32
Results.....	36
Discussion.....	40
Chapter 4: Effects of lipid and urea extraction on stable isotope values ($\delta^{13}\text{C}$ and $\delta^{15}\text{N}$) of two batoids: a call for more species-specific investigations.....	46
Introduction	47
Methods.....	49
Results.....	52
Discussion.....	55
Chapter 5: Trophic roles of rays in sandflat foodwebs	62
Introduction	63
Methods.....	64
Results.....	66
Discussion.....	73
Chapter 6: General Discussion	79
Synthesis of main results	79
Roles of rays as ecosystem engineers.....	81
Future directions.....	83
References	86

Appendix A	115
Appendix B	119
Appendix C	124
Appendix D	127

List of Tables

Table 2.1 Details of acoustic tracks for individual <i>Himantura australis</i> (Ha), <i>Pastinachus ater</i> (Pa), and <i>Glaucostegus typus</i> (Gt) tracked at Lucinda. ROM: Rate of movement.....	14
Table 2.2 Total (95 %) and core (50 %) kernel utilisation distributions (KUD in km ²) from acoustic tracking, drone tracking, and combined methods for <i>Himantura australis</i> and <i>Pastinachus ater</i> at Lucinda. Habitat-use estimates reflect: KUD for all individuals (Total); mean ± standard deviation KUD for individual rays (Individual); and KUD based on the locations of feeding events (Foraging)...	15
Table 3.1 Definitions of feeding types and feeding event parameters used in drone track analyses.	33
Table 4.1 Standard ellipse parameters eccentricity (<i>E</i>) and the angle between the semi-major axis of the standard ellipse and the x- axis (θ) for <i>Himantura australis</i> and <i>Pastinachus ater</i> stable isotope values ($\delta^{13}\text{C}$ and $\delta^{15}\text{N}$) in bulk (BK), lipid extracted (LE), urea extracted (UE), and lipid and urea-extracted (ULE) samples from both muscle and plasma tissues. θ values are expressed in degrees..	55
Table 5.1 Sample size, mean size, size range, and mean stable isotope values ($\delta^{13}\text{C}$ and $\delta^{15}\text{N}$) of <i>Aetobatus ocellatus</i> , <i>Aetomylaeus vespertilio</i> , <i>Glaucostegus typus</i> , <i>Himantura australis</i> , <i>Maculabatus toshi</i> , <i>Pastinachus ater</i> , <i>Pateobatis fai</i> , and <i>Urogymnus granulatus</i> captured at Lucinda. Sample sizes in parentheses indicate the number of muscle and plasma samples analysed, respectively.....	67
Table 5.2 $\delta^{13}\text{C}$ and $\delta^{15}\text{N}$ stable isotope standard ellipse eccentricity (<i>E</i>) and semi-major axis angle (θ) from muscle and plasma tissues of juvenile <i>Glaucostegus typus</i> , <i>Himantura australis</i> , <i>Pastinachus ater</i> , and <i>Urogymnus granulatus</i>	71
Table 5.3 $\delta^{13}\text{C}$ and $\delta^{15}\text{N}$ stable isotope standard ellipse eccentricity (<i>E</i>) and semi-major axis angle (θ) from muscle and plasma tissues of juvenile <i>Himantura australis</i> and <i>Pastinachus ater</i> from 2017–2019.	71
Table 5.4 Probability (%) of species A falling within the niche space (standard ellipse area) of species B based on 10^4 estimated standard ellipse areas for muscle and plasma stable isotope values of <i>Glaucostegus typus</i> , <i>Himantura australis</i> , <i>Pastinachus ater</i> , and <i>Urogymnus granulatus</i>	73
Table 5.5 Probability (%) of an individual from group A falling within the standard ellipse niche space of group B based on 10^4 estimated standard ellipse areas. Overlap probabilities were only determined between species in the same years and across years within a species. Groups are coded by species (<i>H.a</i> = <i>Himantura australis</i> and <i>P.a</i> = <i>Pastinachus ater</i>) and year for muscle and plasma tissues.	74

List of Figures

Figure 1.1 Thesis outline detailing the aims and how the functional roles of rays will be evaluated for each chapter. This figure will be repeated on the title page of each chapter, highlighting the aims and functional roles to be assessed in the chapter.....	5
Figure 1.2 Location of the Lucinda sandflat in Queensland, Australia.....	6
Figure 2.1 95 % (white) and 50 % (red) kernel utilisation distributions of <i>Pastinachus ater</i> (n=7), <i>Glaucostegus typus</i> (n=1), and <i>Himantura australis</i> (n=5) acoustic tracks at Lucinda.....	16
Figure 2.2 Movement paths of <i>Himantura australis</i> (Ha), <i>Pastinachus ater</i> (Pa), and <i>Glaucostegus typus</i> (Gt) individuals acoustically tracked at Lucinda. Blue and black contours represent 50 and 95 % kernel utilisation distributions (KUD) during low tide periods. Red and white contours represent 50 and 95 % KUD during high tide periods. Different coloured lines represent different tracking days (n=2 – 5).	18
Figure 2.3 Single day activity patterns of individual <i>Himantura australis</i> (Ha), <i>Pastinachus ater</i> (Pa), and <i>Glaucostegus typus</i> (Gt) acoustically tracked at Lucinda. Black lines represent the distance travelled in one-minute intervals and red lines demarcate the boundaries of ebb (E), low (L), flood (F), and high (H) tide periods.....	19
Figure 2.4 Boxplots of the mean a) rate of movement (ROM) and b) ten-point linearity by tidal phase for individual <i>Himantura australis</i> (white) and <i>Pastinachus ater</i> (grey) tracked (acoustic telemetry) at Lucinda. Boxes represent the first and third quartiles with whiskers extending to data points within 1.5 times the inter-quartile range. Horizontal black lines represent the median and individual points represent outliers.	20
Figure 2.5 Water temperatures experienced across all tracking days for the four juvenile <i>Pastinachus ater</i> individuals tracked with temperature sensors at Lucinda. Note: the time scale on the x-axis is different for each figure.....	21
Figure 2.6 Boxplots of a) rate of movement (ROM), b) linearity, and c) feeding rate for <i>Himantura australis</i> (white) and <i>Pastinachus ater</i> (grey) tracked with drones at Lucinda. Boxes represent the first and third quartiles with whiskers extending to data points within 1.5 times the inter-quartile range. Horizontal black lines represent the median and individual points represent outliers.	22
Figure 2.7 Kernel utilisation distributions from a) all drone tracks of <i>Himantura australis</i> and <i>Pastinachus ater</i> at Lucinda, and b) all feeding event locations. KUDs for <i>H. australis</i> are represented as white (95 %) and red (50 %) contours. KUDs for <i>P. ater</i> are represented as black (95 %) and blue (50 %) contours.....	24
Figure 2.8 95 % (white) and 50 % (red) kernel utilisation distributions for <i>Himantura australis</i> and <i>Pastinachus ater</i> from combined acoustic and drone tracks.	25

Figure 3.1 Drone video screenshots of a) an Australian whipray (<i>Himantura australis</i>) and recently formed feeding pit (black box), b) close-up of the feeding pit with length (solid arrow) and width (dashed arrow) identified, and c) foraging <i>H. australis</i> with the sagittal (solid line) and transverse (dashed line) planes identified. The dashed line in a) shows the disc width measurement of the focal ray. The colour and contrast of the feeding pit area has been adjusted for clarity.....	34
Figure 3.2 Size distribution of <i>Pastinachus ater</i> and <i>Himantura australis</i> tracked with drones at Lucinda separated into five cm bins.....	37
Figure 3.3 Relationship between the natural log of feeding pit area and a) natural log of feeding time and b) ray disc width. Points indicate feeding events with excavation feeding as the primary feeding type (blue) or without excavation feeding (white) that resulted in a measured feeding scar. Predicted linear relationships are shown for excavation events (dashed line) or non-excavation events (solid line). Points are shown for both <i>Himantura australis</i> and <i>Pastinachus ater</i>	38
Figure 3.4 Feeding (a), pit formation (b), and bioturbation (c) rates of <i>Himantura australis</i> (H.a) and <i>Pastinachus ater</i> (P.a) from all drone tracks at Lucinda. Boxes represent the first and third quartiles with whiskers extending to data points within 1.5 time the inter-quartile range. Horizontal black lines represent the median and individual points represent outliers.....	39
Figure 3.5 a) Frequency and b) proportion of feeding events with excavation (EX), water jetting (WJ), suction (SU), and non-disruptive (ND) feeding as the primary feeding type for <i>Himantura australis</i> and <i>Pastinachus ater</i> . c) The proportion of total sediment volume turned over by each feeding type. d) The frequency of feeding pits in each size category and feeding type. e) The total volume of all feeding pits in each size category by feeding type. Pit size categories: P1 (100 cm ² < area < 250 cm ²), P2 (250 cm ² < area < 500 cm ²), P3 (500 cm ² < area < 1000cm ²), and P4 (area > 1000 cm ²).	40
Figure 3.6 a) Frequency and b) proportion of feeding events with excavation (EX), water jetting (WJ), suction (SU), and non-disruptive (ND) feeding as the primary feeding type for large (>54 cm DW) and small (<54 cm DW) <i>Himantura australis</i> . c) The proportion of total sediment volume turned over by each feeding type. d) The frequency of feeding pits in each size category by feeding type. e) The total volume of all feeding pits in each size category by feeding type. Pit size categories: P1 (100 cm ² < area < 250 cm ²), P2 (250 cm ² < area < 500 cm ²), P3 (500 cm ² < area < 1000 cm ²), and P4 (area > 1000 cm ²).	41
Figure 3.7 Extent and density of foraging activity of a) <i>Himantura australis</i> and <i>Pastinachus ater</i> and b) large (> 54 cm DW) and small (< 54 cm DW) <i>H. australis</i> (H.a) drone tracked at Lucinda.....	42
Figure 4.1 Mean ± SD differences between bulk and treatment samples for a) δ13C, b) δ15N, and c) C:N ratios in muscle and plasma tissues of the batoids <i>Pastinachus ater</i> and <i>Himantura australis</i> . Bars represent lipid extracted (LE), urea extracted (UE), and urea and lipid extracted (ULE) treatments.	

Asterisks (*) indicate significant differences at $\alpha=0.05$ corrected for multiple comparisons using the sequential Bonferroni adjustment.....	53
Figure 4.2 Left: $\delta^{13}\text{C}$ and $\delta^{15}\text{N}$ values in muscle tissue from a) <i>Himantura australis</i> and b) <i>Pastinachus ater</i> for bulk (BK), lipid-extracted (LE), urea-extracted (UE), and urea and lipid extracted (ULE) samples. Solid lines represent standard ellipse areas (SEA). Right: Boxes represent the 50, 75, and 95 % Bayesian credible intervals for SEA. Black dots show the mode SEA and red dots show the small sample-size corrected SEA (SEAc).....	54
Figure 4.3 Left: $\delta^{13}\text{C}$ and $\delta^{15}\text{N}$ values in plasma tissue from a) <i>Himantura australis</i> and b) <i>Pastinachus ater</i> for bulk (BK), lipid-extracted (LE), urea-extracted (UE), and urea and lipid extracted (ULE) samples. Solid lines represent standard ellipse areas (SEA). Right: Boxes represent the 50, 75, and 95 % Bayesian credible intervals for SEA. Black dots show the mode SEA and red dots show the small sample-size corrected SEA (SEAc).....	56
Figure 4.4 $\delta^{13}\text{C}$ and $\delta^{15}\text{N}$ of bulk (BK) and urea-extracted (UE) samples from <i>Himantura australis</i> (●) and <i>Pastinachus ater</i> (▲) a) muscle tissue and b) plasma tissue. Solid lines represent standard ellipse areas for <i>H. australis</i> (solid lines) and <i>P. ater</i> (dashed lines).....	57
Figure 5.1 Mean \pm SE $\delta^{13}\text{C}$ and $\delta^{15}\text{N}$ for all species captured at Lucinda. Primary producers are labelled to the right. * indicates $\delta^{13}\text{C}$ values from Abrantes et al. (2015).....	68
Figure 5.2 $\delta^{13}\text{C}$ and $\delta^{15}\text{N}$ values and standard ellipse areas (SEA) for all teleost carnivores (red) and rays (blue) sampled at Lucinda.....	69
Figure 5.3 Mean \pm SE $\delta^{13}\text{C}$ and $\delta^{15}\text{N}$ for all ray species captured and sampled at Lucinda for both muscle and plasma tissues.....	69
Figure 5.4 Left: $\delta^{13}\text{C}$ and $\delta^{15}\text{N}$ values and standard ellipse areas (SEA) for a) muscle and b) plasma tissues from <i>Glaucostegus typus</i> (G.t), <i>Himantura australis</i> (H.a), <i>Pastinachus ater</i> (P.a), and <i>Urogymnus granulatus</i> (U.g) sampled at Lucinda. Small sample size corrected SEA (SEAc) are presented for <i>U. granulatus</i> and legends are the same for both plots. Right: 50, 75, and 95 % Bayesian credible intervals for SEA for each species. Black dots show the mode SEA and red dots show the SEAc.....	70
Figure 5.5 Left: $\delta^{13}\text{C}$ and $\delta^{15}\text{N}$ values and small sample size corrected standard ellipse areas (SEAc) for a) muscle and b) plasma tissues from <i>Himantura australis</i> (red) and <i>Pastinachus ater</i> (blue) sampled at Lucinda by year. Only two <i>H. australis</i> were sampled in 2018 and these samples are excluded from the plot. Right: 50, 75, and 95 % Bayesian credible intervals for SEAc for each species (<i>Ha</i> = <i>H. australis</i> , <i>Pa</i> = <i>P. ater</i>) and year combination. Black dots show the mode SEA and red dots show the SEAc.....	72

Figure 6.1 Conceptual diagram illustrating the functional roles of rays on coastal sandflats. Line thickness represents the relative impact of roles for *Himantura australis* (left) and *Pastinachus ater* (right). The width of ecosystem engineering lines represents the spatial scale over which roles are performed on sandflats for each species (solid lines) and for both species combined (dashed line). The vertical dashed line indicates foraging habitat partitioning. Ecosystem engineering roles include: the number and size of feeding pits, sediment turnover, habitat creation, and accumulation of detritus.....80

Chapter 1: Introduction

Function can be defined as “the movement or storage of energy or material” (Bellwood *et al.* 2019). At the ecosystem level, however, function extends beyond simply moving and storing energy or material, and also includes services provided to other organisms, both directly and indirectly (Jax 2005). Knowledge of the ecological roles of animals is crucial for understanding ecosystem function (Piraino, Fanelli & Boero 2002; Davidson, Detling & Brown 2012). Roles are often based on diet, feeding mode, and trophic position (Root 1967; Degraaf, Tilghman & Anderson 1985; Elliott *et al.* 2007), as these relate directly to predator-prey relationships and energy flow within foodwebs (Polis & Strong 1996; Ritchie & Johnson 2009). Trophic roles are only part of the story, however, as animals may also influence ecosystem function through movement (Bauer & Hoyer 2014; Buelow & Sheaves 2015) and by altering habitats (Wright & Jones 2006). For example, ecosystem engineers (e.g. beavers altering stream hydrodynamics by building dams (Burchsted & Daniels 2014)) regulate the amount of habitat and resources available to other organisms through physical modification of the environment (Jones, Lawton & Shachak 1997) and can have a significant impact on biodiversity and ecosystem productivity (Coleman & Williams 2002; Byers *et al.* 2006). Additionally, movements between different habitats can facilitate connectivity that is crucial for maintaining energy flux (Polis, Anderson & Holt 1997; Sheaves 2009), gene flow (Frisk, Jordaan & Miller 2014), species diversity, and predator-prey relationships (Sheaves 2005; Berkstrom *et al.* 2013). Thus, roles of animals are not based on a single trait, so assessment requires a trait-based approach that includes all facets of animal ecology with the potential to impact ecosystem function (Violle *et al.* 2007; Enquist *et al.* 2015).

Functional roles can be assessed by directly linking individual phenotypes with ecosystem processes or services (Jax 2005; Bellwood *et al.* 2019). As a result, species are often organised into functional groups based on similar morphologies, behaviours, or diets (Bellwood & Choat 1990; Dehling *et al.* 2016). While these functional groupings can explain what functions are performed (e.g. ecosystem engineering), trait expression (e.g. body size) may differ among species or individuals, which can influence realized contributions to ecosystem function (Zhao *et al.* 2014; Sanders, Vogel & Knop 2015; Bejarano *et al.* 2017). Additionally, the suite of traits contributing to ecosystem performance (i.e. functional traits) may also differ among species (Violle *et al.* 2007; Brandl & Bellwood 2014; Maire *et al.* 2015), and the combination of all functional traits represents a species’ functional niche (Rosenfeld 2002). Consequently, it is critical to assess the expression and variability of functional traits at the individual and species levels to accurately assess realized functional roles and determine species-specific contributions to ecosystem functioning.

The range of functional roles for the whole community is termed its functional diversity and is an effective measure for assessing the resilience of a community to disturbance (Wellnitz & Poff 2001; Mouillot *et al.* 2013). When there is high overlap among functional niches, there is high redundancy, which can help buffer the effects of disturbance because if one species is removed, the remaining species will be able to maintain ecosystem function (Walker 1992; Yachi & Loreau 1999). When there is low overlap, each species is fulfilling a unique role in the community and functions are complementary (Brandl & Bellwood 2014). Although functional complementarity may enhance ecosystem function (Moran-Lopez *et al.* 2020), low functional redundancy makes communities more vulnerable to disturbance (Petchey *et al.* 2007). Under traditional species-richness paradigms, high biodiversity is predicted to provide insurance against disturbance (Yachi & Loreau 1999). However, this is not necessarily the case. For example, examination of functional diversity among coral reef fish showed that redundancy is low within functional groups (Bellwood, Hoey & Choat 2003; Hoey & Bellwood 2009; Brandl & Bellwood 2014; Mouillot *et al.* 2014), despite high species richness. Instead, species perform a unique suite of ecosystem functions and overall functioning is maintained through complementarity (Burkepile & Hay 2008; Bejarano *et al.* 2017).

Coral reefs, and other ecosystems along tropical coastlines, are increasingly exposed to high levels of disturbance due to human activity, development, and climate change (Lotze *et al.* 2006; Hoegh-Guldberg *et al.* 2007; Sheaves *et al.* 2014; Unsworth *et al.* 2018). As a result, it is critical to assess the functional roles of species in these habitats and assess the level of functional redundancy/complementarity among species to fully understand the consequences of disturbance. Sandflats and sandy beaches are among the most extensive habitats along global coastlines (Short 2006), yet these habitats have received relatively little ecological study within the tropics (Abrantes *et al.* 2015a; Schlacher *et al.* 2015). Sandflats are dynamic habitats; subject to constant erosion from the influence of waves and tides (Schlacher *et al.* 2015; Short 2006) and are often reliant on nutrient subsidies from adjacent ecosystems (Savage *et al.* 2012; Gladstone-Gallagher *et al.* 2016). Functional studies in sandflats have primarily focussed on invertebrates and infauna (Lohrer, Thrush & Gibbs 2004; Needham *et al.* 2011; Lohrer *et al.* 2016); however, the abundance of invertebrates can provide an abundant food source for both terrestrial and marine predators (Thrush *et al.* 1994; Gihwala, Pillay & Varughese 2017), which likely contribute to important ecosystem functions.

Batoids (Superorder Batoidea) are a diverse group of primarily marine fishes, with 633 described species in 26 families (Last *et al.* 2016). Due to their flattened morphology, batoids (hereafter referred to as ‘rays’) are well adapted to shallow-water habitats and are often the most abundant large predators in intertidal sandflats (Vaudo & Heithaus 2009; Pierce, Scott-Holland & Bennett 2011). Rays are among the most threatened groups of marine fishes according to the IUCN

Red List of Threatened Species, with global population declines occurring because of targeted fishing and by-catch (Dulvy *et al.* 2014; Dulvy *et al.* 2017). Globally, 20 % of ray species are threatened with extinction (Critically Endangered, Endangered, or Vulnerable), and an additional 10 % are considered Near-Threatened (Last *et al.* 2016). Furthermore, nearly half (44 %) of examined ray species are classified as Data Deficient and numerous newly described species have yet to be evaluated (Last *et al.* 2016). Dulvy *et al.* (2017) identified tropical stingrays as a priority group for conservation because their large body size and affinity for coastal habitats make them vulnerable to fishing pressure from poorly regulated fisheries. Adding to these concerns is a general lack of information about the functional roles of rays and the ecological consequences of species decline (Martins *et al.* 2018; Flowers, Heithaus & Papastamatiou 2020).

Hypothesized roles of rays include facilitating nutrient and energetic links between habitats, mesopredator roles in marine foodwebs, and bioturbation of sediments. Juvenile rays are often resident in coastal nurseries (Vaudo & Heithaus 2012; Cerutti-Pereyra *et al.* 2014), and may provide frequent energetic links between adjacent habitats over the short-term through daily tidal migrations (Davy, Simpfendorfer & Heupel 2015; Martins *et al.* 2020) among components of coastal ecosystem mosaics (Sheaves 2009; Nagelkerken *et al.* 2015). Over the long-term, energetic links may occur on a larger scale through ontogenetic (Aguiar, Valentin & Rosa 2009; White *et al.* 2014; Ajemian & Powers 2016) or long-distance migrations (Collins, Heupel & Simpfendorfer 2008; Ajemian & Powers 2014). Rays also facilitate energy flow between primary consumers and top predators as mesopredators in marine foodwebs (Ritchie & Johnson 2009; Navia, Cortes & Mejia-Falla 2010; Bornatowski *et al.* 2014). High overlap in resource use among sympatric rays suggests redundancy in trophic roles, which may aid ecosystem stability (Vaudo & Heithaus 2011; Navia *et al.* 2017). In other cases, evidence of resource partitioning suggests roles may be more specialized (O'Shea *et al.* 2013; Barria, Coll & Navarro 2015; Pardo *et al.* 2015). Rays are also recognised as substantial bioturbators, with bioturbation occurring during the excavation of benthic invertebrate prey (Myrick & Flessa 1996; O'Shea *et al.* 2012; Takeuchi & Tamaki 2014). This bioturbation is important for structuring sediments, oxygen penetration, and nutrient cycling (Lohrer, Thrush & Gibbs 2004; Mermilliod-Blondin & Rosenberg 2006; Harris *et al.* 2016). In addition, ray foraging often creates distinctive pits or depressions which can provide habitat for other organisms and serve as depositional centres for detritus (Vanblaricom 1982; D'Andrea, Aller & Lopez 2002; D'Andrea, Lopez & Aller 2004; O'Shea *et al.* 2012). Consequently, rays may function as both bioturbators and ecosystem engineers.

Excluding dietary studies, research examining the roles of rays in sandflat ecology have focussed on a single species (Hines *et al.* 1997; Takeuchi & Tamaki 2014) or have treated all species

as equals in terms of their ecosystem function (Grant 1983; Myrick & Flessa 1996; D'Andrea, Lopez & Aller 2004; O'Shea *et al.* 2012). Recent applications of trait-based approaches to assess functional roles have revealed that there is often less functional redundancy in ecological communities than previously thought (Petchey *et al.* 2007; Brandl & Bellwood 2014; Mouillot *et al.* 2014). Where previously many species were assumed to fulfill the same ecological roles, it is now recognised that these roles may be subdivided into narrower functional niches that are filled by only a few or, in some cases, only a single species. Given the diversity in morphology and the abundance of rays in intertidal sandflats, it is likely that functional roles are not equal across species.

The overall aim of this study was to assess the functional roles of rays in coastal sandflats and establish the level of functional redundancy/complementarity among sympatric species. Specifically, I examined individual and species-specific behaviours and resource use to directly link behaviour with function. In Chapter 2, I identified patterns and drivers of diurnal movements to assess the potential for rays to function as energetic links between habitats (Fig. 1.1). Additionally, I identified core foraging habitats to determine where bioturbation and ecosystem engineering impacts were occurring. I quantified bioturbation and ecosystem engineering roles in Chapter 3 by empirically linking foraging behaviour, ray size, and feeding pit sizes (Fig. 1.1). In Chapters 4 and 5 I examined the trophic roles of rays (Fig. 1.1). I determined best practices for treating ray tissues for stable isotope analysis in chapter 4 and these methods were applied to determine the trophic level, niche size, and overlaps among ray species in chapter 5 (Fig. 1.1).

Study Site Description

Fieldwork and data collection for all thesis chapters occurred at the sandflat near Lucinda, QLD, Australia (18.5327° S, 146.3347° E) (Fig. 1.2). The high-level of detail required to gain a comprehensive understanding of functional roles required intensive fieldwork and observations. To achieve this, focus was placed on a single site to collect a high volume of high-quality data using a multi-methods approach.

The Lucinda sandflat is extensive and is exposed >1 km seaward during lowest astronomical tide. Although most of the sandflat is exposed at low tide, the sandflat has heterogenous topography, with numerous gullies between sandbars that remain submerged (≤ 1 m depth). Tidal fluctuations at Lucinda follow a mixed semi-diurnal cycle and have a maximum amplitude of four meters at lowest astronomical tide. The sandflat has eastern exposure and is predominantly sandy substrate but has a small enclosed bay at the Northern end with an early successional mangrove forest and sand/mud substrate (Fig. 1.2). Preliminary observations of ray fauna at Lucinda identified the broad cowtail stingray (*Pastinachus ater*) and Australian whipray (*Himantura australis*) as the

Assessing the Functional Roles of Rays in Coastal Sandflats

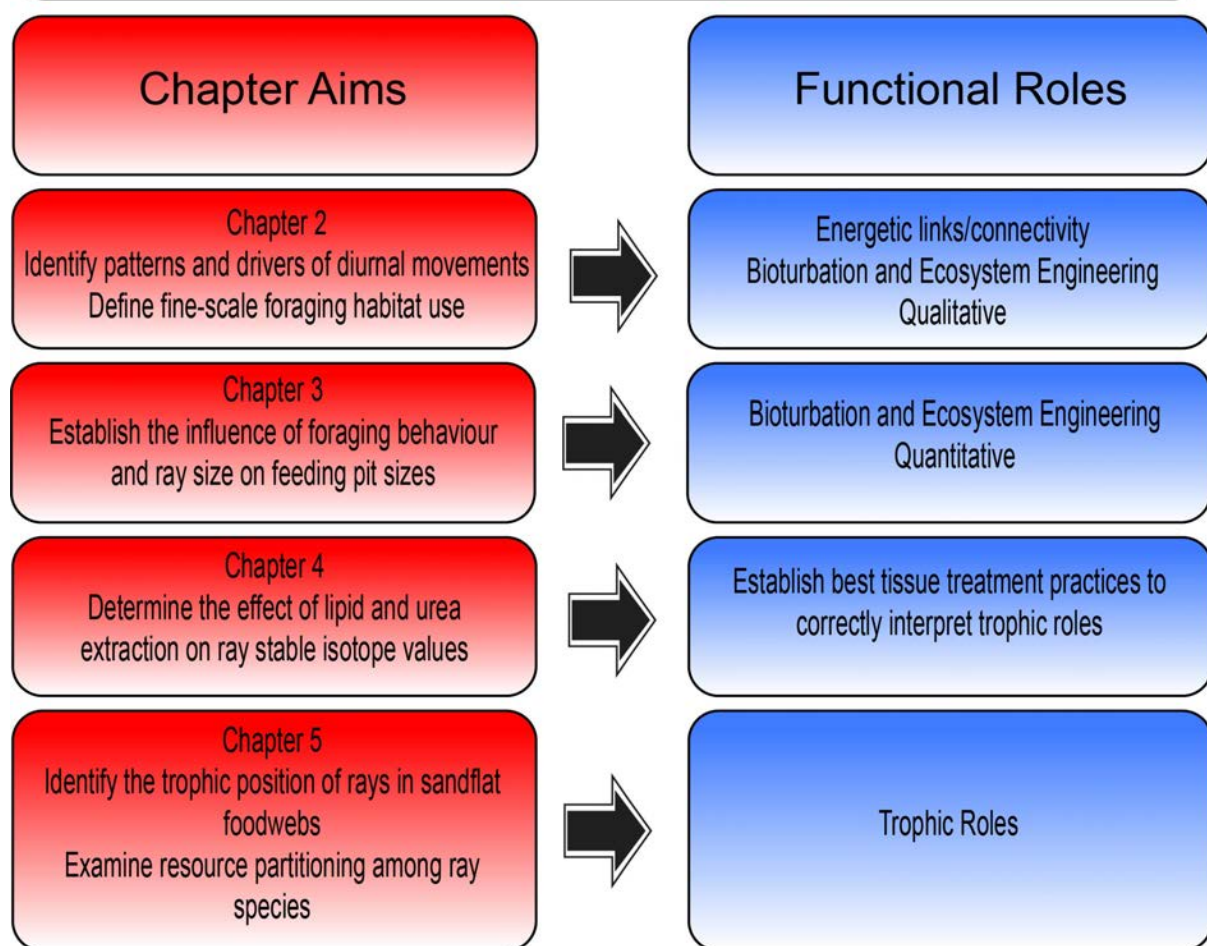


Figure 1.1 Thesis outline detailing the aims and how the functional roles of rays will be evaluated for each chapter. This figure will be repeated on the title page of each chapter, highlighting the aims and functional roles to be assessed in the chapter.

most abundant species (K. Crook unpublished data), and these two species were the primary focus of this thesis. *Pastinachus ater* and *H. australis* have a wide distribution across northern Australia (Last *et al.* 2016) and commonly co-occur in high abundance (Vaudo & Heithaus 2009; O'Shea *et al.* 2013; Cerutti-Pereyra *et al.* 2014). Consequently, defining the functional roles of these two species at Lucinda is likely reflective of processes happening at a broad scale throughout Australia.

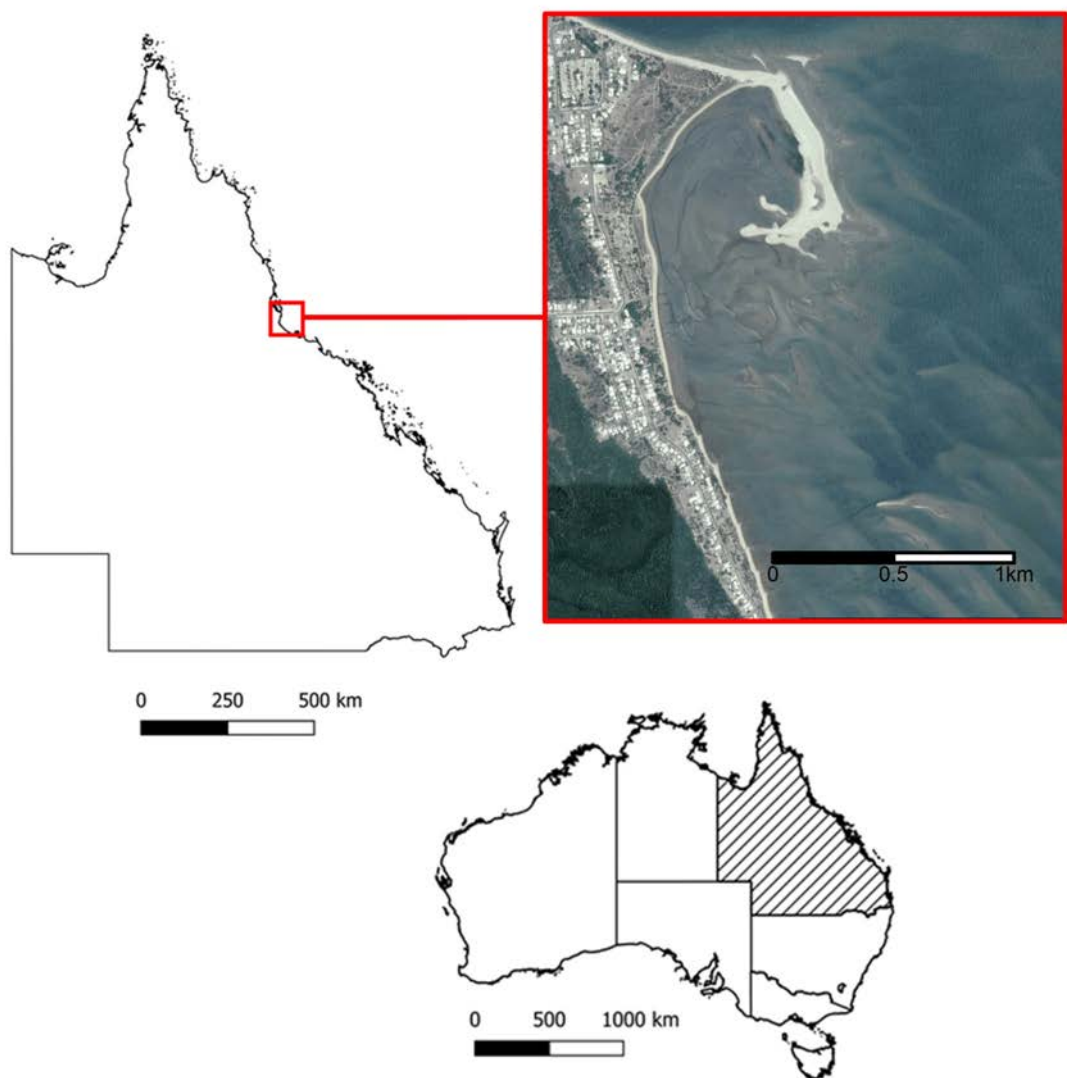
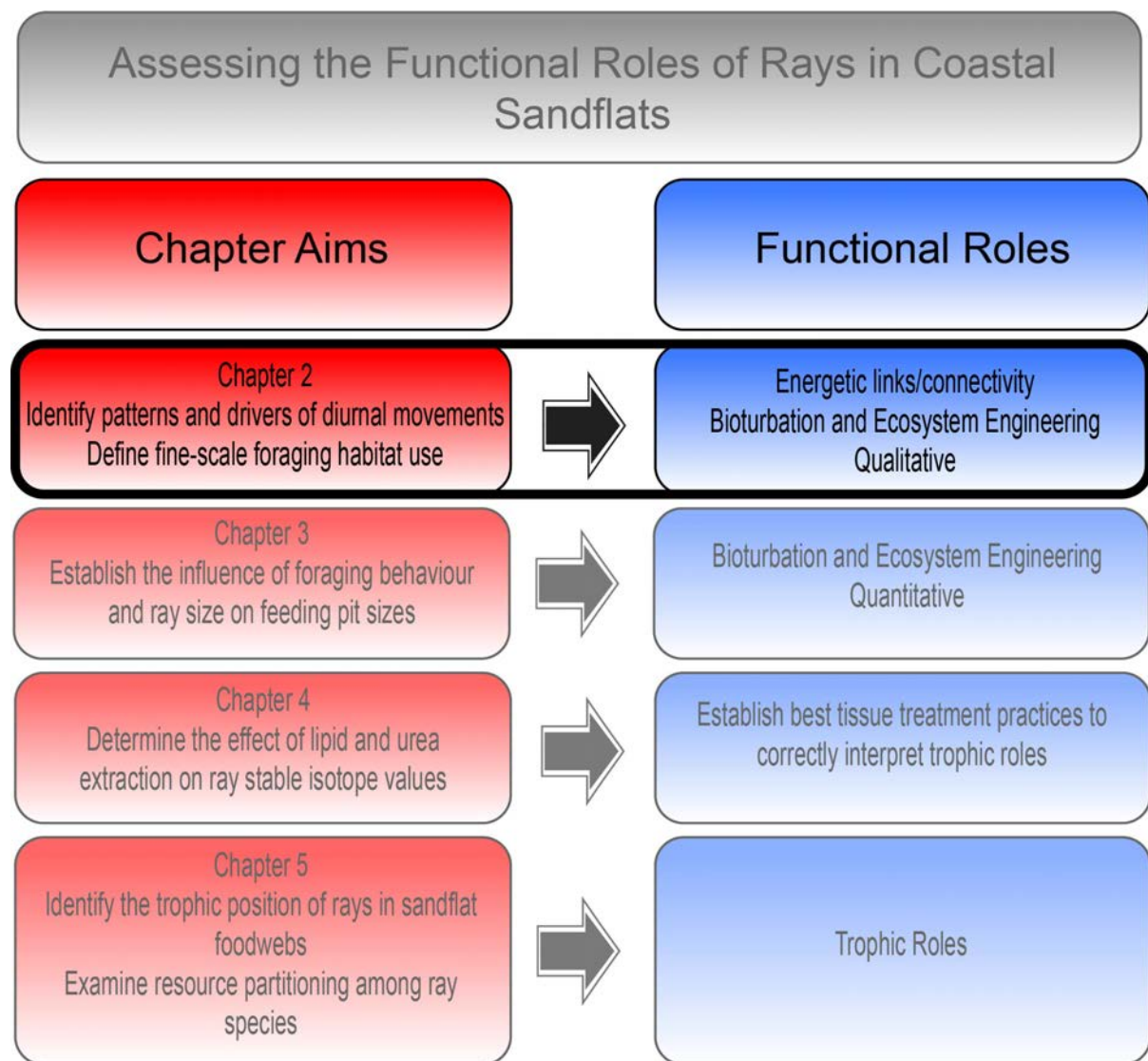


Figure 1.2 Location of the Lucinda sandflat in Queensland, Australia.

Chapter 2: Eye in the sky: Drone observations identify foraging habitat partitioning among sympatric stingrays



This chapter has been submitted for publication in *Animal Behaviour*. The submitted manuscript has been modified to fit with the style of the thesis and avoid unnecessary redundancies.

Crook, KA., Sheaves, M., Barnett, A. Eye in the sky: drone observations identify foraging habitat partitioning among sympatric stingrays. *Animal Behaviour*. Submitted.

Contributions: K Crook designed the study, performed all data collection and statistical analyses, and wrote the manuscript. A Barnett and M Sheaves aided with study design and provided editorial support.

Introduction

Understanding the drivers of animal movement is an important process for understanding the evolution of behaviour. In a broad sense, long distance migration has evolved to maximize fitness, and the drivers include access to mating opportunities, abundant prey resources, and avoidance of adverse environmental conditions (Alerstam, Hedenstrom & Akesson 2003; Chapman, Reynolds & Wilson 2015). Long-distance migrants include birds (Kirby *et al.* 2008), ungulates (Fryxell, Greever & Sinclair 1988; Bergman, Schaefer & Luttich 2000), marine mammals (Riekkola *et al.* 2020), fish (Barnett *et al.* 2011; Barnett *et al.* 2019; Queiroz *et al.* 2019), and insects (Chapman, Reynolds & Wilson 2015), with migrations generally occurring on an annual or seasonal basis. Smaller-scale migrations are also common, but shorter travel distances allow these migrations to occur more frequently (Wurtsbaugh & Neverman 1988; Corp, Gorman & Speakman 1997; Meyer, Papastamatiou & Holland 2007). Daily migrations may also maximize fitness by maintaining short-term needs, including foraging, predator avoidance, and thermoregulation (Vernes, Marsh & Winter 1995; Gibson 2003; Krumme 2009), although the drivers are not always mutually exclusive.

Animal movements facilitate nutrient transfer, and the spatial and temporal scales at which migrations occur influence their ecological importance (Bauer & Hoye 2014; Buelow & Sheaves 2015). For example, annual migrations can create resource pulses; short duration, high magnitude events that drive ecosystem productivity (Ostfeld & Keesing 2000; Nowlin, Vanni & Yang 2008). Daily migrations occur over smaller spatial scales but, because they occur more frequently, may also be important in driving nutrient dynamics (Albeke, Nibbelink & Ben-David 2015; Subalusky *et al.* 2015; Francis & Cote 2018). In coastal marine environments, daily migrations are often necessary due to tidal fluctuations. As water levels rise, previously exposed areas become submerged, allowing mobile organisms access to habitats and resources that are unavailable at low tide (Krumme, Saint-Paul & Rosenthal 2004; Sheaves 2005; Castellanos-Galindo, Krumme & Willis 2010). In the tropics, coastal seascapes have a mosaic of interconnected habitats (Sheaves 2009) and fish often rely on multiple habitats across the tidal cycle for foraging and refuge which increases connectivity (Nagelkerken *et al.* 2015).

Use of shallow coastal areas by rays is often attributed to use as nursery habitat (Martins *et al.* 2018) and may be primarily driven by predator avoidance (Davy, Simpfendorfer & Heupel 2015). The shallow-water refuge hypothesis predicts that juveniles can gain refuge from predation in shallow, intertidal habitats as the larger body size of predators limits access to these areas (Paterson & Whitfield 2000). Vaudo and Heithaus (2013) concluded habitat use of multiple ray species in Shark Bay, Western Australia was driven by predator avoidance, overriding potential thermoregulatory and

foraging benefits of other areas. Indeed, despite high numbers of ray feeding pits in the intertidal (Vaudo & Heithaus 2009), the authors argued that foraging was not driving habitat use due to depauperate prey fauna in nearshore areas (Vaudo & Heithaus 2013). In other areas, however, invertebrate abundance peaks in the intertidal, suggesting these areas may be profitable foraging patches for rays (Dittmann 2000; Sheaves, Dingle & Mattone 2016).

To fully understand how and why rays are using coastal sandflats, it is crucial to directly link behaviour with habitat use and place these observations within the context of overall movement patterns. Traditional tracking methods such as active and passive acoustic telemetry do not provide direct observation of the animals so detailed behavioural information, such as foraging habitats, must be inferred from habitat types used, environmental conditions, and organismal biology. New technologies, such as animal borne cameras (Marshall *et al.* 2007; Stewart *et al.* 2019), accelerometer loggers (Payne *et al.* 2016; Royer *et al.* 2020), and drones (Gallagher, Papastamatiou & Barnett 2018; Raoult, Tusetto & Williamson 2018; Schofield *et al.* 2019), can complement traditional tracking techniques to directly relate habitat use and behaviour. The aim of this chapter was to identify the drivers of diurnal movements and identify foraging habitats of sympatric rays using a novel combination of acoustic telemetry and drone tracking.

Methods

Acoustic tracking

Rays were captured at the Lucinda sandflat using a 30 m seine net (8 mm mesh) when sighted while wading through the water. Once sighted, the target ray was encircled with the seine net and then captured using a large dipnet. After capture, rays were measured to the nearest mm (disc width for stingrays, total length for giant guitarfish), sexed (presence (male) or absence (female) of claspers), and tagged with Hallprint Inc. cinch up loop tags through one of the spiracles. Vemco V13 continuous acoustic transmitters were attached to the spiracle tags using small cable ties. Acoustic transmitters pinged at frequencies between 60 and 81kHz at a rate of one ping every one or two seconds depending on the tag. Four transmitters were also equipped with temperature sensors. The tagging procedure was completed in <10 minutes and all rays were released as close as possible to the capture location. Post-release, rays typically rested on the bottom for 5–10 minutes before resuming normal behaviour (burying or swimming). Burying behaviour was determined as normal behaviour if the ray was observed buried prior to capture.

Rays were tracked using a Vemco VR-100 receiver and a VH-110 directional hydrophone from a small inflatable vessel with an electric trolling motor. Due to the propensity for rays to use shallow (<1m deep) water, most rays were tracked on foot by pushing the vessel through the water.

The motor was only used for tracking when water depths were >1m or when movement rates were too great to keep up with on foot. As far as possible, detection levels were maintained at 70–90 decibels throughout the tracking period. Pursuit was stopped if the ray was visually sighted or if detections were >95 decibels to avoid startling the ray and influencing its behaviour. GPS positions were continuously recorded on the VR-100 receiver with each detection and were additionally recorded every five minutes with a handheld GPS. The position of the vessel during tracking was assumed to be the location of the ray. Rays were only tracked during daylight hours, with tracks commencing after the ray was released and resumed normal behaviour and finishing at sunset or the ray was lost. Individual rays were tracked for up-to three consecutive days during tidal periods with morning and evening high tides due to the logistics of launching and retrieving the vessel.

Drone Tracking

Drone tracking was limited to early mornings (sunrise – 9:30am) when winds were <25 km hr⁻¹ and tidal amplitude was <3m as these conditions provided the best visibility (i.e. minimized the influence of sun glare, waves, and current). DJI Phantom 3 Standard drones were used for tracking with live imagery displayed on an Apple iPad mini4 in the DJI Go application. Drones were hand-launched from the beach and flown in a haphazard search pattern at 10–15 m altitude with the camera angled directly downwards. Once a ray was sighted on the tablet screen, the pilot descended the drone to 3-5m altitude with the focal ray centred in the field of view and started the video recording. The optimal tracking altitude was selected so the drone was low enough to record behavioural details, but high enough so that the rotors did not disturb the water. In all tracks, the focal ray did not change its behaviour in response to the drone; therefore, drone presence likely had minimal influence on ray behaviour.

Rays were followed manually with the drone by applying minor steering inputs along the pitch (forwards/backwards) and roll (left/right) axes to maintain the position of the ray in the centre of the field of view. Rays were tracked until the drone battery level was reduced to 20 % capacity or the ray was no longer visible on the tablet screen, at which point video recording was stopped and the pilot returned the drone to the launch point. After each flight, the battery was immediately swapped out for a fresh one and the drone was launched again to search for and begin tracking a different individual. For consecutive flights, the search pattern was directed away from the final position of the previous ray to avoid tracking the same individual. Up to seven drone tracks were conducted per sampling day in this manner. Due to the high density (> 50 rays ha⁻¹) and high abundance (hundreds of individuals) of rays at Lucinda (K. Crook unpublished data), it was unlikely that the same individual would be tracked repeatedly. Consequently, all rays tracked over the course

of the study were treated as different individuals. Initially, the first ray observed during drone flights was tracked; however, later in the study, either *Pastinachus ater* or *Himantura australis* were targeted to reach the desired sample size for each species.

Longer drone tracks were completed using two drones to determine if behaviour observations during short tracks were representative of ray behaviour over longer periods. Long tracks were flown following the same methods as for short tracks; however, when the tracking drone battery declined to 30 %, a second drone was launched to continue the track. The second drone was launched at least 10 m away from the pilot of the tracking drone to prevent signal interference and was flown at minimum 15 m higher than the tracking drone to avoid a potential collision. The second drone was flown manually towards the tracking drone and positioned so that the tracking drone was in the centre of the tablet screen with the camera angled directly downwards. Once the second drone was in place and the focal ray was visually sighted, the tracking drone was flown away and returned to land. The second drone pilot then descended to tracking altitude (3–5 m), started the video recording, and continued tracking the focal ray. Drones were repeatedly swapped out in this manner until the focal ray was lost or all seven batteries had been used.

Data Filtering

Prior to analysis, acoustic tracking detection data were filtered to include only one detection per minute and to remove detections prior to finding the ray or after tracking had ceased using the ‘adehabitatLT’ package in R (Calenge 2006). On the first tracking day, detections immediately post-release were excluded until normal behaviour was resumed (5 – 10 min). If the ray was lost at any point during the track, this was noted and detections during these periods (i.e. when detections were irregular and < 70 decibels) were excluded from analyses. GPS coordinates were converted to Universal Trans Mercator (UTM) so distances could be calculated in meters. After filtering, each track was divided into ‘flood’, ‘ebb’, ‘high’, and ‘low’ tide periods. High and low tides were defined as ±1.5 hours from slack high and low tides, respectively, using local tide charts with flood and ebb tide periods defined as the rising and falling periods between the two. The tidal range for each track was calculated as the sum of the change in tide height over the duration of the track based on predicted tide heights from local tide charts.

For drone tracks, flight information stored in the DJI GO application was uploaded to an online storage platform (AirData) using the HD sync iPad application at the end of each tracking day. For each drone track, GPS locations (latitude and longitude), date and time, flight time, drone height above take-off location, and whether the drone was recording video were obtained from the flight

logs. GPS locations were recorded at a frequency of 10 Hz, but flight logs were filtered to include only one GPS position per second. Additionally, flight logs were filtered to only include positions when the drone was recording video so the drone position could be matched up with the video recording. The position of the drone was used as the position of the focal ray. For long tracks, flight logs for successive flights of the same individual were merged into a single file and relocations with overlapping date and time were removed. A 10 second simple moving average transformation was applied to GPS locations to correct for wind drift and imprecise control inputs. Once flight logs had been filtered, coordinates were converted to UTM. Tidal phases were categorised in the same way as for acoustic tracking. All short tracks occurred within a single tidal phase, but long tracks spanned over both flood and high tides in some cases.

Video Analysis

Drone videos were watched using VLC media player to record feeding events. Feeding behaviour was categorized as ‘Non-disruptive’, ‘Suction’, ‘Water Jetting’, or ‘Excavation’ (See Table 3.1) and a feeding event was recorded for every instance of foraging behaviour. The video time at the onset of foraging was recorded and matched with the drone flight log to determine the location of each feeding event. The feeding rate for each drone track was calculated as the number of feeding events divided by the tracking time (events hr⁻¹).

Data Analysis

For all tracks, rate of movement (ROM) was calculated as the distance travelled in meters for every minute of tracking (m min⁻¹). Distances between relocations were calculated by creating movement trajectories using the ‘adehabitatLT’ R package (Calenge 2006). For acoustic tracks, ROM was simply the distance travelled between successive one-minute relocations averaged over the entire track and within each tidal phase. For short drone tracks, ROM was determined for the entire track as the distance travelled divided by the time tracked. ROM for long tracks was determined in the same way over the full track but also divided by tidal phase if tracked across both flood and high tides. Distances travelled for all tracks was determined by the sum of the distances between all relocations.

The tortuosity of movement paths was evaluated using a short-term linearity index, modified from Benhamou (2004) (e.g. Simpfendorfer, Wiley and Yeiser (2010); Martins *et al.* (2020)), as the distance between the first relocation and the tenth relocation of the track divided by the total distance travelled over the 10 relocations (~10 minutes for acoustic tracking, ~10 seconds for drone tracking). The linearity index (LI), ranging from zero (non-linear movement) to one (linear movement), was calculated for every 10 adjacent relocations, sequentially removing the oldest and

adding the next relocation for the entire track and for tidal phases within each track. Mean LI values were calculated for each track and tidal phase for both drone and acoustic tracks.

Habitat use was examined by calculating kernel utilization distributions (KUD) from ray relocations using the ‘adehabitatHR’ R package (Calenge 2006). The 95 % KUD was used to represent total habitat use and the 50 % KUD as core habitat use. For acoustic tracking, total and core habitat use were determined for each species by combining all relocations from all tracked individuals. Habitat-use estimates were also calculated by individual (across all tracking days) and then averaged for each species. Drone track habitat use was only calculated per species due to the limited tracking time for each individual and was determined for short and long tracks combined. Foraging habitat use was calculated for each species based the location of all observed feeding events.

All statistical analyses were conducted using R statistical computing software (R Core Team 2018) and habitat use maps were generated using satellite imagery from the ‘ggmap’ package (Kahle & Wickham 2013). ROM and feeding rate data were all non-normal and could not be coerced to normal distributions using transformations so non-parametric statistical tests were used. Kruskal-Wallis tests were used for comparisons among tidal phases for acoustic tracks and short drone tracks with post-hoc Dunn tests to compare between groups. Flood and high tide periods for long drone tracks were compared with Mann-Whitney U tests. All tests of significance were evaluated at $\alpha=0.05$ and the Benjamini-Hochberg procedure was applied to adjust p-values from multiple comparisons to reduce the probability of type I error. Correlations between continuous variables were assessed using Pearson’s correlation tests for habitat use as these data fit the assumptions of normality and Spearman’s rho correlation tests for non-normal data.

Results

Acoustic tracking

Thirteen individual rays were tracked at Lucinda over a total of 38 tracking days between Sept 2017 and June 2019. Tracks were completed for seven *Pastinachus ater* (18 days), five *Himantura australis* (18 days), and one giant guitarfish (*Glaucostegus typus*; 2 days) with track durations ranging from 2.5–11.2 hours (mean \pm SD: 8.9 ± 2 hours, Table 2.1). All tagged rays were juveniles based on published sizes at maturity (Last *et al.* 2016) and a lack of clasper calcification for males (Table 2.1). Rays were tracked for up-to three consecutive days and all rays were re-detected on the sandflat following the first day of tracking. In cases where individuals were tracked for <3 days, tracking was suspended due to poor weather conditions or equipment malfunction. Two individuals (*Ha055* and *Ha184*) were tracked for three consecutive days and then for an additional

Table 2.1 Details of acoustic tracks for individual *Himantura australis* (Ha), *Pastinachus ater* (Pa), and *Glaucostegus typus* (Gt) tracked at Lucinda. ROM: Rate of movement.

ID	Disc Width (mm)	Sex	Date	Distance (m)	Duration (hr)	ROM (m min ⁻¹)	Linearity
<i>Ha055</i>	510	M	2017-09-22	1127	8.5	2.22	0.760
			2017-09-23	1134	9.3	2.04	0.487
			2017-09-24	4466	9.2	8.10	0.568
			2017-09-29	3752	9.6	6.62	0.558
			2017-09-30	3567	11.2	5.33	0.601
<i>Pa035</i>	440	F	2017-12-12	2473	5.9	7.09	0.532
			2017-12-13	4772	10.3	7.80	0.670
			2017-12-14	4354	10.4	6.98	0.606
<i>Gt097</i>	1000 ^a	F	2017-12-16	6914	9.7	12.04	0.687
			2017-12-17	10231	11.2	15.22	0.637
<i>Pa146</i>	400	F	2018-04-24	5290	10.0	8.83	0.562
			2018-04-25	4963	10.0	8.26	0.766
<i>Pa147</i>	458	F	2018-05-09	2186	6.6	5.58	0.682
			2018-05-10	5174	10.7	8.10	0.624
			2018-05-11	5027	10.2	8.23	0.751
<i>Ha148</i>	328	F	2018-05-23	2769	2.6	18.96	0.771
			2018-05-24	4814	9.5	8.48	0.715
			2018-05-25	4883	10.3	7.93	0.694
<i>Pa149</i>	507	F	2018-06-20	2361	7.9	4.99	0.576
			2018-06-21	6290	10.6	9.90	0.510
			2018-06-22	5156	10.8	7.98	0.565
<i>Pa192</i>	450	F	2018-09-18	3444	7.6	7.69	0.546
			2018-09-19	4798	10.9	7.35	0.730
			2018-09-20	4975	10.4	8.00	0.728
<i>Ha184</i>	394	M	2018-10-04	1460	5.9	4.22	0.575
			2018-10-05	1856	8.3	3.74	0.648
			2018-10-06	2008	9.1	3.70	0.780
			2018-10-18	2163	10.0	3.61	0.679
			2018-10-19	2406	9.6	4.20	0.611
<i>Pa187</i>	494	M	2018-11-16	2093	7.5	4.68	0.629

<i>Pa181</i>	581	M	2019-04-27	813	5.2	2.62	0.600
			2019-04-28	3444	9.8	5.89	0.714
			2019-04-29	4664	10.1	7.71	0.765
<i>Ha190</i>	770	M	2019-05-29	2589	5.0	8.72	0.681
			2019-05-30	4137	10.1	6.87	0.661
			2019-06-12	6436	10.2	10.53	0.673
<i>Ha186</i>	343	M	2019-06-11	3215	5.7	9.51	0.677
			2019-06-13	2342	8.8	4.44	0.611

^aStretch total length for *G. typus*

two days 1–2 weeks later. For all but two tracking days, tracking was terminated when there was insufficient light to continue the track, with the remaining two tracks ending when the ray could no longer be detected in water depths <20 cm. Daily travel distances for individual rays ranged from 813–10231 m (mean: 3804 ± 1911 m, Table A1). Variability in track time and distances were largely due to shorter tracking time on the first tracking day due to the time it took to catch and tag a ray (Table 2.1).

Table 2.2 Total (95 %) and core (50 %) kernel utilisation distributions (KUD in km²) from acoustic tracking, drone tracking, and combined methods for *Himantura australis* and *Pastinachus ater* at Lucinda. Habitat-use estimates reflect: KUD for all individuals (Total); mean ± standard deviation KUD for individual rays (Individual); and KUD based on the locations of feeding events (Foraging).

Track Type	Estimate	<i>Himantura australis</i>		<i>Pastinachus ater</i>	
		95 % KUD	50 % KUD	95 % KUD	50 % KUD
Acoustic	Total	1.53	0.30	1.41	0.38
	Individual	0.68 ± 0.30	0.13 ± 0.06	0.64 ± 0.15	0.13 ± 0.03
Drone	Total	0.23	0.03	0.51	0.10
	Foraging	0.22	0.03	0.42	0.09
Combined	Total	1.55	0.32	1.43	0.39

Overall, individual rays restricted habitat use to within the sandflat boundary and habitat use was similar among species (Table 2.2) (Fig. 2.1). All tagged rays were detected on the sandflat for the entire battery life of the tag (29–48 days), suggesting rays may be resident to the sandflat over the short-term. Estimated total habitat areas (95 % KUD) were 1.5 and 1.4 km² for *H. australis* and *P. ater*, respectively, with smaller core use areas (50 % KUD) restricted to 0.3 and 0.4 km² (Table 2.2). The *G. typus* individual used a total area of 1.0 km² and a core area of 0.2 km² over two tracking days. Habitat use of individual rays was similar for *H. australis* and *P. ater* but in each case was

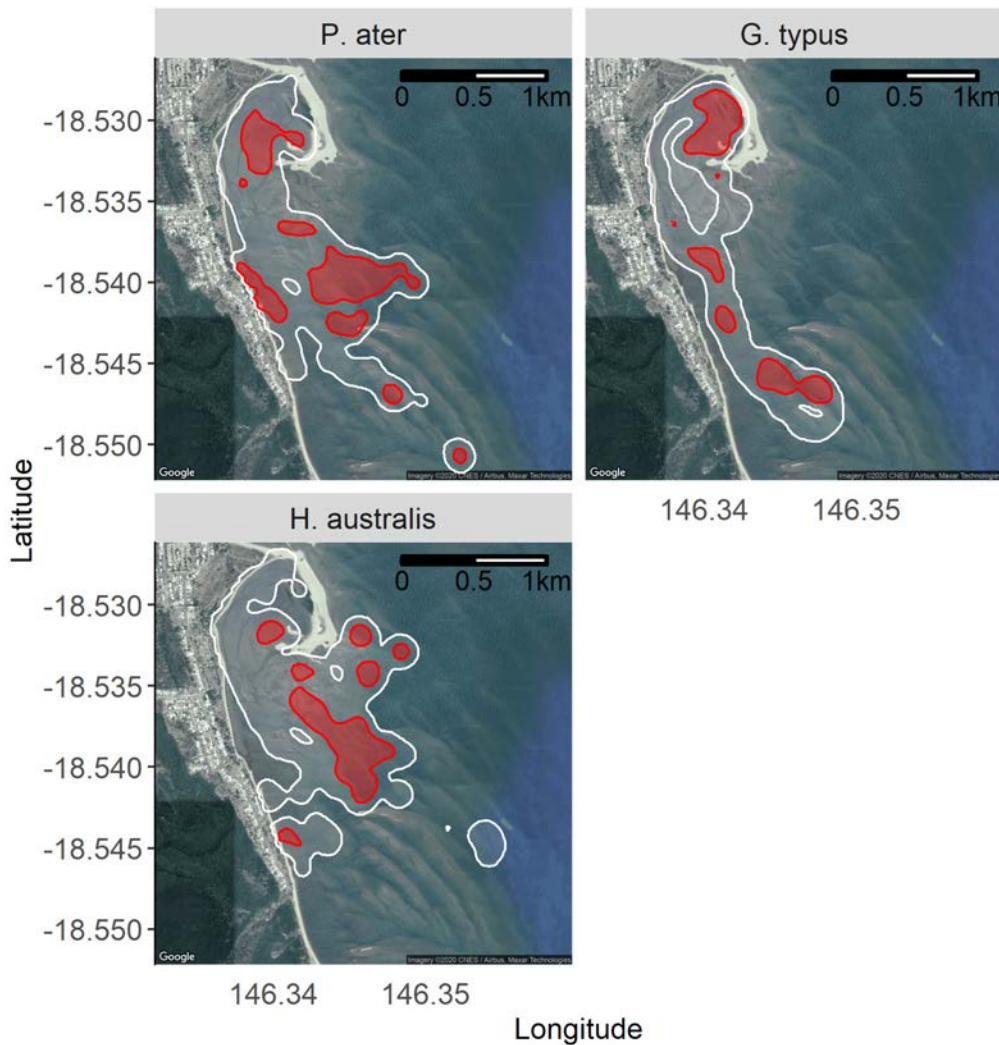
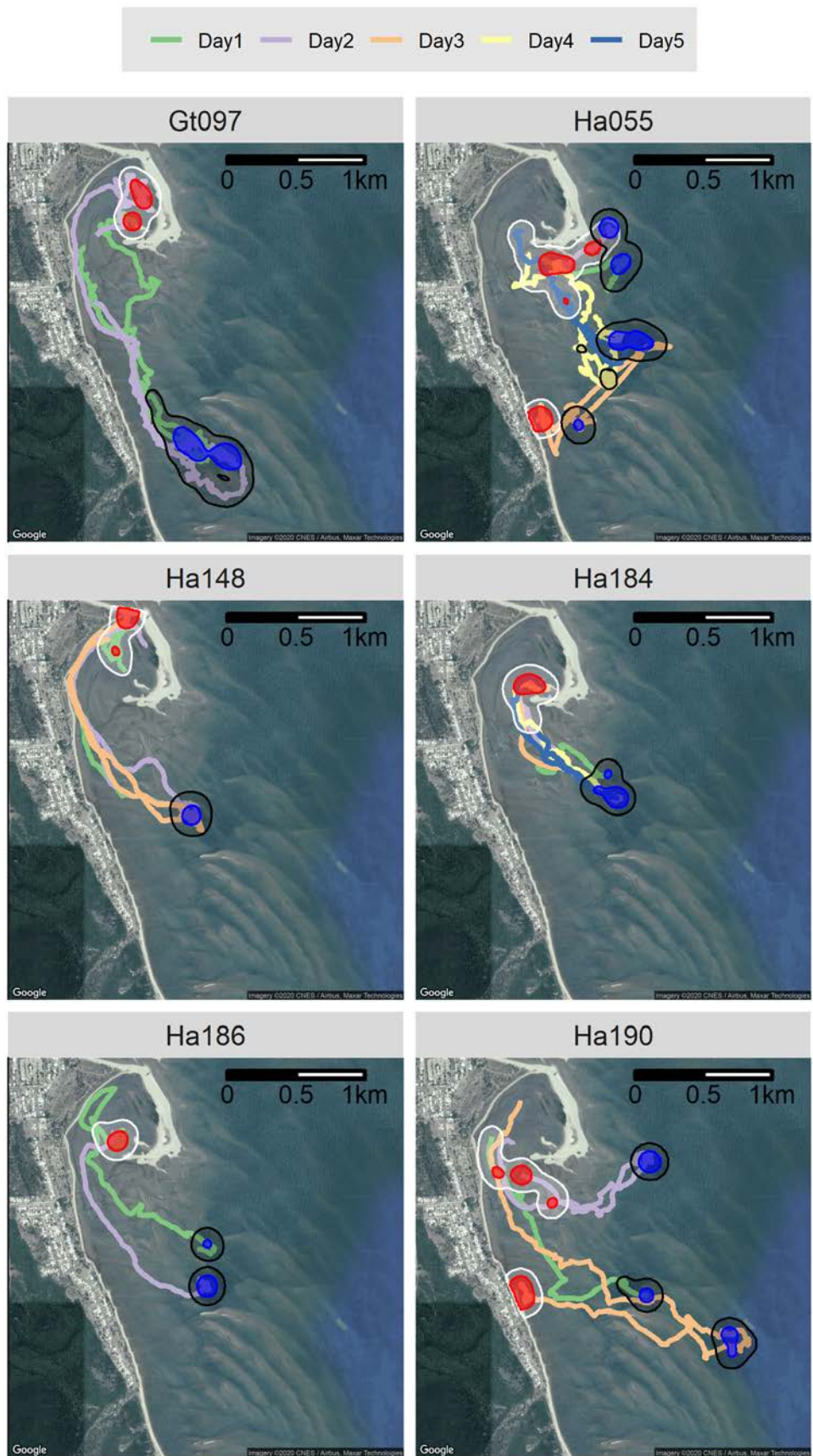


Figure 2.1 95 % (white) and 50 % (red) kernel utilisation distributions of *Pastinachus ater* (n=7), *Glaucostegus typus* (n=1), and *Himantura australis* (n=5) acoustic tracks at Lucinda.

smaller than overall species habitat area (Table 2.2). Both total and core habitat areas were positively correlated with disc width (Table A1) but there was no significant correlation between habitat use and time-tracked or tidal range (Table A1), suggesting that rays used similar habitats across sampling days.

The activity patterns and habitat use of *H. australis* and *P. ater* at Lucinda were coupled with the tidal cycle. During high tides, rays used the enclosed bay at the northern end of the sandflat or shallow flats adjacent to the beach (Fig. 2.2). During low tides, rays rested in shallow gullies between exposed sandbars and remained stationary for extended periods (Fig. 2.2 and 2.3). Movements during running tides were direct paths between core low and high tide areas and followed predictable patterns, with tracks often following identical paths across tidal cycles and sampling days



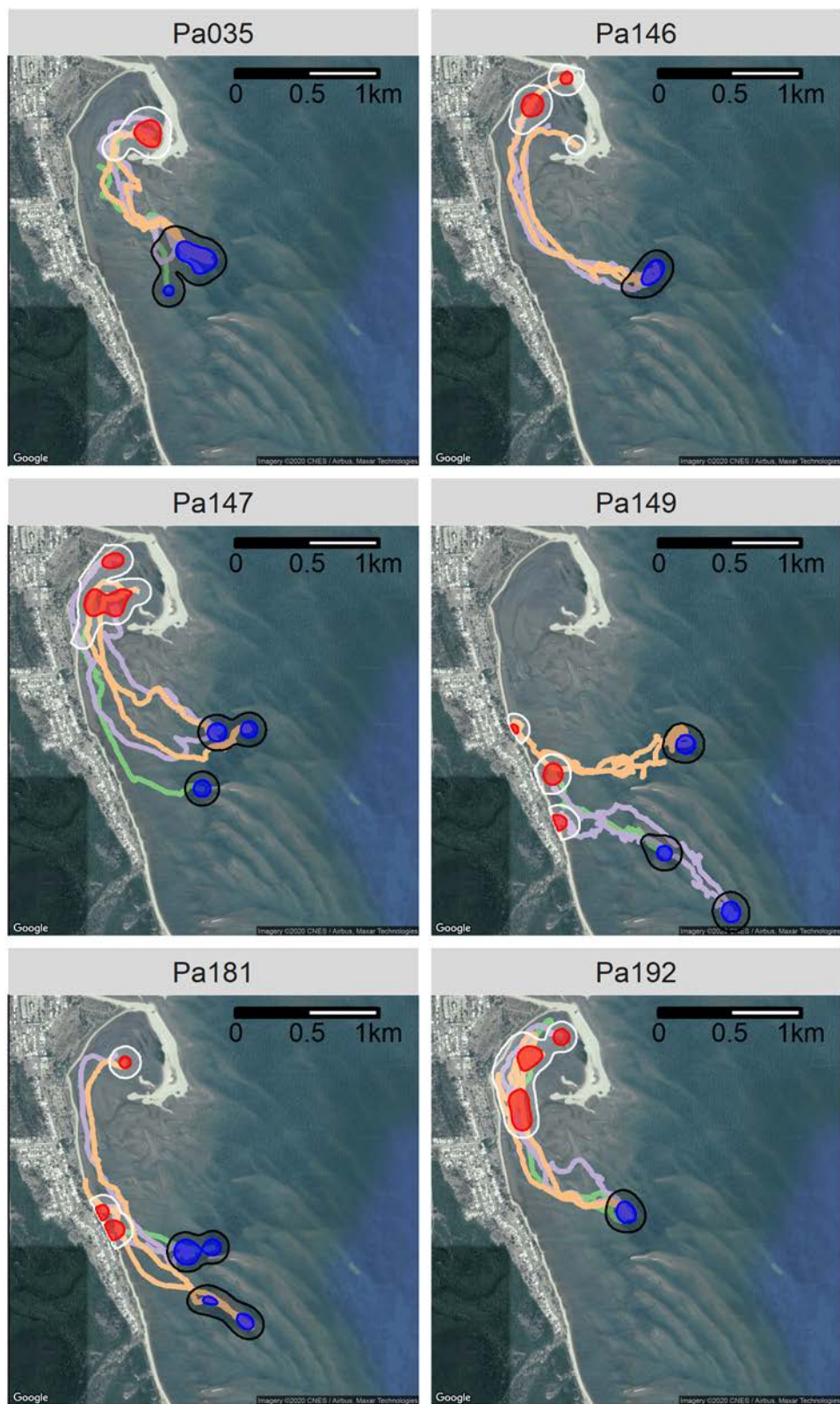


Figure 2.2 Movement paths of *Himantura australis* (Ha), *Pastinachus ater* (Pa), and *Glaucostegus typus* (Gt) individuals acoustically tracked at Lucinda. Blue and black contours represent 50 and 95 % kernel utilisation distributions (KUD) during low tide periods. Red and white contours represent 50 and 95 % KUD during high tide periods. Different coloured lines represent different tracking days ($n=2 - 5$).

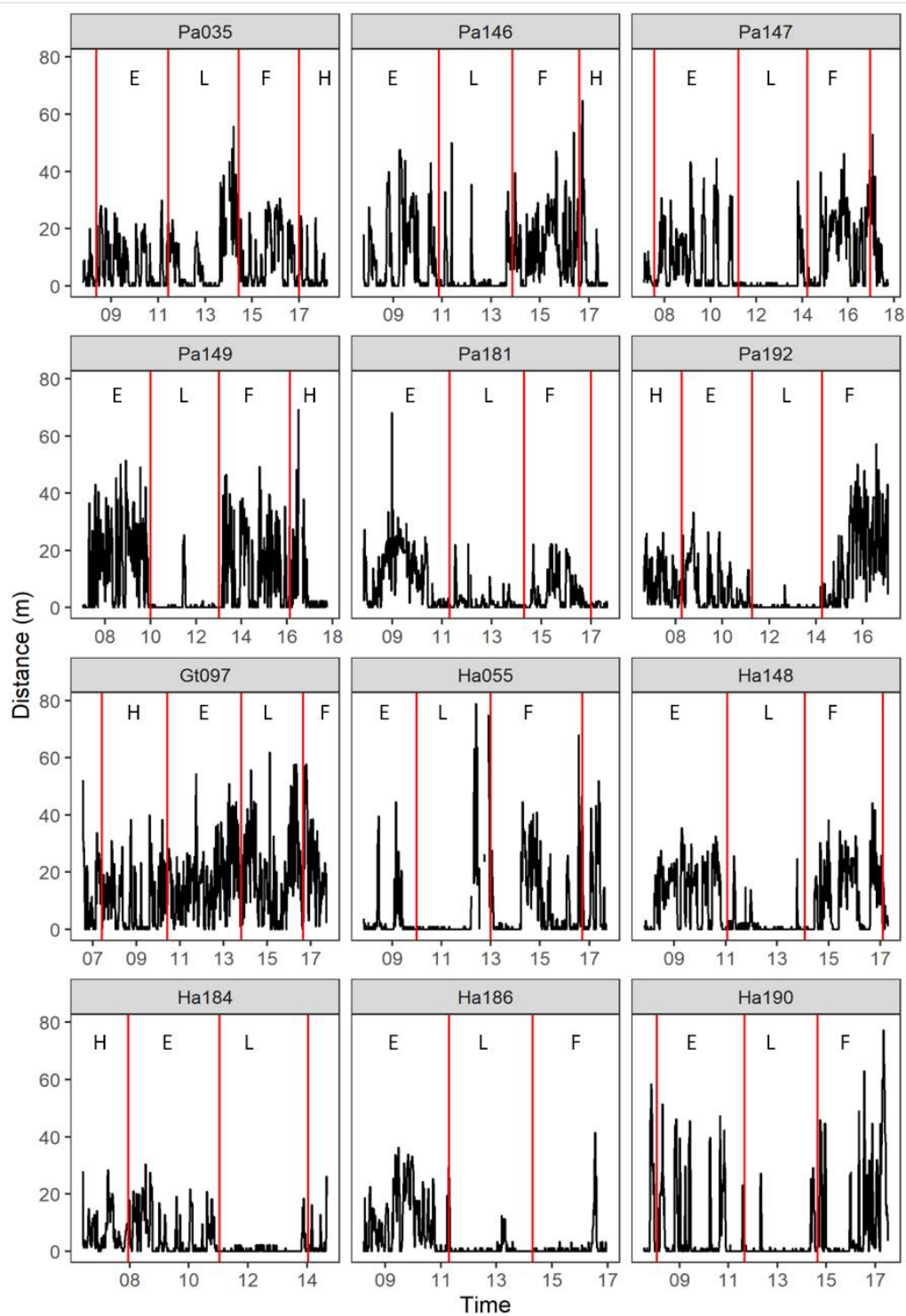


Figure 2.3 Single day activity patterns of individual *Himantura australis* (Ha), *Pastinachus ater* (Pa), and *Glaucostegus typus* (Gt) acoustically tracked at Lucinda. Black lines represent the distance travelled in one-minute intervals and red lines demarcate the boundaries of ebb (E), low (L), flood (F), and high (H) tide periods.

(Fig. 2.2). Activity patterns during running tides were highly variable, with short periods of inactivity interspersed with bursts of movement or sustained travel (Fig. 2.3). The activity of the lone *G. typus* differed from those of *H. australis* and *P. ater*, with no extended period of inactivity at low tide and more sustained periods of movement across the tidal cycle (Fig. 2.3).

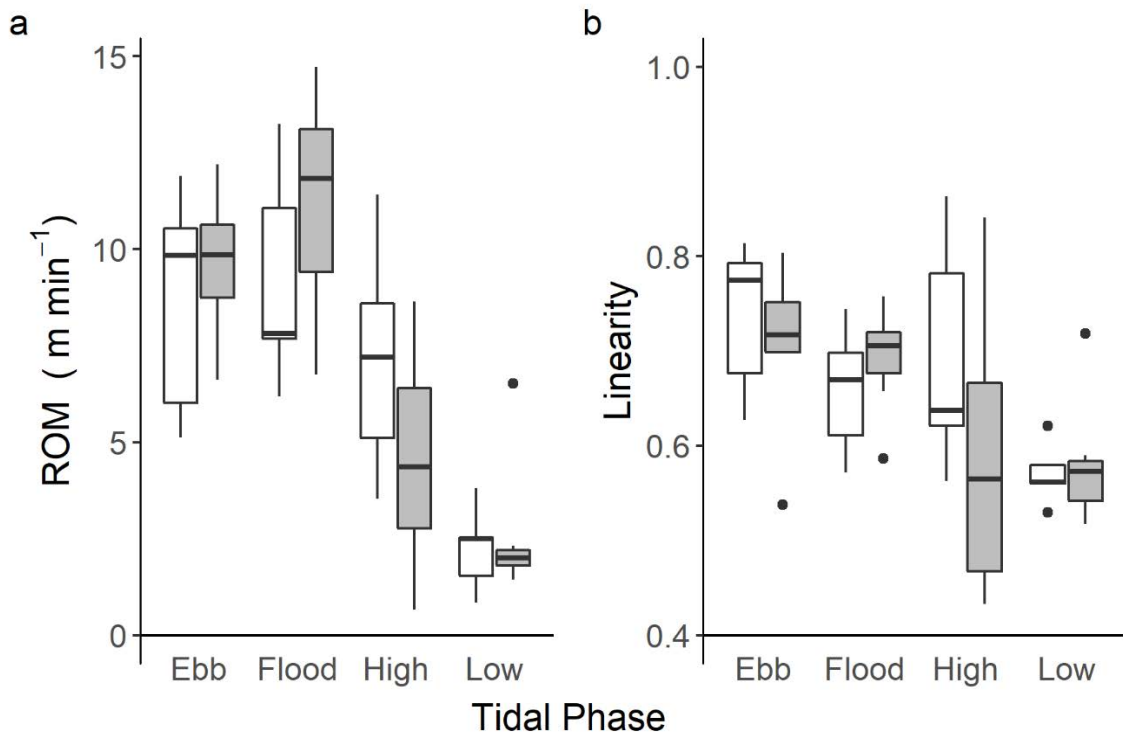


Figure 2.4 Boxplots of the mean a) rate of movement (ROM) and b) ten-point linearity by tidal phase for individual *Himantura australis* (white) and *Pastinachus ater* (grey) tracked (acoustic telemetry) at Lucinda. Boxes represent the first and third quartiles with whiskers extending to data points within 1.5 times the inter-quartile range. Horizontal black lines represent the median and individual points represent outliers.

Rates of movement (ROM) were variable among individuals and tracking days (Table 2.1) but were similar between *P. ater* and *H. australis* (mean \pm SD: 7.1 ± 1.3 and $6.7 \pm 2.4 \text{ m min}^{-1}$, respectively). Mean ROM was higher for the single *G. typus* across two tracking days (13.6 m min^{-1}) but was not statistically compared with the other two species. ROM was not significantly correlated with ray size nor with tidal range (Table A1) but differed among tidal phases for both *P. ater* and *H. australis* (Fig. 2.4a) (Table A2). Consistent with activity patterns, ROM was highest during running tides (flood and ebb) and lowest and least variable during low tides for both species (Fig. 2.4a) (Table A2). High tide ROM was highly variable and was generally lower than during running tides although this pattern was more evident for *P. ater* (Fig. 2.4a). Mean linearity was also highest during running tides and lowest during low tides (Fig. 2.4b); however, linearity values were above 0.5 during all tidal

phases (Fig. 2.4b) and over full tracks (Table 2.1) indicating that rays follow linear trajectories throughout the tidal cycle.

The four *P. ater* tracked with temperature sensors experienced a wide range of temperatures with a minimum of 18.3°C in the dry (cool) season and a maximum of 34.9°C at the start of the wet (warm) season. The maximum temperature range experienced by an individual in a single day was 10.3°C (22.8–33.9°C); however, the variation in temperature did not influence activity patterns as temperature increased steadily throughout the day (Fig. 2.5) and activity patterns were similar for all individuals (Fig. 2.2 and 2.3).

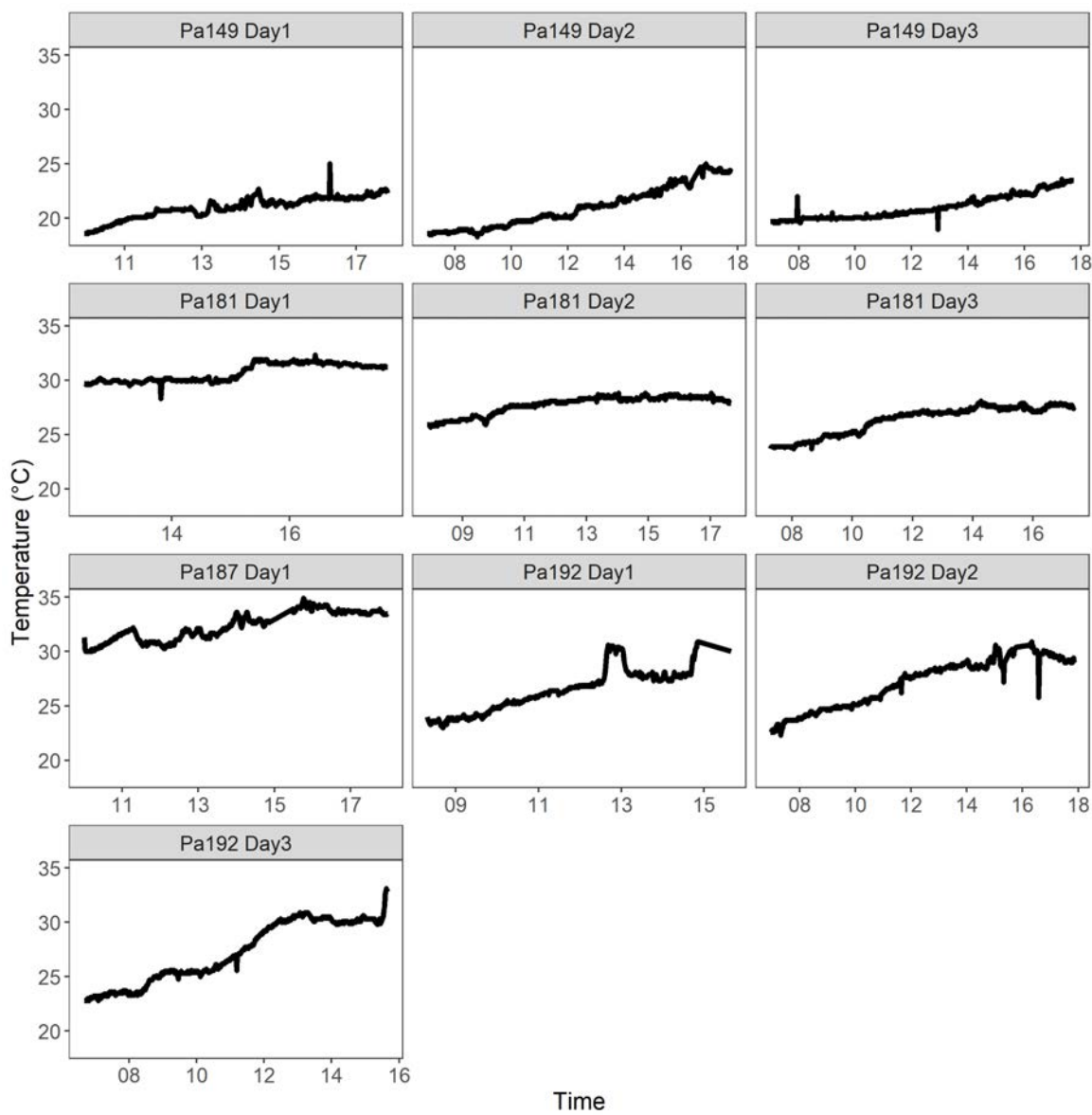


Figure 2.5 Water temperatures experienced across all tracking days for the four juvenile *Pastinachus ater* individuals tracked with temperature sensors at Lucinda. Note: the time scale on the x-axis is different for each figure.

Drone Tracking

Between Dec 2017 and Sept 2019, 125 short (*P. ater*: n=63, *H. australis*: n=62) and 11 long (*P. ater*: n=5, *H. australis*: n=6) drone tracks were flown at Lucinda. Short tracks were spread evenly among flood, high, and ebb tide periods and ranged from 5–20 minutes with a mean \pm SD duration of 14.6 ± 3.6 min. Long tracks ranged from 37–107 minutes with a mean \pm SD of 79.9 ± 23.9 min and only covered flood and high tide periods. Trends in ROM, linearity, and feeding rates were similar for long and short tracks (Fig. A3); therefore, all tracks were combined for analyses.

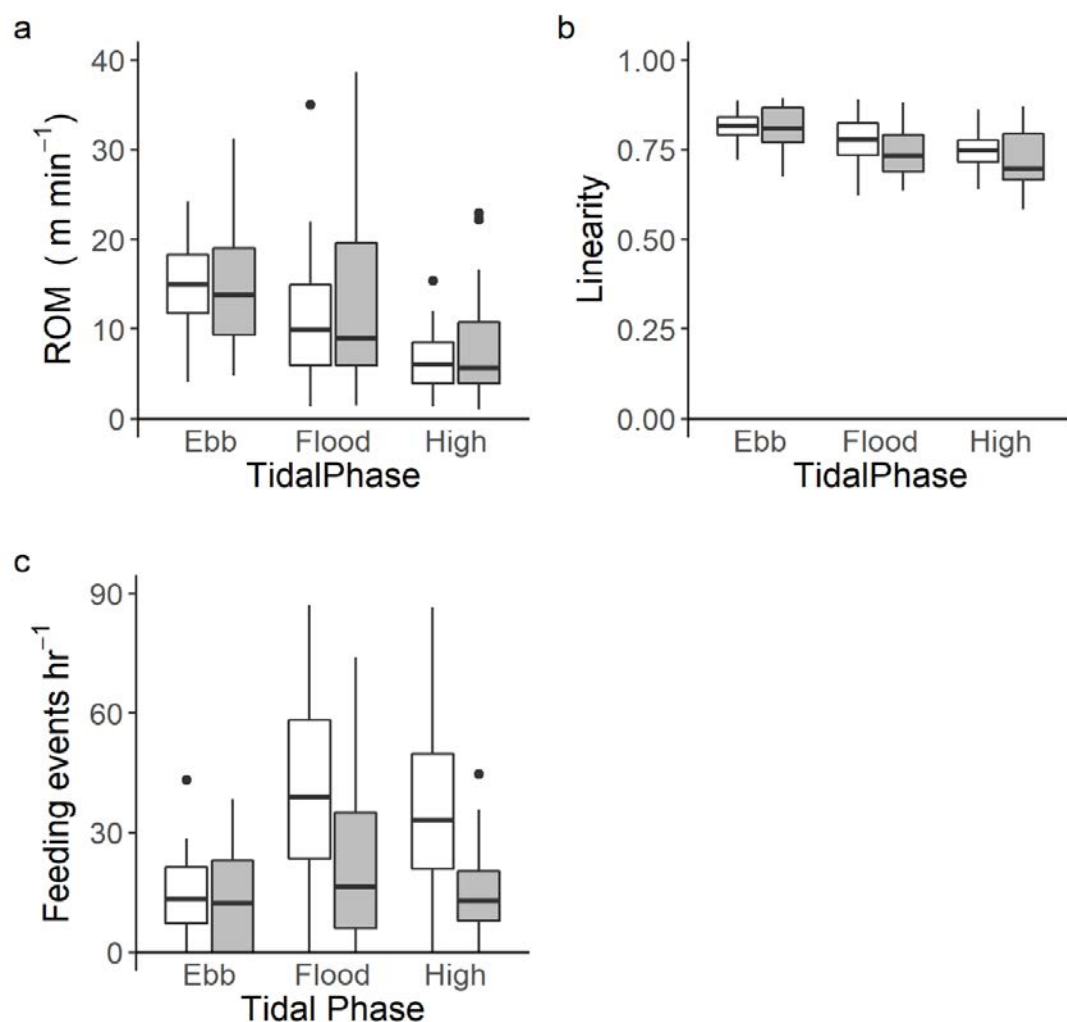


Figure 2.6 Boxplots of a) rate of movement (ROM), b) linearity, and c) feeding rate for *Himantura australis* (white) and *Pastinachus ater* (grey) tracked with drones at Lucinda. Boxes represent the first and third quartiles with whiskers extending to data points within 1.5 times the inter-quartile range. Horizontal black lines represent the median and individual points represent outliers.

Consistent with acoustic tracking, drone track ROM and linearity were similar for *H. australis* and *P. ater* and showed similar trends among tidal phases. Drone track ROM was highest during ebbing tides and lowest during high tides (Fig. 2.6a) (Table A4). Linearity values were also highest during ebb tides and lowest during high tides; however, all linearity values were >0.6 indicating linear movement for all individuals and tidal phases which is consistent with acoustic tracking (Fig. 2.6b).

Feeding rates were highly variable among individuals of both species but median foraging rates were higher for *H. australis* than for *P. ater* (28.8 vs. 13.1 events hr⁻¹) (Fig. 2.6c). Median feeding rates were nearly identical for long and short tracks and were consistent throughout the year (Fig. A5). Feeding rates of *H. australis* were higher during flood and high tides than during ebb tides whereas *P. ater* foraged at a consistent rate throughout the tidal cycle (Fig. 2.6c) (Table A4).

Drone KUD

Contrary to acoustic tracking, total and core habitat use estimates from drone tracks were smaller for *H. australis* than for *P. ater* (Fig. 2.7a) (Table 2.1). Core habitat use was predominantly used for feeding as most feeding events occurred in core habitats for both species (Fig. 2.7a). Consistently, core habitat use based solely on the locations of feeding scars was nearly identical to core drone track habitat use (Table 2.2). Despite overlap in total habitat use, core foraging habitats had minimal overlap between the two species, suggesting foraging habitat partitioning is occurring on a fine scale (Fig. 2.7b).

Combined KUD

To see if habitat use matched up with feeding locations, feeding locations from drone tracks were overlaid onto habitat use maps from acoustic tracking separated into flood, high, and ebb tides. For *P. ater*, all feeding scars were contained within the total habitat area for both flood and ebb tides and only a few high tide feeding scars fell outside the total habitat area (Fig. A6). Core habitats matched up well with foraging locations for flood and high tides but mostly fell outside core areas for ebbing tides (Fig. A6). Foraging locations of *H. australis* were within the 95 % KUD for flood and ebb tides but most high tide feeding scars occurred outside both core and total habitat use areas (Fig. A6). Combining drone and acoustic tracks gave similar habitat use estimates as for acoustic tracks only (Table 2.2); however, combined tracks showed larger core areas in the enclosed bay at the northern end of the beach where the majority of drone tracking took place (Fig. 2.8).

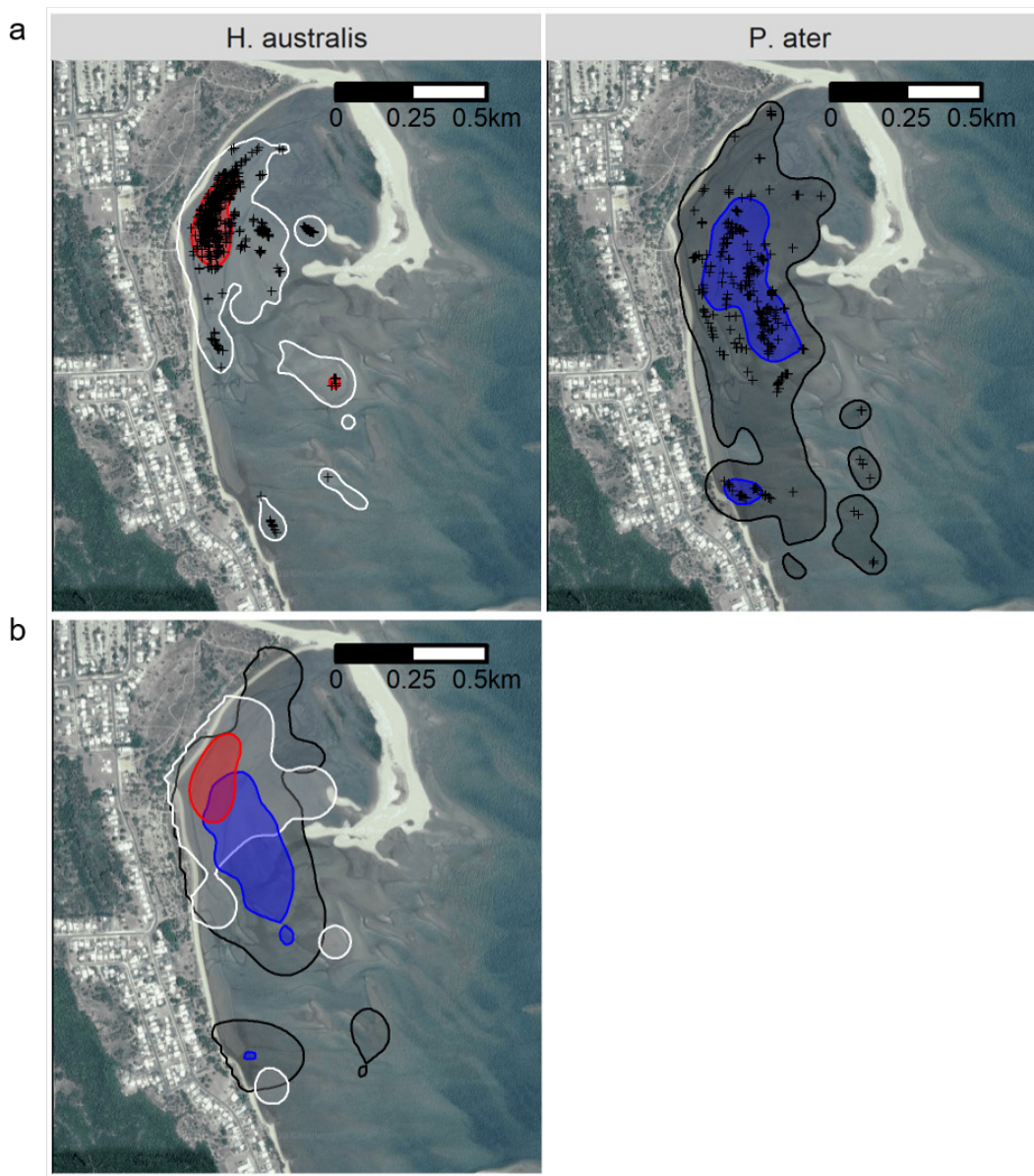


Figure 2.7 Kernel utilisation distributions from a) all drone tracks of *Himantura australis* and *Pastinachus ater* at Lucinda, and b) all feeding event locations. KUDs for *H. australis* are represented as white (95 %) and red (50 %) contours. KUDs for *P. ater* are represented as black (95 %) and blue (50 %) contours.

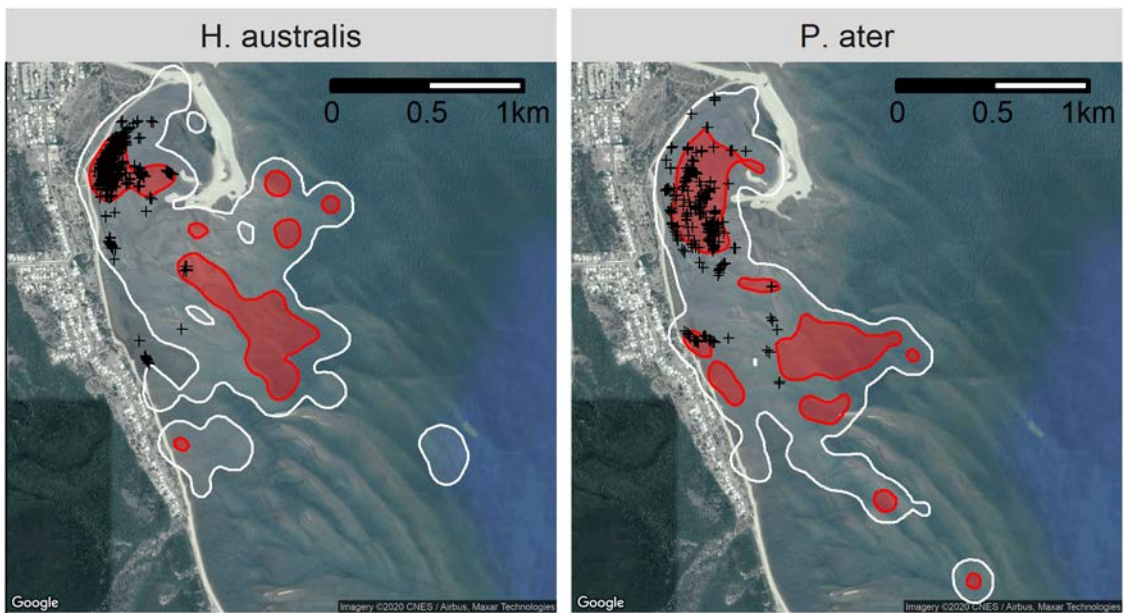


Figure 2.8 95 % (white) and 50 % (red) kernel utilisation distributions for *Himantura australis* and *Pastinachus ater* from combined acoustic and drone tracks.

Discussion

This study is the first to use a combination of acoustic tracking and drone tracking to investigate the fine-scale habitat use and behaviour of free-ranging marine animals. The combination of methods allowed us to not only establish habitat use and movement patterns but to identify specific behaviours and pinpoint when and where those behaviours were occurring. Acoustic tracking determined that movements of juvenile *Pastinachus ater* and *Himantura australis* were restricted to within the sandflat boundary, tightly coupled with the tidal cycle, and repeated across individuals and sampling days. The addition of drone tracking revealed that despite overall habitat use being similar, the two species foraged in discrete areas of the sandflat. Foraging activity was largely restricted to habitats only accessible during late flood and high tide periods which suggests that daily tidal migrations of juvenile rays may primarily be driven by access to foraging opportunities in the intertidal. Thus, the added dimension of placing behavioural observations within the context of overall habitat use allows a more thorough understanding of the drivers of animal movement and can illuminate fine-scale differences among sympatric species.

Tides have a significant influence on movement patterns and habitat use of organisms in coastal marine and estuarine environments (Gibson 2003; Krumme 2009). In the present study, juvenile *H. australis* and *P. ater* concentrated foraging activity in the intertidal and all rays moved quickly and in linear trajectories towards core foraging areas during flooding tides. In tropical sand and mudflats, macro-invertebrate richness, abundance, and biomass peaks in the low-intertidal and

these areas may serve as profitable foraging patches for benthic invertivores (Sheaves, Dingle & Mattone 2016). Animals can maximize energy intake and decrease search times by returning to areas with abundant prey or where prey has been previously encountered (Davoren, Montevecchi & Anderson 2003; Weimerskirch *et al.* 2007; Wakefield *et al.* 2015). Consistently, rays at Lucinda repeatedly used the same intertidal foraging habitats, suggesting tidal migrations are likely driven by access to predictable prey patches.

The time and depths at which fish can access intertidal habitats is determined by body size (Bretsch & Allen 2006). Shallower body depths of small fish allow them to enter intertidal areas earlier and for longer periods than large fish. Rays have a relatively high biomass among sandflat fauna; however, their flattened body shape affords them access to intertidal habitats earlier in the tidal cycle than teleosts with similar biomass and foraging strategies (e.g. golden trevally). Indeed, juvenile *Urogymnus granulatus* and *Pastinachus ater* at nearby Orpheus Island, Australia followed the edge of the tide to access intertidal areas as soon as they flooded (Davy, Simpfendorfer & Heupel 2015; Martins *et al.* 2020). Juvenile *H. australis* and *P. ater* at Lucinda followed similar patterns and used shallow (<1m) water throughout the tidal cycle. The ability to remain in shallow water means rays can stay in depths that afford them refuge from predation and can access foraging patches earlier and for longer than potential teleost competitors. Consistently, rays at Lucinda foraged intensely in the intertidal while it was submerged and then retreated only as far as necessary to remain submerged (< 1m) at ebb and low tides. During low tide periods, rays remained stationary for extended periods (>2 hours) and were often buried (K. Crook pers obs.). Additionally, ray feeding pits were absent or in low abundance in low tide habitats (K. Crook pers. obs.) which suggests rays are primarily resting during low tides.

Temperature may also influence habitat selection, particularly among poikilotherms as their body temperature and metabolism are regulated by ambient temperatures (Sunday *et al.* 2014). Consequently, movements may occur to remain at thermal optimum temperatures or to exploit thermal heterogeneity in the environment to gain a physiological advantage (Blouin-Demers & Weatherhead 2001; Martin & Huey 2008). Among rays, Dabruzzi *et al.* (2013) suggest juveniles in tropical marine environments exploit a narrow temperature range and move with the tidal cycle to remain at optimum temperatures. Movements consistent with remaining within a thermal optimum would result in individuals experiencing minimal daily temperature fluctuations which was not observed in this study. The four individuals tracked with temperature sensors showed there was no influence of temperature on activity patterns or habitat selection as temperatures increased linearly throughout the day and activity patterns were consistent across all individuals. Although no *H. australis* were tagged with temperature sensors, the similarity in movement patterns with *P. ater*

suggests that neither species is moving in response to temperature heterogeneity or to exploit optimum temperature gradients.

The large temperature variation experienced daily and throughout the year by juvenile rays at Lucinda suggests that juvenile rays have a wide thermal tolerance and activity levels may not be limited by metabolism. Atlantic stingrays (*Dasyatis sabina*) have extreme thermal tolerances and have among the highest abilities to acclimate to extreme temperatures among measured animals (Fangue & Bennett 2003). Dabruzzi *et al.* (2013) noted that the bluespotted fantail ray (*Taeniura lymma*) has a high thermal optimum temperature but metabolism increased more than expected past the optimum temperature. Thus, even in thermally tolerant stingrays, high temperatures in the warm season may result in higher metabolic costs than during the winter when waters are cooler. Dale, Drazen and Holland (2013) suggest that metabolism is the most significant component of juvenile energy budgets and foraging rates must be high to compensate for these high metabolic costs. Consequently, the high feeding rates of rays at Lucinda may be necessary to offset high metabolic costs, particularly in the warmer months. Alternatively, if prey is not limited, high water temperatures may increase digestion rates which may aid juvenile rays in maximizing growth (Hight & Lowe 2007; Papastamatiou *et al.* 2015). The perpetual use of intertidal areas by rays at Lucinda indicates that benefits such as foraging, predation refuge, and potentially growth outweigh any increased metabolic costs experienced due to large fluctuations in temperature.

The habitat use, residency (at least one month), and high abundance across years (K.Crook unpublished data) of juvenile rays at Lucinda support that the sandflat is a nursery area for these species (Heupel, Carlson & Simpfendorfer 2007; Heupel *et al.* 2019). Nursery areas function by providing opportunity for juveniles to feed and grow with reduced predation pressure and, consequently, contribute more recruits to the breeding population (Beck *et al.* 2001; Nagelkerken *et al.* 2015). Nurseries are seldom perfect, however, and often require a trade-off between maximizing growth and maximizing survival (Heupel *et al.* 2007; Heithaus 2007). High foraging rates and use of shallow water throughout the tidal cycle suggest that juvenile rays at Lucinda have access to abundant prey and may not be required to trade-off growth and survival. As a result, the Lucinda nursery may be higher quality than areas with depauperate prey communities or higher predation pressure (Vaudo & Heithaus 2009; Davy, Simpfendorfer & Heupel 2015); however, examination of prey distribution and abundance at Lucinda warrants future study.

Daily migrations between discrete foraging and resting areas within the sandflat boundary suggest that juvenile rays may transport energy and nutrients between areas. Daily use of foraging and resting sites can have a significant influence on nutrient dynamics in resting sites through

deposition of allochthonous resources via defecation or excretion (Reef, Feller & Lovelock 2014; Albeke, Nibbelink & Ben-David 2015; Subalusky *et al.* 2015). Although ray foraging and resting sites at Lucinda are only spaced 1–2 km apart, the consistent transfer of intertidal nutrients to the subtidal may be important for subtidal productivity (Allgeier, Yeager & Layman 2013). Over the long term, rays may transfer sandflat productivity offshore through ontogenetic migration (Mumby 2006; Chin *et al.* 2013). Individual habitat use at Lucinda was positively correlated with body size, suggesting that as individuals grow, they range over larger areas possibly due to reduced predation risk or increased energetic demand (Heithaus 2007; Papastamatiou *et al.* 2009). The gradual home range expansion of large juveniles may increase connectivity by using both nursery and adult habitats prior to permanent emigration from the nursery (Aguiar, Valentin & Rosa 2009). My results show weak support for this gradual transition occurring at Lucinda; however, longer term tracking studies and identification of adult habitats are required to confirm the scale and frequency of connectivity.

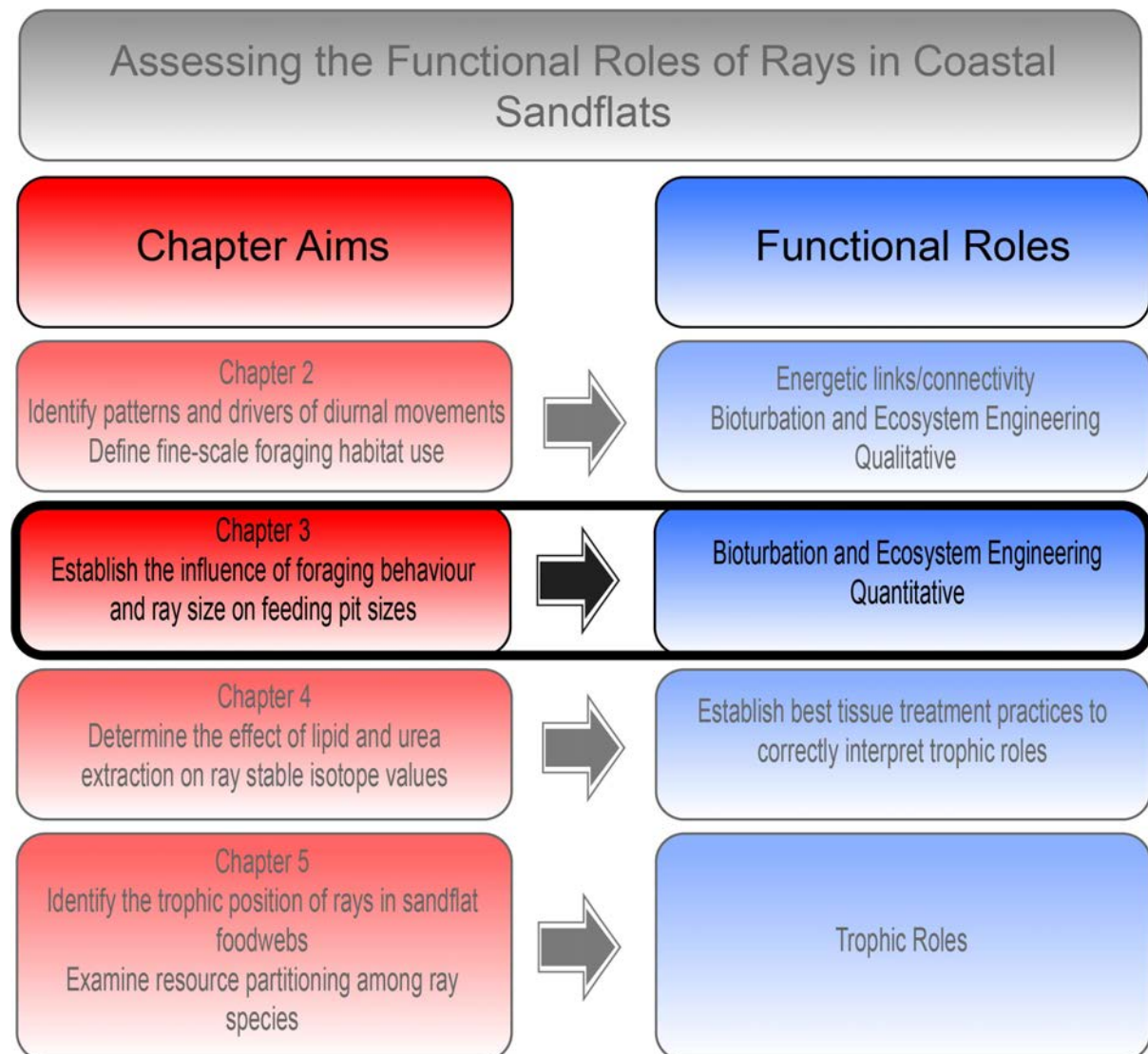
Despite overall habitat use being similar, drone tracking revealed that core foraging habitats of *P. ater* and *H. australis* were segregated on a fine scale. *Himantura australis* foraged twice as often as *P. ater* but concentrated foraging activity in a small area. Although *P. ater* foraged less often, core foraging habitat covered an area three times larger than core foraging habitat for *H. australis*. Foraging habitat partitioning has been suggested as a mechanism for co-existence among sympatric rays (O'Shea *et al.* 2013); however, this study is the first to define species-specific foraging habitats based on direct observations of feeding behaviour. *Pastinachus ater* and *H. australis* in Western Australia exhibit different dietary preferences, with *P. ater* consuming mostly polychaetes and *H. australis* consuming more brachyuran crabs and penaeid prawns (Vaudo & Heithaus 2011; O'Shea *et al.* 2013). Consequently, the observed segregation of foraging habitats may reflect the distributions of preferred prey which warrants future investigation. Additionally, differences in feeding rate and habitat use suggest that the magnitude and spatial impact of bioturbation and ecosystem engineering roles of rays may also differ between species.

Foraging behaviour and habitat use can be influenced by both diel and tidal cycles (Gibson 2003; Krumme, Saint-Paul & Rosenthal 2004; Brenner & Krumme 2007). Sampling limitations (i.e. launching the vessel at high tides for acoustic tracking, sun and wind conditions for drone tracking) prevented time of day and tidal phase being matched up for each tracking method, which may have contributed to the mismatch between high tide habitat use and feeding locations for *H. australis* (Fig. A7). The sampling times resulted in acoustic tracking being biased towards low tide periods and an incomplete estimate of high tide habitat use. Drone tracking was limited to late flood, high, and early ebb tide periods which contributed to an underestimate of total habitat use; however, this

timing filled in the high tide gaps from acoustic tracking. Thus, the sampling limitations and biases of each method complemented each other to provide a more complete picture of habitat use throughout the tidal cycle (Fig. 2.8).

This study highlights the importance of linking animal behaviour with habitat use to understand the drivers and implications of animal movement. By using a novel combination of acoustic tracking and drone tracking, I obtained detailed habitat use data over the entire tidal cycle and identified the spatial extent and intensity of foraging activity for two sympatric rays. Results suggest that daily intertidal migrations of rays are driven by access to profitable prey patches in the shallow intertidal, which also offers predation refuge. Consequently, intertidal sandflats may be high quality nursery areas for rays; however, further assessment of prey and predator assemblages are needed. Additionally, frequent foraging migrations between intertidal foraging habitats and subtidal resting areas suggest rays may form energetic links between the two. Future studies should evaluate the importance of this nutrient transport for subtidal productivity and investigate the implications of foraging rate and habitat selection on bioturbation roles. Overall, results highlight the value of combining high-resolution behavioural information with traditional tracking data to determine the drivers of animal movements and assess their implications for ecosystem function.

Chapter 3: All rays are not created equal: Species-specific foraging behaviours define the functional roles of sympatric stingrays.



This chapter has been submitted for publication in *Functional Ecology*. The submitted manuscript has been modified to fit with the style of the thesis and avoid unnecessary redundancies.

Crook, KA., Sheaves, M., Barnett, A. All rays are not created equal: Species-specific foraging behaviours define the functional roles of sympatric stingrays. *Functional Ecology*. Submitted.

Contributions: K Crook designed the study, performed all data collection and statistical analyses, and wrote the manuscript. A Barnett and M Sheaves aided with study design and provided editorial support.

Introduction

In sedimentary habitats, bioturbation is important for structuring sediments, oxygen penetration, and nutrient cycling (Lohrer, Thrush & Gibbs 2004; Mermilliod-Blondin & Rosenberg 2006; Harris *et al.* 2016). Bioturbation occurs in both terrestrial and aquatic environments through the activity of living organisms, particularly burrowing activities of invertebrates and mammals (Suchanek & Colin 1986; Rao *et al.* 2014) and foraging activities of macrofauna such as bandicoots (Valentine *et al.* 2012), echidnas (Eldridge & Mensinga 2007), rays (Takeuchi & Tamaki 2014), walrus (Ray *et al.* 2006), turtles (Lazar *et al.* 2011), and whales (Oliver & Slattery 1985). Beyond their effect on sediment and biogeochemical processes, the depressions and burrows created by bioturbation can collect detritus and serve as habitat for other organisms meaning that bioturbators can also act as ecosystem engineers (Meysman, Middelburg & Heip 2006).

How species function in terms of bioturbation and ecosystem engineering is directly influenced by the number and size of feeding pits or burrows. Large excavations penetrate deeper, disturb more sediment, and accumulate more organic matter than smaller pits (Yager, Nowell & Jumars 1993; Eldridge & Mensinga 2007). On the other hand, small pits and burrows are often more abundant (Myrick & Flessa 1996; O'Shea *et al.* 2012), so that the combined impact of numerous small pits may equal or exceed that of fewer large pits (Takeuchi & Tamaki 2014; Haussmann 2017). The presence of excavations increases habitat heterogeneity and individual decisions governing where excavations are made further influence their contribution to ecosystem function. As a result, determining the spatial distribution, number, and size of excavations is critical for assessing individual- and species-specific functional roles.

Rays are common bioturbators of coastal sandflats and disturb sediments by jetting water through their mouths or gills in combination with pectoral fin flapping to excavate buried invertebrates (Smith & Merriner 1985; Dean, Bizzarro & Summers 2007; Wilga *et al.* 2012). This foraging behaviour disrupts sediments and often creates depressions or pits that can remain in the environment for several days (Valentine *et al.* 1994; Myrick & Flessa 1996; O'Shea *et al.* 2012). As sandflats are dynamic habitats; subject to constant erosion from the influence of waves and tides (Short 2006; Schlacher *et al.* 2015), nutrient subsidies do not settle and instead form wracks on the beach or are transported offshore (Yager, Nowell & Jumars 1993). Ray feeding pits can provide shelter from tide and wave action and may accumulate detritus; providing nutrient subsidies for other organisms (Vanblaricom 1982). Ray pits consistently contain elevated quantities of organic matter relative to the surrounding sandflat (D'Andrea, Aller & Lopez 2002) and this increase in

nutrients may provide foraging opportunities for other sandflat fauna (Vanblaricom 1982; O'Shea *et al.* 2012).

Feeding pit size is assumed to be proportional to ray size, and pit creation rates assumed to be equal among size classes (Valentine *et al.* 1994; Takeuchi & Tamaki 2014). Based on these assumptions, it seems logical that individual large rays play more important bioturbation and ecosystem engineering roles; however, there is limited empirical evidence supporting these assumptions. Additionally, there is little information on species-specific feeding rates and pit sizes. Myrick and Flessa (1996) found that pits created by round rays (*Urotrygon halleri*) were smaller and more abundant than pits made by larger bat rays (*Myliobatis californicus*) and suggest that *U. halleri* are either more abundant or feed more often than *M. californicus*. Thus, differences in body size and foraging behaviour among sympatric rays likely play a role in determining feeding pit sizes and, consequently, in determining species-specific functional roles. The objective of this study was to investigate the influence of foraging behaviour and ray size on the abundance, size, and distribution of feeding pits to establish the functional roles of sympatric stingrays on coastal sandflats.

Methods

The same long and short drone track videos from Chapter 2 were analysed in greater detail to record specific foraging behaviours. Foraging behaviour was identified based on previous observations of ray foraging behaviour, kinematics, and morphology (Ebert & Cowley 2003; Dean & Motta 2004; Sasko *et al.* 2006; Wilga *et al.* 2012) and four distinct feeding types were identified: 'Suction', 'Water jetting', 'Excavation', and 'Non-disruptive' feeding (Table 3.1). For each foraging event identified in Chapter 2, the feeding type, feeding time, and presence/absence of a feeding scar was recorded (Table 3.1). Feeding time was not recorded for non-disruptive feeding as rays were generally not stationary during this feeding type. If more than one feeding type was observed in a single event, behaviours were separated into 'Primary' and 'Secondary' behaviours (Table 3.1). Foraging events where the ray was observed feeding prior to the tracking interval or if foraging continued after tracking ceased were excluded from analyses as feeding time could not be determined. The GPS coordinates for each foraging event were recorded as the position of the focal ray at the onset of foraging.

Ray and pit measurements

For each drone track video, five screenshots were taken of the focal ray when the disc was flat against the substrate with the disc margins clearly visible. The video time of each screenshot was recorded and disc width (DW) was measured in pixels using Image J software (Fig. 3.1a). To convert

Table 3.1 Definitions of feeding types and feeding event parameters used in drone track analyses.

Term	Definition
Feeding Types	
Suction	Focal ray stationary and ejecting streams of sediment from both spiracles simultaneously. Often preceded by a flattening of the disc against the substrate.
Water Jetting	Focal ray stationary with sediment plumes emanating from the disc margins.
Excavation	Repeated and rhythmic raising and lowering of the rostrum and/or pectoral fins resulting in large sediment plumes emanating from the anterior and lateral disc margins.
Non-disruptive	Focal ray stationary or moving slowly forwards or backwards. Puffs of sediment emanating from the anterior disc margin with non-rhythmic raising and lowering of the rostrum. Does not result in formation of a feeding pit.
Feeding Event Parameters	
Primary Feeding	Feeding type that occurred for the longest duration during each feeding event.
Secondary Feeding	Feeding type that occurred in the feeding event for shorter duration than the primary feeding type. Recorded as “None” if only one foraging behaviour observed.
Feeding time	Duration from the visible onset of foraging behaviour until the focal ray moved away. Duration was measured for the entire event and not separated by primary and secondary behaviours.
Feeding scar	Recorded if ray foraging left a visible mark on the sediment OR if foraging behaviour was likely to have left a mark based on previous observations. Not recorded if the ray was observed foraging in an existing feeding pit (see below).
Feeding pit	Newly formed feeding scars with predicted areas $\geq 100 \text{ cm}^2$.

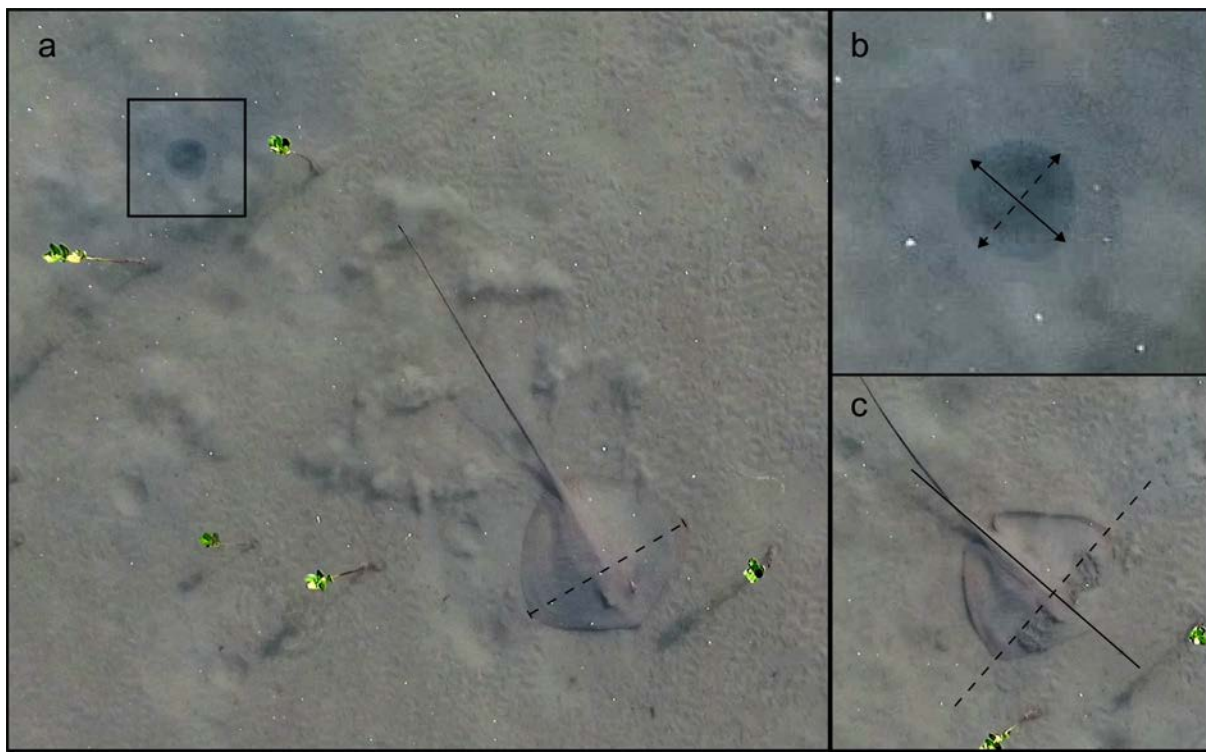


Figure 3.1 Drone video screenshots of a) an Australian whipray (*Himantura australis*) and recently formed feeding pit (black box), b) close-up of the feeding pit with length (solid arrow) and width (dashed arrow) identified, and c) foraging *H. australis* with the sagittal (solid line) and transverse (dashed line) planes identified. The dashed line in a) shows the disc width measurement of the focal ray. The colour and contrast of the feeding pit area has been adjusted for clarity.

measurements from pixels to cm, videos of 60 and 80 cm DW ray decoys were recorded from 3, 5, 7, 10, 12, and 15 m altitudes to define the relationship between drone height and image resolution. Decoy screenshots were taken from each height and size (pixels) was measured in the same manner as for ray DW. Image resolution (cm pixel^{-1}) at each drone height was calculated by dividing the known decoy size (cm) by the measured size (pixels). Using linear regression, I defined the relationship between image resolution and drone height and used this relationship to determine the image resolution for each focal ray screenshot (Fig. B1). DW measurements in pixels were multiplied by the image resolution to determine focal ray DW in cm for each screenshot. For each track, focal ray DW was recorded as the mean DW across all screenshots. To assess the accuracy of DW measurements, videos of 20, 40, 60, and 80 cm decoys were taken from 10 m altitude on three separate occasions and screenshots were measured following the same method. The mean \pm SD difference between measured and actual decoy size was calculated to estimate the measurement error.

Feeding scars were measured following the same procedure. Screenshots were taken when the feeding scar margins were clearly visible and not obstructed by stirred up sediment (Fig. 3.1b). The length and width were measured in pixels as the maximum diameter along the sagittal plane of the feeding ray and maximum diameter along the transverse plane of the feeding ray, respectively (Fig. 3.1b,c). To reduce the influence of measurement variability on scar size (pooled DW standard deviation ± 4.3 cm), scar dimensions were standardized relative to focal ray size. As much as possible, feeding scar and ray DW screenshots were taken in the same video frame (Fig. 3.1a). If focal ray DW could not be measured in the same frame, a DW screenshot was taken as soon as possible before or after the scar screenshot when the drone was flying at the same height. Scar dimensions in pixels were converted to a proportion of ray DW and then converted to cm by multiplying by the mean DW in cm. The area of each measured feeding scar was estimated based on the area of an ellipse:

$$Area = \pi * \frac{Length}{2} * \frac{Width}{2} \quad (1)$$

Predicting sizes of non-visible feeding scars

Feeding scar areas were modelled with linear mixed models in the ‘lme4’ R package (Bates *et al.* 2015) to determine factors influencing feeding scar size. The measured area of each scar was modelled with feeding time, primary and secondary feeding types, ray DW, and species as predictor variables with individual as a random effect. Area and feeding time were natural log transformed to normalize residuals and separate variance structures were adopted for secondary feeding type to account for heteroscedasticity. The best mixed model was selected by starting with a saturated model including all interactions and subsequently removing non-significant terms until all terms were significant at $\alpha = 0.05$ (Zuur *et al.* 2009). The sizes of non-visible scars were predicted from the best fit linear mixed model. Feeding scars with predicted areas < 100 cm² were excluded from volume analyses as these were not considered feeding pits (Table 3.1) and would likely be filled in during running tides.

Pit Volume

Bioturbation impact of individual rays was assessed by estimating feeding pit volumes based on the relationship between pit area and volume. To define this relationship, I physically measured the length, width, and depth of 50 recently formed feeding pits of various sizes on the Lucinda sandflat. Newly formed pits were identified and measured based on the presence and position of excavated sediment mounds around the pit margins (Hines *et al.* 1997; Takeuchi & Tamaki 2014).

The volume of each measured pit was calculated assuming a semi-ellipsoid shape (O'Shea *et al.* 2012):

$$\text{Pit Volume} = \frac{4}{3}\pi\left(\frac{\text{Length}}{2} * \frac{\text{Width}}{2} * \text{Depth}\right)/2 \quad (2)$$

Pit area was calculated using equation (1) and the area to volume relationship was modelled using a self-starting non-linear least squares regression in R (R Core Team 2018) assuming a logistic relationship (Takeuchi & Tamaki 2014). The logistic relationship was then used to estimate the volume of all feeding pits observed during drone tracks.

Data Analysis

Foraging data was summarised for all drone tracks to include the number of foraging events, the number of feeding pits created, and the total volume of all feeding pits in each track. Foraging and bioturbation rates were calculated by dividing the number of feeding events, pits, and total pit volume by the tracking time. Correlations among feeding rates, bioturbation rates, and DW were evaluated using Pearson correlation tests. Feeding and bioturbation rates were natural log transformed for correlation tests to normalize residuals. For each feeding event, pit sizes were categorized as P0 (no feeding scar or scar area $<100 \text{ cm}^2$), P1 ($100 \text{ cm}^2 \leq \text{area} < 250 \text{ cm}^2$), P2 ($250 \text{ cm}^2 \leq \text{area} < 500 \text{ cm}^2$), P3 ($500 \text{ cm}^2 \leq \text{area} < 1000 \text{ cm}^2$), and P4 ($\text{area} > 1000 \text{ cm}^2$). The total volume of all pits in each category was determined to assess the influence of pit size and feeding behaviour on bioturbation. The spatial extent and intensity of foraging activity was assessed using kernel density estimation (based on GPS coordinates of feeding events) in the 'stat_density2d' function from the 'ggplot2' R package (Wickham 2016) and visualized with the 'ggmap' R package (Kahle & Wickham 2013).

Results

Foraging behaviour was observed in 112 of 132 drone tracks (101 short; 11 long) and resulted in 1107 feeding events and 745 feeding pits. Based on estimated size-at-maturity, all tracked individuals were juveniles (Last *et al.* 2016). Tracked *H. australis* were larger than *P. ater* (mean \pm SD DW 53.9 ± 13.2 and 42.2 ± 11.6 cm, respectively) and tracks covered a wider size range (Fig. 3.2). Tracked *H. australis* were divided into 'Small' (<54 cm DW) and 'Large' (≥ 54 cm DW) size categories based on the mean DW but size classes were not separated for *P. ater* because only a few large individuals were tracked (Fig. 3.2). DW measurements were accurate to 1.1 ± 6.3 cm and the absolute value of the difference between measured and actual sizes was 5.6 ± 2.9 cm.

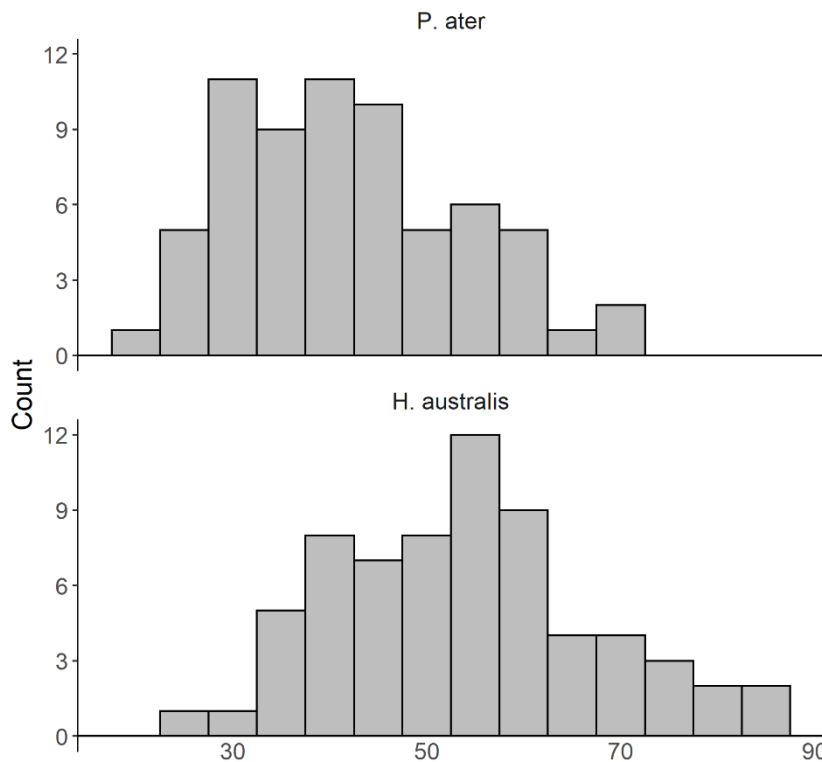


Figure 3.2 Size distribution of *Pastinachus ater* and *Himantura australis* tracked with drones at Lucinda separated into five cm bins.

The best-fit linear mixed model based on 394 measured feeding scars determined that feeding time, feeding type (primary and secondary), and ray size had a significant influence on feeding pit size (Table B2). Species had no influence on pit size and was excluded from the best model (Table B3). Longer feeding times resulted in larger feeding pits and the largest pits were made by excavation feeding (Fig. 3.3a). Disc width positively influenced pit size (Fig. 3.3b); however, both feeding time and feeding type had a stronger influence on pit size (Table B2). Plotting predicted versus actual pit sizes showed that the model overestimated small pit areas and underestimated large pit areas relative to a perfect 1:1 relationship (Fig. B4). Predicted pit sizes from all observed foraging events ranged from 100–3158 cm² (mean ± SD: 420 ± 434 cm²) and the size distribution was strongly skewed towards smaller pits for both species (Fig. B5). Feeding pits physically measured on the sandflat ranged in size from 7–70 cm in maximum diameter, 2–41 cm in depth, 38–3354 cm² in area, and 59–86092 cm³ in volume. The logistic relationship between pit area and volume (Fig. B6a) predicted volumes ranging from 3007–73511 cm³ (mean ± SD: 6191 ± 7801 cm³). Similar to pit areas, the logistic fit overestimated small pit volumes and underestimated large pit volumes (Fig. B6b).

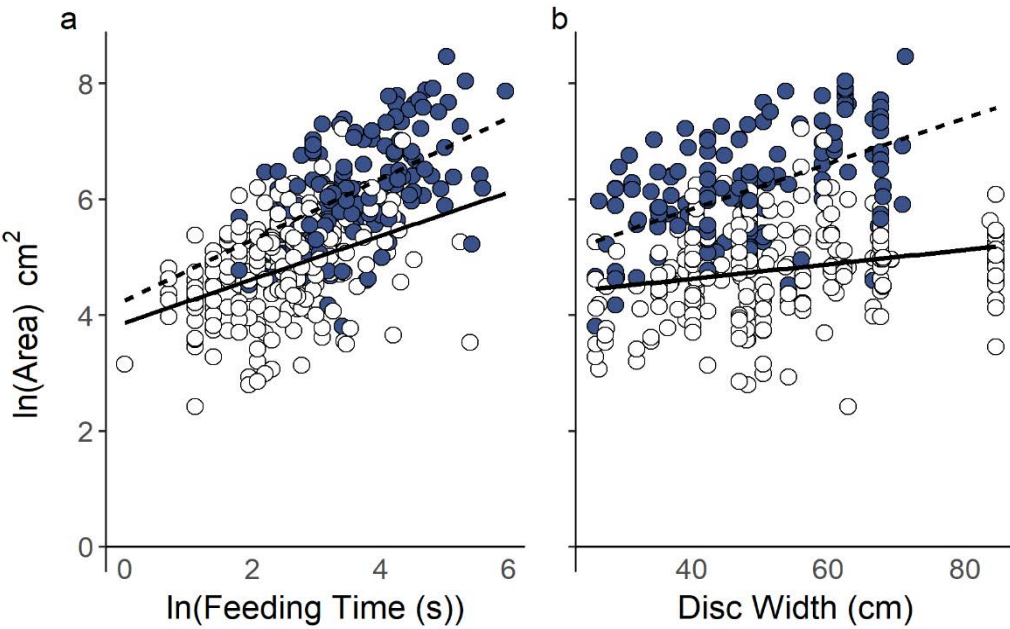


Figure 3.3 Relationship between the natural log of feeding pit area and a) natural log of feeding time and b) ray disc width. Points indicate feeding events with excavation feeding as the primary feeding type (blue) or without excavation feeding (white) that resulted in a measured feeding scar. Predicted linear relationships are shown for excavation events (dashed line) or non-excavation events (solid line). Points are shown for both *Himantura australis* and *Pastinachus ater*.

Among individual rays, *H. australis* were observed foraging twice as often as *P. ater* (mean \pm SD 35.1 ± 27.8 vs. 17.7 ± 15.4 events hr⁻¹) and made three times as many feeding pits (26.9 \pm 24.9 vs. 8.4 ± 8.5 pits hr⁻¹) (Fig. 3.4a,b). Neither feeding rate nor pit formation rate were significantly correlated with disc width for either species; however, bioturbation rates were positively correlated with both DW and pit formation rate (Table B7). Consequently, individual *H. australis* had higher bioturbation rates than individual *P. ater* (Fig. 3.4c).

Most feeding events included only a single feeding type (90 % for *P. ater*, 60 % for *H. australis*) (Fig. B8a), but primary foraging behaviours differed between species. *Pastinachus ater* used non-disruptive feeding most often followed by water jetting and excavation feeding but suction feeding was never observed (Fig. 3.5a,b). *Himantura australis* were rarely observed using non-disruptive feeding and used water jetting most often followed by excavation and suction feeding (Fig. 3.5a,b). Foraging behaviour also differed among size classes for *H. australis*. Suction feeding, water jetting, and excavation feeding occurred equally among large individuals; however, small *H. australis* used water jetting most often and were rarely observed suction feeding (Fig. 3.6a,b). Secondary feeding was more common among large *H. australis* with suction feeding being the dominant secondary feeding type (Fig. B8b).

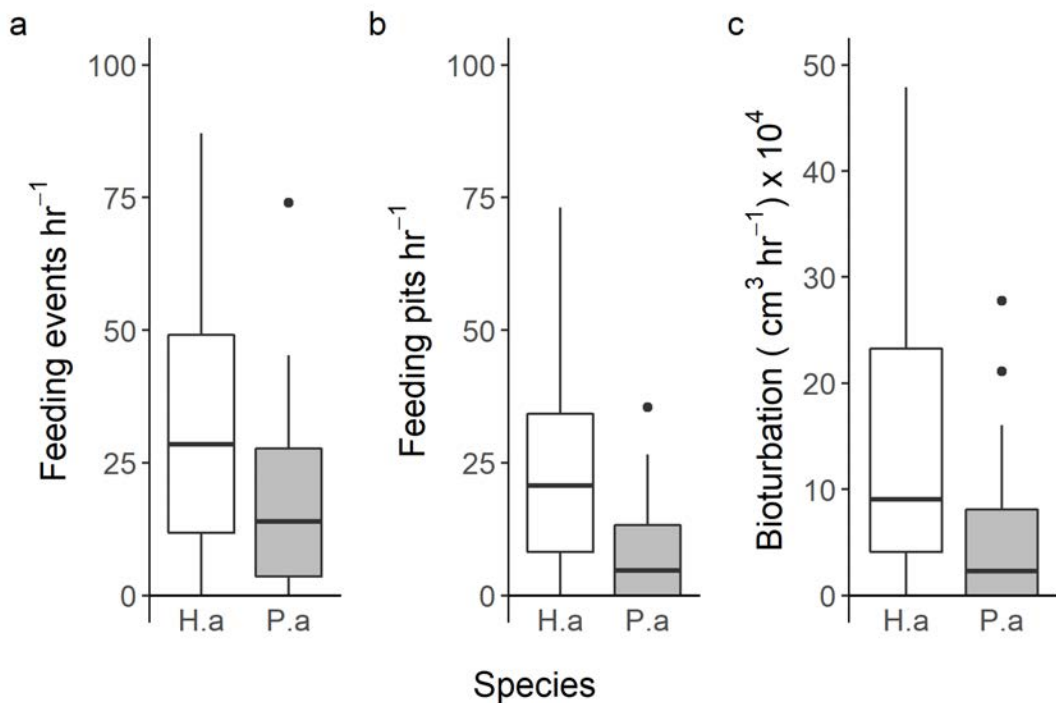


Figure 3.4 Feeding (a), pit formation (b), and bioturbation (c) rates of *Himantura australis* (H.a) and *Pastinachus ater* (P.a) from all drone tracks at Lucinda. Boxes represent the first and third quartiles with whiskers extending to data points within 1.5 time the inter-quartile range. Horizontal black lines represent the median and individual points represent outliers.

Total sediment turnover from all feeding pits across all individuals was four times higher for *H. australis* ($3.71 \times 10^6 \text{ cm}^3$) than for *P. ater* ($9.01 \times 10^5 \text{ cm}^3$). Although excavation feeding was used less often than other feeding types (22 and 31 % of feeding events for *P. ater* and *H. australis*, respectively), it accounted for 58 % and 67 % of the total sediment turnover (Fig. 3.5b,c). For both species, excavation feeding accounted for all of the largest feeding pits (P4) whereas most smaller pits (P1 and P2) were made by less disruptive feeding behaviours (water jetting for *P. ater*; suction and water jetting for *H. australis*) (Fig. 3.5d). All pit sizes contributed similarly to total sediment turnover for *P. ater* (Fig. 3.5e). For *H. australis*, P4 pits accounted for the most excavated sediment despite fewer P4 pits being made (P4: n=52; P1: n=289) (Fig. 3.5d,e). Small and large *H. australis* made similar numbers of P1 and P3 pits, but more P2 were made by small rays (Fig. 3.6d). Large *H. australis* made all but three P4 pits, which accounted for the most sediment turnover (Fig. 3.6d,e).

The spatial extent of foraging and bioturbation impact on the sandflat also differed between species. *Himantura australis* foraging activity was densely concentrated in a small area, whereas *P. ater* foraged less intensely but pits covered a broader sandflat area (Fig. 3.7a). There was minimal overlap of the two species core foraging areas (Fig. 3.7a) (Fig. 2.7b). The spatial extent and density of foraging activity was similar between size classes of *H. australis* (Fig. 3.7b).

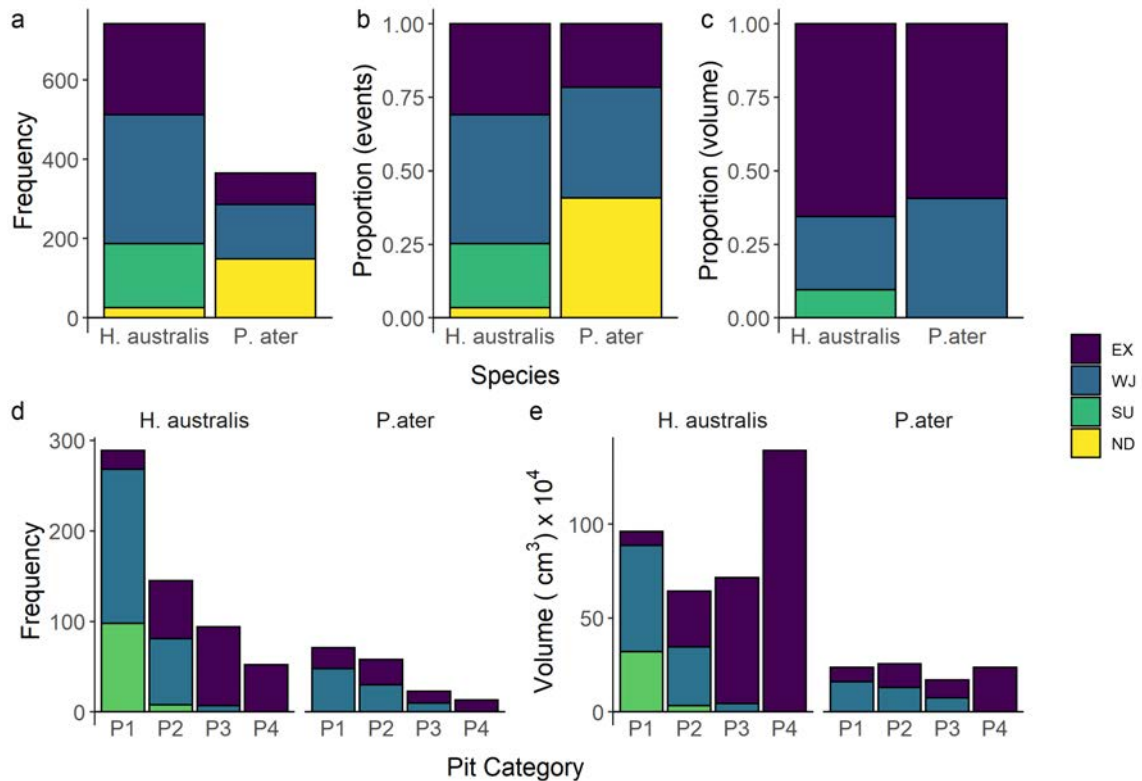


Figure 3.5 a) Frequency and b) proportion of feeding events with excavation (EX), water jetting (WJ), suction (SU), and non-disruptive (ND) feeding as the primary feeding type for *Himantura australis* and *Pastinachus ater*. c) The proportion of total sediment volume turned over by each feeding type. d) The frequency of feeding pits in each size category and feeding type. e) The total volume of all feeding pits in each size category by feeding type. Pit size categories: P1 ($100 \text{ cm}^2 \leq \text{area} < 250 \text{ cm}^2$), P2 ($250 \text{ cm}^2 \leq \text{area} < 500 \text{ cm}^2$), P3 ($500 \text{ cm}^2 \leq \text{area} < 1000 \text{ cm}^2$), and P4 ($\text{area} > 1000 \text{ cm}^2$).

Discussion

Foraging patterns of sympatric stingray species on the Lucinda sandflat present a complex picture of their functional roles. Frequent foraging by both *Himantura australis* and *Pastinachus ater* support their roles as bioturbators and ecosystem engineers but differences in foraging rates and behaviour suggest the spatial extent and magnitude of those roles differ between species.

Pastinachus ater individuals favoured non-disruptive feeding, which did not create feeding pits, whereas *H. australis* individuals were rarely observed non-disruptive feeding and made three times as many feeding pits. Despite higher feeding rates, *H. australis* concentrated foraging activity in a small area whereas *P. ater* foraged less often but over a broader area. Overall, results suggest that *H. australis* may have an intense localised impact in terms of bioturbation and ecosystem engineering roles, but *P. ater* may aid with nutrient dispersal over a broader area. This suggests that the functional roles of *H. australis* and *P. ater* are different, yet complementary, which may enhance

ecosystem productivity. Therefore, functional roles cannot be determined from presumed feeding roles but need to be defined based on species-specific foraging behaviour and habitat use.

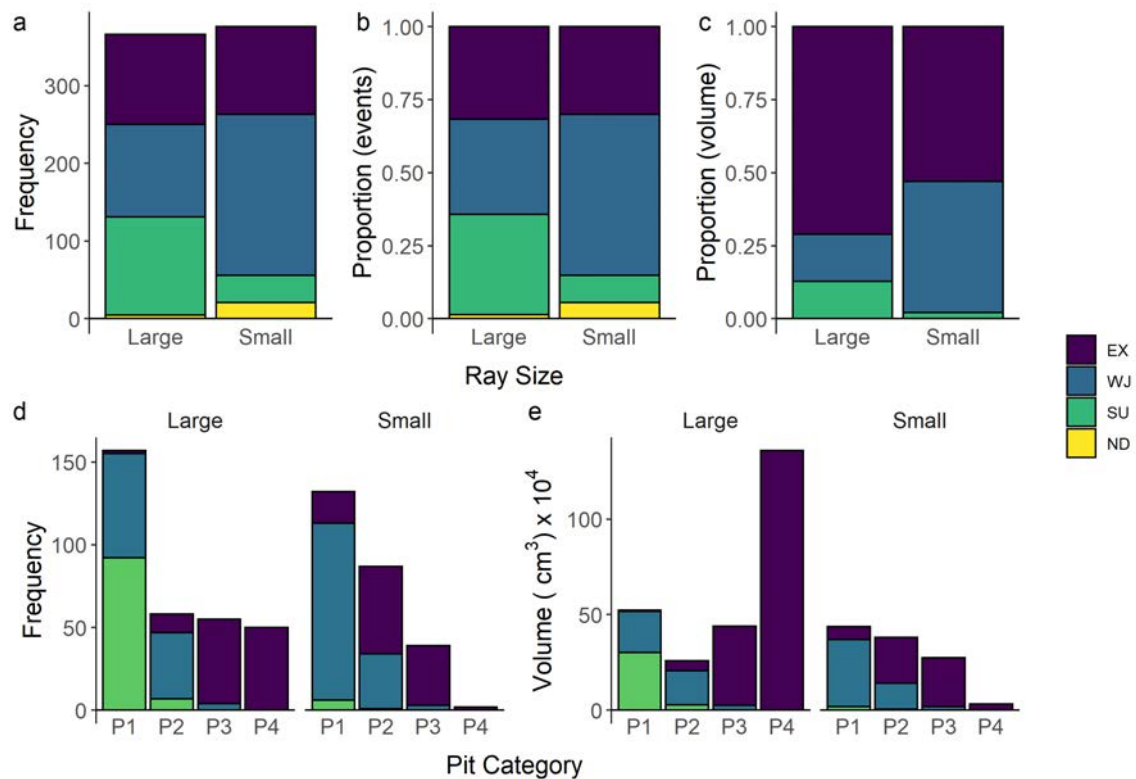


Figure 3.6 a) Frequency and b) proportion of feeding events with excavation (EX), water jetting (WJ), suction (SU), and non-disruptive (ND) feeding as the primary feeding type for large (>54 cm DW) and small (<54 cm DW) *Himantura australis*. c) The proportion of total sediment volume turned over by each feeding type. d) The frequency of feeding pits in each size category by feeding type. e) The total volume of all feeding pits in each size category by feeding type. Pit size categories: P1 ($100 \text{ cm}^2 \leq \text{area} < 250 \text{ cm}^2$), P2 ($250 \text{ cm}^2 \leq \text{area} < 500 \text{ cm}^2$), P3 ($500 \text{ cm}^2 \leq \text{area} < 1000 \text{ cm}^2$), and P4 ($\text{area} > 1000 \text{ cm}^2$).

For species that physically modify their habitats, where and how often those modifications occur directly influences their functional roles (Pillay *et al.* 2011; Alvarez *et al.* 2015). For example, steephead parrotfish (*Chlorurus microrhinos*) perform important algal removal and bioerosion roles in coral reef systems but their functional impacts are only realized in small foraging areas (Welsh & Bellwood 2012). At Lucinda, *H. australis* foraged intensely but foraging activity was restricted to a small core area. In contrast, *P. ater* foraged less often but spread foraging activity over a broader sandflat area that had minimal overlap with *H. australis* foraging areas. Differences in space use among species that perform similar roles can enhance ecosystem function through behavioural complementarity (Moran-Lopez *et al.* 2020). Under a complementarity framework, *H. australis* and

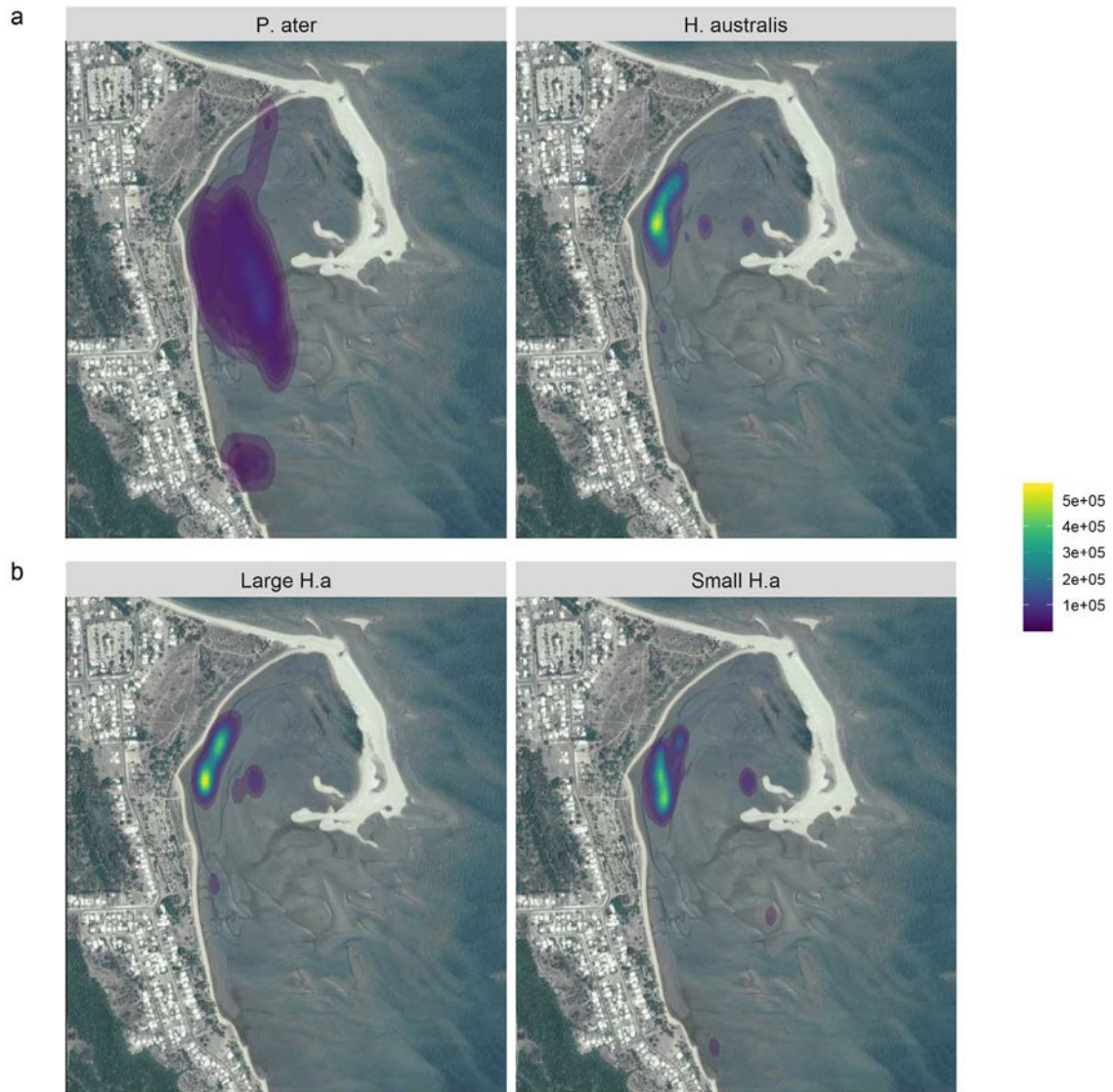


Figure 3.7 Extent and density of foraging activity of a) *Himantura australis* and *Pastinachus ater* and b) large (> 54 cm DW) and small (< 54 cm DW) *H. australis* (H.a) drone tracked at Lucinda.

P. ater foraging habitat partitioning spreads bioturbation and ecosystem engineering services across a broader sandflat area than either species acting alone.

Species are often classified into functional groups based on feeding apparatus and dentition as these can be strong predictors of ecosystem function (Bellwood & Choat 1990; Dehling *et al.* 2016; Lellys *et al.* 2019). A similar relationship between feeding apparatus and diets has been suggested for rays; however, direct links between morphology, diets, and behaviour are rare (Dean, Bizzarro & Summers 2007). Differences in habitat use and behaviour within functional groups can lead to discordance between morphology and diet, which has critical ramifications for interpreting functional roles (Bellwood *et al.* 2006; Murray, Douglas & Solan 2014). In the present study, *H. australis* and *P. ater* were both observed excavation feeding, which resulted in the largest feeding

pits; yet individuals of both species used multiple feeding types, often favouring less disruptive feeding behaviours and, consequently, smaller feeding pits. Indeed, despite their excavation capability, *P. ater* used non-disruptive feeding most often, a behaviour that was rarely observed for *H. australis*. Non-disruptive feeding did not create feeding pits, and the frequent use of this feeding type contributed to lower pit formation and bioturbation rates among individual *P. ater*. In contrast, *H. australis* favoured suction (large individuals) and water jetting (small individuals), both of which formed feeding pits and contributed to bioturbation. These behavioural differences combined with habitat partitioning highlight the important distinction between the fundamental and realized foraging niches of sympatric species for determining functional roles.

Although the present study focused on *H. australis* and *P. ater*, opportunistic drone tracks of four other ray species were completed at Lucinda (K. Crook unpublished data). Further observation is needed to establish foraging rates for the other species; however, preliminary observations suggest that eagle rays (*Aetobatus ocellatus*) have similar foraging rates to *H. australis*, whereas giant guitarfish (*Glaucostegus typus*) were not observed making any feeding pits. The reduced pectoral fin mobility of *G. typus* may prevent excavation feeding and, consequently, this species may rely on non-disruptive or alternative feeding behaviours and may have minimal contribution to bioturbation and ecosystem engineering functions. On the other hand, pink whiprays (*Pateobatis fai*) and mangrove whiprays (*Urogymnus granulatus*) were observed using the same feeding behaviours (suction, water jetting, and excavation) as *H. australis*, and, consequently, may have similar functional roles. Thus, differences in feeding rates and behaviour are likely common among co-existing rays and further differences in feeding behaviour, movement patterns, and habitat selection likely exist that will have important implications for determining functional roles.

Body size governs species performance and can play a central role in establishing functional roles (Barneche *et al.* 2014; Sanders, Vogel & Knop 2015). For example, large parrotfish (Labridae) make larger feeding scars and excavate more substratum than small individuals, due to stronger jaws and larger gape size (Bonaldo & Bellwood 2008; Lellys *et al.* 2019). Small individuals do not excavate any substratum and, as a result, do not perform the bioerosion roles of larger individuals (Bonaldo & Bellwood 2008). My results show that, all else being equal, larger rays make larger feeding pits and, therefore, bioturbation rates are positively correlated with disc width. Results do not, however, support the generalisation that ray size can be assumed based on pit size (Valentine *et al.* 1994; Takeuchi & Tamaki 2014). Although the largest feeding pits were made by large individuals, the distribution of pit sizes for both large and small rays were strongly skewed towards smaller pits. Among burrowing organisms, burrow volume is positively correlated with body size but burrow size and overall excavation rates can vary based on site conditions, individual behaviour, and abundance

(Schlacher *et al.* 2016; Haussmann 2017; Clark *et al.* 2019). Foraging excavation sizes may similarly be dependent on foraging effort and behaviour (Abenspergtraun, Dickman & Deboer 1991; Lopez-Fernandez *et al.* 2014; Gihwala, Pillay & Varughese 2017). Consistently, feeding pit sizes at Lucinda were more strongly influenced by foraging time and foraging behaviour than ray size. Therefore, it is critical to establish the factors governing individual foraging decisions that influence feeding pit sizes to better predict functional roles across a range of ecological contexts.

Foraging theory predicts that prey density and quality directly influence the foraging success and behaviour of predators (Charnov 1976; Friedlaender *et al.* 2020). The size of foraging excavations made by echidnas (*Tachyglossus aculeatus*) are positively related to prey density and also vary depending on the type of prey consumed (Abenspergtraun, Dickman & Deboer 1991). The type, density, size, and burrowing depth of invertebrate prey consumed by rays may similarly influence feeding pit sizes. For example, ghost shrimp (Callianassidae) can burrow to depths greater than 1m (Shimoda & Tamaki 2004) whereas polychaetes and soldier crabs (Mictyridae) often only burrow to depths of a few cm (Maitland & Maitland 1992; Velasquez & Navarro 1993). Thus, rays foraging for ghost shrimp and rays foraging for polychaetes or soldier crabs likely make pits of different depths due to the excavation requirements for accessing preferred prey. The high pit formation rates of *H. australis* suggest foraging for prey embedded deeper in the sediment whereas *P. ater* may rely on shallower prey that can be accessed through non-disruptive feeding. Although I cannot comment on ray diets or prey composition at Lucinda, in Western Australia, *P. ater* forages primarily on polychaetes whereas diets of *H. australis* are dominated by crabs and prawns (Vaudo & Heithaus 2011; O'Shea *et al.* 2013). The foraging habitat partitioning (Chapter 2) and differences in foraging behaviour between *H. australis* and *P. ater* is consistent with dietary partitioning; however, further work is needed to link foraging behaviour with prey type to understand patterns of prey selection and bioturbation that may serve as indicators of biological activity on sandflats.

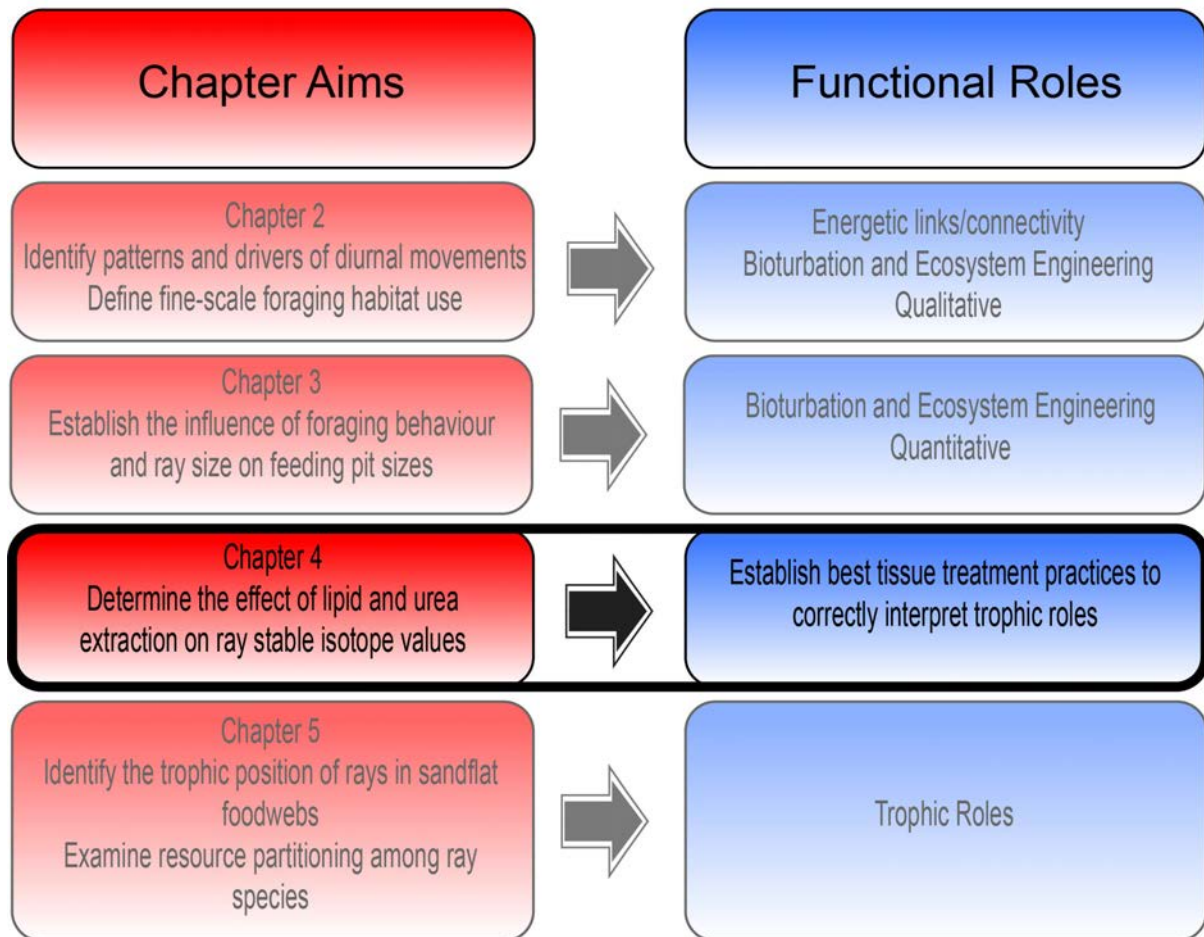
The estimates of stingray bioturbation rates in this study are based on several assumptions and predictive equations and, thus, there is a level of uncertainty surrounding them. While my assumptions surrounding pit size and the relationship between pit area and volume are consistent with other studies (O'Shea *et al.* 2012; Takeuchi & Tamaki 2014), I caution against direct comparisons of bioturbation rates with other studies. Similarly, the high variability in feeding rates among individual rays makes it difficult to use mean feeding rates to extrapolate bioturbation rates across tidal cycles, days, or years. Despite these limitations, all assumptions were consistent for both species so comparisons between species and conclusions regarding the influence of behaviour on pit size are valid. Additionally, the high feeding rates suggest that rays play a significant bioturbation role on the sandflat irrespective of the error surrounding bioturbation estimates. Combined with the

observed differences in foraging behaviour and habitat partitioning, results suggest functional roles of rays are complementary and provide novel insight into the complexity of establishing the functional roles of sympatric species.

Overall, results from this study suggest that differences in foraging habitat selection and behaviour have critical implications for the functional roles of sympatric stingrays. High bioturbation rates indicate that *H. australis* has a localized bioturbation and ecosystem engineering role on the sandflat, whereas *P. ater* may have a broader nutrient deposition footprint. Thus, the functional roles of sympatric species are dependent on complex interactions between feeding behaviour, intensity, and habitat use and, consequently, caution should be taken when assuming similar functional roles between closely related species.

Chapter 4: Effects of lipid and urea extraction on stable isotope values ($\delta^{13}\text{C}$ and $\delta^{15}\text{N}$) of two batoids: a call for more species-specific investigations

Assessing the Functional Roles of Rays in Coastal Sandflats



This chapter has been published in *Limnology and Oceanography: Methods*. The published manuscript has been modified to fit with the style of the thesis and avoid unnecessary redundancies.

Crook, K.A., Barnett, A., Sheaves, M. & Abrantes, K. (2019) Effects of lipid and urea extraction on stable isotope values ($\delta^{13}\text{C}$ and $\delta^{15}\text{N}$) of two batoids: A call for more species-specific investigations. *Limnology and Oceanography-Methods*, **17, 565–574.**

Contributions: K Crook designed the study, performed all data collection and statistical analyses, and wrote the manuscript. A Barnett and K Abrantes aided with study design and provided editorial support. M Sheaves provided editorial support.

Introduction

Studying animal diets is critical to understanding their ecology. Analysis of stable isotope ratios in animal tissues, in particular $\delta^{13}\text{C}$ and $\delta^{15}\text{N}$, has become commonplace in dietary studies for its power to trace trophic pathways through foodwebs and elucidate patterns in resource use (DeNiro & Epstein 1981; Peterson & Fry 1987; Post 2002). Ecologists typically use $\delta^{13}\text{C}$ in animal tissues to determine the source of primary production in consumer diets (DeNiro & Epstein 1978; Tieszen *et al.* 1983; Hobson, Alisauskas & Clark 1993; Peterson 1999) and $\delta^{15}\text{N}$ to assess the trophic level of consumers within a food web (DeNiro & Epstein 1981; Post 2002; Vanderklift & Ponsard 2003). The use of stable isotopes to trace consumer resource use is advantageous over traditional methods such as gut content analysis as stable isotope sampling can be less invasive (e.g. small tissue sample collected for stable isotopes versus lethal sampling (O'Shea *et al.* 2013) or gut flushing (Barnett *et al.* 2010b; Elston, von Brandis & Cowley 2015) to collect stomach contents) and can shed light on resources used over longer time periods (Tieszen *et al.* 1983; Hussey *et al.* 2012a), as opposed to just the most recently consumed prey items.

Although useful to study animal diets, the use of stable isotopes comes with several assumptions which need to be considered to draw appropriate conclusions (Peterson & Fry 1987; Hussey *et al.* 2012a; Vander Zanden *et al.* 2015). For example, lipid content in animal tissues can vary among individuals, species, and tissues depending on body condition and physiology (Lorrain *et al.* 2002; Post *et al.* 2007; Hussey *et al.* 2012b). Since lipids are depleted in ^{13}C in relation to proteins, lipid content can significantly affect the $\delta^{13}\text{C}$ values of consumer tissues (Bodin, Le Loc'h & Hily 2007; Post *et al.* 2007). To remove biases associated with lipid content, it is suggested that either lipids are removed from the samples prior to $\delta^{13}\text{C}$ analysis (Sotiropoulos, Tonn & Wassenaar 2004; Bodin, Le Loc'h & Hily 2007; Hussey *et al.* 2012b), or that mathematical equations that normalize the samples to a similarly low lipid content are used (Post *et al.* 2007; Logan *et al.* 2008; Elliott, Davis & Elliott 2014).

Because lipids are depleted in ^{13}C in relation to proteins, lipid extraction techniques applied to lipid-rich samples generally lead to increases in $\delta^{13}\text{C}$ (Post *et al.* 2007; Abrantes *et al.* 2012). At the same time, because lipids have relatively more carbon atoms than proteins, lipid removal leads to a decrease in the ratio of carbon to nitrogen (C:N ratio), to values close to pure protein (~3) (Kiljunen *et al.* 2006; Post *et al.* 2007). Therefore, C:N ratios (which are generally measured along with $\delta^{13}\text{C}$ and $\delta^{15}\text{N}$) can be used as indicators of lipid content and it is generally accepted that, in dietary studies, lipids should be removed if C:N ratios are >3.5 to prevent bias in $\delta^{13}\text{C}$ associated with variation in lipid content (Post *et al.* 2007).

Although lipid extraction methods are used to correct biases in $\delta^{13}\text{C}$ due to differences in lipid content, $\delta^{15}\text{N}$ may also be affected by lipid extraction (Murry *et al.* 2006; Bodin, Le Loc'h & Hily 2007; Yurkowski *et al.* 2015). The influence of lipid extraction on $\delta^{15}\text{N}$ appears to vary depending on the extraction method (Doucette, Wissel & Somers 2010). Polar solvents (e.g. chloroform-methanol) remove lipids from a sample but also remove non-lipid components (Dobush, Ankney & Krementz 1985), resulting in increases in $\delta^{15}\text{N}$ values following lipid extraction (Sweeting, Polunin & Jennings 2006; Newsome, Clementz & Koch 2010; Hussey *et al.* 2012b). Non-polar solvents (e.g. petroleum ether) remove only structural lipids and fewer non-lipid compounds (Dobush, Ankney & Krementz 1985) and generally have a minimal effect on $\delta^{15}\text{N}$ values (Doucette, Wissel & Somers 2010; Kaufman *et al.* 2014). Kim and Koch (2012), however, found that petroleum ether may also increase $\delta^{15}\text{N}$ values, highlighting the need to understand how chemical treatments affect both $\delta^{13}\text{C}$ and $\delta^{15}\text{N}$ values for the specific tissue and taxa of interest.

The unique physiology of elasmobranchs leads to additional challenges in interpreting stable isotope values due to the retention of urea in body tissues for osmoregulatory purposes (Hazon *et al.* 2003; Hammerschlag 2006). Urea is enriched in ^{14}N relative to pure protein due to lighter isotopes reacting faster and being preferentially selected during amination processes (Gannes, del Rio & Koch 1998). Thus, high urea concentrations in elasmobranch tissues lower $\delta^{15}\text{N}$ values, and this can result in an underestimation of trophic positions (Kim & Koch 2012; Carlisle *et al.* 2017). Experimental studies examining the influence of urea on elasmobranch $\delta^{15}\text{N}$ have illustrated that urea-extracted tissues generally have higher $\delta^{15}\text{N}$ and C:N ratios relative to untreated tissues although results are not consistent across all species (Kim & Koch 2012; Li *et al.* 2016; Burgess & Bennett 2017; Carlisle *et al.* 2017). The increase in C:N ratio following urea-extraction has important implications for assessing tissue lipid content based on the C:N ratios. Carlisle *et al.* (2017) suggest that the influence of urea on the C:N ratio can mask lipid content and lead to conclusions that lipids do not need to be removed due to C:N ratios <3.5 when, in fact, C:N ratios following urea extraction may be >3.5 and, thus, lipids should be extracted.

There is considerable variability in the effects of lipid and urea extraction on elasmobranch stable isotope values among species. In studies evaluating the effect of lipid extraction on multiple elasmobranch species, $\delta^{13}\text{C}$ values increased in eight of 21 (Hussey *et al.* 2012b), seven of seven (Li *et al.* 2016), and three of ten species (Carlisle *et al.* 2017). Carlisle *et al.* (2017) also observed a decrease in $\delta^{13}\text{C}$ in three species tested; all three were rays. Effects of urea extraction show more consistent results among species with increases in $\delta^{15}\text{N}$ in seven of seven in Li *et al.* (2016) and seven of ten species in Carlisle *et al.* (2017). While Hussey *et al.* (2012b) did not explicitly test the influence

of urea extraction, $\delta^{15}\text{N}$ increased for 13 of 21 species following lipid extraction and they suggest that the chloroform-methanol solution used extracts soluble urea in addition to lipids.

The variability in the effect of lipid and urea extraction on $\delta^{13}\text{C}$ / $\delta^{15}\text{N}$ among species suggests variability in lipid/urea content in elasmobranch tissues, which may also bias interpretations of trophic niche size. Isotopic niche sizes and overlaps are often used to assess resource partitioning and competition among co-existing species (Eloranta, Knudsen & Amundsen 2013; Karlson, Gorokhova & Elmgren 2015) or to assess functional roles of species in different communities (Sanders, Vogel & Knop 2015). Considering the influence of lipid and urea extraction on $\delta^{13}\text{C}$ and $\delta^{15}\text{N}$ values of elasmobranch tissues, it is reasonable to expect that these extraction methods will also affect estimates of isotope niche sizes and overlaps.

Given the broad application of stable isotope analysis to the study of elasmobranch ecology, there is a critical need to further understand the inherent biases that may result from decisions to extract or not extract lipids and urea from tissues prior to analysis. To date, only a handful of studies have investigated lipid/urea extraction on stable isotope values and the coverage of these empirical studies represents <5 % of the ~1150 described elasmobranch species. Among existing studies, the range of species examined is largely biased towards sharks (Hussey *et al.* 2012b; Churchill, Heithaus & Grubbs 2015; Li *et al.* 2016; Shipley *et al.* 2017) and existing studies on rays have mostly focused on deep-water skates (Carlisle *et al.* 2017). Additionally, there is considerable ambiguity among results from existing studies, and yet those are frequently cited as reason to extract or not extract lipid/urea for previously untested species, with no guarantees that methods are appropriate for the species in question. Thus, there is imminent need for investigation into the effects of lipid and urea extraction methods on stable isotope values for a wider range of elasmobranch species, to produce a generalized understanding and ensure the correct decisions are made on a species by species basis. I investigated the influence of lipid and urea extraction on the stable isotope values of muscle and blood plasma tissues of two sympatric rays: the cowtail stingray (*Pastinachus ater*) and the Australian whipray (*Himantura australis*). Specifically, my aim was to determine how extraction methods influence $\delta^{13}\text{C}$, $\delta^{15}\text{N}$, and C:N ratios in muscle and plasma tissues of these previously untested species, assess if the effect of treatment methods is similar for the two species, and evaluate how lipid and urea extraction influence estimates of isotopic niche size and overlap of these two sympatric batoids.

Methods

Rays were captured at Lucinda using seine nets following the methods from Chapter 2. Muscle samples from each ray were collected using a 5mm diameter biopsy punch inserted into the

middle of the pectoral fin. Blood samples were collected using syringes fitted with 21-gauge needles and heparinized with sodium heparin. Needles were inserted into the caudal vein near the base of the tail and ~1 mL of blood was drawn. Blood samples, along with sodium heparin were transferred to 2 mL microcentrifuge tubes to prevent blood from clotting. Sodium heparin was chosen due to its minimal influence on blood plasma stable isotope values (Lemons *et al.* 2012). Muscle and blood samples were stored on ice until return to the laboratory where blood samples were immediately centrifuged at 7200 rpm for three minutes to separate the red blood cells from the plasma. Once separated, the plasma portion was pipetted into 2 mL plastic microcentrifuge tubes and frozen, along with the muscle samples at -20°C.

Sample Processing

Muscle and blood samples from 10 individuals from each species were selected for stable isotope analysis. Muscle samples were dried in a 60°C drying oven for 24–48 hours and then homogenized using a blunt-ended probe. Plasma samples were thawed, pipetted onto glass microscope slides, and dried in a 60°C drying oven for 2–4 hours. Once dry, the plasma was scraped off the microscope slide into glass scintillation vials and dried for a further 24–48 hours. Homogenized muscle and plasma samples were separated into four equal subsamples for analysis in one of four treatments: bulk analysis (BK), lipid extraction (LE), urea extraction (UE), and lipid and urea extraction (ULE). Some samples were not large enough to be split into four and, in those cases, the individual with insufficient tissue was excluded and a new individual was selected for analysis of the specific tissue (muscle or plasma). If no individual was available for sampling, the ULE treatment was excluded ($n=1$). Details of which individuals were sampled for each treatment can be seen in Appendix C (Tables C1 and C2).

Lipid and urea extraction were performed manually following the procedure outlined in Kim and Koch (2012). Briefly, lipid extraction samples were submerged in 10 mL of petroleum ether and agitated for 15 minutes. Samples were then decanted, and the process was repeated. After a second round of lipid extraction, samples were dried in a 60°C oven for 24–48 hours. Petroleum ether was chosen for lipid extraction as it is a non-polar solvent which extracts fewer non-lipid components from the tissue (Dobush, Ankney & Krementz 1985). The commonly used chloroform-methanol solution has been shown to remove urea from elasmobranch tissues in addition to lipids (Hussey *et al.* 2012b; Churchill, Heithaus & Grubbs 2015); therefore, I selected the non-polar petroleum ether to tease apart the influence of lipid and urea extraction on isotope values. For urea extraction, samples were submerged in 10 mL of de-ionized water (DIW) and agitated for 15 minutes. After 15 minutes, the samples were decanted, and the process was repeated two more times. After the third

round of urea extraction, samples were dried in a 60°C oven for 24–48 hours. Samples undergoing both lipid and urea extraction were treated first with the lipid extraction method followed by urea extraction. Once dry, samples were weighed to 1.0 ± 0.2 mg using a microbalance and encapsulated in tin capsules. Encapsulated samples were sent to the UC Davis Stable Isotope Facility (University of California), where they were analyzed using a stable isotope ratio mass spectrometer to determine $\delta^{13}\text{C}$, $\delta^{15}\text{N}$, %C and %N. Results had a precision of ± 0.05 to 0.14 ‰ for $\delta^{13}\text{C}$ and ± 0.04 to 0.11 ‰ for $\delta^{15}\text{N}$ (SD), calculated from replicate samples of laboratory standards calibrated against NIST standard reference material. Duplicate samples of ray tissues were not performed due to having an insufficient amount of tissue. Delta notation of isotope values is expressed relative to international standards (Vienna PeeDee Belemnite for carbon and air for nitrogen).

Data Analysis

Pairwise comparisons were performed between all treatments to assess how lipid and urea extraction methods influence $\delta^{13}\text{C}$, $\delta^{15}\text{N}$ and C:N ratios. Paired Wilcoxon Signed-Rank tests were used to compare $\delta^{13}\text{C}$ and $\delta^{15}\text{N}$ among treatments as the variances differed among treatments, assessed using Mauchly's test of sphericity due to the repeated-measures design. C:N ratios were compared using paired t-tests as these met the assumptions of normality and sphericity. P-values for multiple comparisons were assessed based on $\alpha=0.05$ and corrected for multiple comparisons using a sequential Bonferroni adjustment. To analyze the effects of sample treatment on isotopic niche sizes, standard ellipse areas (SEA) were calculated using Stable Isotope Bayesian Ellipses in R (SIBER) (Jackson *et al.* 2011). Comparisons of the 95 % credible intervals were used to determine if niche sizes differed among treatments. Ellipse parameters eccentricity (E) and θ were qualitatively assessed for each treatment. The eccentricity value of an ellipse ranges from zero (a perfect circle) to one (an elongated ellipse along one axis) and θ is the angle between the semi-major ellipse axis and the x-axis (0–180°) (Jackson *et al.* 2011; Reid *et al.* 2016). Theta values close to zero indicate variability along the x-axis and theta → 90 degrees indicates variability along the y-axis (Reid *et al.* 2016). The amount of overlap between individual ellipses in bivariate niche space was calculated as the 95 % probability of the estimated niche space from one treatment occurring within the trophic niche space of another treatment (Swanson *et al.* 2015). Niche overlap was calculated using the ‘nicheRover’ package in R (Swanson *et al.* 2015; R Core Team 2018). All statistical analyses were performed in R (R Core Team 2018).

Results

Overall, the effect of lipid and urea extraction on $\delta^{13}\text{C}$, $\delta^{15}\text{N}$, and C:N ratios in muscle and plasma tissues was similar for both species. Results from all pairwise comparisons among treatments are listed in Appendix C (Table C3).

In general, lipid extraction did not significantly alter $\delta^{13}\text{C}$, $\delta^{15}\text{N}$, or C:N ratios for muscle or plasma tissues (Fig. 4.1). The effect of lipid extraction was highly variable among individual stingrays, particularly for $\delta^{13}\text{C}$ in muscle tissue (Fig. 4.1a). $\delta^{13}\text{C}$ values increased for four of ten and six of ten individuals of *Pastinachus ater* and *Himantura australis*, respectively, following lipid extraction with the remaining individuals showing a decrease or no change in $\delta^{13}\text{C}$ values (Table C1). Pairwise comparisons between lipid-extracted and bulk samples revealed statistically significant differences in $\delta^{13}\text{C}$ only for *P. ater* plasma and for C:N ratios for *H. australis* muscle; however, the magnitudes of these differences were small ($-0.2 \pm 0.2\text{‰}$ and $-0.1 \pm 0.1\text{‰}$, respectively) and not ecologically significant. The C:N ratios in bulk muscle and plasma samples were <3.5 for both species and the lack of change in C:N ratios following lipid extraction suggests that lipid content in muscle and plasma tissues of these two rays is low.

In contrast to lipid extraction, DIW rinses to remove urea led to significant changes in $\delta^{13}\text{C}$, $\delta^{15}\text{N}$, and C:N ratios. For muscle tissue, urea extraction significantly increased $\delta^{15}\text{N}$ and C:N for both species, but did not affect $\delta^{13}\text{C}$ values (Fig. 4.1). Similar increases in $\delta^{15}\text{N}$ values were observed for all individuals of both *P. ater* and *H. australis*, with mean changes of $+0.9 \pm 0.2\text{‰}$ and $+1.1 \pm 0.3\text{‰}$, respectively (Fig. 4.1b). Similarly, C:N ratios of all individual stingrays increased following urea-extraction ($+0.7 \pm 0.2\text{‰}$ for *P. ater* and $+0.7 \pm 0.1\text{‰}$ for *H. australis*) (Fig. 4.1c) (Table C1). Urea extraction led to variable changes in muscle $\delta^{13}\text{C}$ among individuals, ranging from -1.3‰ to $+1.3\text{‰}$ for *P. ater* (mean \pm SD: $-0.2 \pm 0.8\text{‰}$) (Fig. 4.1a) (Table C1). Changes in muscle $\delta^{13}\text{C}$ values were less variable for *H. australis* (-0.3‰ to $+0.6\text{‰}$) with an overall (non-significant) mean increase of $+0.2 \pm 0.3\text{‰}$ (Fig. 4.1a).

In contrast to muscle tissue, urea extraction had a significant effect on plasma $\delta^{13}\text{C}$ and resulted in significantly lower $\delta^{13}\text{C}$ for both species (*P. ater*: $-1.9 \pm 0.3\text{‰}$; *H. australis*: $-1.3 \pm 0.2\text{‰}$) (Fig. 4.1a). Again, in contrast to the increase in muscle $\delta^{15}\text{N}$ with urea extraction, $\delta^{15}\text{N}$ decreased in plasma tissue from both species following urea extraction (*P. ater*: $-0.5 \pm 0.4\text{‰}$; *H. australis*: $-0.3 \pm 0.3\text{‰}$), although the difference was only significant for *P. ater* (Fig. 4.1b). As with muscle, C:N ratios were significantly higher in urea-extracted plasma samples than in bulk samples for both *P. ater* and *H. australis* (Fig. 4.1c) with mean increases of $+2.3 \pm 0.2$ and $+2.5 \pm 0.2$, respectively.

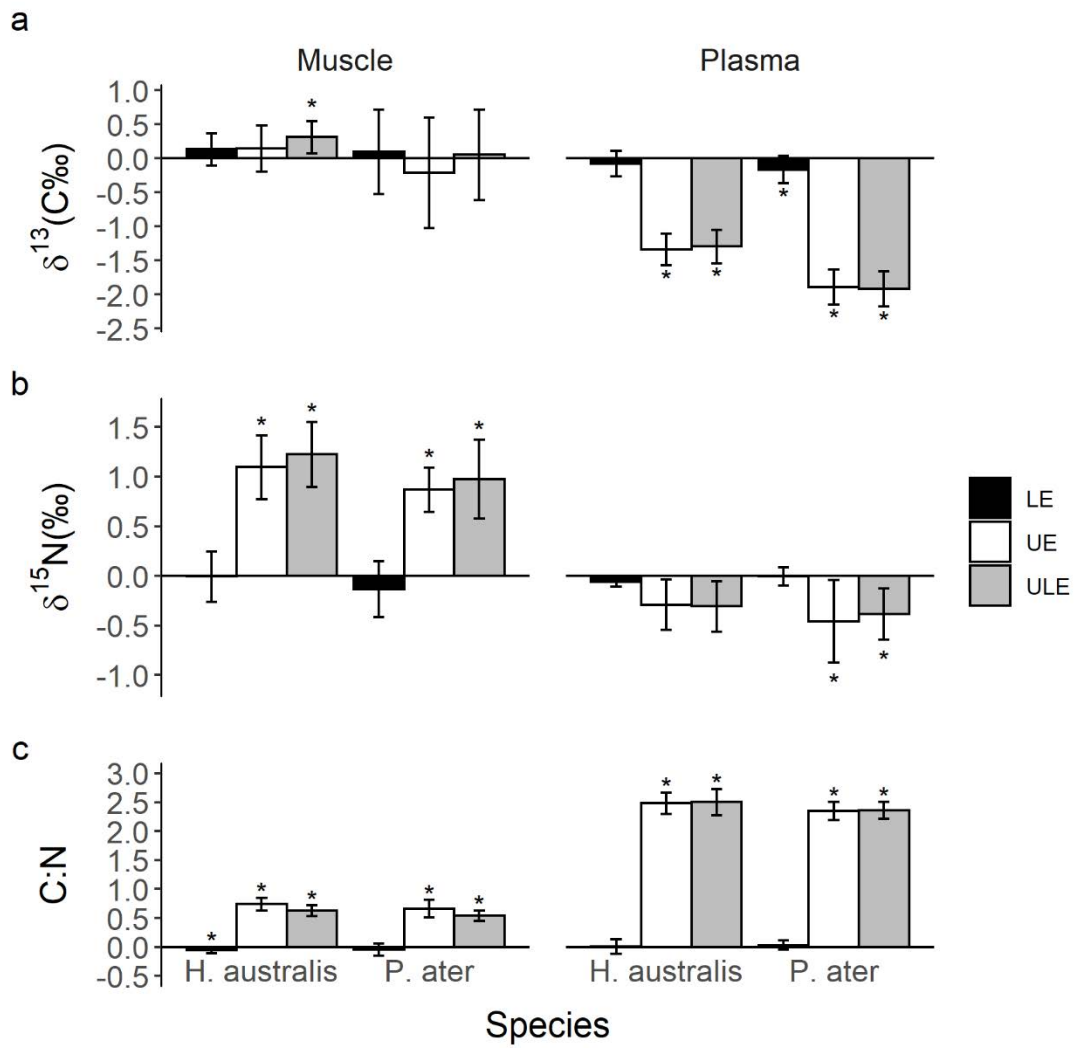


Figure 4.1 Mean \pm SD differences between bulk and treatment samples for a) $\delta^{13}\text{C}$, b) $\delta^{15}\text{N}$, and c) C:N ratios in muscle and plasma tissues of the batoids *Pastinachus ater* and *Himantura australis*. Bars represent lipid extracted (LE), urea extracted (UE), and urea and lipid extracted (ULE) treatments. Asterisks (*) indicate significant differences at $\alpha=0.05$ corrected for multiple comparisons using the sequential Bonferroni adjustment.

Tissues that underwent both lipid and urea extraction (ULE) showed the same patterns as those that only underwent urea extraction (Figs. 4.1–4.3). The only difference apparent for ULE tissues that was not present for UE treatment was a small increase in muscle $\delta^{13}\text{C}$ for *H. australis* ($+0.3 \pm 0.2\text{ ‰}$).

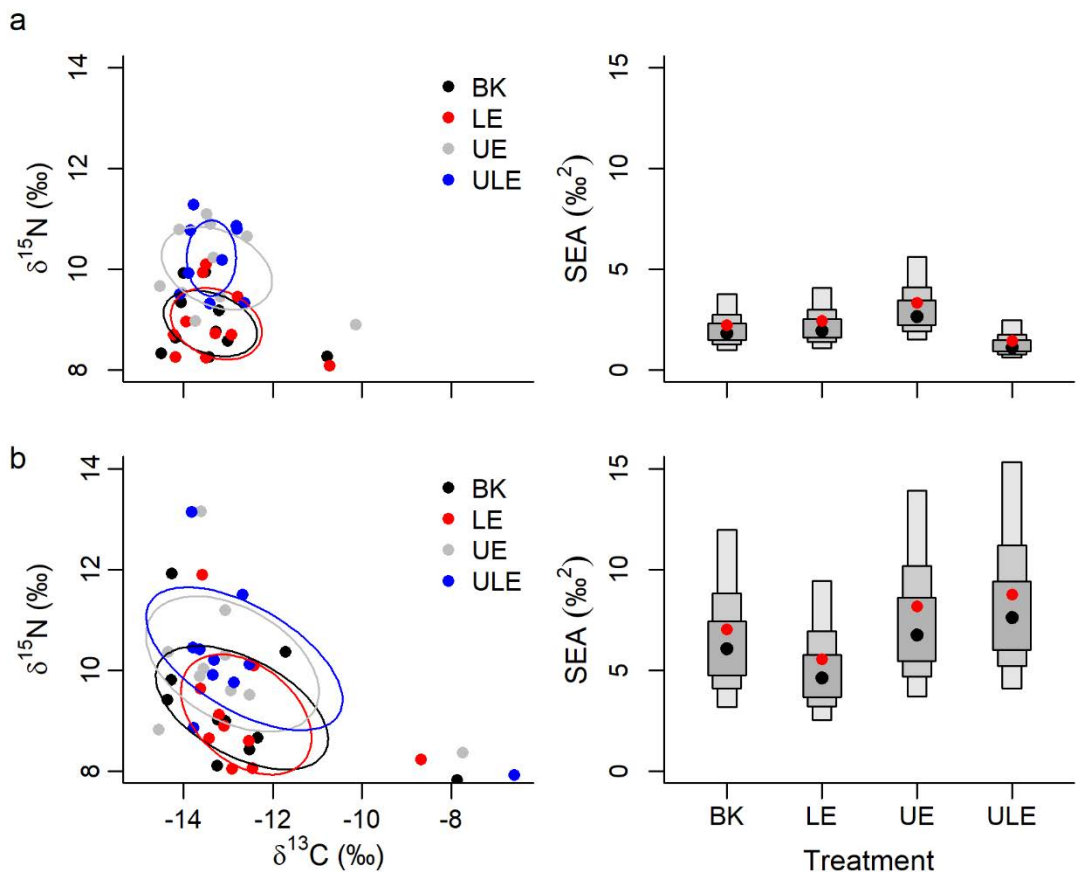


Figure 4.2 Left: $\delta^{13}\text{C}$ and $\delta^{15}\text{N}$ values in muscle tissue from a) *Himantura australis* and b) *Pastinachus ater* for bulk (BK), lipid-extracted (LE), urea-extracted (UE), and urea and lipid extracted (ULE) samples. Solid lines represent standard ellipse areas (SEA). Right: Boxes represent the 50, 75, and 95 % Bayesian credible intervals for SEA. Black dots show the mode SEA and red dots show the small sample-size corrected SEA (SEA_c).

Regarding niche sizes, lipid and urea extraction methods did not affect the standard ellipse areas for muscle or plasma tissues of *P. ater* or *H. australis*, as the 95 % credible intervals of the standard ellipse areas of all treatments overlapped, suggesting no influence of extraction methods on estimated niche size (Figs. 4.2 and 4.3). Qualitative analysis of ellipse parameters indicated that ellipse shape (E) and angle (θ) remained relatively unchanged following all treatments for muscle tissue (Table 4.1), further suggesting that treatment methods do not influence variability in stable isotope values. The change in θ observed for *H. australis* muscle following the ULE treatment is a result of the exclusion of the ULE treatment for one individual which had the most extreme isotope values for the other treatments (Fig. 4.2a). For plasma, ellipse shape was similar among all treatments; however, θ decreased for both species following UE and ULE treatments (Table 4.1), reflecting decreased variability in $\delta^{15}\text{N}$ and increased variability in $\delta^{13}\text{C}$.

Table 4.1 Standard ellipse parameters eccentricity (E) and the angle between the semi-major axis of the standard ellipse and the x- axis (θ) for *Himantura australis* and *Pastinachus ater* stable isotope values ($\delta^{13}\text{C}$ and $\delta^{15}\text{N}$) in bulk (BK), lipid extracted (LE), urea extracted (UE), and lipid and urea-extracted (ULE) samples from both muscle and plasma tissues. θ values are expressed in degrees.

Treatment	<i>H. australis</i>				<i>P. ater</i>			
	Muscle		Plasma		Muscle		Plasma	
	E	θ	E	θ	E	θ	E	θ
BK	0.83	-16.5	0.92	67.1	0.88	-23.7	0.77	65.8
LE	0.77	-16.6	0.88	75.4	0.77	-31.1	0.82	62.1
UE	0.81	-18.7	0.93	37.0	0.83	-24.2	0.77	34.4
ULE	0.68	89.2	0.92	41.6	0.90	-26.1	0.87	22.0

Despite no significant changes in estimated niche size following sample treatment, the positions of the standard ellipses shifted in bivariate niche space following urea-extraction treatments (UE and ULE) for both muscle and plasma of both species. Based on similar observed shifts for UE and ULE treatments, isotopic niche overlap was only calculated for bulk and urea-extracted treatments. The probability of UE samples occupying the same trophic niche space as bulk samples for muscle and plasma, respectively, was 45 and 26 % for *H. australis* and 78 and 37 % for *P. ater* (Fig. 4.4). When comparing muscle samples between species, the probability of *H. australis* occurring within the trophic niche of *P. ater* did not change following urea-extraction (96 % and 97 % for BK and UE, respectively; Fig. 4.4a); however, the probability of *P. ater* occurring within the trophic niche space of *H. australis* increased from 40 % (BK) to 62 % after urea-extraction (Fig. 4.4a). In plasma, the probability of *H. australis* occurring within the trophic niche space of *P. ater* decreased from 96 to 82 % for BK and UE samples, respectively (Fig. 4.4b). Similarly, the probability of *P. ater* occurring within the trophic niche space of *H. australis* decreased following urea-extraction from 39 % (BK) to 32 % (Fig. 4.4b).

Discussion

My results support the recommendation that urea be extracted from ray muscle tissue prior to stable isotope analysis due to increases in $\delta^{15}\text{N}$ and C:N ratios following urea extraction (Burgess & Bennett 2017; Carlisle *et al.* 2017). In contrast, $\delta^{13}\text{C}$ and C:N ratios did not change following lipid

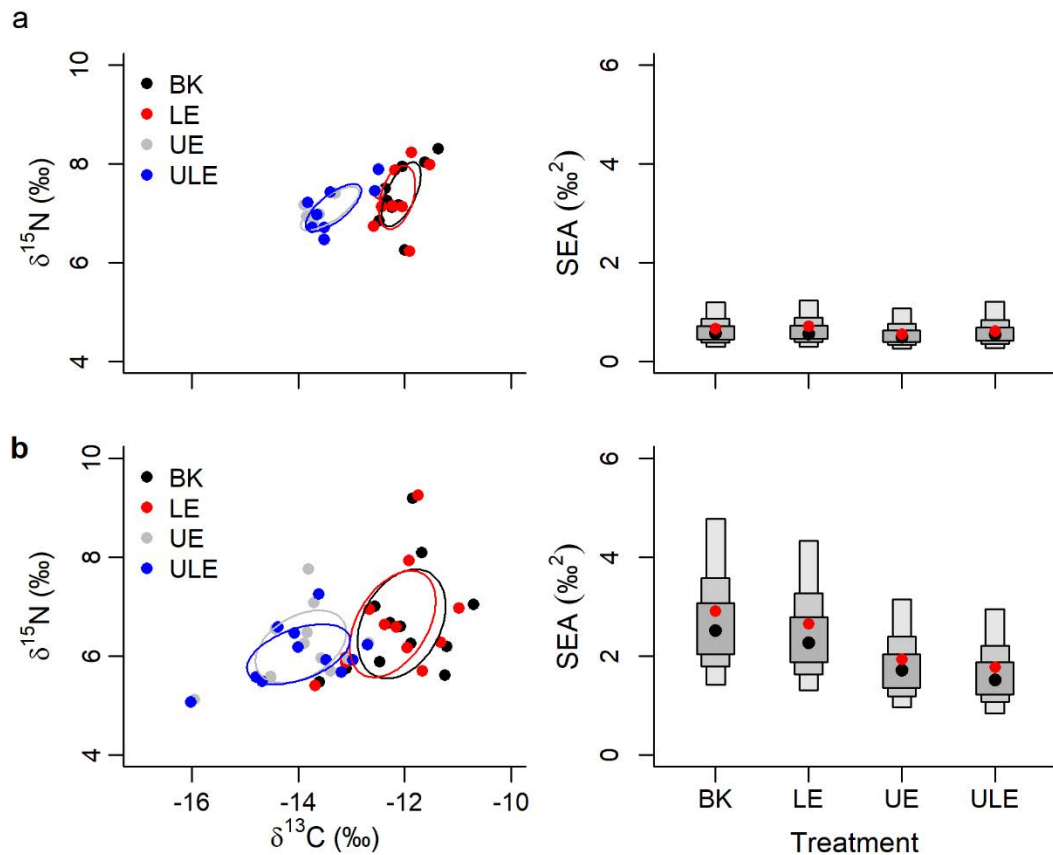


Figure 4.3 Left: $\delta^{13}\text{C}$ and $\delta^{15}\text{N}$ values in plasma tissue from a) *Himantura australis* and b) *Pastinachus ater* for bulk (BK), lipid-extracted (LE), urea-extracted (UE), and urea and lipid extracted (ULE) samples. Solid lines represent standard ellipse areas (SEA). Right: Boxes represent the 50, 75, and 95 % Bayesian credible intervals for SEA. Black dots show the mode SEA and red dots show the small sample-size corrected SEA (SEAc).

extraction, suggesting muscle lipid content was low. Additionally, I observed no changes in isotopic niche size estimates following any extraction method indicating low variability in both lipid and urea content among individuals of the same species. Although no change in niche size was observed, the niche position shifted in bivariate space following urea-extraction. The observed shift in trophic niche position reflected the increase in $\delta^{15}\text{N}$ following urea-extraction which suggests that untreated samples underestimated trophic position. Additionally, the probability of *Pastinachus ater* isotope values falling within the trophic niche space of *Himantura australis* increased following urea extraction. Overall, results suggest that for *P. ater* and *H. australis* muscle tissue, urea should be extracted prior to stable isotope analysis to accurately assess trophic position and niche overlap but lipid extraction is not required due to low tissue lipid content in these two species.

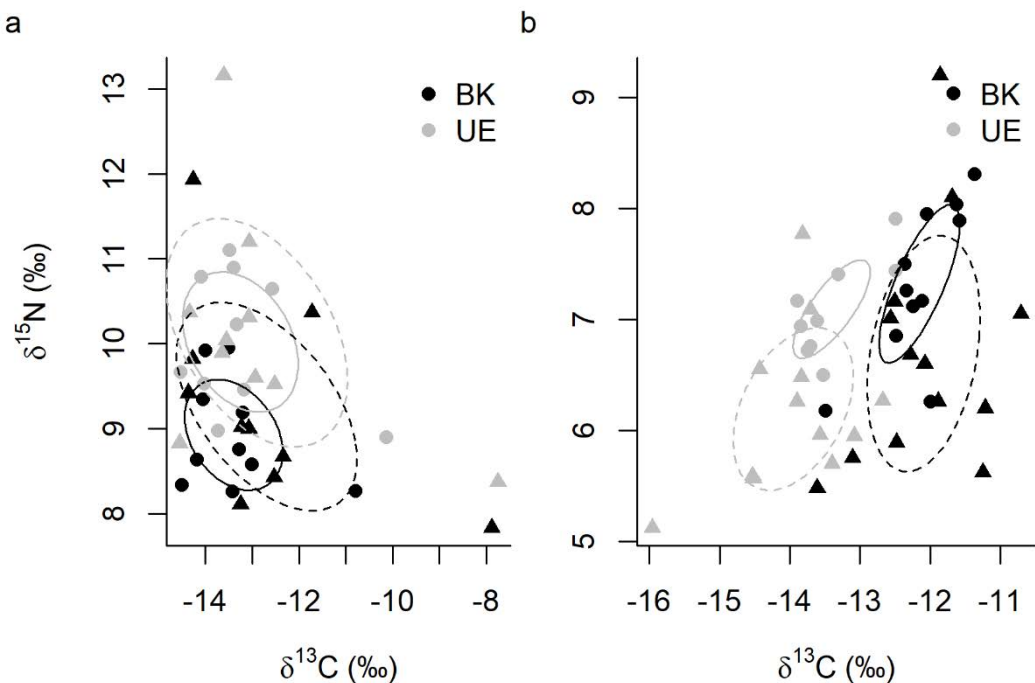


Figure 4.4 $\delta^{13}\text{C}$ and $\delta^{15}\text{N}$ of bulk (BK) and urea-extracted (UE) samples from *Himantura australis* (●) and *Pastinachus ater* (▲) a) muscle tissue and b) plasma tissue. Solid lines represent standard ellipse areas for *H. australis* (solid lines) and *P. ater* (dashed lines).

Urea extraction is recommended for elasmobranch tissues (Kim & Koch 2012; Li *et al.* 2016; Burgess & Bennett 2017; Carlisle *et al.* 2017) due to urea retention in body tissues for osmoregulation (Hazon *et al.* 2003), and because urea is relatively depleted in ^{14}N (Gannes, del Rio & Koch 1998). In the present study, urea extraction led to a $\sim 1\text{ \textperthousand}$ increase in $\delta^{15}\text{N}$ values of stingray muscle tissue ($+0.9 \pm 0.2\text{ \textperthousand}$ for *P. ater*; $+1.1 \pm 0.3\text{ \textperthousand}$ for *H. australis*). These shifts in $\delta^{15}\text{N}$ fall within the range of those observed in muscle tissue from other elasmobranchs ($+1.7\text{ \textperthousand}$, Kim and Koch (2012); $+0.5\text{--}1.1\text{ \textperthousand}$, Carlisle *et al.* (2017); $+0.9\text{--}1.4\text{ \textperthousand}$, Li *et al.* (2016)) and closely match shifts observed in a closely related species (coral sea maskray, *Neotrygon trigonoides*: $+1.0\text{ \textperthousand}$, (Burgess & Bennett 2017)).

Shifts in $\delta^{15}\text{N}$ following urea-extraction have important implications for the evaluation of trophic levels. Using the estimated trophic discrimination factor of $2.3\text{ \textperthousand}$ for elasmobranch muscle tissue (Hussey *et al.* 2010), calculated trophic levels of urea-extracted tissues can be up to 0.5 trophic levels higher than those calculated from bulk samples (Li *et al.* 2016; Carlisle *et al.* 2017). Consistently, increases in $\delta^{15}\text{N}$ following urea-extraction in this study correspond to trophic level shifts of $+0.4$ and 0.5 levels for *P. ater* and *H. australis*, respectively, based on the $2.3\text{ \textperthousand}$ $\delta^{15}\text{N}$ trophic discrimination factor for muscle tissue. Note, however, that estimates of trophic discrimination

values for elasmobranchs have largely focused on shark tissues (Hussey *et al.* 2010; Kim *et al.* 2012; Malpica-Cruz *et al.* 2012), with little to no evidence evaluating if these are appropriate for application to ray tissues. Thus, experimental investigation into trophic discrimination factors for rays needs to be undertaken to more accurately identify perceived trophic level shifts in ray tissues following urea-extraction.

Similar to $\delta^{15}\text{N}$ values, C:N ratios also significantly increased in muscle tissue following urea-extraction for both species. C:N ratios are frequently used to infer tissue lipid content and decisions to extract or not extract lipids from tissues are often made based on these inferences (Kiljunen *et al.* 2006; Sweeting, Polunin & Jennings 2006; Post *et al.* 2007). Pure protein has an expected C:N ratio of ~ 3 and it is accepted in the literature that lipids need not be removed in tissues with C:N ratios < 3.5 (Post *et al.* 2007). Following this rule, numerous studies evaluating elasmobranch resource use with stable isotopes have chosen not to extract lipids due to C:N ratios similar or often lower than those of pure protein (e.g. Abrantes and Barnett (2011), Vaudo and Heithaus (2011), Madigan *et al.* (2015)). The increase in C:N ratio following urea-extraction in the present study, as in other studies (Kim & Koch 2012; Li *et al.* 2016; Carlisle *et al.* 2017), suggests that C:N ratios are not a good proxy for lipid content in tissues containing urea, and that the influence of urea on C:N ratios can mask lipid content, and may lead to incorrect decisions to not extract lipids (Carlisle *et al.* 2017). However, the C:N ratios of *P. ater* and *H. australis* muscle both before (2.5 and 2.6) and after urea-extraction (3.2 and 3.3) suggest that batoid lipid content is generally low, and that lipid extraction is not required. This is supported by the lack of change in $\delta^{13}\text{C}$, C:N ratios, eccentricity, or ellipse θ following lipid extraction. While my results are consistent with many species examined in Carlisle *et al.* (2017) and Li *et al.* (2016), C:N ratios of four out of 14 elasmobranch species examined by Carlisle *et al.* (2017) shifted above 3.5 following urea-extraction, suggesting that, for those species, lipids should be extracted prior to $\delta^{13}\text{C}$ analysis. Although lipid content in elasmobranch muscle tissue is generally low, some species (e.g. spiny dogfish (*Squalus acanthias*), Greenland shark (*Somniosus microcephalus*), whale shark (*Rhincodon typus*)) have high lipid content and require lipid extraction prior to $\delta^{13}\text{C}$ analysis (Logan & Lutcavage 2010; Hussey *et al.* 2012a; Carlisle *et al.* 2017).

The influence of urea-extraction on stingray plasma differed from its influence on muscle. DIW rinses led to a decrease in both $\delta^{13}\text{C}$ and $\delta^{15}\text{N}$ in plasma tissues and, as with muscle, to an increase in C:N ratios. The increase in C:N ratio above 3.5 following urea-extraction likely does not indicate high lipid content in plasma, however, as the C:N ratio of ~ 3 for pure protein is assumed for muscle tissue and for other tissues, the C:N ratio of lipid-free tissue is more variable (Post *et al.* 2007). Kim and Koch (2012) also showed a decrease in $\delta^{13}\text{C}$ in leopard shark (*Triakis semifasciata*) plasma following urea-extraction and an increase in C:N ratio but did not observe any changes in

$\delta^{15}\text{N}$. They suggest the decrease in $\delta^{13}\text{C}$ was likely due to altered amino acid composition in plasma following urea-extraction, that did not occur for muscle tissue; however, decreases in $\delta^{13}\text{C}$ were also observed for red blood cells despite no changes in amino acid composition, suggesting other organic carbon is being removed by DIW rinses (Kim & Koch 2012). Elasmobranch plasma has low concentrations of free amino acids relative to muscle tissue and red-blood cells but high concentrations of urea (Boyd *et al.* 1977; Bedford 1983; Cain, Harms & Segars 2004). The high concentration of urea in plasma suggests that urea-extracted plasma should have higher $\delta^{15}\text{N}$ than bulk samples, but that was not observed in the present study. Instead, there was a decrease in $\delta^{15}\text{N}$ following urea-extraction, suggesting that DIW rinses are causing additional biochemical modifications of plasma tissue. In support, ellipse θ decreased for plasma following urea extraction indicating greater variability in $\delta^{13}\text{C}$ and decreased variability in $\delta^{15}\text{N}$. Thus, it is likely that DIW rinses are removing urea from plasma tissues but this effect is masked by the unexplained changes in $\delta^{13}\text{C}$. Results obtained from ray plasma tissues highlight the need for further study to determine the biochemical influences of DIW on elasmobranch plasma, to confirm that DIW rinses are removing urea from plasma, and that urea in elasmobranch plasma is indeed enriched in ^{14}N . Thus, I agree with the suggestion of Kim and Koch (2012), that urea should not be removed prior to analysis of stable isotope ratios of ray plasma tissues.

The documented biases that result from the effects of lipid and urea content in elasmobranch tissues need to be corrected to accurately infer resource use and trophic position from stable isotope values (Hussey *et al.* 2012a; 2012b; Kim & Koch 2012; Carlisle *et al.* 2017). As such, treatments to correct for the effect of lipid/urea content are expected to decrease the variability in stable isotopic values among individuals and, therefore, decrease estimates of isotopic niche sizes. In this study, however, and despite significant changes in $\delta^{13}\text{C}$ and $\delta^{15}\text{N}$ following urea-extraction, I did not observe any difference in trophic niche sizes among treatments. To my knowledge, this is the first study to investigate the influence of lipid and urea-extraction on estimated trophic niche sizes in elasmobranchs. A similar analysis has been performed for teleost species, where McNicholl *et al.* (2018) investigated trophic niche size of co-occurring forage fish and found that, following lipid extraction, estimated niche size decreased for polar cod (*Boreogadus saida*) but not for capelin (*Mallotus villosus*). The difference in niche size for cod but not for capelin can be attributed to cod individuals having higher variability in lipid content than capelin as was evidenced by their C:N ratios (McNicholl *et al.* 2018). This supports the conclusion that lipid extraction will decrease estimated niche size for species with variable lipid content but not when lipid content is more homogeneous among individuals. Therefore, the lack of change in isotopic niche sizes observed following lipid and urea extraction in this study suggests that among individual

variation for each species is low for both lipid and urea content. This is further supported by the similar eccentricity and θ values for muscle tissue among all treatments within a species.

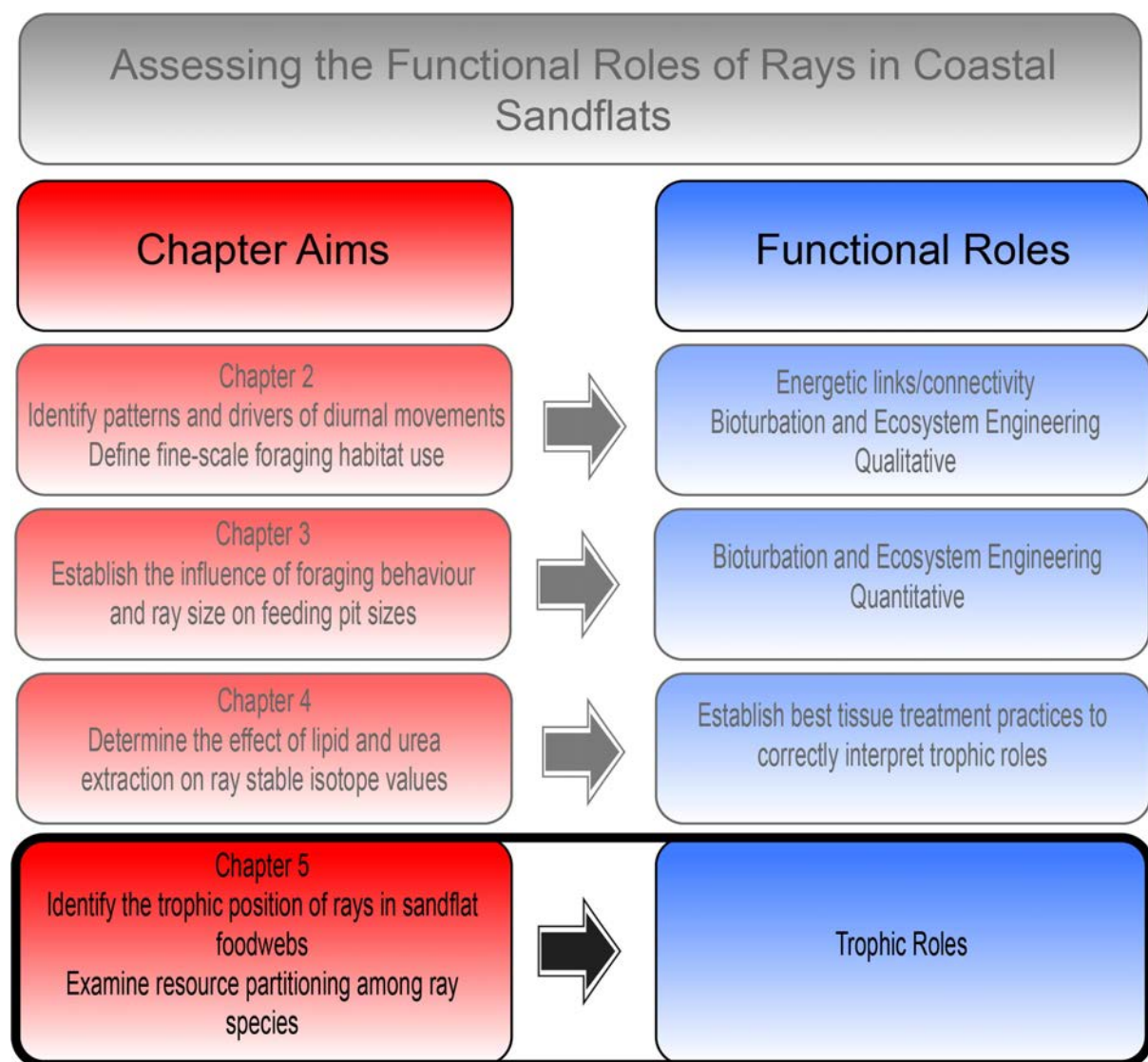
Despite no changes in estimates of trophic niche size following urea extraction, the probability of isotope values for *P. ater* muscle tissue falling within *H. australis* niche space increased from 40 to 62 % following urea extraction. Similarly, McNicholl *et al.* (2018) found that the probability of cod occurring within the trophic niche of capelin was 53 % for bulk samples but increased to 83 % following lipid extraction due to the high lipid content in polar cod tissues. The increased probability of overlap observed following urea extraction suggests that while among individual variation in urea content may be low, urea content may differ in muscle tissue between the two species.

Individual rays sampled for this study were all very similar in size (Tables C1 and C2) and it is possible that inclusion of larger or smaller individuals may increase the variability of lipid and urea content. Additionally, variation in body condition may also affect the isotope values of individuals, which may be more or less pronounced depending on environmental conditions and food availability during sampling (Gannes, del Rio & Koch 1998; Bearhop *et al.* 2004). Individuals assessed in this study were all sampled during Austral winter so variation in body condition due to seasonality should be minimal. Although sample sizes for each treatment were small, I do not believe that this had any influence on my ability to detect patterns in the effects of lipid/urea extraction on isotope values and estimates of niche size and overlap. Using Bayesian inference to calculate the 95 % credible intervals of standard ellipse area (SEA_B) is unbiased regardless of sample size (Jackson *et al.* 2011); therefore, conclusions regarding the influence of treatment methods on niche size and overlap are appropriate based on a sample size of 10.

Overall, results from this study corroborate results from previous studies suggesting that removal of urea from elasmobranch muscle tissue significantly increases both $\delta^{15}\text{N}$ and C:N ratios but has minimal effect on $\delta^{13}\text{C}$. Lipid extraction using petroleum ether did not affect $\delta^{13}\text{C}$, $\delta^{15}\text{N}$, or C:N of ray muscle or plasma tissues, supporting that lipid content in ray tissues is low. Thus, for the two species tested here, I recommend urea extraction from muscle tissue prior to stable isotope analysis, but lipid extraction is not required. The influence of urea-extraction on plasma in this study did not agree with expected results for urea removal, therefore, I caution the use of extraction methods on plasma tissues and stress the need for more in-depth investigations on the biochemical reactions occurring in plasma tissues following standard extraction methods. Overall, these results contribute to the sparse coverage in the literature examining the influence of lipid/urea extraction on elasmobranch stable isotope values and I advocate for more species-specific investigations to

identify generalized patterns among elasmobranch groups and establish protocols for best practices. Therefore, when no species-specific data is available, I recommend pilot samples (e.g. 10 individuals) be sent for analysis to determine the influence of lipid/urea extraction prior to analysis of the entire sample set.

Chapter 5: Trophic roles of rays in sandflat foodwebs



Introduction

Direct predator-prey interactions govern energy flow in foodwebs, and knowledge of these relationships is critical for understanding ecosystem function (Polis & Strong 1996; Ripple *et al.* 2014). Species at different trophic levels can propagate direct and indirect effects of disturbance through the foodweb by either top-down or bottom-up processes (Elmhagen & Rushton 2007; Heithaus *et al.* 2008; Ritchie & Johnson 2009; Van Colen *et al.* 2015). With current high levels of anthropogenic and climate change induced pressure on global ecosystems, it is critical to identify and understand the relationships in ecological communities, so that the effects of disturbance can be understood (Hughes *et al.* 2003; Folke *et al.* 2004; Hughes *et al.* 2018). Foodwebs with high complexity are expected to have high trophic redundancy due to high numbers of trophic links among consumers and to be better suited to withstand disturbance (Yachi & Loreau 1999; Dunne, Williams & Martinez 2004). Consistently, species that are part of more trophic pathways are more important in propagating effects throughout the foodweb, and the loss of those species will have more severe effects on foodweb structure and function (Bornatowski *et al.* 2014; Navia *et al.* 2016).

Due to global declines in shark and ray populations, recent attention has been given to the trophic roles of elasmobranchs (Heithaus *et al.* 2008; Dulvy *et al.* 2014; 2017). Sharks have traditionally been considered apex predators in marine systems (Stevenson *et al.* 2007; Barnett *et al.* 2017). However, recent evidence suggests that apex predatory roles are performed by few highly mobile shark species, and that species such as reef sharks play mesopredator roles similar to piscivorous teleosts (Heupel *et al.* 2014; Roff *et al.* 2016). Indeed, topological analyses of complex marine foodwebs shows that while apex predators have unique trophic roles, there is high redundancy among mesopredators (Bornatowski *et al.* 2014; Navia *et al.* 2016; Navia *et al.* 2017). Mesopredator assemblages are often diverse and can occupy multiple trophic levels (Thillainath *et al.* 2016; Navia *et al.* 2017; Mulas *et al.* 2019). Given the breadth of species sizes, feeding modes, and life history strategies among so-called ‘mesopredators’, functional redundancy among this trophic guild warrants closer examination.

The diversity in mesopredator assemblages suggests the potential for competition to exist among sympatric species. In the face of competition, sympatric species can partition resources to maximize fitness, and this can be an evolutionary driver of morphological differences (Schoener 1974; Davies *et al.* 2007). Co-existence can also occur among similar species (Scheffer & van Nes 2006). For example, multi-species ray communities are often made up of species that share similar morphologies (Vaudo & Heithaus 2009; Pierce, Scott-Holland & Bennett 2011). Dietary analyses of sympatric species have determined that despite high dietary overlap (Vaudo & Heithaus 2011; Yick,

Tracey & White 2011; O'Shea *et al.* 2013), resources are partitioned based on the quantities of each prey type consumed (Marshall, Kyne & Bennett 2008; Elston *et al.* 2020), habitat use (O'Shea *et al.* 2013), and morphology (Barria, Coll & Navarro 2015; Pardo *et al.* 2015). Although these differences are evident in stomach content analysis, stable isotope studies suggest high levels of functional redundancy among sympatric species (Vaudo & Heithaus 2011; Elston *et al.* 2020). Additionally, existing stable isotope studies on rays have focussed on their trophic relationships to other elasmobranchs (Vaudo & Heithaus 2011; Heithaus *et al.* 2013; Shipley *et al.* 2018; Elston *et al.* 2020). Consequently, trophic relationships and niche comparisons of rays with teleost mesopredators are lacking. In this Chapter, stable isotope analysis was used to determine if rays occupy a unique trophic niche in sandflat foodwebs and evaluate the level of functional redundancy in trophic roles of sympatric rays.

Methods

Rays were captured at the Lucinda sandflat following methods outlined in Chapter 2, and tissue samples were collected and stored for stable isotope analysis as outlined in Chapter 4 (Crook *et al.* 2019). To place rays within the context of the sandflat foodweb, samples from primary producers, invertebrates, and fish were also collected at Lucinda. Green leaves were hand-picked from the mangroves *Rhizophora* sp., *Sonneratia* sp., and *Avicennia* sp. as well as the macroalga *Caulerpa taxifolia*. Each primary producer sample consisted of three leaves from an individual plant. Fish were collected using an 8mm mesh, 30m long seine net. White muscle samples were collected from the dorsal musculature posterior to the pectoral fin using 5mm diameter biopsy punches for individuals >150mm total length, but smaller individuals were euthanized in an ice bucket slurry and muscle samples were excised in the laboratory. The total length (mm) was measured for all sampled fish.

Longline sampling (200 m mainline with 25 size 8/0 or 12/0 hooks) was conducted in 2016 and 2017 to sample sharks and large teleosts; however, no individuals from either group were captured. Benthic invertebrates were sieved (500µm) from sediment samples collected using a 10 cm diameter PVC corer, and were opportunistically collected when observed active on the sandflat (e.g. soldier crabs *Mictyris longicarpus*) or when captured in seine nets. Ghost shrimp (*Trypaea australiensis*) were collected using a suction pump as their presence was observed (burrows) but none were captured in sediment cores. Invertebrates were euthanized along with fish. Where possible, muscle tissue was collected. Chelae muscle was collected for *T. australiensis* and *M. longicarpus*, abdominal muscle for prawns and muscular foot from gastropods. For small bivalves,

the shell was removed and the whole body was analysed. For *T. australiensis*, *M. longicarpus*, and bivalves, tissue from three to five individuals were combined to make up one sample.

Sample Processing

Ray muscle and plasma samples were processed for stable isotope analysis following the best practices identified in Chapter 4 (urea extraction for muscle, no treatment for plasma). Samples from other species were dried, weighed, and encapsulated for stable isotope analysis following the same procedures as for ray samples (Chapter 4), but were not treated for lipid or urea extraction. Lipid extraction has a minimal influence on muscle $\delta^{13}\text{C}$ values for invertebrates and lean fish (Post *et al.* 2007; Ricca *et al.* 2007), and urea extraction is only recommended for elasmobranchs (Kim & Koch 2012; Carlisle *et al.* 2017). Encapsulated samples were sent to the UC Davis Stable Isotope Facility (University of California), where they were analyzed using a stable isotope ratio mass spectrometer to determine $\delta^{13}\text{C}$ and $\delta^{15}\text{N}$. Results are expressed in delta notation relative to international standards (Vienna PeeDee Belemnite for carbon and air for nitrogen) with a precision of $\pm 0.00\text{--}0.16 \text{\textperthousand}$ for $\delta^{13}\text{C}$ and $\pm 0.05\text{--}0.28 \text{\textperthousand}$ for $\delta^{15}\text{N}$ (SD), calculated from replicate samples of laboratory standards.

Data Analysis

Mean stable isotope values were calculated for all species sampled, and resulting values were plotted to assess the structure of the sandflat foodweb. Samples were then organized into four general categories: primary producers, invertebrates, fish, and rays. Invertebrates were further grouped into broad taxonomic groups (bivalves, decapod crustaceans, and gastropods) and fish into trophic groups based on diets following Abrantes and Sheaves (2009) (Table D1). The trophic position of each group was determined by comparing $\delta^{15}\text{N}$ values with the primary producer baseline. Fish and invertebrates were classified as primary or secondary consumers based on diets and classifications in Abrantes and Sheaves (2009). Ray muscle isotope values were used to assess trophic position.

For rays, muscle and plasma stable isotope values were also used to assess long- (muscle) and short-term (plasma) resource use. Metabolically active tissues (e.g. liver and blood plasma) have faster incorporation rates and represent resource use over shorter periods (several months), whereas tissues with slower turnover rates (e.g. muscle and bone collagen) represent average resource use over longer periods (>1 year) (Tieszen *et al.* 1983; Kim *et al.* 2012). Analysis of stable isotope values in tissues with different incorporation rates can provide an indication of dietary consistency or shifts in resource use over time (Bond, Jardine & Hobson 2016; Yurkowski *et al.* 2016).

For ray species with ≥ 5 samples for both muscle and plasma, standard ellipse areas (SEA) were calculated using the R package ‘SIBER’ (Jackson *et al.* 2011) to compare long- and short-term isotopic niche sizes. Small sample size corrected standard ellipses (SEAc) were plotted for species with sample sizes < 20 . Differences in niche sizes among species were determined by assessing if the 95 % credible intervals overlapped for 10^5 estimated Bayesian SEAs (SEA_B). Resource partitioning was assessed using the ‘nicheROVER’ R package (Swanson *et al.* 2015), as the probability of an individual from one species falling within the niche space (SEA) of another. Ellipse parameters eccentricity (E) and θ were calculated to qualitatively compare ellipse shape between species (as elongate ellipses have E close to one and more circular ellipses have E close to zero), and to determine if variability was driven by $\delta^{13}\text{C}$ (θ closer to 0°) or $\delta^{15}\text{N}$ (θ closer to 90°) (Reid *et al.* 2016) (Chapter 4). Niche sizes and overlaps were further compared within and among species across years for species with at least five individuals sampled in multiple years. All statistical analyses were performed in R (R Core Team 2018).

Results

Rays were captured and sampled at the Lucinda sandflat between June 2017 and June 2019. In total, 186 individuals were captured comprising eight species (Table 5.1). Muscle and plasma samples were collected from 131 and 117 individuals, respectively (Table 5.1). All captured individuals were juveniles, based on published size at maturity, clasper calcification for males, or estimated based on maximum adult size for poorly studied species (Last *et al.* 2016). Ray catches were dominated numerically by *Pastinachus ater*, *Himantura australis*, and *Glaucostegus typus* (92 % of all individuals) with low numbers (≤ 5 individuals) for all other species (Table 5.1). For all species, most individuals fell within a narrow size range so the relationship between size and isotope values was not explored; however, the most extreme carbon and nitrogen values were observed for both small and large juveniles so it is unlikely that a pattern exists for the size range captured at Lucinda. Additionally, seasonal changes in diet were not explored as most individuals were sampled in the dry season between June and August. In addition to rays, 15 fish, six invertebrate, and four primary producer species were sampled (Table D1). $\delta^{13}\text{C}$ values from primary producers not sampled at Lucinda were included, based on values from estuaries along the QLD coast in Abrantes *et al.* (2015b).

There was high variability in $\delta^{13}\text{C}$ values among sandflat consumers (Fig. 5.1) with mean \pm SE $\delta^{13}\text{C}$ values ranging from -20.2 for the detritivore *Valamugil buchanani* to $-13.3 \pm 1.5\text{‰}$ for the herbivore *Arrhamphus sclerolepis* (Table D1). Mean $\delta^{13}\text{C}$ for rays was $-13.5 \pm 0.2\text{‰}$ and was similar among species except for *Urogymnus granulatus* ($-17.8 \pm 1.0\text{‰}$) which had lower $\delta^{13}\text{C}$ values (Fig.

5.2) (Table 5.1). All sandflat consumers had mean $\delta^{13}\text{C}$ values closest to macroalgae ($-15.5 \pm 0.2 \text{‰}$) sampled at Lucinda, but were also similar to seagrass, microphytobenthos (MPB), and plankton $\delta^{13}\text{C}$ from Abrantes *et al.* (2015b). The 8 ‰ difference between the lowest consumer $\delta^{13}\text{C}$ value (*V. buchanani*) and mangroves ($-28.5 \pm 0.2 \text{‰}$) suggests Lucinda consumers are not relying on mangrove derived nutrients (Fig. 5.1).

Table 5.1 Sample size, mean size, size range, and mean stable isotope values ($\delta^{13}\text{C}$ and $\delta^{15}\text{N}$) of *Aetobatus ocellatus*, *Aetomylaeus vespertilio*, *Glaucostegus typus*, *Himantura australis*, *Maculabatus toshi*, *Pastinachus ater*, *Pateobatis fai*, and *Urogymnus granulatus* captured at Lucinda. Sample sizes in parentheses indicate the number of muscle and plasma samples analysed, respectively.

Species	n	Muscle		Plasma	
		Mean \pm SD size (mm)	Size range (mm)	Mean \pm SD $\delta^{13}\text{C}(\text{‰})$	Mean \pm SD $\delta^{15}\text{N}(\text{‰})$
<i>A. ocellatus</i>	2(2,1)	683 \pm 94	616–750	-14.3, \pm 7.3	9.0, 9.0
<i>A. vespertilio</i>	1(0,0)	876			
<i>G. typus</i>	42(34,28)	621 \pm 380	330–1870	-14.3 \pm 0.7	10.3 \pm 0.4
<i>H. australis</i>	31(28,24)	403 \pm 132	277–900	-14.1 \pm 2.0	10.0 \pm 0.8
<i>M. toshi</i>	4(4,1)	225 \pm 41	166–260	-13.6 \pm 0.4	10.1 \pm 0.4
<i>P. ater</i>	98(55,58)	415 \pm 48	290–570	-12.6 \pm 1.7	10.3 \pm 1.5
<i>P. fai</i>	3(3,0)	682 \pm 60	630–748	-13.6 \pm 0.0	11.1 \pm 0.8
<i>U. granulatus</i>	5(5,5)	470 \pm 89	374–570	-17.8 \pm 2.3	8.8 \pm 0.4
					-15.2 \pm 1.4
					7.3 \pm 0.3

Primary consumer $\delta^{15}\text{N}$ values were $6.9 \pm 0.2 \text{‰}$ for invertebrates (all species except *Nassarius* sp.) and $7.0 \pm 0.3 \text{‰}$ for fish (detritivores and herbivores, excluding *Liza vaigiensis*, for which $\delta^{15}\text{N}$ was much higher than that of the other species) reflecting a 2.2 and 2.3 ‰ difference from mean primary producer $\delta^{15}\text{N}$ ($4.7 \pm 0.2 \text{‰}$), respectively (Fig. 5.1). Rays and fish secondary consumers (carnivores and planktivores) had similar average $\delta^{15}\text{N}$ values ($10.2 \pm 0.1 \text{‰}$ and $10.1 \pm 0.1 \text{‰}$, respectively) (Fig. 5.1). The barramundi *Lates calcarifer* had the highest $\delta^{15}\text{N}$ (10.9‰), 4 ‰ higher than primary consumers, suggesting a food web with 3.3 trophic levels, if a 3 ‰ trophic discrimination factor (Vanderklift & Ponsard 2003) is considered. Like $\delta^{13}\text{C}$, $\delta^{15}\text{N}$ values were similar among ray species except for *U. granulatus* and *A. ocellatus* which had lower $\delta^{15}\text{N}$ values ($8.8 \pm 0.2 \text{‰}$ and 8.5‰ , respectively) (Fig. 5.2a). The relative position of rays in the bivariate niche space was consistent for long- and short-term indicators of resource use (muscle and plasma tissue, respectively) (Fig. 5.2); however, $\delta^{13}\text{C}$ values were consistently higher in plasma than in muscle

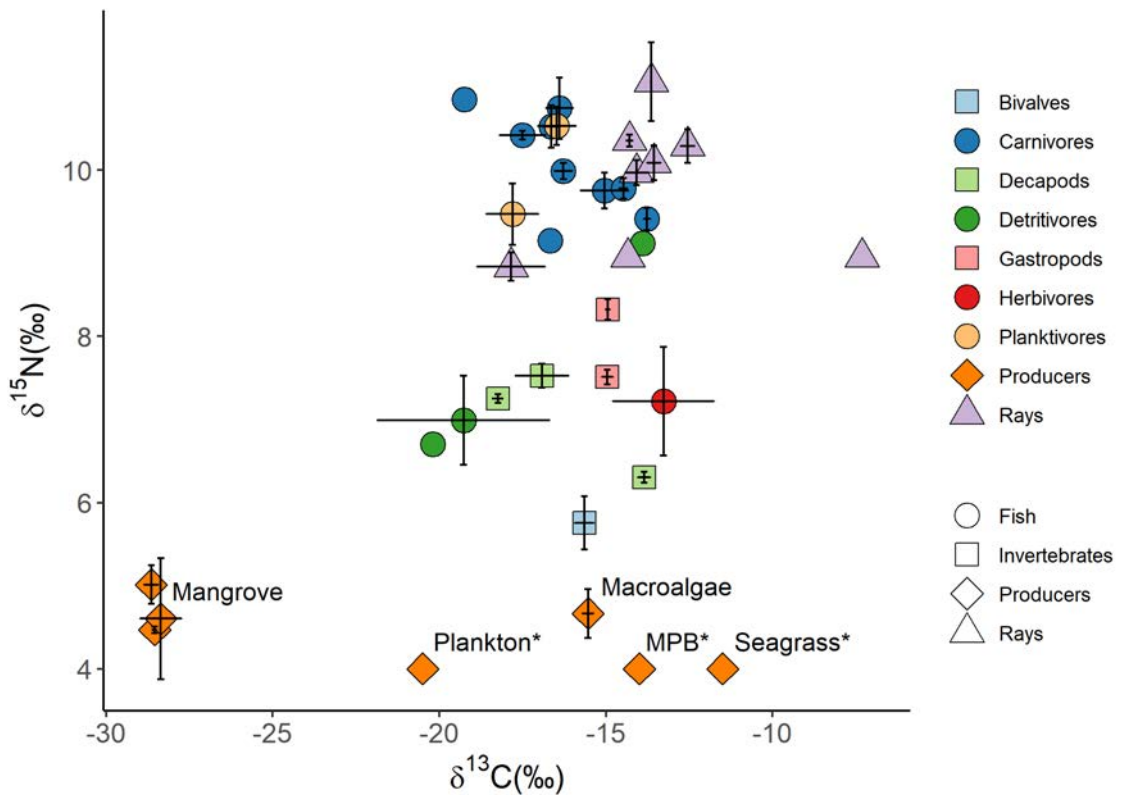


Figure 5.1 Mean \pm SE $\delta^{13}\text{C}$ and $\delta^{15}\text{N}$ for all species captured at Lucinda. Primary producers are labelled to the right. * indicates $\delta^{13}\text{C}$ values from Abrantes et al. (2015).

samples (0.3 ‰ *P. ater* to 2.6 ‰ for *U. granulatus*) (Fig. 5.2) and $\delta^{15}\text{N}$ values consistently lower in plasma than in muscle (1.5 ‰ for *U. granulatus* to 2.7 ‰ for *P. ater*) (Table 5.1). The single *Aetobatus ocellatus* with both muscle and plasma samples was the only exception, with plasma $\delta^{13}\text{C}$ lower than muscle $\delta^{13}\text{C}$ (Fig. 5.2) (Table 5.1).

Niche size

Rays and teleost secondary consumers had minimal overlap in isotopic niche space, and niche space was smaller for teleosts than for rays (Fig. 5.3), despite that teleosts sampled comprised more species, and of different trophic ecologies (Abrantes & Sheaves 2009). Individual *P. ater* had the highest variability in stable isotope values and, consistently, *P. ater* had the largest niche size (standard ellipse area) among the four species with $n \geq 5$ (Fig. 5.4). The long-term niche size of *P. ater* was significantly larger than niche sizes of *G. typus* and *U. granulatus* (Fig. 5.4a). Although long-term niche size was also larger for *P. ater* than for *H. australis*, the 95 % credible intervals (CI) of these two species overlapped (Fig. 5.4a). *Glaucostegus typus* occupied the smallest niche space, with a distinctly smaller niche than *H. australis* and *P. ater*. The 95 % CI for *U. granulatus* niche size overlapped with *G. typus* and *H. australis* but had smaller niche space than *P. ater* (Fig. 5.4a). Short-

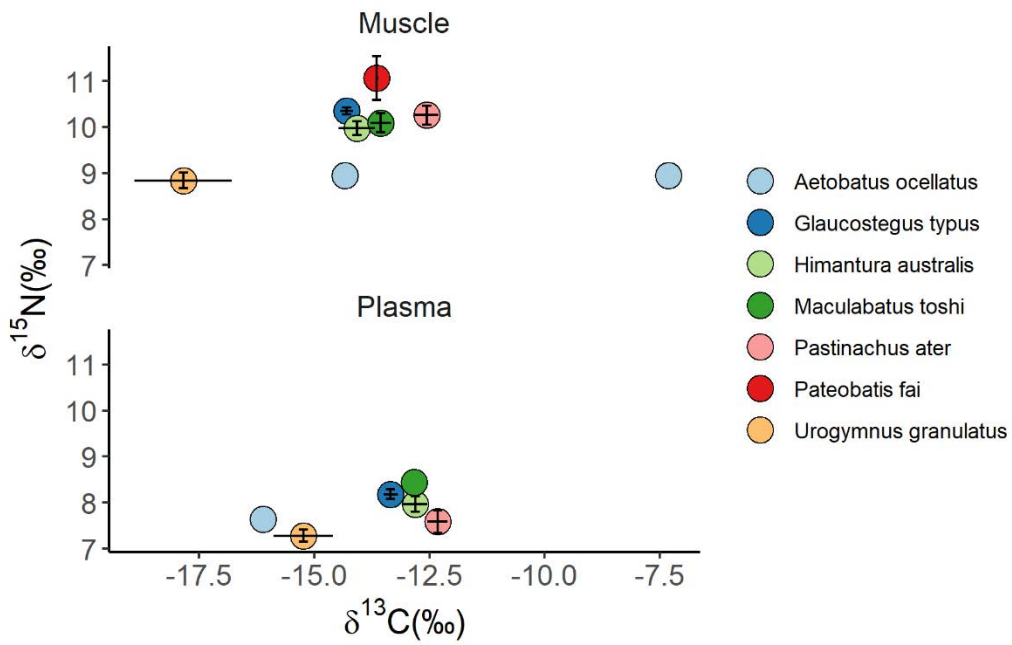


Figure 5.3 Mean \pm SE $\delta^{13}\text{C}$ and $\delta^{15}\text{N}$ for all ray species captured and sampled at Lucinda for both muscle and plasma tissues.

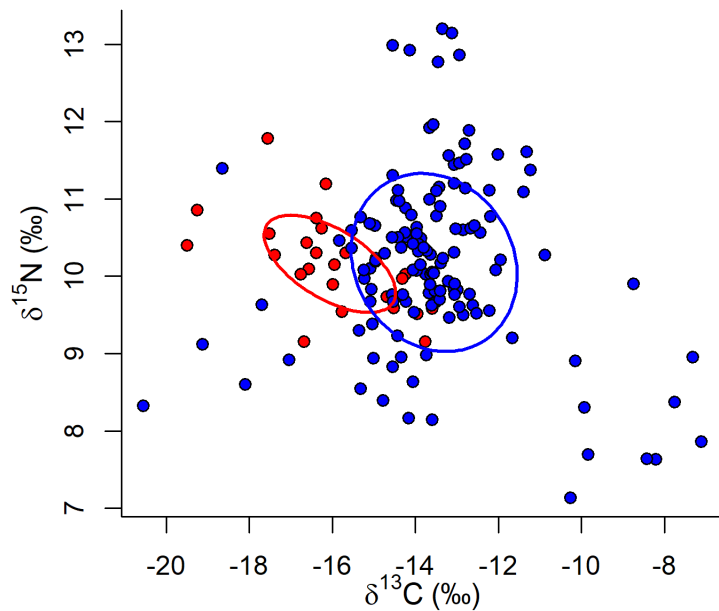


Figure 5.2 $\delta^{13}\text{C}$ and $\delta^{15}\text{N}$ values and standard ellipse areas (SEA) for all teleost carnivores (red) and rays (blue) sampled at Lucinda.

term niche sizes were similar to long-term sizes and showed the same pattern among species (Fig. 5.4). Short-term niche size of *P. ater* was significantly larger than those of the other four species, and

G. typus occupied the smallest niche space (Fig. 5.4b). As for long-term diets, short-term niche size of *G. typus* was smaller than *H. australis* and the 95 % credible interval overlapped with *U. granulatus*, which was only distinct from *P. ater* (Fig. 5.4b). For all species, SEA based on muscle tissue had the highest variability along the $\delta^{13}\text{C}$ axis indicated by $|\theta|$ closer to zero than to 90° (Table 5.2). Plasma ellipses also showed more variation along the $\delta^{13}\text{C}$ axis except for *P. ater* which showed the most variation in $\delta^{15}\text{N}$ ($\theta = 62.19^\circ$) (Table 5.2).

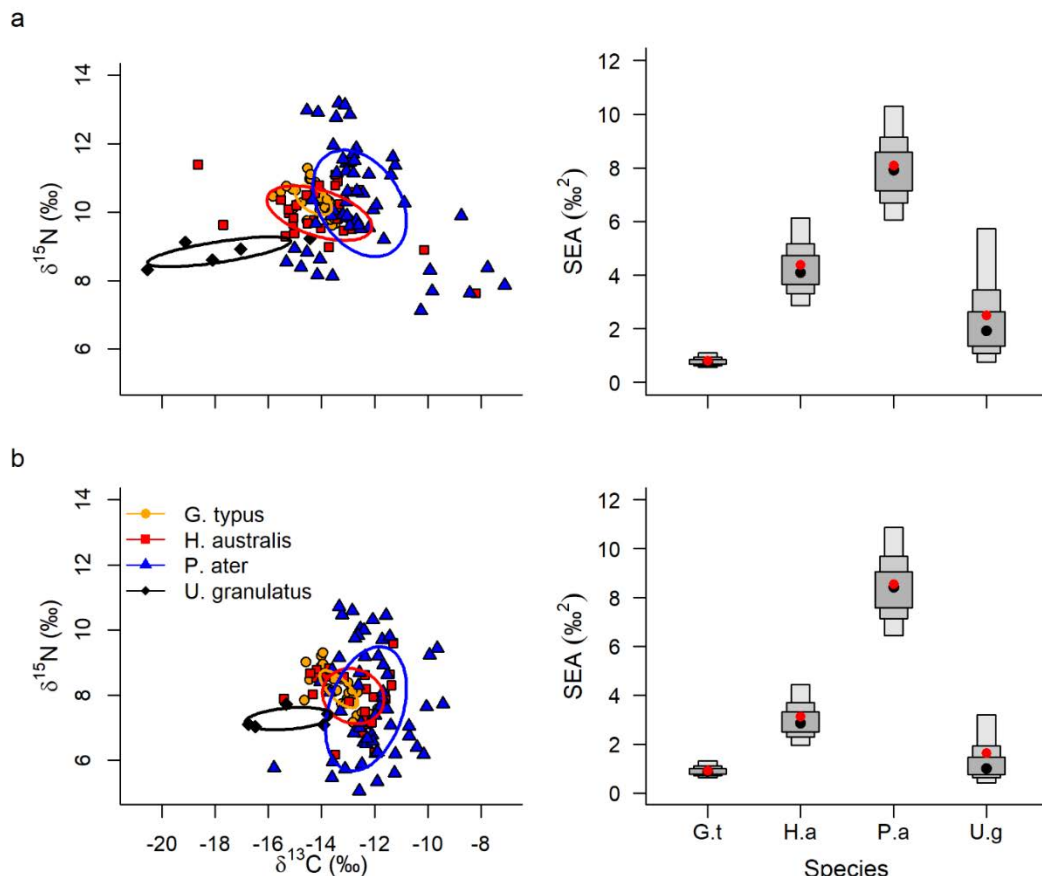


Figure 5.4 Left: $\delta^{13}\text{C}$ and $\delta^{15}\text{N}$ values and standard ellipse areas (SEA) for a) muscle and b) plasma tissues from *Glaucostegus typus* (G.t), *Himantura australis* (H.a), *Pastinachus ater* (P.a), and *Urogymnus granulatus* (U.g) sampled at Lucinda. Small sample size corrected SEA (SEAc) are presented for *U. granulatus* and legends are the same for both plots. Right: 50, 75, and 95 % Bayesian credible intervals for SEA for each species. Black dots show the mode SEA and red dots show the SEAc.

Analysis of niche sizes across years for *H. australis* and *P. ater* indicated that long-term niche size was similar over time. *Pastinachus ater* niche space was largest in 2018 but the 95 % CIs overlapped for all years (Fig. 5.5a). Similarly, *H. australis* niche size did not differ between 2017 and 2019 nor from *P. ater* niche size in either year (Fig. 5.5a). Over the short-term, *P. ater* again occupied

the largest niche space in 2018 and 95 % CIs overlapped for all years (Fig. 5.5b). Short-term niche space was consistent across years for *H. australis* and was smaller than *P. ater* niche space in both 2017 and 2019; however, the 95 % CIs overlapped between the two species in 2019 (Fig. 5.5b). The shape of *H. australis* ellipses (E) were similar across years for long term resource use, with most variability along the $\delta^{13}\text{C}$ axis (Table 5.3). Over the short-term, there was more variability along the $\delta^{15}\text{N}$ axis in 2017 ($\theta = 63.67^\circ$) and along the $\delta^{13}\text{C}$ axis in 2019 ($\theta = 21.80^\circ$) (Fig. 5.5b) (Table 5.3). Niche shape was more variable across years for *P. ater* (Fig. 5.5). Long-term resource use for individuals sampled in 2017 and 2018 showed more variation along the $\delta^{13}\text{C}$ axis whereas 2019 resource use varied more in $\delta^{15}\text{N}$. Over the short-term, *P. ater* resource use varied mostly along the $\delta^{15}\text{N}$ axis across years ($\theta > 72^\circ$).

Table 5.2 $\delta^{13}\text{C}$ and $\delta^{15}\text{N}$ stable isotope standard ellipse eccentricity (E) and semi-major axis angle (θ) from muscle and plasma tissues of juvenile *Glaucostegus typus*, *Himantura australis*, *Pastinachus ater*, and *Urogymnus granulatus*.

Species	Muscle		Plasma	
	E	θ	E	θ
<i>G. typus</i>	0.88	-23.01	0.92	-36.20
<i>H. australis</i>	0.94	-12.54	0.70	-9.46
<i>P. ater</i>	0.72	-34.82	0.75	62.19
<i>U. granulatus</i>	0.99	6.79	0.98	3.84

Table 5.3 $\delta^{13}\text{C}$ and $\delta^{15}\text{N}$ stable isotope standard ellipse eccentricity (E) and semi-major axis angle (θ) from muscle and plasma tissues of juvenile *Himantura australis* and *Pastinachus ater* from 2017–2019.

Species	Year	Muscle		Plasma	
		E	θ	E	θ
<i>H. australis</i>	2017	0.93	-14.18	0.93	63.67
	2019	0.95	-23.55	0.94	21.80
<i>P. ater</i>	2017	0.77	-28.57	0.71	74.06
	2018	0.55	-28.28	0.65	72.70
	2019	0.99	-54.01	0.92	87.82

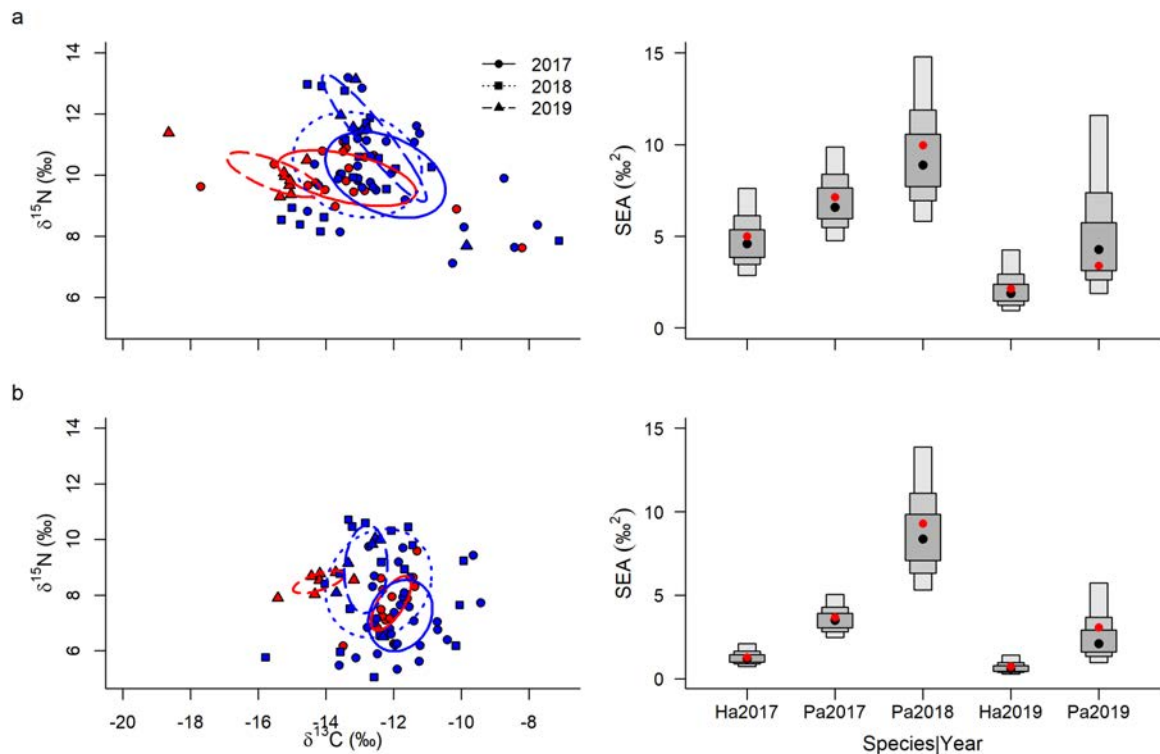


Figure 5.5 Left: $\delta^{13}\text{C}$ and $\delta^{15}\text{N}$ values and small sample size corrected standard ellipse areas (SEAc) for a) muscle and b) plasma tissues from *Himantura australis* (red) and *Pastinachus ater* (blue) sampled at Lucinda by year. Only two *H. australis* were sampled in 2018 and these samples are excluded from the plot. Right: 50, 75, and 95 % Bayesian credible intervals for SEAc for each species (*Ha* = *H. australis*, *Pa* = *P. ater*) and year combination. Black dots show the mode SEA and red dots show the SEAc.

Niche overlap

The probability of an individual of one species occurring in the niche space of another suggests that resource partitioning is occurring among rays at Lucinda (Fig. 5.4; Table 5.4). *Glaucostegus typus* individuals were most likely to occur in the niche space of *H. australis* and *P. ater*; however, these species had low probability of occurring within the niche space of *G. typus*, likely due to its small niche size (Fig. 5.4; Table 5.4). Overall, there was low probability of *P. ater* occurring in the niche space of any other species (Table 5.4). *Himantura australis* had the highest probability of overlapping with *P. ater* and the probability of overlap was higher for plasma than for muscle tissue (Table 5.4). The niche space of *U. granulatus* was separate from all other species with low probabilities (<3 %) of any other species occurring within its niche space and similarly low probabilities of *U. granulatus* occurring within the niche space any other species (Table 5.4).

Table 5.4 Probability (%) of species A falling within the niche space (standard ellipse area) of species B based on 10^4 estimated standard ellipse areas for muscle and plasma stable isotope values of *Glaucostegus typus*, *Himantura australis*, *Pastinachus ater*, and *Urogymnus granulatus*.

Tissue	Species A	Species B			
		<i>G. typus</i>	<i>H. australis</i>	<i>P. ater</i>	<i>U. granulatus</i>
Muscle	<i>G. typus</i>	-	68.0	44.6	0.2
	<i>H. australis</i>	8.1	-	41.0	1.7
	<i>P. ater</i>	2.9	14.8	-	0.7
	<i>U. granulatus</i>	0.0	4.1	4.8	-
Plasma	<i>G. typus</i>	-	53.0	53.9	1.3
	<i>H. australis</i>	11.7	-	66.3	3.0
	<i>P. ater</i>	3.4	13.4	-	1.5
	<i>U. granulatus</i>	0.9	7.5	15.5	-

Despite similar niche sizes across years, overlap probabilities support a trophic shift over time for both *H. australis* and *P. ater*. *Himantura australis* sampled in 2017 had a 7 % probability of occurring in the 2019 niche space based on long-term resource use and 0 % probability based on short-term resource use (Fig. 5.5; Table 5.5). Similarly, *H. australis* had 38.5 and 58.1 % probabilities of overlap with *P. ater* for long- and short-term resource use, respectively in 2017 whereas overlap probabilities decreased to 0.0 and 12.6 %, respectively in 2019 (Table 5.5). Individual *P. ater* were more likely to occur in the niche space of *H. australis* in 2017 than in 2019 (Table 5.5) and individuals sampled in both 2017 and 2019 were most likely to fall within 2018 niche space (Table 5.5).

Discussion

Stable isotope values of consumers and primary producers at the Lucinda sandflat support a foodweb consisting of ~3.3 trophic levels, with rays occupying similar trophic position to teleost carnivores. Despite having similar $\delta^{15}\text{N}$ values, there was minimal overlap between the trophic niches between rays and teleosts, suggesting the two groups have distinct trophic roles. Among ray species, niche size and relative position in isotopic niche space were similar for muscle and plasma tissues, suggesting resource use is restricted to the sandflat resource pool. Despite being limited to the sandflat, niche size and position in isotopic niche space varied among species and suggest resource partitioning is occurring. There were variable levels of niche overlap among juvenile *Glaucostegus typus*, *Himantura australis*, and *Pastinachus ater*, but *Urogymnus granulatus* occupied

the most unique niche space. Niche size also differed among species with *P. ater* having the largest trophic niche, suggesting they may be generalist foragers whereas *G. typus*, *U. granulatus*, and *H. australis* occupied smaller niche spaces and may forage on smaller resource pools or in specific areas. Results highlight that functional redundancy in mesopredator communities is complex and may be lower than expected based on simple trophic level comparisons. Consequently, the functional roles of mesopredators may be maintained by complementarity rather than redundancy, which raises concerns for response to disturbance.

Table 5.5 Probability (%) of an individual from group A falling within the standard ellipse niche space of group B based on 10^4 estimated standard ellipse areas. Overlap probabilities were only determined between species in the same years and across years within a species. Groups are coded by species (*H.a* = *Himantura australis* and *P.a* = *Pastinachus ater*) and year for muscle and plasma tissues.

Tissue	Group A	Group B				
		<i>H.a</i> 2017	<i>H.a</i> 2019	<i>P.a</i> 2017	<i>P.a</i> 2018	<i>P.a</i> 2019
Muscle	<i>H.a</i> 2017	-	7.0	38.5	-	-
	<i>H.a</i> 2019	16.3	-	-	-	0.0
	<i>P.a</i> 2017	23.7	-	-	39.3	9.9
	<i>P.a</i> 2018	-	-	26.7	-	8.6
	<i>P.a</i> 2019	-	0.0	32.8	35.5	-
Plasma	<i>H.a</i> 2017	-	0.0	58.1	-	-
	<i>H.a</i> 2019	0.0	-	-	-	12.6
	<i>P.a</i> 2017	12.6	-	-	40.9	5.8
	<i>P.a</i> 2018	-	-	13.0	-	9.8
	<i>P.a</i> 2019	-	2.2	7.8	66.6	-

Restricted movements of juvenile *H. australis*, *P. ater*, and *G. typus* within the sandflat boundary (Chapter 2) combined with only juveniles being captured at Lucinda supports that the sandflat is a nursery for multiple ray species (Martins *et al.* 2018). Residency to nursery areas is common among rays (Vaudo & Heithaus 2012; Cerutti-Pereyra *et al.* 2014; Martins *et al.* 2018) and, as such, diets are likely restricted to the range prey items available within the nursery (Dale *et al.* 2011). Multi-tissue stable isotope analysis can shed light on the consistency of resource use over varying time scales (Tieszen *et al.* 1983; Matich, Heithaus & Layman 2011; Yurkowski *et al.* 2016).

Although $\delta^{13}\text{C}$ and $\delta^{15}\text{N}$ values differed for muscle and plasma tissues of all ray species captured at Lucinda, the relative position of each species in isotopic niche space was similar for both tissues. Differences in isotope values among tissues from the same individual commonly occur due to tissue-specific fractionation and/or isotopic routing (Hussey *et al.* 2010; Kim *et al.* 2012) and may not reflect differences in diets. For example, Kim *et al.* (2012) determined that the diet-tissue discrimination factor for carbon ($\Delta^{13}\text{C}$) was lower in muscle than in plasma of leopard sharks (*Triakis semifasciata*) but $\Delta^{15}\text{N}$ was higher in plasma which is consistent with the tissue differences observed at Lucinda. Additionally, niche sizes representing short- and long-term resource use were similar for all ray species, supporting prolonged use of the same resource pool and residency to the sandflat.

Species sharing the same habitat can minimize competition and facilitate co-existence through resource partitioning (Davies *et al.* 2007). At Lucinda, there were medium to high levels of overlap among stable isotope niche spaces of *G. typus*, *H. australis*, and *P. ater*, but *U. granulatus* occupied distinct niche space. Examination of resource partitioning among sympatric rays using stable isotopes has shown high levels of overlap among species; however, analysis of stomach contents has revealed that prey groups are consumed in different quantities (Vaudo & Heithaus 2011; Elston *et al.* 2020). For example, juvenile *U. granulatus* in The Seychelles primarily consumed decapod crustaceans (Callianassidae and Portunidae) whereas *P. ater* diets consisted mostly of small bivalves (Elston *et al.* 2020). Consistently, these species may also partition resources based on space use as *U. granulatus* use mangrove habitats more often than *P. ater* (Davy, Simpfendorfer & Heupel 2015; Kanno *et al.* 2019; Martins *et al.* 2020). Although it is unclear if *U. granulatus* consume more mangrove derived nutrients, increased foraging in mangrove habitats would result in more negative $\delta^{13}\text{C}$ values; consistent with isotope values of *U. granulatus* and *P. ater* at Lucinda. Stomach contents of *H. australis* and *P. ater* in Western Australia also suggest resource partitioning which was not evident in their stable isotope values (Vaudo & Heithaus 2011; O'Shea *et al.* 2013). *Himantura australis* diets primarily consisted of brachyuran crabs and penaeid prawns whereas *P. ater* consumed mostly polychaetes in both Shark Bay, WA (Vaudo & Heithaus 2011) and Ningaloo, WA (O'Shea *et al.* 2013). In the present study, *H. australis* and *P. ater* foraged in different areas of the Lucinda sandflat (Chapter 2) and used different foraging behaviours (Chapter 3) which suggests that resources may be partitioned at a greater level than is evident in isotope values.

Resource partitioning between *P. ater* and *H. australis* was more evident when analysing samples across years. *Himantura australis* niche space had high overlap with *P. ater* in 2017 but occupied distinct niche space in 2019. *H. australis* had lower $\delta^{13}\text{C}$ in 2019, and short-term resource use indicated no overlap with 2017 diets. *Pastinachus ater* niche space shifted less across years, but also indicated a decrease in $\delta^{13}\text{C}$ from 2017 to 2019. Since results from Chapters 2 and 3 suggest that

foraging behaviour and habitat use of these two species were consistent over time, it is likely that prey preferences did not change over this period. Alternatively, the carbon sources used by invertebrate prey may have changed. Benthic feeding invertebrates often rely on multiple sources of primary production, depending on their relative availability (Bouillon *et al.* 2002; Kristensen, Kristensen & Mangion 2010; Abrantes *et al.* 2013) and the amounts of each source consumed will influence consumer $\delta^{13}\text{C}$ values. For example, increased reliance on mangrove-derived nutrients generally decreases $\delta^{13}\text{C}$ values in consumer tissues, while increased reliance of seagrass-derived nutrients would lead to an increase in $\delta^{13}\text{C}$ (Nabeel *et al.* 2010; Feng *et al.* 2014; Abrantes *et al.* 2015b). Although I cannot comment on the relative availability of the different primary producers at Lucinda over the study period, shifts in ray $\delta^{13}\text{C}$ could have resulted from shifts in availability of a particular producer (e.g. decrease in seagrass cover/increase mangrove cover), which could have affected *H. australis* prey more than *P. ater* prey.

Stingrays are continuous feeders (Gilliam & Sullivan 1993; Jacobsen & Bennett 2013) and consume large numbers of small prey throughout the day (Ebert & Cowley 2003; Pardo *et al.* 2015). The broad range in diets has led some to classify rays as ‘generalists’ (Gilliam & Sullivan 1993; Collins *et al.* 2007). Although the broad trophic niche of *P. ater* at Lucinda supports generalist foraging, the small niche size of *G. typus* suggests specialized use of a small resource pool. Previous studies have suggested that *P. ater* forages over wider areas than other species (Vaudo & Heithaus 2012; Cerutti-Pereyra *et al.* 2014), which may provide them access to a wider range of prey. Consistently, *P. ater* at Lucinda foraged over a broader sandflat area than *H. australis* (Chapters 2 and 3), and this was reflected in the isotopic niche sizes of the two species. Niche size of *H. australis* was intermediate between *G. typus* and *P. ater* but the intense localized foraging during flood and high tides (Chapter 2) suggests specialized foraging for *H. australis*. Although I cannot comment on prey densities at Lucinda, the high feeding rates of *H. australis* (Chapters 2 and 3) are also consistent with density dependent foraging observed for other rays (Hines *et al.* 1997; Ajemian, Powers & Murdoch 2012). Predator consumption rates are expected to increase with increasing prey density (Holling 1965; Eggleston, Lipcius & Hines 1992). In support, foraging rates for *H. australis* were high during flood and high tide periods but dropped at ebbing tides as rays moved out of core foraging areas, with minimal foraging occurring in other areas of the sandflat (Chapter 2). Foraging rates of *P. ater* were consistent throughout the tidal cycle suggesting prey may be distributed over larger areas but have lower densities.

Resource partitioning and different levels of specialist and generalist feeding of juvenile rays at Lucinda have important implications for the understanding of their trophic roles. Structural complexity is important for buffering disturbance in foodwebs, and species with more trophic

connections are deemed more important (Bornatowski *et al.* 2014; Navia *et al.* 2016). As a generalist forager, *P. ater* may have more links with primary invertebrates than ray species with more limited diets like *G. typus*. On the other hand, resource partitioning by specialist feeders may result in complementary trophic roles for species occupying distinct niche spaces (e.g. *U. granulatus*). Differences in abundance among ray species will also influence their trophic roles. Based on seine net catch rates and drone surveys of ray fauna (K. Crook unpublished data), *Pastinachus ater*, *H. australis*, and *G. typus* are abundant on the sandflat and may play stronger roles through increased top-down pressure on prey populations. Additionally, the higher feeding rate of *H. australis* (Chapters 2 and 3) suggests this species may have a disproportionately high impact on prey populations. All other ray species were caught/observed in low numbers; however, small or more cryptic species may be underrepresented due to the sampling methods.

As prey, rays are thought to be important for propagating indirect effects of top predator declines to lower trophic levels (Heithaus *et al.* 2008). Large sharks are commonly cited as ray predators (e.g. Vaudo and Heithaus (2013)) and rays are commonly found in diets of multiple shark species (Cliff & Dudley 1991; Cliff 1995; Simpfendorfer, Goodreid & McAuley 2001; Barnett *et al.* 2010a). In particular, rays may be important prey of great hammerhead sharks (*Sphyrna mokarran*) (Gallagher & Klimley 2018; Raoult *et al.* 2019). Although great hammerheads have been observed foraging in shallow intertidal areas (Roemer, Gallagher & Hammerschlag 2016), prey can gain refuge in shallow water as hammerhead swimming performance decreases in depths when the dorsal fin and tail are not completely submerged (Doan & Kajiura 2020). Although I did not perform comprehensive sampling of the Lucinda foodweb, large sharks were never observed (K. Crook pers. obs.) and are likely transient visitors, forming weak trophic links with juvenile rays. Rays may, however, form more important trophic links with large sharks as adults when they use deeper water. Teleost mesopredators, on the other hand, may be exposed to higher levels of predation from resident and transient piscivores (Baker & Sheaves 2009) and have more trophic connections in the sandflat foodweb. Indeed, topological analysis of complex foodwebs have illustrated that teleost mesopredators have a stronger influence on foodweb interactions than mesopredator elasmobranchs (Navia *et al.* 2016).

Results from this study suggest that trophic roles extend beyond simple assessments of trophic level and morphology. Rays and teleost carnivores occupied similar trophic levels, but the trophic niches of these two groups had minimal overlap, likely resulting from teleost mesopredators lacking the excavation capability of rays. Consequently, teleost mesopredators do not contribute to bioturbation and ecosystem engineering roles whereas the functional roles of rays extend beyond feeding interactions and are dominated by the physical structuring of benthic habitats (Chapter 3).

Resource partitioning identified in this Chapter suggests further differences in bioturbation and ecosystem engineering may exist among ray species due to limited overlap of *U. granulatus* resource use with other species and potentially specialized foraging by *G. typus*. Consequently, the functional roles cannot be assumed based solely on assumed trophic positions and trophic levels but are also dependent on complex interactions of diet and foraging behaviour.

Chapter 6: General Discussion

Synthesis of main results

The multi-methods approach applied in the present study provides the most comprehensive assessment to-date of the functional roles of rays in coastal sandflats. Existing studies have focused on broad ecosystem functions (e.g. trophic ecology, bioturbation) for a single species or treated all ray species as equals, particularly in terms of bioturbation roles (Flowers, Heithaus & Papastamatiou 2020). Although results from this study showed that sympatric rays contribute to the same broad-scale ecosystem functions, differences in habitat use (Chapter 2), foraging behaviour (Chapter 3), and resource use (Chapter 5) revealed that functional roles are complementary and are driven by species-specific behaviours (Fig. 6.1).

Rays at Lucinda made repeated tidal migrations between intertidal foraging areas and low tide resting areas (Chapter 2), suggesting that rays provide frequent energetic links between intertidal and subtidal zones. The frequent excavation of feeding pits confirms bioturbation and ecosystem engineering roles; however, differences in foraging intensity, behaviour, and habitat use among juvenile rays support functional complementarity (Chapters 2 and 3) (Fig. 6.1). Intense foraging and frequent use of disruptive foraging behaviours resulted in higher bioturbation rates for *H. australis* than for *P. ater* which favoured non-disruptive feeding (Chapter 3). Conversely, *H. australis* concentrated foraging activity in a small area, confining ecosystem engineering impacts to a small region whereas *P. ater* foraged over a broader area and may have a wider impact (Chapter 3) (Fig. 6.1).

The differences in foraging rate and habitat selection between *H. australis* and *P. ater* were reflected in their trophic niche sizes. *Pastinachus ater* had the largest niche space of all species supporting generalist feeding over a broad area (Chapter 5) but *H. australis* had a smaller niche and foraging rates were consistent with density dependent foraging. Resource partitioning was also evident in trophic niches of *Urogymnus granulatus* and *Glaucostegus typus*, suggesting bioturbation and ecosystem engineering roles may be further segregated among species (Chapter 5). In the overall sandflat foodweb, rays were positioned at similar trophic levels to teleost carnivores; however, rays occupied unique niche space (Chapter 5). This result is not unexpected as teleost carnivores have different feeding modes and lack the excavation capability of rays to access invertebrates buried deep in the sediment. Thus, rays not only occupy a unique trophic position, but bioturbation and ecosystem engineering roles are also unique among sandflat predators. Therefore, rays are keystone species on coastal sandflats and conservation of ray populations is crucial for maintaining sandflat ecosystem function.

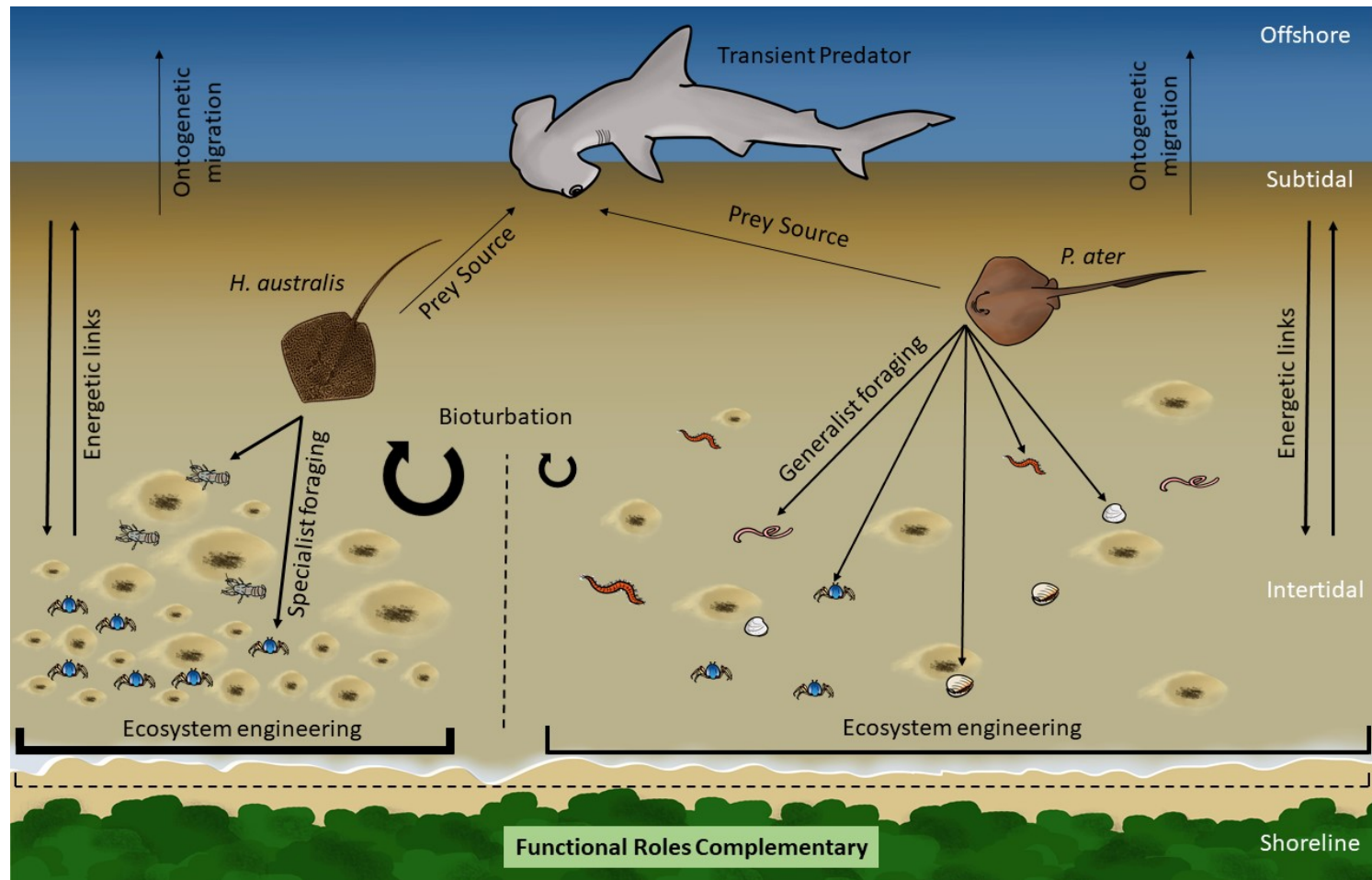


Figure 6.1 Conceptual diagram illustrating the functional roles of rays on coastal sandflats. Line thickness represents the relative impact of roles for *Himantura australis* (left) and *Pastinachus ater* (right). The width of ecosystem engineering lines represents the spatial scale over which roles are performed on sandflats for each species (solid lines) and for both species combined (dashed line). The vertical dashed line indicates foraging habitat partitioning. Ecosystem engineering roles include: the number and size of feeding pits, sediment turnover, habitat creation, and accumulation of detritus.

Beyond assessing the functional roles of rays in sandflats, this study showed that sandflats are essential habitats for juvenile rays. Rays at Lucinda restricted habitat use to within the sandflat boundary (Chapter 2) and resource use was consistent with the sandflat resource pool over the short- and long-term (Chapter 5). Combined with the fact that all rays observed, captured, and tracked were juveniles, results support that the Lucinda sandflat is a nursery area for multiple ray species. The flattened body shape of rays makes them well adapted to exploiting shallow sandflats that provide simultaneous refuge from predation and access to profitable foraging patches (Chapter 2). Consequently, the Lucinda sandflat may be high-value nursery area for rays and contribute a high number of recruits to offshore adult populations over the long-term (Fig. 6.1). Over the short-term, residency and repeated use of the same foraging habitats within the nursery suggest that significant ecosystem engineering occurs on an ongoing basis and likely has a structuring influence in coastal sandflats.

Roles of rays as ecosystem engineers

Ecosystem engineers are often considered keystone species due to their ability to physically modify habitats and alter ecosystem dynamics. For example, dam building by beavers (*Castor canadensis*) significantly alters stream and river flows and, consequently, creates new habitats, alters nutrient dynamics, and changes community composition (Naiman, Johnston & Kelley 1988; Burchsted & Daniels 2014). These new habitats are maintained on the scale of years to decades depending on environmental conditions and dam maintenance by beaver populations (Naiman, Johnston & Kelley 1988; Fryxell 2001). More frequent small-scale engineering activities can also have significant impacts on ecosystem dynamics. Persistent, year-round foraging activity of superb lyrebirds (*Menura novaehollandiae*) in Australian forests results in greater litter and soil turnover than for any other terrestrial engineer (Maisey *et al.* 2020). Like lyrebirds, juvenile rays at Lucinda forage repeatedly and intensely in the same areas and, like beavers, this engineering activity may alter the hydrodynamics of the system.

Sandflats and sandy beaches are dynamic habitats with malleable sediment that is constantly being re-worked by waves and tidal currents (Schlacher *et al.* 2008; 2015). Ray bioturbation has been considered trivial compared to erosion by tidal currents (Grant 1983); however, the significant quantities of sediment disturbed by foraging rays (Chapter 3) suggests otherwise. Indeed, conservative extrapolation (assuming foraging for 5hr per day) from the median bioturbation rate for individual *H. australis* suggests the sediment excavated by an individual ray may exceed $205.4\text{m}^3\text{yr}^{-1}$. Combined with high abundance of individuals, significant year-round foraging in the same areas by rays may not only be important for nutrient cycling but may physically

alter the hydrodynamics and topography of the sandflat through sandbank erosion. Indeed, recent expansion of the present study has documented sandbank erosion caused by *H. australis* excavation feeding may be altering the flow of a tropical estuary, overriding the traditional erosion processes in these systems (Bryce, Larcombe & Ridd 1998).

Sandflat resource pools are reliant on allochthonous subsidies from the marine environment (Spiller *et al.* 2010; Schlacher *et al.* 2013; 2015). In the absence of benthic structure, subsidies wash up and form wracks on the beach (Yager, Nowell & Jumars 1993; Spiller *et al.* 2010). As discussed in Chapter 3, ray pits increase habitat heterogeneity and accumulate detritus which is important for nutrient cycling and dispersal on sandflats (Vanblaricom 1982; D'Andrea, Aller & Lopez 2002). The amount and source of organic matter collected by pits is influenced by location (Polis, Anderson & Holt 1997; Eldridge & Mensinga 2007). In this regard, *P. ater* foraged over an area three times larger than *H. australis* (9 vs. 3 ha, respectively; Chapter 2), and therefore *P. ater* has a broader nutrient dispersal footprint. Furthermore, *P. ater* pits may capture more material coming from offshore due to their more seaward position whereas *H. australis* pits may accumulate more mangrove detritus from the adjacent developing mangrove forest (Chapters 2 and 3). The source of detritus accumulating in ray pits will affect nutrient cycling because decomposition rates differ among detrital sources (Rossi 2007; Crawshaw *et al.* 2019). Seagrass and macroalgal detritus have faster decomposition rates and contribute more to overall nutrient flux than mangrove detritus (Holmer & Olsen 2002; Rossi 2007), which may explain low reliance on mangrove-derived carbon among consumers at Lucinda (Chapter 5).

The accumulation, burial, and decomposition of detritus may form a positive feedback loop with ray foraging that has the potential to re-enforce and enhance ecosystem productivity. Ray pits remain on sandflats for periods of days to weeks depending on environmental conditions (Grant 1983; D'Andrea, Lopez & Aller 2004; O'Shea *et al.* 2012) and accumulate detritus at higher rates than the surrounding sediment (Vanblaricom 1982; Yager, Nowell & Jumars 1993). As pits are filled in, the accumulated detritus is buried and broken down by microbes and detritivores (Holmer & Olsen 2002; Rossi 2007; Crawshaw *et al.* 2019). At a future high tide, ray foraging will release the trapped nutrients and create a new feeding pit which will re-start the cycle. It is unclear how this process contributes to ecosystem function or productivity, but it is likely an influential process on nutrient cycling in unvegetated sand and mudflats.

In addition to influencing nutrient dynamics, ecosystem engineering can facilitate foraging opportunities for other species that are otherwise unavailable. Ray foraging fluidizes the sediment and can disturb or dislodge prey into the water column. Commensal foraging on disturbed prey has

been observed for double-crested cormorants (*Phalacrocorax auratus*) (Kajiura *et al.* 2009) and several teleost species (Vanblaricom 1982; Kiszka, Heithaus & Quod 2015). Anecdotal observations of fish following rays from drone tracks suggest that commensal relationships may also occur at Lucinda, although the outcomes of these events were not determined. Additionally, numerous invertebrate species were observed using ray pits while the sandflat was submerged, and in pits retaining water at low tide. The accumulation of detritus and water retention in ray pits may serve as low tide foraging refuges for both fish and invertebrates (O'Shea *et al.* 2012). How rays are facilitating access to prey resources (i.e. are these isolated, opportunistic events or is commensal foraging a repeated strategy) and the potential for pits to act as low tide refuges warrants future investigation.

Future directions

Ecosystem engineers can affect habitat heterogeneity at both patch and landscape scales (Wright & Jones 2006; Coverdale *et al.* 2016; Grossman, Hayward & Gibb 2019). Habitat heterogeneity is important in maintaining biodiversity and connectivity; therefore, it is critical to monitor the long-term effects of ecosystem engineers on habitat heterogeneity and structure at large spatial scales (Tews *et al.* 2004; Wright & Jones 2006; Parsons *et al.* 2016). In the present study, I quantified ecosystem engineering effects of juvenile rays at individual and species levels but did not quantify engineering at the sandflat scale which warrants further investigation. Ecosystem effects of beaver re-introductions in Europe have been determined using repeated drone surveys to map affected areas (Puttock *et al.* 2015). Similar mapping applications should be undertaken at sandflats with frequent ray foraging activity to monitor the effect of engineering activity on hydrodynamics and sandflat topography.

As discussed in Chapter 3, the density, type, and depth of invertebrate prey likely has a strong influence on the size and distribution of ray feeding pits. For example, Takeuchi and Tamaki (2014) found small feeding pits of red stingray (*Hemitrygon akajei*) foraging for ghost shrimp (Callianassidae) were concentrated in areas with high prey density. High prey density may decrease the foraging effort required to capture prey resulting in a smaller feeding pit. Alternatively, small pits may indicate prey is close to sediment surface. Establishing the relationship between prey density, prey type, prey depth, ray foraging behaviour, and pit size is critical for predicting the functional roles of rays across ecological contexts. In tropical Australia, invertebrate densities peak in the low intertidal, suggesting intertidal sand and mud flats are productive areas (Dittmann 2000; Sheaves, Dingle & Mattone 2016). Invertebrate hotspots are likely important foraging grounds for rays, supporting the intense, localised foraging of *H. australis* in a small area at Lucinda. Heterogeneous

distributions of prey are common in nature and patches with dense concentrations of animals are biologically and ecologically important (Polis, Anderson & Holt 1997; Davoren 2013). Direct links between ray foraging behaviour and prey type/density may allow biologically active areas to be identified by the presence of ray pits. Ray pits are conspicuous and commonly observed on sand and mudflats around the world (Myrick & Flessa 1996; Hines *et al.* 1997; D'Andrea, Lopez & Aller 2004; O'Shea *et al.* 2012; Takeuchi & Tamaki 2014). By linking the presence of ray pits with biological activity, managers may be able to quickly identify the ecological value of unvegetated habitats which will aid in decision making for coastal developments.

Although this study focussed intensely on a single sandflat, similarities in ray behaviour, habitat use, and community structure allow insights to be made across study sites. Multi-species ray assemblages are common in shallow coastal habitats around the globe (Vaudo & Heithaus 2009; Bishop *et al.* 2016; Elston *et al.* 2020). In Australia, ray communities in coastal areas share many of the same species (Vaudo & Heithaus 2009; Pierce, Scott-Holland & Bennett 2011; Cerutti-Pereyra *et al.* 2014; Kanno *et al.* 2019) and patterns in resource partitioning and habitat use are consistent across studies (Vaudo & Heithaus 2011; 2012; O'Shea *et al.* 2013; Cerutti-Pereyra *et al.* 2014; Martins *et al.* 2020) and with the present study. The integrated use of acoustic telemetry, drone tracking, and stable isotope analysis in the present study provided a comprehensive look at ray ecology on the sandflat and allowed direct conclusions to be made about behaviour and function. Evidence of resource and habitat partitioning of the same and closely related species in different ecological contexts suggests that functional roles may be consistent for ray species across sites. Given that movement and dietary information is already available from previous studies, addition of drone tracking to identify foraging behaviour, foraging habitats, and pit formation rates can fill in the gaps to quantify functional roles across multiple contexts.

Studies on movements and diets of stingrays (Dasyatidae) have mostly focussed on juveniles due to their abundance in coastal habitats (Vaudo & Heithaus 2009; Cerutti-Pereyra *et al.* 2014; Davy, Simpfendorfer & Heupel 2015) but there is limited information for adult rays. Separation of adult and juvenile habitats (Aguiar, Valentin & Rosa 2009) suggests that adults are involved in different foodwebs and, consequently, may have different functional roles. For example, shifts to deeper habitats by adult rays may expose them to higher levels of predation by large sharks which are more common in deeper waters (Heithaus 2007; Vaudo & Heithaus 2013). Additionally, studies have suggested that diets of rays change with ontogeny (Marshall, Kyne & Bennett 2008; Jacobsen & Bennett 2012). Juvenile prey selection is limited by gape size, a constraint that may be relieved with larger body size, leading to diet and habitat shifts in accordance with increased foraging ability or energetic requirements (Heithaus 2007; Dale *et al.* 2011; Lim *et al.* 2019). Increased gape size may

allow large individuals to consume large epibenthic crustaceans. Reliance on epibenthic prey would not require excavation, and, therefore, decrease bioturbation and ecosystem engineering functions that are driving the functional roles of juveniles. Consequently, identification of movement patterns, diets, and foraging behaviour of adult rays warrant investigation to establish how functional roles of rays change through ontogeny.

References

- Abenspergtraun, M., Dickman, C.R. & Deboer, E.S. (1991) Patch use and prey defense in a mammalian myrmecophage, the echidna (*Tachyglossus aculeatus*) (monotremata, tachyglossidae) - a test of foraging efficiency in captive and free-ranging animals. *Journal of Zoology*, **225**, 481-493. doi: 10.1111/j.1469-7998.1991.tb03830.x.
- Abrantes, K. & Sheaves, M. (2009) Food web structure in a near-pristine mangrove area of the Australian Wet Tropics. *Estuarine Coastal and Shelf Science*, **82**, 597-607. doi: 10.1016/j.ecss.2009.02.021.
- Abrantes, K.G. & Barnett, A. (2011) Intrapopulation variations in diet and habitat use in a marine apex predator, the broadnose sevengill shark *Notorynchus cepedianus*. *Marine Ecology Progress Series*, **442**, 133-148. doi: 10.3354/meps09395.
- Abrantes, K.G., Barnett, A., Baker, R. & Sheaves, M. (2015a) Habitat-specific food webs and trophic interactions supporting coastal-dependent fishery species: an Australian case study. *Reviews in Fish Biology and Fisheries*, **25**, 337-363. doi: 10.1007/s11160-015-9385-y.
- Abrantes, K.G., Barnett, A., Marwick, T.R. & Bouillon, S. (2013) Importance of terrestrial subsidies for estuarine food webs in contrasting East African catchments. *Ecosphere*, **4**, 33. doi: 10.1890/es12-00322.1.
- Abrantes, K.G., Johnston, R., Connolly, R.M. & Sheaves, M. (2015b) Importance of mangrove carbon for aquatic food webs in wet-dry tropical estuaries. *Estuaries and Coasts*, **38**, 383-399. doi: 10.1007/s12237-014-9817-2.
- Abrantes, K.G., Semmens, J.M., Lyle, J.M. & Nichols, P.D. (2012) Normalisation models for accounting for fat content in stable isotope measurements in salmonid muscle tissue. *Marine Biology*, **159**, 57-64. doi: 10.1007/s00227-011-1789-1.
- Aguiar, A.A., Valentin, J.L. & Rosa, R.S. (2009) Habitat use by *Dasyatis americana* in a south-western Atlantic oceanic island. *Journal of the Marine Biological Association of the United Kingdom*, **89**, 1147-1152. doi: 10.1017/s0025315409000058.
- Ajemian, M.J. & Powers, S.P. (2014) Towed-float satellite telemetry tracks large-scale movement and habitat connectivity of myliobatid stingrays. *Environmental Biology of Fishes*, **97**, 1067-1081. doi: 10.1007/s10641-014-0296-x.
- Ajemian, M.J. & Powers, S.P. (2016) Seasonality and ontogenetic habitat partitioning of cownose rays in the Northern Gulf of Mexico. *Estuaries and Coasts*, **39**, 1234-1248. doi: 10.1007/s12237-015-0052-2.

- Ajemian, M.J., Powers, S.P. & Murdoch, T.J.T. (2012) Estimating the potential impacts of large mesopredators on benthic resources: integrative assessment of spotted eagle ray foraging ecology in Bermuda. *PLoS ONE*, **7**, 17. doi: 10.1371/journal.pone.0040227.
- Albeke, S.E., Nibbelink, N.P. & Ben-David, M. (2015) Modeling behavior by coastal river otter (*Lontra canadensis*) in response to prey availability in Prince William Sound, Alaska: a spatially-explicit individual-based approach. *PLoS ONE*, **10**, 27. doi: 10.1371/journal.pone.0126208.
- Alerstam, T., Hedenstrom, A. & Akesson, S. (2003) Long-distance migration: evolution and determinants. *Oikos*, **103**, 247-260. doi: 10.1034/j.1600-0706.2003.12559.x.
- Allgeier, J.E., Yeager, L.A. & Layman, C.A. (2013) Consumers regulate nutrient limitation regimes and primary production in seagrass ecosystems. *Ecology*, **94**, 521-529. doi: 10.1890/12-1122.1.
- Alvarez, M.F., Addino, M., Iribarne, O. & Botto, F. (2015) Combined engineering effects of clams and crabs on infaunal assemblages and food availability in intertidal systems. *Marine Ecology Progress Series*, **540**, 57-71. doi: 10.3354/meps11478.
- Baker, R. & Sheaves, M. (2009) Overlooked small and juvenile piscivores dominate shallow-water estuarine "refuges" in tropical Australia. *Estuarine Coastal and Shelf Science*, **85**, 618-626. doi: 10.1016/j.ecss.2009.10.006.
- Barneche, D.R., Kulbicki, M., Floeter, S.R., Friedlander, A.M., Maina, J. & Allen, A.P. (2014) Scaling metabolism from individuals to reef-fish communities at broad spatial scales. *Ecology Letters*, **17**, 1067-1076. doi: 10.1111/ele.12309.
- Barnett, A., Abrantes, K., Stevens, J.D., Yick, J.L., Frusher, S.D. & Semmens, J.M. (2010a) Predator-prey relationships and foraging ecology of a marine apex predator with a wide temperate distribution. *Marine Ecology Progress Series*, **416**, 189-200. doi: 10.3354/meps08778.
- Barnett, A., Abrantes, K.G., Stevens, J.D. & Semmens, J.M. (2011) Site fidelity and sex-specific migration in a mobile apex predator: implications for conservation and ecosystem dynamics. *Animal Behaviour*, **81**, 1039-1048. doi: 10.1016/j.anbehav.2011.02.011.
- Barnett, A., Braccini, M., Dudgeon, C.L., Payne, N.L., Abrantes, K.G., Sheaves, M. & Snelling, E.P. (2017) The utility of bioenergetics modelling in quantifying predation rates of marine apex predators: ecological and fisheries implications. *Scientific Reports*, **7**, 10. doi: 10.1038/s41598-017-13388-y.
- Barnett, A., McAllister, J.D., Semmens, J., Abrantes, K., Sheaves, M. & Awruch, C. (2019) Identification of essential habitats: including chimaeras into current shark protected areas. *Aquatic Conservation-Marine and Freshwater Ecosystems*, **29**, 865-880. doi: 10.1002/aqc.3087.

- Barnett, A., Redd, K.S., Frusher, S.D., Stevens, J.D. & Semmens, J.M. (2010b) Non-lethal method to obtain stomach samples from a large marine predator and the use of DNA analysis to improve dietary information. *Journal of Experimental Marine Biology and Ecology*, **393**, 188-192. doi: 10.1016/j.jembe.2010.07.022.
- Barria, C., Coll, M. & Navarro, J. (2015) Unravelling the ecological role and trophic relationships of uncommon and threatened elasmobranchs in the western Mediterranean Sea. *Marine Ecology Progress Series*, **539**, 225-240. doi: 10.3354/meps11494.
- Bates, D., Machler, M., Bolker, B.M. & Walker, S.C. (2015) Fitting linear mixed-effects models using lme4. *Journal of Statistical Software*, **67**, 1-48. doi: 10.18637/jss.v067.i01.
- Bauer, S. & Hoye, B.J. (2014) Migratory animals couple biodiversity and ecosystem functioning worldwide. *Science*, **344**, 1242552. doi: 10.1126/science.1242552.
- Bearhop, S., Adams, C.E., Waldron, S., Fuller, R.A. & Macleod, H. (2004) Determining trophic niche width: a novel approach using stable isotope analysis. *Journal of Animal Ecology*, **73**, 1007-1012. doi: 10.1111/j.0021-8790.2004.00861.x.
- Beck, M.W., Heck, K.L., Able, K.W., Childers, D.L., Eggleston, D.B., Gillanders, B.M., Halpern, B., Hays, C.G., Hoshino, K., Minello, T.J., Orth, R.J., Sheridan, P.F. & Weinstein, M.R. (2001) The identification, conservation, and management of estuarine and marine nurseries for fish and invertebrates. *Bioscience*, **51**, 633-641. doi: 10.1641/0006-3568(2001)051[0633:Tcamo]2.0.Co;2.
- Bedford, J.J. (1983) The composition of the fluid compartments of two chondrichthyans, *Callorhynchus millii* and *Squalus acanthias*. *Comparative Biochemistry and Physiology, Part A: Molecular & Integrative Physiology*, **76**, 75-80.
- Bejarano, S., Jouffray, J.B., Chollett, I., Allen, R., Roff, G., Marshall, A., Steneck, R., Ferse, S.C.A. & Mumby, P.J. (2017) The shape of success in a turbulent world: wave exposure filtering of coral reef herbivory. *Functional Ecology*, **31**, 1312-1324. doi: 10.1111/1365-2435.12828.
- Bellwood, D.R. & Choat, J.H. (1990) A functional-analysis of grazing in parrotfishes (family scaridae) - the ecological implications. *Environmental Biology of Fishes*, **28**, 189-214. doi: 10.1007/bf00751035.
- Bellwood, D.R., Hoey, A.S. & Choat, J.H. (2003) Limited functional redundancy in high diversity systems: resilience and ecosystem function on coral reefs. *Ecology Letters*, **6**, 281-285. doi: 10.1046/j.1461-0248.2003.00432.x.
- Bellwood, D.R., Streit, R.P., Brandl, S.J. & Tebbett, S.B. (2019) The meaning of the term 'function' in ecology: a coral reef perspective. *Functional Ecology*, **33**, 948-961. doi: 10.1111/1365-2435.13265.

- Bellwood, D.R., Wainwright, P.C., Fulton, C.J. & Hoey, A.S. (2006) Functional versatility supports coral reef biodiversity. *Proceedings of the Royal Society B-Biological Sciences*, **273**, 101-107. doi: 10.1098/rspb.2005.3276.
- Benhamou, S. (2004) How to reliably estimate the tortuosity of an animal's path: straightness, sinuosity, or fractal dimension? *Journal of Theoretical Biology*, **229**, 209-220. doi: 10.1016/j.jtbi.2004.03.016.
- Bergman, C.M., Schaefer, J.A. & Luttich, S.N. (2000) Caribou movement as a correlated random walk. *Oecologia*, **123**, 364-374. doi: 10.1007/s004420051023.
- Berkstrom, C., Lindborg, R., Thyresson, M. & Gullstrom, M. (2013) Assessing connectivity in a tropical embayment: fish migrations and seascape ecology. *Biological Conservation*, **166**, 43-53. doi: 10.1016/j.biocon.2013.06.013.
- Bishop, J.M., Moore, A.B.M., Alsaffar, A.H. & Ghaffar, A.R.A. (2016) The distribution, diversity and abundance of elasmobranch fishes in a modified subtropical estuarine system in Kuwait. *Journal of Applied Ichthyology*, **32**, 75-82. doi: 10.1111/jai.12980.
- Blouin-Demers, G. & Weatherhead, P.J. (2001) An experimental test of the link between foraging, habitat selection and thermoregulation in black rat snakes *Elaphe obsoleta obsoleta*. *Journal of Animal Ecology*, **70**, 1006-1013. doi: 10.1046/j.0021-8790.2001.00554.x.
- Bodin, N., Le Loc'h, F. & Hily, C. (2007) Effect of lipid removal on carbon and nitrogen stable isotope ratios in crustacean tissues. *Journal of Experimental Marine Biology and Ecology*, **341**, 168-175. doi: 10.1016/j.jembe.2006.09.008.
- Bonaldo, R.M. & Bellwood, D.R. (2008) Size-dependent variation in the functional role of the parrotfish *Scarus rivulatus* on the Great Barrier Reef, Australia. *Marine Ecology Progress Series*, **360**, 237-244. doi: 10.3354/meps07413.
- Bond, A.L., Jardine, T.D. & Hobson, K.A. (2016) Multi-tissue stable-isotope analyses can identify dietary specialization. *Methods in Ecology and Evolution*, **7**, 1428-1437. doi: 10.1111/2041-210x.12620.
- Bornatowski, H., Navia, A.F., Braga, R.R., Abilhoa, V. & Correa, M.F.M. (2014) Ecological importance of sharks and rays in a structural foodweb analysis in southern Brazil. *ICES Journal of Marine Science*, **71**, 1586-1592. doi: 10.1093/icesjms/fsu025.
- Bouillon, S., Koedam, N., Raman, A.V. & Dehairs, F. (2002) Primary producers sustaining macro-invertebrate communities in intertidal mangrove forests. *Oecologia*, **130**, 441-448. doi: 10.1007/s004420100814.

- Boyd, T.A., Cha, C.J., Forster, R.P. & Goldstein, L. (1977) Free amino acids in tissues of the skate *Raja erinacea* and the stingray *Dasyatis sabina*: effects of environmental dilution. *Journal of Experimental Zoology*, **199**, 435-442. doi: 10.1002/jez.1401990318.
- Brandl, S.J. & Bellwood, D.R. (2014) Individual-based analyses reveal limited functional overlap in a coral reef fish community. *Journal of Animal Ecology*, **83**, 661-670. doi: 10.1111/1365-2656.12171.
- Brenner, M. & Krumme, U. (2007) Tidal migration and patterns in feeding of the four-eyed fish *Anableps anableps* L. in a north Brazilian mangrove. *Journal of Fish Biology*, **70**, 406-427. doi: 10.1111/j.1095-8649.2007.01313.x.
- Bretsch, K. & Allen, D.M. (2006) Tidal migrations of nekton in salt marsh intertidal creeks. *Estuaries and Coasts*, **29**, 474-486. doi: 10.1007/bf02784995.
- Bryce, S., Larcombe, P. & Ridd, P.V. (1998) The relative importance of landward-directed tidal sediment transport versus freshwater flood events in the Normanby River estuary, Cape York Peninsula, Australia. *Marine Geology*, **149**, 55-78. doi: 10.1016/s0025-3227(98)00013-9.
- Buelow, C. & Sheaves, M. (2015) A birds-eye view of biological connectivity in mangrove systems. *Estuarine Coastal and Shelf Science*, **152**, 33-43. doi: 10.1016/j.ecss.2014.10.014.
- Burchsted, D. & Daniels, M.D. (2014) Classification of the alterations of beaver dams to headwater streams in northeastern Connecticut, USA. *Geomorphology*, **205**, 36-50. doi: 10.1016/j.geomorph.2012.12.029.
- Burgess, K.B. & Bennett, M.B. (2017) Effects of ethanol storage and lipid and urea extraction on $\delta^{15}\text{N}$ and $\delta^{13}\text{C}$ isotope ratios in a benthic elasmobranch, the bluespotted maskray *Neotrygon kuhlii*. *Journal of Fish Biology*, **90**, 417-423. doi: 10.1111/jfb.13164.
- Burkepile, D.E. & Hay, M.E. (2008) Herbivore species richness and feeding complementarity affect community structure and function on a coral reef. *Proceedings of the National Academy of Sciences of the United States of America*, **105**, 16201-16206. doi: 10.1073/pnas.0801946105.
- Byers, J.E., Cuddington, K., Jones, C.G., Talley, T.S., Hastings, A., Lambrinos, J.G., Crooks, J.A. & Wilson, W.G. (2006) Using ecosystem engineers to restore ecological systems. *Trends in Ecology & Evolution*, **21**, 493-500. doi: 10.1016/j.tree.2006.06.002.
- Cain, D.K., Harms, C.A. & Segars, A. (2004) Plasma biochemistry reference values of wild-caught southern stingrays (*Dasyatis americana*). *Journal of Zoo and Wildlife Medicine*, **35**, 471-476. doi: 10.1638/03-107.
- Calenge, C. (2006) The package "adehabitat" for the R software: a tool for the analysis of space and habitat use by animals. *Ecological Modelling*, **197**, 516-519. doi: 10.1016/j.ecolmodel.2006.03.017.

- Carlisle, A.B., Litvin, S.Y., Madigan, D.J., Lyons, K., Bigman, J.S., Ibarra, M. & Bizarro, J.J. (2017) Interactive effects of urea and lipid content confound stable isotope analysis in elasmobranch fishes. *Canadian Journal of Fisheries and Aquatic Sciences*, **74**, 419-428. doi: 10.1139/cjfas-2015-0584.
- Castellanos-Galindo, G.A., Krumme, U. & Willis, T.J. (2010) Tidal influences on fish distributions on tropical eastern Pacific rocky shores (Colombia). *Marine Ecology Progress Series*, **416**, 241-254. doi: 10.3354/meps08768.
- Cerutti-Pereyra, F., Thums, M., Austin, C.M., Bradshaw, C.J.A., Stevens, J.D., Babcock, R.C., Pillans, R.D. & Meekan, M.G. (2014) Restricted movements of juvenile rays in the lagoon of Ningaloo Reef, Western Australia - evidence for the existence of a nursery. *Environmental Biology of Fishes*, **97**, 371-383. doi: 10.1007/s10641-013-0158-y.
- Chapman, J.W., Reynolds, D.R. & Wilson, K. (2015) Long-range seasonal migration in insects: mechanisms, evolutionary drivers and ecological consequences. *Ecology Letters*, **18**, 287-302. doi: 10.1111/ele.12407.
- Charnov, E.L. (1976) Optimal foraging - attack strategy of a mantid. *American Naturalist*, **110**, 141-151. doi: 10.1086/283054.
- Chin, A., Heupel, M.R., Simpfendorfer, C.A. & Tobin, A.J. (2013) Ontogenetic movements of juvenile blacktip reef sharks: evidence of dispersal and connectivity between coastal habitats and coral reefs. *Aquatic Conservation-Marine and Freshwater Ecosystems*, **23**, 468-474. doi: 10.1002/aqc.2349.
- Churchill, D.A., Heithaus, M.R. & Grubbs, R.D. (2015) Effects of lipid and urea extraction on $\delta^{15}\text{N}$ values of deep-sea sharks and hagfish: can mathematical correction factors be generated? *Deep-Sea Research Part II Topical Studies in Oceanography*, **115**, 103-108. doi: 10.1016/j.dsr2.2014.12.013.
- Clark, T.J., Bonnet-Lebrun, A.S., Campioni, L., Catry, P. & Wakefield, E. (2019) The depth of sooty shearwater *Ardenna grisea* burrows varies with habitat and increases with competition for space. *Ibis*, **161**, 192-197. doi: 10.1111/ibi.12631.
- Cliff, G. (1995) Sharks caught in the protective gill nets off Kwazulu-Natal, South-Africa .8. the great hammerhead shark *Sphyrna mokarran* (Ruppell). *South African Journal of Marine Science-Suid-Afrikaanse Tydskrif Vir Seewetenskap*, **15**, 105-114.
- Cliff, G. & Dudley, S.F.J. (1991) Sharks caught in the protective gill nets off Natal, South-Africa .4. the bull shark *Carcharhinus leucas* Valenciennes. *South African Journal of Marine Science-Suid-Afrikaanse Tydskrif Vir Seewetenskap*, **10**, 253-270.

- Coleman, F.C. & Williams, S.L. (2002) Overexploiting marine ecosystem engineers: potential consequences for biodiversity. *Trends in Ecology & Evolution*, **17**, 40-44. doi: 10.1016/s0169-5347(01)02330-8.
- Collins, A.B., Heupel, M.R., Hueter, R.E. & Motta, P.J. (2007) Hard prey specialists or opportunistic generalists? an examination of the diet of the cownose ray, *Rhinoptera bonasus*. *Marine and Freshwater Research*, **58**, 135-144. doi: 10.1071/mf05227.
- Collins, A.B., Heupel, M.R. & Simpfendorfer, C.A. (2008) Spatial distribution and long-term movement patterns of cownose rays *Rhinoptera bonasus* within an estuarine river. *Estuaries and Coasts*, **31**, 1174-1183. doi: 10.1007/s12237-008-9100-5.
- Corp, N., Gorman, M.L. & Speakman, J.R. (1997) Ranging behaviour and time budgets of male wood mice *Apodemus sylvaticus* in different habitats and seasons. *Oecologia*, **109**, 242-250. doi: 10.1007/s004420050079.
- Coverdale, T.C., Kartzinel, T.R., Grabowski, K.L., Shriner, R.K., Hassan, A.A., Goheen, J.R., Palmer, T.M. & Pringle, R.M. (2016) Elephants in the understory: opposing direct and indirect effects of consumption and ecosystem engineering by megaherbivores. *Ecology*, **97**, 3219-3230. doi: 10.1002/ecy.1557.
- Crawshaw, J., O'Meara, T., Savage, C., Thomson, B., Baltar, F. & Thrush, S.F. (2019) Source of organic detritus and bivalve biomass influences nitrogen cycling and extracellular enzyme activity in estuary sediments. *Biogeochemistry*, **145**, 315-335. doi: 10.1007/s10533-019-00608-y.
- Crook, K.A., Barnett, A., Sheaves, M. & Abrantes, K. (2019) Effects of lipid and urea extraction on stable isotope values ($\delta^{13}\text{C}$ and $\delta^{15}\text{N}$) of two batoids: A call for more species-specific investigations. *Limnology and Oceanography-Methods*, **17**, 565-574. doi: 10.1002/lom3.10333.
- D'Andrea, A.F., Aller, R.C. & Lopez, G.R. (2002) Organic matter flux and reactivity on a South Carolina sandflat: the impacts of porewater advection and macrobiological structures. *Limnology and Oceanography*, **47**, 1056-1070. doi: 10.4319/lo.2002.47.4.1056.
- D'Andrea, A.F., Lopez, G.R. & Aller, R.C. (2004) Rapid physical and biological particle mixing on an intertidal sandflat. *Journal of Marine Research*, **62**, 67-92. doi: 10.1357/00222400460744627.
- Dabruzz, T.F., Bennett, W.A., Rummer, J.L. & Fangue, N.A. (2013) Juvenile ribbontail stingray, *Taeniura lymma* (Forsskål, 1775) (Chondrichthyes, Dasyatidae), demonstrate a unique suite of physiological adaptations to survive hyperthermic nursery conditions. *Hydrobiologia*, **701**, 37-49. doi: 10.1007/s10750-012-1249-z.

- Dale, J.J., Drazen, J.C. & Holland, K.N. (2013) Stingray life history trade-offs associated with nursery habitat use inferred from a bioenergetics model. *Marine Biology*, **160**, 3181-3192. doi: 10.1007/s00227-013-2305-6.
- Dale, J.J., Wallsgrove, N.J., Popp, B.N. & Holland, K.N. (2011) Nursery habitat use and foraging ecology of the brown stingray *Dasyatis lata* determined from stomach contents, bulk and amino acid stable isotopes. *Marine Ecology Progress Series*, **433**, 221-236. doi: 10.3354/meps09171.
- Davidson, A.D., Detling, J.K. & Brown, J.H. (2012) Ecological roles and conservation challenges of social, burrowing, herbivorous mammals in the world's grasslands. *Frontiers in Ecology and the Environment*, **10**, 477-486. doi: 10.1890/110054.
- Davies, T.J., Meiri, S., Barraclough, T.G. & Gittleman, J.L. (2007) Species co-existence and character divergence across carnivores. *Ecology Letters*, **10**, 146-152. doi: 10.1111/j.1461-0248.2006.01005.x.
- Davoren, G. (2013) Distribution of marine predator hotspots explained by persistent areas of prey. *Marine Biology*, **160**, 3043-3058. doi: 10.1007/s00227-013-2294-5.
- Davoren, G.K., Montevecchi, W.A. & Anderson, J.T. (2003) Search strategies of a pursuit-diving marine bird and the persistence of prey patches. *Ecological Monographs*, **73**, 463-481. doi: 10.1890/02-0208.
- Davy, L.E., Simpfendorfer, C.A. & Heupel, M.R. (2015) Movement patterns and habitat use of juvenile mangrove whiprays (*Himantura granulata*). *Marine and Freshwater Research*, **66**, 481-492. doi: 10.1071/mf14028.
- Dean, M.N., Bizarro, J.J. & Summers, A.P. (2007) The evolution of cranial design, diet, and feeding mechanisms in batoid fishes. *Integrative and Comparative Biology*, **47**, 70-81. doi: 10.1093/icb/icm034.
- Dean, M.N. & Motta, P.J. (2004) Feeding behavior and kinematics of the lesser electric ray, *Narcine brasiliensis* (Elasmobranchii : Batoidea). *Zoology*, **107**, 171-189. doi: 10.1016/j.zool.2004.04.002.
- Degraaf, R.M., Tilghman, N.G. & Anderson, S.H. (1985) Foraging guilds of North American birds. *Environmental Management*, **9**, 493-536. doi: 10.1007/bf01867324.
- Dehling, D.M., Jordano, P., Schaefer, H.M., Bohning-Gaese, K. & Schleuning, M. (2016) Morphology predicts species' functional roles and their degree of specialization in plant-frugivore interactions. *Proceedings of the Royal Society B-Biological Sciences*, **283**, 7. doi: 10.1098/rspb.2015.2444.

- DeNiro, M.J. & Epstein, S. (1978) Influence of diet on the distribution of carbon isotopes in animals. *Geochimica et Cosmochimica Acta*, **42**, 495-506.
- DeNiro, M.J. & Epstein, S. (1981) Influence of diet on the distribution of nitrogen isotopes in animals. *Geochimica et Cosmochimica Acta*, **45**, 341-351.
- Dittmann, S. (2000) Zonation of benthic communities in a tropical tidal flat of north-east Australia. *Journal of Sea Research*, **43**, 33-51. doi: 10.1016/s1385-1101(00)00004-6.
- Doan, M.D. & Kajiura, S.M. (2020) Adult blacktip sharks (*Carcharhinus limbatus*) use shallow water as a refuge from great hammerheads (*Sphyrna mokarran*). *Journal of Fish Biology*, **96**, 1530-1533. doi: 10.1111/jfb.14342.
- Dobush, G.R., Ankney, C.D. & Krementz, D.G. (1985) The effect of apparatus, extraction time, and solvent type on lipid extractions of snow geese. *Canadian Journal of Zoology*, **63**, 1917-1920. doi: 10.1139/z85-285.
- Doucette, J.L., Wissel, B. & Somers, C.M. (2010) Effects of lipid extraction and lipid normalization on stable carbon and nitrogen isotope ratios in double-crested cormorants: implications for food web studies. *Waterbirds*, **33**, 273-284. doi: 10.1675/063.033.0302.
- Dulvy, N.K., Fowler, S.L., Musick, J.A., Cavanagh, R.D., Kyne, P.M., Harrison, L.R., Carlson, J.K., Davidson, L.N.K., Fordham, S.V., Francis, M.P., Pollock, C.M., Simpfendorfer, C.A., Burgess, G.H., Carpenter, K.E., Compagno, L.J.V., Ebert, D.A., Gibson, C., Heupel, M.R., Livingstone, S.R., Sanciangco, J.C., Stevens, J.D., Valenti, S. & White, W.T. (2014) Extinction risk and conservation of the world's sharks and rays. *eLife*, **3**, 34. doi: 10.7554/eLife.00590.
- Dulvy, N.K., Simpfendorfer, C.A., Davidson, L.N.K., Fordham, S.V., Brautigam, A., Sant, G. & Welch, D.J. (2017) Challenges and priorities in shark and ray conservation. *Current Biology*, **27**, R565-R572. doi: 10.1016/j.cub.2017.04.038.
- Dunne, J.A., Williams, R.J. & Martinez, N.D. (2004) Network structure and robustness of marine food webs. *Marine Ecology Progress Series*, **273**, 291-302. doi: 10.3354/meps273291.
- Ebert, D.A. & Cowley, P.D. (2003) Diet, feeding behaviour and habitat utilisation of the blue stingray *Dasyatis chrysonota* (Smith, 1828) in South African waters. *Marine and Freshwater Research*, **54**, 957-965. doi: 10.1071/mf03069.
- Egginton, D.B., Lipcius, R.N. & Hines, A.H. (1992) Density-dependent predation by blue crabs upon infaunal clam species with contrasting distribution and abundance patterns. *Marine Ecology Progress Series*, **85**, 55-68. doi: 10.3354/meps085055.
- Eldridge, D.J. & Mensinga, A. (2007) Foraging pits of the short-beaked echidna (*Tachyglossus aculeatus*) as small-scale patches in a semi-arid Australian box woodland. *Soil Biology & Biochemistry*, **39**, 1055-1065. doi: 10.1016/j.soilbio.2006.11.016.

- Elliott, K.H., Davis, M. & Elliott, J.E. (2014) Equations for lipid normalization of carbon stable isotope ratios in aquatic bird eggs. *PLoS ONE*, **9**, e83597. doi: 10.1371/journal.pone.0083597.
- Elliott, M., Whitfield, A.K., Potter, I.C., Blaber, S.J.M., Cyrus, D.P., Nordlie, F.G. & Harrison, T.D. (2007) The guild approach to categorizing estuarine fish assemblages: a global review. *Fish and Fisheries*, **8**, 241-268. doi: 10.1111/j.1467-2679.2007.00253.x.
- Elmhagen, B. & Rushton, S.P. (2007) Trophic control of mesopredators in terrestrial ecosystems: top-down or bottom-up? *Ecology Letters*, **10**, 197-206. doi: 10.1111/j.1461-0248.2006.01010.x.
- Eloranta, A.P., Knudsen, R. & Amundsen, P.A. (2013) Niche segregation of coexisting Arctic charr (*Salvelinus alpinus*) and brown trout (*Salmo trutta*) constrains food web coupling in subarctic lakes. *Freshwater Biology*, **58**, 207-221. doi: 10.1111/fwb.12052.
- Elston, C., Cowley, P.D., von Brandis, R.G. & Fisk, A. (2020) Dietary niche differentiation in a mesopredatory dasyatid assemblage. *Marine Biology*, **167**, 89. doi:
- Elston, C., von Brandis, R.G. & Cowley, P.D. (2015) Gastric lavage as a non-lethal method for stingray (Myliobatiformes) diet sampling. *African Journal of Marine Science*, **37**, 415-419. doi: 10.2989/1814232x.2015.1076519.
- Enquist, B.J., Norberg, J., Bonser, S.P., Violette, C., Webb, C.T., Henderson, A., Sloat, L.L. & Savage, V.M. (2015) Scaling from traits to ecosystems: developing a general trait driver theory via integrating trait-based and metabolic scaling theories. *Advances in Ecological Research, Vol 52: Trait-Based Ecology - from Structure to Function* (eds S. Pawar, G. Woodward & A.I. Dell), pp. 249-318. Elsevier Academic Press Inc, San Diego.
- Fangue, N.A. & Bennett, W.A. (2003) Thermal tolerance responses of laboratory-acclimated and seasonally acclimatized Atlantic stingray, *Dasyatis sabina*. *Copeia*, 315-325.
- Feng, J.X., Guo, J.M., Huang, Q., Jiang, J.X., Huang, G.M., Yang, Z.W. & Lin, G.H. (2014) Changes in the community structure and diet of benthic macrofauna in invasive *Spartina alterniflora* wetlands following restoration with native mangroves. *Wetlands*, **34**, 673-683. doi: 10.1007/s13157-014-0533-2.
- Flowers, K.I., Heithaus, M.R. & Papastamatiou, Y.P. (2020) Buried in the sand: uncovering the ecological roles and importance of rays. *Fish and Fisheries*, doi: 10.1111/faf.12508.
- Folke, C., Carpenter, S., Walker, B., Scheffer, M., Elmqvist, T., Gunderson, L. & Holling, C.S. (2004) Regime shifts, resilience, and biodiversity in ecosystem management. *Annual Review of Ecology Evolution and Systematics*, **35**, 557-581. doi: 10.1146/annurev.ecolsys.35.021103.105711.
- Francis, F.T. & Cote, I.M. (2018) Fish movement drives spatial and temporal patterns of nutrient provisioning on coral reef patches. *Ecosphere*, **9**, 14. doi: 10.1002/ecs2.2225.

- Friedlaender, A.S., Bowers, M.T., Cade, D., Hazen, E.L., Stimpert, A.K., Allen, A.N., Calambokidis, J., Fahlbusch, J., Segre, P., Visser, F., Southall, B.L. & Goldbogen, J.A. (2020) The advantages of diving deep: fin whales quadruple their energy intake when targeting deep krill patches. *Functional Ecology*, **34**, 497-506. doi: 10.1111/1365-2435.13471.
- Frisk, M.G., Jordaan, A. & Miller, T.J. (2014) Moving beyond the current paradigm in marine population connectivity: are adults the missing link? *Fish and Fisheries*, **15**, 242-254. doi: 10.1111/faf.12014.
- Fryxell, J.M. (2001) Habitat suitability and source-sink dynamics of beavers. *Journal of Animal Ecology*, **70**, 310-316. doi: 10.1046/j.1365-2656.2001.00492.x.
- Fryxell, J.M., Greever, J. & Sinclair, A.R.E. (1988) Why are migratory ungulates so abundant. *American Naturalist*, **131**, 781-798. doi: 10.1086/284822.
- Gallagher, A.J. & Klimley, A.P. (2018) The biology and conservation status of the large hammerhead shark complex: the great, scalloped, and smooth hammerheads. *Reviews in Fish Biology and Fisheries*, **28**, 777-794. doi: 10.1007/s11160-018-9530-5.
- Gallagher, A.J., Papastamatiou, Y.P. & Barnett, A. (2018) Apex predatory sharks and crocodiles simultaneously scavenge a whale carcass. *Journal of Ethology*, **36**, 205-209. doi: 10.1007/s10164-018-0543-2.
- Gannes, L.Z., del Rio, C.M. & Koch, P. (1998) Natural abundance variations in stable isotopes and their potential uses in animal physiological ecology. *Comparative Biochemistry and Physiology, Part A: Molecular & Integrative Physiology*, **119**, 725-737. doi: 10.1016/s1095-6433(98)01016-2.
- Gibson, R.N. (2003) Go with the flow: tidal migration in marine animals. *Hydrobiologia*, **503**, 153-161. doi: 10.1023/b:hydr.0000008488.33614.62.
- Gihwala, K.N., Pillay, D. & Varughese, M. (2017) Differential impacts of foraging plasticity by greater flamingo *Phoenicopterus roseus* on intertidal soft sediments. *Marine Ecology Progress Series*, **569**, 227-242. doi: 10.3354/meps12069.
- Gilliam, D. & Sullivan, K.M. (1993) Diet and feeding-habits of the southern stingray *Dasyatis americana* in the central Bahamas. *Bulletin of Marine Science*, **52**, 1007-1013.
- Gladstone-Gallagher, R.V., Lohrer, A.M., Lundquist, C.J. & Pilditch, C.A. (2016) Effects of detrital subsidies on soft-sediment ecosystem function are transient and source-dependent. *PLoS ONE*, **11**, 18. doi: 10.1371/journal.pone.0154790.
- Grant, J. (1983) The relative magnitude of biological and physical sediment reworking in an intertidal community. *Journal of Marine Research*, **41**, 673-689. doi: 10.1357/002224083788520469.

- Grossman, B.F., Hayward, M.W. & Gibb, H. (2019) An experimental test of the multi-scalar impacts of digging mammal reintroductions on invertebrate burrows. *Soil Biology & Biochemistry*, **132**, 101-110. doi: 10.1016/j.soilbio.2019.02.003.
- Hammerschlag, N. (2006) Osmoregulation in elasmobranchs: a review for fish biologists, behaviourists and ecologists. *Marine and Freshwater Behaviour and Physiology*, **39**, 209-228. doi: 10.1080/10236240600815820.
- Harris, R.J., Pilditch, C.A., Greenfield, B.L., Moon, V. & Kroncke, I. (2016) The influence of benthic macrofauna on the erodibility of intertidal sediments with varying mud content in three New Zealand estuaries. *Estuaries and Coasts*, **39**, 815-828. doi: 10.1007/s12237-015-0036-2.
- Haussmann, N.S. (2017) Soil movement by burrowing mammals: a review comparing excavation size and rate to body mass of excavators. *Progress in Physical Geography*, **41**, 29-45. doi: 10.1177/0309133316662569.
- Hazon, N., Wells, A., Pillans, R.D., Good, J.P., Anderson, W.G. & Franklin, C.E. (2003) Urea based osmoregulation and endocrine control in elasmobranch fish with special reference to euryhalinity. *Comparative Biochemistry and Physiology, Part B: Biochemistry & Molecular Biology*, **136**, 685-700. doi: 10.1016/s1096-4959(03)00280-x.
- Heithaus, M.R. (2007) Nursery areas as essential shark habitats: a theoretical perspective. *American Fisheries Society Symposium*, **50**, 3-13.
- Heithaus, M.R., Frid, A., Wirsing, A.J. & Worm, B. (2008) Predicting ecological consequences of marine top predator declines. *Trends in Ecology & Evolution*, **23**, 202-210. doi: 10.1016/j.tree.2008.01.003.
- Heithaus, M.R., Vaudo, J.J., Kreicker, S., Layman, C.A., Krutzen, M., Burkholder, D.A., Gastrich, K., Bessey, C., Sarabia, R., Cameron, K., Wirsing, A., Thomson, J.A. & Dunphy-Daly, M.M. (2013) Apparent resource partitioning and trophic structure of large-bodied marine predators in a relatively pristine seagrass ecosystem. *Marine Ecology Progress Series*, **481**, 225-237. doi: 10.3354/meps10235.
- Heupel, M.R., Carlson, J.K. & Simpfendorfer, C.A. (2007) Shark nursery areas: concepts, definition, characterization and assumptions. *Marine Ecology Progress Series*, **337**, 287-297. doi: 10.3354/meps337287.
- Heupel, M.R., Kanno, S., Martins, A.P.B. & Simpfendorfer, C.A. (2019) Advances in understanding the roles and benefits of nursery areas for elasmobranch populations. *Marine and Freshwater Research*, **70**, 897-907. doi: 10.1071/mf18081.
- Heupel, M.R., Knip, D.M., Simpfendorfer, C.A. & Dulvy, N.K. (2014) Sizing up the ecological role of sharks as predators. *Marine Ecology Progress Series*, **495**, 291-298. doi: 10.3354/meps10597.

- Hight, B.V. & Lowe, C.G. (2007) Elevated body temperatures of adult female leopard sharks, *Triakis semifasciata*, while aggregating in shallow nearshore embayments: evidence for behavioral thermoregulation? *Journal of Experimental Marine Biology and Ecology*, **352**, 114-128. doi: 10.1016/j.jembe.2007.07.021.
- Hines, A.H., Whitlatch, R.B., Thrush, S.F., Hewitt, J.E., Cummings, V.J., Dayton, P.K. & Legendre, P. (1997) Nonlinear foraging response of a large marine predator to benthic prey: eagle ray pits and bivalves in a New Zealand sandflat. *Journal of Experimental Marine Biology and Ecology*, **216**, 191-210. doi: 10.1016/s0022-0981(97)00096-8.
- Hobson, K.A., Alisauskas, R.T. & Clark, R.G. (1993) Stable-nitrogen isotope enrichment in avian-tissues due to fasting and nutritional stress - implications for isotopic analyses of diet. *Condor*, **95**, 388-394. doi: 10.2307/1369361.
- Hoegh-Guldberg, O., Mumby, P.J., Hooten, A.J., Steneck, R.S., Greenfield, P., Gomez, E., Harvell, C.D., Sale, P.F., Edwards, A.J., Caldeira, K., Knowlton, N., Eakin, C.M., Iglesias-Prieto, R., Muthiga, N., Bradbury, R.H., Dubi, A. & Hatziolos, M.E. (2007) Coral reefs under rapid climate change and ocean acidification. *Science*, **318**, 1737-1742. doi: 10.1126/science.1152509.
- Hoey, A.S. & Bellwood, D.R. (2009) Limited functional redundancy in a high diversity system: single species dominates key ecological process on coral reefs. *Ecosystems*, **12**, 1316-1328. doi: 10.1007/s10021-009-9291-z.
- Holling, C.S. (1965) The functional response of predators to prey density and its role in mimicry and population regulation. *The Memoirs of the Entomological Society of Canada*, **97**, 5-60.
- Holmer, M. & Olsen, A.B. (2002) Role of decomposition of mangrove and seagrass detritus in sediment carbon and nitrogen cycling in a tropical mangrove forest. *Marine Ecology Progress Series*, **230**, 87-101. doi: 10.3354/meps230087.
- Hughes, T.P., Baird, A.H., Bellwood, D.R., Card, M., Connolly, S.R., Folke, C., Grosberg, R., Hoegh-Guldberg, O., Jackson, J.B.C., Kleypas, J., Lough, J.M., Marshall, P., Nystrom, M., Palumbi, S.R., Pandolfi, J.M., Rosen, B. & Roughgarden, J. (2003) Climate change, human impacts, and the resilience of coral reefs. *Science*, **301**, 929-933. doi: 10.1126/science.1085046.
- Hughes, T.P., Kerry, J.T., Baird, A.H., Connolly, S.R., Dietzel, A., Eakin, C.M., Heron, S.F., Hoey, A.S., Hoogenboom, M.O., Liu, G., McWilliam, M.J., Pears, R.J., Pratchett, M.S., Skirving, W.J., Stella, J.S. & Torda, G. (2018) Global warming transforms coral reef assemblages. *Nature*, **556**, 492-496. doi: 10.1038/s41586-018-0041-2.
- Hussey, N.E., Brush, J., McCarthy, I.D. & Fisk, A.T. (2010) $\delta^{15}\text{N}$ and $\delta^{13}\text{C}$ diet-tissue discrimination factors for large sharks under semi-controlled conditions. *Comparative Biochemistry and*

Physiology, Part A: Molecular & Integrative Physiology, **155**, 445-453. doi:

10.1016/j.cbpa.2009.09.023.

- Hussey, N.E., MacNeil, M.A., Olin, J.A., McMeans, B.C., Kinney, M.J., Chapman, D.D. & Fisk, A.T. (2012a) Stable isotopes and elasmobranchs: tissue types, methods, applications and assumptions. *Journal of Fish Biology*, **80**, 1449-1484. doi: 10.1111/j.1095-8649.2012.03251.x.
- Hussey, N.E., Olin, J.A., Kinney, M.J., McMeans, B.C. & Fisk, A.T. (2012b) Lipid extraction effects on stable isotope values ($\delta^{13}\text{C}$ and $\delta^{15}\text{N}$) of elasmobranch muscle tissue. *Journal of Experimental Marine Biology and Ecology*, **434**, 7-15. doi: 10.1016/j.jembe.2012.07.012.
- Jackson, A.L., Inger, R., Parnell, A.C. & Bearhop, S. (2011) Comparing isotopic niche widths among and within communities: SIBER - Stable Isotope Bayesian Ellipses in R. *Journal of Animal Ecology*, **80**, 595-602. doi: 10.1111/j.1365-2656.2011.01806.x.
- Jacobsen, I.P. & Bennett, M.B. (2012) Feeding ecology and dietary comparisons among three sympatric *Neotrygon* (Myliobatoidei: Dasyatidae) species. *Journal of Fish Biology*, **80**, 1580-1594. doi: 10.1111/j.1095-8649.2011.03169.x.
- Jacobsen, I.P. & Bennett, M.B. (2013) A comparative analysis of feeding and trophic level ecology in stingrays (Rajiformes; Myliobatoidei) and electric rays (Rajiformes: Torpedinoidei). *PLoS ONE*, **8**, 10. doi: 10.1371/journal.pone.0071348.
- Jax, K. (2005) Function and "functioning" in ecology: what does it mean? *Oikos*, **111**, 641-648. doi: 10.1111/j.1600-0706.2005.13851.x.
- Jones, C.G., Lawton, J.H. & Shachak, M. (1997) Positive and negative effects of organisms as physical ecosystem engineers. *Ecology*, **78**, 1946-1957. doi: 10.1890/0012-9658(1997)078[1946:Paneeoo]2.0.Co;2.
- Kahle, D. & Wickham, H. (2013) ggmap: spatial visualization with ggplot2. *R Journal*, **5**, 144-161. doi: 10.32379/rj.2013.05.01.10000.
- Kajiura, S.M., Macesic, L.J., Meredith, T.L., Cocks, K.L. & Dirk, L.J. (2009) Commensal foraging between double-crested cormorants and a southern stingray. *Wilson Journal of Ornithology*, **121**, 646-648. doi: 10.1676/08-122.1.
- Kanno, S., Schlaff, A.M., Heupel, M.R. & Simpfendorfer, C.A. (2019) Stationary video monitoring reveals habitat use of stingrays in mangroves. *Marine Ecology Progress Series*, **621**, 155-168. doi: 10.3354/meps12977.
- Karlson, A.M.L., Gorokhova, E. & Elmgren, R. (2015) Do deposit-feeders compete? Isotopic niche analysis of an invasion in a species-poor system. *Scientific Reports*, **5**, 8. doi: 10.1038/srep09715.
- Kaufman, T.J., Pajuelo, M., Bjorndal, K.A., Bolten, A.B., Pfaller, J.B., Williams, K.L. & Vander Zanden, H.B. (2014) Mother-egg stable isotope conversions and effects of lipid extraction and

ethanol preservation on loggerhead eggs. *Conservation Physiology*, **2**, 13. doi: 10.1093/conphys/cou049.

Kiljunen, M., Grey, J., Sinisalo, T., Harrod, C., Immonen, H. & Jones, R.I. (2006) A revised model for lipid-normalizing $\delta^{13}\text{C}$ values from aquatic organisms, with implications for isotope mixing models. *Journal of Applied Ecology*, **43**, 1213-1222. doi: 10.1111/j.1365-2664.2006.01224.x.

Kim, S.L., Casper, D.R., Galvan-Magana, F., Ochoa-Diaz, R., Hernandez-Aguilar, S.B. & Koch, P.L. (2012) Carbon and nitrogen discrimination factors for elasmobranch soft tissues based on a long-term controlled feeding study. *Environmental Biology of Fishes*, **95**, 37-52. doi: 10.1007/s10641-011-9919-7.

Kim, S.L. & Koch, P.L. (2012) Methods to collect, preserve, and prepare elasmobranch tissues for stable isotope analysis. *Environmental Biology of Fishes*, **95**, 53-63. doi: 10.1007/s10641-011-9860-9.

Kirby, J.S., Stattersfield, A.J., Butchart, S.H.M., Evans, M.I., Grimmett, R.F.A., Jones, V.R., O'Sullivan, J., Tucker, G.M. & Newton, I. (2008) Key conservation issues for migratory land- and waterbird species on the world's major flyways. *Bird Conservation International*, **18**, S49-S73. doi: 10.1017/s0959270908000439.

Kiszka, J.J., Heithaus, M.R. & Quod, J.P. (2015) Stingrays as possible facilitators for foraging trevallies in a nearshore sandflat. *Marine Biodiversity*, **45**, 625-626. doi: 10.1007/s12526-014-0304-6.

Kristensen, D.K., Kristensen, E. & Mangion, P. (2010) Food partitioning of leaf-eating mangrove crabs (Sesarminae): experimental and stable isotope ($\delta^{13}\text{C}$ and $\delta^{15}\text{N}$) evidence. *Estuarine Coastal and Shelf Science*, **87**, 583-590. doi: 10.1016/j.ecss.2010.02.016.

Krumme, U. (2009) Diel and tidal movements by fish and decapods linking tropical coastal ecosystems. *Ecological Connectivity among Tropical Coastal Ecosystems* (ed. I. Nagelkerken), pp. 271-324. Springer Netherlands, Dordrecht.

Krumme, U., Saint-Paul, U. & Rosenthal, H. (2004) Tidal and diel changes in the structure of a nekton assemblage in small intertidal mangrove creeks in northern Brazil. *Aquatic Living Resources*, **17**, 215-229. doi: 10.1051/alr:2004019.

Last, P., Naylor, G., Séret, B., White, W., de Carvalho, M. & Stehmann, M. (2016) *Rays of the World*. CSIRO publishing.

Lazar, B., Gracan, R., Katic, J., Zavodnik, D., Jaklin, A. & Tvrkovic, N. (2011) Loggerhead sea turtles (*Caretta caretta*) as bioturbators in neritic habitats: an insight through the analysis of benthic molluscs in the diet. *Marine Ecology-an Evolutionary Perspective*, **32**, 65-74. doi: 10.1111/j.1439-0485.2010.00402.x.

- Lellys, N.T., de Moura, R.L., Bonaldo, R.M., Francini, R.B. & Gibran, F.Z. (2019) Parrotfish functional morphology and bioerosion on SW Atlantic reefs. *Marine Ecology Progress Series*, **629**, 149-163. doi: 10.3354/meps13102.
- Lemons, G.E., Eguchi, T., Lyon, B.N., LeRoux, R. & Seminoff, J.A. (2012) Effects of blood anticoagulants on stable isotope values of sea turtle blood tissue. *Aquatic Biology*, **14**, 201-206. doi: 10.3354/ab00397.
- Li, Y.K., Zhang, Y.Y., Hussey, N.E. & Dai, X.J. (2016) Urea and lipid extraction treatment effects on $\delta^{15}\text{N}$ and $\delta^{13}\text{C}$ values in pelagic sharks. *Rapid Communications in Mass Spectrometry*, **30**, 1-8. doi: 10.1002/rcm.7396.
- Lim, K.C., Chong, V.C., Lim, P.E., Yurimoto, T. & Loh, K.H. (2019) Feeding ecology of three sympatric species of stingrays on a tropical mudflat. *Journal of the Marine Biological Association of the United Kingdom*, **99**, 999-1007. doi: 10.1017/s0025315418000759.
- Logan, J.M., Jardine, T.D., Miller, T.J., Bunn, S.E., Cunjak, R.A. & Lutcavage, M.E. (2008) Lipid corrections in carbon and nitrogen stable isotope analyses: comparison of chemical extraction and modelling methods. *Journal of Animal Ecology*, **77**, 838-846. doi: 10.1111/j.1365-2656.2008.01394.x.
- Logan, J.M. & Lutcavage, M.E. (2010) Stable isotope dynamics in elasmobranch fishes. *Hydrobiologia*, **644**, 231-244. doi: 10.1007/s10750-010-0120-3.
- Lohrer, A.M., Thrush, S.F. & Gibbs, M.M. (2004) Bioturbators enhance ecosystem function through complex biogeochemical interactions. *Nature*, **431**, 1092-1095. doi: 10.1038/nature03042.
- Lohrer, A.M., Townsend, M., Hailes, S.F., Rodil, I.F., Cartner, K., Pratt, D.R. & Hewitt, J.E. (2016) Influence of New Zealand cockles (*Austrovenus stutchburyi*) on primary productivity in sandflat-seagrass (*Zostera muelleri*) ecotones. *Estuarine Coastal and Shelf Science*, **181**, 238-248. doi: 10.1016/j.ecss.2016.08.045.
- Lopez-Fernandez, H., Arbour, J., Willis, S., Watkins, C., Honeycutt, R.L. & Winemiller, K.O. (2014) Morphology and efficiency of a specialized foraging behavior, sediment sifting, in neotropical cichlid fishes. *PLoS ONE*, **9**, 9. doi: 10.1371/journal.pone.0089832.
- Lorrain, A., Paulet, Y.M., Chauvaud, L., Savoye, N., Donval, A. & Saout, C. (2002) Differential $\delta^{13}\text{C}$ and $\delta^{15}\text{N}$ signatures among scallop tissues: implications for ecology and physiology. *Journal of Experimental Marine Biology and Ecology*, **275**, 47-61. doi: 10.1016/s0022-0981(02)00220-4.
- Lotze, H.K., Lenihan, H.S., Bourque, B.J., Bradbury, R.H., Cooke, R.G., Kay, M.C., Kidwell, S.M., Kirby, M.X., Peterson, C.H. & Jackson, J.B.C. (2006) Depletion, degradation, and recovery potential of estuaries and coastal seas. *Science*, **312**, 1806-1809. doi: 10.1126/science.1128035.

- Madigan, D.J., Brooks, E.J., Bond, M.E., Gelsleichter, J., Howey, L.A., Abercrombie, D.L., Brooks, A. & Chapman, D.D. (2015) Diet shift and site-fidelity of oceanic whitetip sharks *Carcharhinus longimanus* along the Great Bahama Bank. *Marine Ecology Progress Series*, **529**, 185-197. doi: 10.3354/meps11302.
- Maire, E., Grenouillet, G., Brosse, S. & Villeger, S. (2015) How many dimensions are needed to accurately assess functional diversity? A pragmatic approach for assessing the quality of functional spaces. *Global Ecology and Biogeography*, **24**, 728-740. doi: 10.1111/geb.12299.
- Maisey, A.C., Haslem, A., Leonard, S.W.J. & Bennett, A.F. (2020) Foraging by an avian ecosystem engineer extensively modifies the litter and soil layer in forest ecosystems. *Ecological Applications*, e02219. doi: 10.1002/eap.2219.
- Maitland, D.P. & Maitland, A. (1992) Penetration of water into blind-ended capillary tubes and its bearing on the functional design of the lungs of soldier crabs *Mictyris longicarpus*. *Journal of Experimental Biology*, **163**, 333-344. doi:
- Malpica-Cruz, L., Herzka, S.Z., Sosa-Nishizaki, O. & Lazo, J.P. (2012) Tissue-specific isotope trophic discrimination factors and turnover rates in a marine elasmobranch: empirical and modeling results. *Canadian Journal of Fisheries and Aquatic Sciences*, **69**, 551-564. doi: 10.1139/f2011-172.
- Marshall, A.D., Kyne, P.M. & Bennett, M.B. (2008) Comparing the diet of two sympatric urolophid elasmobranchs (*Trygonoptera testacea* Muller & Henle and *Urolophus kapalensis* Yearsley & Last): evidence of ontogenetic shifts and possible resource partitioning. *Journal of Fish Biology*, **72**, 883-898. doi: 10.1111/j.1095-8649.2007.01762.x.
- Marshall, G., Bakhtiari, M., Shepard, M., Tweedy, J., Rasch, D., Abernathy, K., Joliff, B., Carrier, J.C. & Heithaus, M.R. (2007) An advanced solid-state animal-borne video and environmental data-logging Device ("CRITTERCAM") for marine research. *Marine Technology Society Journal*, **41**, 31-38. doi: 10.4031/002533207787442240.
- Martin, T.L. & Huey, R.B. (2008) Why "Suboptimal" is optimal: Jensen's inequality and ectotherm thermal preferences. *American Naturalist*, **171**, E102-E118. doi: 10.1086/527502.
- Martins, A.P.B., Heupel, M.R., Bierwagen, S.L., Chin, A. & Simpfendorfer, C. (2020) Diurnal activity patterns and habitat use of juvenile *Pastinachus ater* in a coral reef flat environment. *PLoS ONE*, **15**, e0228280. doi: 10.1371/journal.pone.0228280.
- Martins, A.P.B., Heupel, M.R., Chin, A. & Simpfendorfer, C.A. (2018) Batoid nurseries: definition, use and importance. *Marine Ecology Progress Series*, **595**, 253-267. doi: 10.3354/meps12545.

- Matich, P., Heithaus, M.R. & Layman, C.A. (2011) Contrasting patterns of individual specialization and trophic coupling in two marine apex predators. *Journal of Animal Ecology*, **80**, 294-305. doi: 10.1111/j.1365-2656.2010.01753.x.
- McNicholl, D.G., Davoren, G.K., Majewski, A.R. & Reist, J.D. (2018) Isotopic niche overlap between co-occurring capelin (*Mallotus villosus*) and polar cod (*Boreogadus saida*) and the effect of lipid extraction on stable isotope ratios. *Polar Biology*, **41**, 423-432. doi: 10.1007/s00300-017-2199-8.
- Mermilliod-Blondin, F. & Rosenberg, R. (2006) Ecosystem engineering: the impact of bioturbation on biogeochemical processes in marine and freshwater benthic habitats. *Aquatic Sciences*, **68**, 434-442. doi: 10.1007/s00027-006-0858-x.
- Meyer, C.G., Papastamatiou, Y.P. & Holland, K.N. (2007) Seasonal, diel, and tidal movements of green jobfish (*Aprion virescens*, Lutjanidae) at remote Hawaiian atolls: implications for marine protected area design. *Marine Biology*, **151**, 2133-2143. doi: 10.1007/s00227-007-0647-7.
- Meysman, F.J.R., Middelburg, J.J. & Heip, C.H.R. (2006) Bioturbation: a fresh look at Darwin's last idea. *Trends in Ecology & Evolution*, **21**, 688-695. doi: 10.1016/j.tree.2006.08.002.
- Moran-Lopez, T., Gonzalez-Castro, A., Morales, J.M. & Nogales, M. (2020) Behavioural complementarity among frugivorous birds and lizards can promote plant diversity in island ecosystems. *Functional Ecology*, **34**, 182-193. doi: 10.1111/1365-2435.13476.
- Mouillot, D., Graham, N.A.J., Villeger, S., Mason, N.W.H. & Bellwood, D.R. (2013) A functional approach reveals community responses to disturbances. *Trends in Ecology & Evolution*, **28**, 167-177. doi: 10.1016/j.tree.2012.10.004.
- Mouillot, D., Villeger, S., Parravicini, V., Kulbicki, M., Arias-Gonzalez, J.E., Bender, M., Chabanet, P., Floeter, S.R., Friedlander, A., Vigliola, L. & Bellwood, D.R. (2014) Functional over-redundancy and high functional vulnerability in global fish faunas on tropical reefs. *Proceedings of the National Academy of Sciences of the United States of America*, **111**, 13757-13762. doi: 10.1073/pnas.1317625111.
- Mulas, A., Bellodi, A., Cannas, R., Carbonara, P., Cau, A., Marongiu, M.F., Pesci, P., Porcu, C. & Follesa, M.C. (2019) Resource partitioning among sympatric elasmobranchs in the central-western Mediterranean continental shelf. *Marine Biology*, **166**, 16. doi: 10.1007/s00227-019-3607-0.
- Mumby, P.J. (2006) Connectivity of reef fish between mangroves and coral reefs: algorithms for the design of marine reserves at seascape scales. *Biological Conservation*, **128**, 215-222. doi: 10.1016/j.biocon.2005.09.042.

- Murray, F., Douglas, A. & Solan, M. (2014) Species that share traits do not necessarily form distinct and universally applicable functional effect groups. *Marine Ecology Progress Series*, **516**, 23-34. doi: 10.3354/meps11020.
- Murry, B.A., Farrell, J.M., Teece, M.A. & Smyntek, P.M. (2006) Effect of lipid extraction on the interpretation of fish community trophic relationships determined by stable carbon and nitrogen isotopes. *Canadian Journal of Fisheries and Aquatic Sciences*, **63**, 2167-2172. doi: 10.1139/f06-116.
- Myrick, J.L. & Flessa, K.W. (1996) Bioturbation rates in Bahia La Choya, Sonora, Mexico. *Ciencias Marinas*, **22**, 23-46.
- Nabeel, M.A., Kathiresan, K., Rajendran, N., Ohnishi, H., Hamaoka, H. & Omori, K. (2010) Contribution by microbes to the foodweb of a mangrove biotope: the approach of carbon and nitrogen stable isotopes. *African Journal of Marine Science*, **32**, 65-70. doi: 10.2989/18142321003714492.
- Nagelkerken, I., Sheaves, M., Baker, R. & Connolly, R.M. (2015) The seascape nursery: a novel spatial approach to identify and manage nurseries for coastal marine fauna. *Fish and Fisheries*, **16**, 362-371. doi: 10.1111/faf.12057.
- Naiman, R.J., Johnston, C.A. & Kelley, J.C. (1988) Alteration of North American streams by beaver. *Bioscience*, **38**, 753-762. doi: 10.2307/1310784.
- Navia, A.F., Cortes, E. & Mejia-Falla, P.A. (2010) Topological analysis of the ecological importance of elasmobranch fishes: a food web study on the Gulf of Tortugas, Colombia. *Ecological Modelling*, **221**, 2918-2926. doi: 10.1016/j.ecolmodel.2010.09.006.
- Navia, A.F., Cruz-Escalona, V.H., Giraldo, A. & Barausse, A. (2016) The structure of a marine tropical food web, and its implications for ecosystem-based fisheries management. *Ecological Modelling*, **328**, 23-33. doi: 10.1016/j.ecolmodel.2016.02.009.
- Navia, A.F., Mejia-Falla, P.A., Lopez-Garcia, J., Giraldo, A. & Cruz-Escalona, V.H. (2017) How many trophic roles can elasmobranchs play in a marine tropical network? *Marine and Freshwater Research*, **68**, 1342-1353. doi: 10.1071/mf16161.
- Needham, H.R., Pilditch, C.A., Lohrer, A.M. & Thrush, S.F. (2011) Context-specific bioturbation mediates changes to ecosystem functioning. *Ecosystems*, **14**, 1096-1109. doi: 10.1007/s10021-011-9468-0.
- Newsome, S.D., Clementz, M.T. & Koch, P.L. (2010) Using stable isotope biogeochemistry to study marine mammal ecology. *Marine Mammal Science*, **26**, 509-572. doi: 10.1111/j.1748-7692.2009.00354.x.

- Nowlin, W.H., Vanni, M.J. & Yang, L.H. (2008) Comparing resource pulses in aquatic and terrestrial ecosystems. *Ecology*, **89**, 647-659. doi: 10.1890/07-0303.1.
- O'Shea, O.R., Thums, M., van Keulen, M., Kempster, R.M. & Meekan, M.G. (2013) Dietary partitioning by five sympatric species of stingray (Dasyatidae) on coral reefs. *Journal of Fish Biology*, **82**, 1805-1820. doi: 10.1111/jfb.12104.
- O'Shea, O.R., Thums, M., van Keulen, M. & Meekan, M. (2012) Bioturbation by stingrays at Ningaloo Reef, Western Australia. *Marine and Freshwater Research*, **63**, 189-197. doi: 10.1071/mf11180.
- Oliver, J.S. & Slattery, P.N. (1985) Destruction and opportunity on the sea-floor - effects of gray whale feeding. *Ecology*, **66**, 1965-1975. doi: 10.2307/2937392.
- Ostfeld, R.S. & Keesing, F. (2000) Pulsed resources and community dynamics of consumers in terrestrial ecosystems. *Trends in Ecology & Evolution*, **15**, 232-237. doi: 10.1016/s0169-5347(00)01862-0.
- Papastamatiou, Y.P., Lowe, C.G., Caselle, J.E. & Friedlander, A.M. (2009) Scale-dependent effects of habitat on movements and path structure of reef sharks at a predator-dominated atoll. *Ecology*, **90**, 996-1008. doi: 10.1890/08-0491.1.
- Papastamatiou, Y.P., Watanabe, Y.Y., Bradley, D., Dee, L.E., Weng, K., Lowe, C.G. & Caselle, J.E. (2015) Drivers of daily routines in an ectothermic marine predator: hunt warm, rest warmer? *PLoS ONE*, **10**, 16. doi: 10.1371/journal.pone.0127807.
- Pardo, S.A., Burgess, K.B., Teixeira, D. & Bennett, M.B. (2015) Local-scale resource partitioning by stingrays on an intertidal flat. *Marine Ecology Progress Series*, **533**, 205-218. doi: 10.3354/meps11358.
- Parsons, M.A., Barkley, T.C., Rachlow, J.L., Johnson-Maynard, J.L., Johnson, T.R., Milling, C.R., Hammel, J.E. & Leslie, I. (2016) Cumulative effects of an herbivorous ecosystem engineer in a heterogeneous landscape. *Ecosphere*, **7**, 17. doi: 10.1002/ecs2.1334.
- Paterson, A.W. & Whitfield, A.K. (2000) Do shallow-water habitats function as refugia for juvenile fishes? *Estuarine Coastal and Shelf Science*, **51**, 359-364. doi: 10.1006/ecss.2000.0640.
- Payne, N.L., Iosilevskii, G., Barnett, A., Fischer, C., Graham, R.T., Gleiss, A.C. & Watanabe, Y.Y. (2016) Great hammerhead sharks swim on their side to reduce transport costs. *Nature Communications*, **7**, 5. doi: 10.1038/ncomms12289.
- Petchey, O.L., Evans, K.L., Fishburn, I.S. & Gaston, K.J. (2007) Low functional diversity and no redundancy in British avian assemblages. *Journal of Animal Ecology*, **76**, 977-985. doi: 10.1111/j.1365-2656.2007.01271.x.

- Peterson, B.J. (1999) Stable isotopes as tracers of organic matter input and transfer in benthic food webs: a review. *Acta Oecologica Oecologia Applicata*, **20**, 479-487. doi: 10.1016/s1146-609x(99)00120-4.
- Peterson, B.J. & Fry, B. (1987) Stable isotopes in ecosystem studies. *Annual Review of Ecology and Systematics*, **18**, 293-320. doi: 10.1146/annurev.ecolsys.18.1.293.
- Pierce, S.J., Scott-Holland, T.B. & Bennett, M.B. (2011) Community composition of elasmobranch fishes utilizing intertidal sand flats in Moreton Bay, Queensland, Australia. *Pacific Science*, **65**, 235-247. doi: 10.2984/65.2.235.
- Pillay, D., Branch, G.M., Dawson, J. & Henry, D. (2011) Contrasting effects of ecosystem engineering by the cordgrass *Spartina maritima* and the sandprawn *Callianassa kraussi* in a marine-dominated lagoon. *Estuarine Coastal and Shelf Science*, **91**, 169-176. doi: 10.1016/j.ecss.2010.10.010.
- Piraino, S., Fanelli, G. & Boero, F. (2002) Variability of species' roles in marine communities: change of paradigms for conservation priorities. *Marine Biology*, **140**, 1067-1074. doi: 10.1007/s00227-001-0769-2.
- Polis, G.A., Anderson, W.B. & Holt, R.D. (1997) Toward an integration of landscape and food web ecology: the dynamics of spatially subsidized food webs. *Annual Review of Ecology and Systematics*, **28**, 289-316. doi: 10.1146/annurev.ecolsys.28.1.289.
- Polis, G.A. & Strong, D.R. (1996) Food web complexity and community dynamics. *The American Naturalist*, **147**, 813-846. doi:
- Post, D.M. (2002) Using stable isotopes to estimate trophic position: models, methods, and assumptions. *Ecology*, **83**, 703-718. doi: 10.2307/3071875.
- Post, D.M., Layman, C.A., Arrington, D.A., Takimoto, G., Quattrochi, J. & Montana, C.G. (2007) Getting to the fat of the matter: models, methods and assumptions for dealing with lipids in stable isotope analyses. *Oecologia*, **152**, 179-189. doi: 10.1007/s00442-006-0630-x.
- Puttock, A.K., Cunliffe, A.M., Anderson, K. & Brazier, R.E. (2015) Aerial photography collected with a multirotor drone reveals impact of Eurasian beaver reintroduction on ecosystem structure. *Journal of Unmanned Vehicle Systems*, **3**, 123-130. doi: 10.1139/juvs-2015-0005.
- Queiroz, N., Humphries, N.E., Couto, A., Vedor, M., Costa, I., Sequeira, A.M.M., Mucientes, G., Santos, A.M., Abascal, F.J., Abercrombie, D.L., Abrantes, K., Acuna-Marrero, D., Afonso, A.S., Afonso, P., Anders, D., Araujo, G., Arauz, R., Bach, P., Barnett, A., Bernal, D., Berumen, M.L., Lion, S.B., Bezerra, N.P.A., Blaison, A.V., Block, B.A., Bond, M.E., Bonfil, R., Bradford, R.W., Braun, C.D., Brooks, E.J., Brooks, A., Brown, J., Bruce, B.D., Byrne, M.E., Campana, S.E., Carlisle, A.B., Chapman, D.D., Chapple, T.K., Chisholm, J., Clarke, C.R., Clua, E.G., Cochran,

J.E.M., Crochelet, E.C., Dagorn, L., Daly, R., Cortes, D.D., Doyle, T.K., Drew, M., Duffy, C.A.J., Erikson, T., Espinoza, E., Ferreira, L.C., Ferretti, F., Filmalter, J.D., Fischer, G.C., Fitzpatrick, R., Fontes, J., Forget, F., Fowler, M., Francis, M.P., Gallagher, A.J., Gennari, E., Goldsworthy, S.D., Gollock, M.J., Green, J.R., Gustafson, J.A., Guttridge, T.L., Guzman, H.M., Hammerschlag, N., Harman, L., Hazin, F.H.V., Heard, M., Hearn, A.R., Holdsworth, J.C., Holmes, B.J., Howey, L.A., Hoyos, M., Hueter, R.E., Hussey, N.E., Huvaneers, C., Irion, D.T., Jacoby, D.M.P., Jewell, O.J.D., Johnson, R., Jordan, L.K.B., Jorgensen, S.J., Joyce, W., Daly, C.A.K., Ketchum, J.T., Klimley, A.P., Kock, A.A., Koen, P., Ladino, F., Lana, F.O., Lea, J.S.E., Llewellyn, F., Lyon, W.S., MacDonnell, A., Macena, B.C.L., Marshall, H., McAllister, J.D., McAuley, R., Meyer, M.A., Morris, J.J., Nelson, E.R., Papastamatiou, Y.P., Patterson, T.A., Penaherrera-Palma, C., Pepperell, J.G., Pierce, S.J., Poisson, F., Quintero, L.M., Richardson, A.J., Rogers, P.J., Rohner, C.A., Rowat, D.R.L., Samoilys, M., Semmens, J.M., Sheaves, M., Shillinger, G., Shivji, M., Singh, S., Skomal, G.B., Smale, M.J., Snyders, L.B., Soler, G., Soria, M., Stehfest, K.M., Stevens, J.D., Thorrold, S.R., Tolotti, M.T., Towner, A., Travassos, P., Tyminski, J.P., Vandeperre, F., Vaudo, J.J., Watanabe, Y.Y., Weber, S.B., Wetherbee, B.M., White, T.D., Williams, S., Zarate, P.M., Harcourt, R., Hays, G.C., Meekan, M.G., Thums, M., Iragoien, X., Eguiluz, V.M., Duarte, C.M., Sousa, L.L., Simpson, S.J., Southall, E.J. & Sims, D.W. (2019) Global spatial risk assessment of sharks under the footprint of fisheries. *Nature*, **572**, 461-466. doi: 10.1038/s41586-019-1444-4.

R Core Team (2018) R: A language and environment for statistical computing. R Foundation for Statistical Computing, Vienna, Austria.

Rao, A.M.F., Malkin, S.Y., Montserrat, F. & Meysman, F.J.R. (2014) Alkalinity production in intertidal sands intensified by lugworm bioirrigation. *Estuarine Coastal and Shelf Science*, **148**, 36-47. doi: 10.1016/j.ecss.2014.06.006.

Raoult, V., Broadhurst, M.K., Peddemors, V.M., Williamson, J.E. & Gaston, T.F. (2019) Resource use of great hammerhead sharks (*Sphyrna mokarran*) off eastern Australia. *Journal of Fish Biology*, **95**, 1430-1440. doi: 10.1111/jfb.14160.

Raoult, V., Tosetto, L. & Williamson, J.E. (2018) Drone-based high-resolution tracking of aquatic vertebrates. *Drones*, **2**, 37. doi: 10.3390/drones2040037

Ray, G.C., McCormick-Ray, J., Berg, P. & Epstein, H.E. (2006) Pacific walrus: benthic bioturbator of Beringia. *Journal of Experimental Marine Biology and Ecology*, **330**, 403-419. doi: 10.1016/j.jembe.2005.12.043.

- Reef, R., Feller, I.C. & Lovelock, C.E. (2014) Mammalian herbivores in Australia transport nutrients from terrestrial to marine ecosystems via mangroves. *Journal of Tropical Ecology*, **30**, 179-188. doi: 10.1017/s0266467414000054.
- Reid, W.D.K., Sweeting, C.J., Wigham, B.D., McGill, R.A.R. & Polunin, N.V.C. (2016) Isotopic niche variability in macroconsumers of the East Scotia Ridge (Southern Ocean) hydrothermal vents: what more can we learn from an ellipse? *Marine Ecology Progress Series*, **542**, 13-24. doi: 10.3354/meps11571.
- Ricca, M.A., Miles, A.K., Anthony, R.G., Deng, X. & Hung, S.S.O. (2007) Effect-of lipid extraction on analyses of stable carbon and stable nitrogen isotopes in coastal organisms of the Aleutian archipelago. *Canadian Journal of Zoology-Revue Canadienne De Zoologie*, **85**, 40-48. doi: 10.1139/z06-187.
- Riekkola, L., Andrews-Goff, V., Friedlaender, A., Zerbini, A.N. & Constantine, R. (2020) Longer migration not necessarily the costliest strategy for migrating humpback whales. *Aquatic Conservation: Marine and Freshwater Ecosystems*, **30**, 937-948. doi: 10.1002/aqc.3295.
- Ripple, W.J., Estes, J.A., Beschta, R.L., Wilmers, C.C., Ritchie, E.G., Hebblewhite, M., Berger, J., Elmhagen, B., Letnic, M., Nelson, M.P., Schmitz, O.J., Smith, D.W., Wallach, A.D. & Wirsing, A.J. (2014) Status and ecological effects of the world's largest carnivores. *Science*, **343**, 1241484. doi: 10.1126/science.1241484.
- Ritchie, E.G. & Johnson, C.N. (2009) Predator interactions, mesopredator release and biodiversity conservation. *Ecology Letters*, **12**, 982-998. doi: 10.1111/j.1461-0248.2009.01347.x.
- Roemer, R.P., Gallagher, A.J. & Hammerschlag, N. (2016) Shallow water tidal flat use and associated specialized foraging behavior of the great hammerhead shark (*Sphyrna mokarran*). *Marine and Freshwater Behaviour and Physiology*, **49**, 235-249. doi: 10.1080/10236244.2016.1168089.
- Roff, G., Doropoulos, C., Rogers, A., Bozec, Y.M., Krueck, N.C., Aurellado, E., Priest, M., Birrell, C. & Mumby, P.J. (2016) The ecological role of sharks on coral reefs. *Trends in Ecology & Evolution*, **31**, 395-407. doi: 10.1016/j.tree.2016.02.014.
- Root, R.B. (1967) Niche exploitation pattern of blue-gray gnatcatcher. *Ecological Monographs*, **37**, 317-350. doi: 10.2307/1942327.
- Rosenfeld, J.S. (2002) Functional redundancy in ecology and conservation. *Oikos*, **98**, 156-162. doi: 10.1034/j.1600-0706.2002.980116.x.
- Rossi, F. (2007) Recycle of buried macroalgal detritus in sediments: use of dual-labelling experiments in the field. *Marine Biology*, **150**, 1073-1081. doi: 10.1007/s00227-006-0438-6.

- Royer, M., Maloney, K., Meyer, C., Cardona, E., Payne, N., Whittingham, K., Silva, G., Blandino, C. & Holland, K. (2020) Scalloped hammerhead sharks swim on their side with diel shifts in roll magnitude and periodicity. *Animal Biotelemetry*, **8**, 11. doi: 10.1186/s40317-020-00196-x.
- Sanders, D., Vogel, E. & Knop, E. (2015) Individual and species-specific traits explain niche size and functional role in spiders as generalist predators. *Journal of Animal Ecology*, **84**, 134-142. doi: 10.1111/1365-2656.12271.
- Sasko, D.E., Dean, M.N., Motta, P.J. & Hueter, R.E. (2006) Prey capture behavior and kinematics of the Atlantic cownose ray, *Rhinoptera bonasus*. *Zoology*, **109**, 171-181. doi: 10.1016/j.zool.2005.12.005.
- Savage, C., Thrush, S.F., Lohrer, A.M. & Hewitt, J.E. (2012) Ecosystem services transcend boundaries: estuaries provide resource subsidies and influence functional diversity in coastal benthic communities. *PLoS ONE*, **7**, 8. doi: 10.1371/journal.pone.0042708.
- Scheffer, M. & van Nes, E.H. (2006) Self-organized similarity, the evolutionary emergence of groups of similar species. *Proceedings of the National Academy of Sciences of the United States of America*, **103**, 6230-6235. doi: 10.1073/pnas.0508024103.
- Schlacher, T.A., Lucrezi, S., Peterson, C.H., Connolly, R.M., Olds, A.D., Althaus, F., Hyndes, G.A., Maslo, B., Gilby, B.L., Leon, J.X., Weston, M.A., Lastra, M., Williams, A. & Schoeman, D.S. (2016) Estimating animal populations and body sizes from burrows: marine ecologists have their heads buried in the sand. *Journal of Sea Research*, **112**, 55-64. doi: 10.1016/j.seares.2016.04.001.
- Schlacher, T.A., Schoeman, D.S., Dugan, J., Lastra, M., Jones, A., Scapini, F. & McLachlan, A. (2008) Sandy beach ecosystems: key features, sampling issues, management challenges and climate change impacts. *Marine Ecology-an Evolutionary Perspective*, **29**, 70-90. doi: 10.1111/j.1439-0485.2007.00204.x.
- Schlacher, T.A., Strydom, S., Connolly, R.M. & Schoeman, D. (2013) Donor-control of scavenging food webs at the land-ocean interface. *PLoS ONE*, **8**, 15. doi: 10.1371/journal.pone.0068221.
- Schlacher, T.A., Weston, M.A., Schoeman, D.S., Olds, A.D., Huijbers, C.M. & Connolly, R.M. (2015) Golden opportunities: a horizon scan to expand sandy beach ecology. *Estuarine Coastal and Shelf Science*, **157**, 1-6. doi: 10.1016/j.ecss.2015.02.002.
- Schoener, T.W. (1974) Resource partitioning in ecological communities. *Science*, **185**, 27-39. doi: 10.1126/science.185.4145.27.
- Schofield, G., Esteban, N., Katselidis, K.A. & Hays, G.C. (2019) Drones for research on sea turtles and other marine vertebrates - a review. *Biological Conservation*, **238**, 10. doi: 10.1016/j.biocon.2019.108214.

- Sheaves, M. (2005) Nature and consequences of biological connectivity in mangrove systems. *Marine Ecology Progress Series*, **302**, 293-305. doi: 10.3354/meps302293.
- Sheaves, M. (2009) Consequences of ecological connectivity: the coastal ecosystem mosaic. *Marine Ecology Progress Series*, **391**, 107-115. doi: 10.3354/meps08121.
- Sheaves, M., Brookes, J., Coles, R., Freckleton, M., Groves, P., Johnston, R. & Winberg, P. (2014) Repair and revitalisation of Australia's tropical estuaries and coastal wetlands: opportunities and constraints for the reinstatement of lost function and productivity. *Marine Policy*, **47**, 23-38. doi: 10.1016/j.marpol.2014.01.024.
- Sheaves, M., Dingle, L. & Mattone, C. (2016) Biotic hotspots in mangrove-dominated estuaries: macro-invertebrate aggregation in unvegetated lower intertidal flats. *Marine Ecology Progress Series*, **556**, 31-43. doi: 10.3354/meps11860.
- Shimoda, K. & Tamaki, A. (2004) Burrow morphology of the ghost shrimp *Nihonotrypaea petalura* (Decapoda : Thalassinidea : Callianassidae) from western Kyushu, Japan. *Marine Biology*, **144**, 723-734. doi: 10.1007/s00227-003-1237-y.
- Shipley, O.N., Brooks, E.J., Madigan, D.J., Sweeting, C.J. & Grubbs, R.D. (2017) Stable isotope analysis in deep-sea chondrichthyans: recent challenges, ecological insights, and future directions. *Reviews in Fish Biology and Fisheries*, **27**, 481-497. doi: 10.1007/s11160-017-9466-1.
- Shipley, O.N., Murchie, K.J., Frisk, M.G., O'Shea, O.R., Winchester, M.M., Brooks, E.J., Pearson, J. & Power, M. (2018) Trophic niche dynamics of three nearshore benthic predators in The Bahamas. *Hydrobiologia*, **813**, 177-188. doi: 10.1007/s10750-018-3523-1.
- Short, A.D. (2006) Australian beach systems - nature and distribution. *Journal of Coastal Research*, **22**, 11-27. doi: 10.2112/05a-0002.1.
- Simpfendorfer, C.A., Goodreid, A.B. & McAuley, R.B. (2001) Size, sex and geographic variation in the diet of the tiger shark, *Galeocerdo cuvier*, from Western Australian waters. *Environmental Biology of Fishes*, **61**, 37-46. doi: 10.1023/a:1011021710183.
- Simpfendorfer, C.A., Wiley, T.R. & Yeiser, B.G. (2010) Improving conservation planning for an endangered sawfish using data from acoustic telemetry. *Biological Conservation*, **143**, 1460-1469. doi: 10.1016/j.biocon.2010.03.021.
- Smith, J.W. & Merriner, J.V. (1985) Food-habits and feeding-behavior of the cownose ray, *Rhinoptera bonasus*, in lower Chesapeake Bay. *Estuaries*, **8**, 305-310. doi: 10.2307/1351491.
- Sotiropoulos, M.A., Tonn, W.M. & Wassenaar, L.I. (2004) Effects of lipid extraction on stable carbon and nitrogen isotope analyses of fish tissues: potential consequences for food web studies. *Ecology of Freshwater Fish*, **13**, 155-160. doi: 10.1111/j.1600-0633.2004.00056.x.

- Spiller, D.A., Piovia-Scott, J., Wright, A.N., Yang, L.H., Takimoto, G., Schoener, T.W. & Iwata, T. (2010) Marine subsidies have multiple effects on coastal food webs. *Ecology*, **91**, 1424-1434. doi: 10.1890/09-0715.1.
- Stevenson, C., Katz, L.S., Micheli, F., Block, B., Heiman, K.W., Perle, C., Weng, K., Dunbar, R. & Witting, J. (2007) High apex predator biomass on remote Pacific islands. *Coral Reefs*, **26**, 47-51. doi: 10.1007/s00338-006-0158-x.
- Stewart, J.D., Smith, T.R., Marsha, G., Abernathy, K., Fonseca-Ponce, I.A., Froman, N. & Stevens, G.M.W. (2019) Novel applications of animal-borne Crittercams reveal thermocline feeding in two species of manta ray. *Marine Ecology Progress Series*, **632**, 145-158. doi: 10.3354/meps13148.
- Subalusky, A.L., Dutton, C.L., Rosi-Marshall, E.J. & Post, D.M. (2015) The hippopotamus conveyor belt: vectors of carbon and nutrients from terrestrial grasslands to aquatic systems in sub-Saharan Africa. *Freshwater Biology*, **60**, 512-525. doi: 10.1111/fwb.12474.
- Suchanek, T.H. & Colin, P.L. (1986) Rates and effects of bioturbation by invertebrates and fishes at Enewetak and Bikini atolls. *Bulletin of Marine Science*, **38**, 25-34. doi:
- Sunday, J.M., Bates, A.E., Kearney, M.R., Colwell, R.K., Dulvy, N.K., Longino, J.T. & Huey, R.B. (2014) Thermal-safety margins and the necessity of thermoregulatory behavior across latitude and elevation. *Proceedings of the National Academy of Sciences of the United States of America*, **111**, 5610-5615. doi: 10.1073/pnas.1316145111.
- Swanson, H.K., Lysy, M., Power, M., Stasko, A.D., Johnson, J.D. & Reist, J.D. (2015) A new probabilistic method for quantifying n-dimensional ecological niches and niche overlap. *Ecology*, **96**, 318-324. doi: 10.1890/14-0235.1.
- Sweeting, C.J., Polunin, N.V. & Jennings, S. (2006) Effects of chemical lipid extraction and arithmetic lipid correction on stable isotope ratios of fish tissues. *Rapid Communications in Mass Spectrometry*, **20**, 595-601. doi: 10.1002/rcm.2347.
- Takeuchi, S. & Tamaki, A. (2014) Assessment of benthic disturbance associated with stingray foraging for ghost shrimp by aerial survey over an intertidal sandflat. *Continental Shelf Research*, **84**, 139-157. doi: 10.1016/j.csr.2014.05.007.
- Tews, J., Brose, U., Grimm, V., Tielborger, K., Wichmann, M.C., Schwager, M. & Jeltsch, F. (2004) Animal species diversity driven by habitat heterogeneity/diversity: the importance of keystone structures. *Journal of Biogeography*, **31**, 79-92. doi: 10.1046/j.0305-0270.2003.00994.x.

- Thillainath, E.C., McIlwain, J.L., Wilson, S.K. & Depczynski, M. (2016) Estimating the role of three mesopredatory fishes in coral reef food webs at Ningaloo Reef, Western Australia. *Coral Reefs*, **35**, 261-269. doi: 10.1007/s00338-015-1367-y.
- Thrush, S.F., Pridmore, R.D., Hewitt, J.E. & Cummings, V.J. (1994) The importance of predators on a sandflat - interplay between seasonal-changes in prey densities and predator effects. *Marine Ecology Progress Series*, **107**, 211-222. doi: 10.3354/meps107211.
- Tieszen, L.L., Boutton, T.W., Tesdahl, K.G. & Slade, N.A. (1983) Fractionation and turnover of stable carbon isotopes in animal-tissues - implications for $\delta^{13}\text{C}$ analysis of diet. *Oecologia*, **57**, 32-37. doi: 10.1007/bf00379558.
- Unsworth, R.K.F., McKenzie, L.J., Nordlund, L.M. & Cullen-Unsworth, L.C. (2018) A changing climate for seagrass conservation? *Current Biology*, **28**, R1229-R1232. doi: 10.1016/j.cub.2018.09.027.
- Valentine, J.F., Heck, K.L., Harper, P. & Beck, M. (1994) Effects of bioturbation in controlling turtlegrass (*Thalassia testudinum* Banks ex König) abundance - evidence from field enclosures and observations in the northern Gulf of Mexico. *Journal of Experimental Marine Biology and Ecology*, **178**, 181-192. doi: 10.1016/0022-0981(94)90035-3.
- Valentine, L.E., Anderson, H., Hardy, G.E.S. & Fleming, P.A. (2012) Foraging activity by the southern brown bandicoot (*Isoodon obesulus*) as a mechanism for soil turnover. *Australian Journal of Zoology*, **60**, 419-423. doi: 10.1071/zo13030.
- Van Colen, C., Thrush, S.F., Parkes, S., Harris, R., Woodin, S.A., Wethey, D.S., Pilditch, C.A., Hewitt, J.E., Lohrer, A.M. & Vincx, M. (2015) Bottom-up and top-down mechanisms indirectly mediate interactions between benthic biotic ecosystem components. *Journal of Sea Research*, **98**, 42-48. doi: 10.1016/j.seares.2014.10.016.
- Vanblaricom, G.R. (1982) Experimental analyses of structural regulation in a marine sand community exposed to oceanic swell. *Ecological Monographs*, **52**, 283-305. doi: 10.2307/2937332.
- Vander Zanden, M.J., Clayton, M.K., Moody, E.K., Solomon, C.T. & Weidel, B.C. (2015) Stable isotope turnover and half-life in animal tissues: a literature synthesis. *PLoS ONE*, **10**, e0116182. doi: 10.1371/journal.pone.0116182.
- Vanderklift, M.A. & Ponsard, S. (2003) Sources of variation in consumer-diet $\delta^{15}\text{N}$ enrichment: a meta-analysis. *Oecologia*, **136**, 169-182. doi: 10.1007/s00442-003-1270-z.
- Vaudo, J.J. & Heithaus, M.R. (2009) Spatiotemporal variability in a sandflat elasmobranch fauna in Shark Bay, Australia. *Marine Biology*, **156**, 2579-2590. doi: 10.1007/s00227-009-1282-2.

- Vaudo, J.J. & Heithaus, M.R. (2011) Dietary niche overlap in a nearshore elasmobranch mesopredator community. *Marine Ecology Progress Series*, **425**, 247-260. doi: 10.3354/meps08988.
- Vaudo, J.J. & Heithaus, M.R. (2012) Diel and seasonal variation in the use of a nearshore sandflat by a ray community in a near pristine system. *Marine and Freshwater Research*, **63**, 1077-1084. doi: 10.1071/mf11226.
- Vaudo, J.J. & Heithaus, M.R. (2013) Microhabitat selection by marine mesoconsumers in a thermally heterogeneous habitat: behavioral thermoregulation or avoiding predation risk? *PLoS ONE*, **8**, 9. doi: 10.1371/journal.pone.0061907.
- Velasquez, C.R. & Navarro, R.A. (1993) The influence of water depth and sediment type on the foraging behavior of whimbrels. *Journal of Field Ornithology*, **64**, 149-157. doi: 10.2307/4123850
- Vernes, K., Marsh, H. & Winter, J. (1995) Home-range characteristics and movement patterns of the red-legged pademelon (*Thylogale stigmatica*) in a fragmented tropical rainforest. *Wildlife Research*, **22**, 699-708. doi: 10.1071/wr9950699.
- Violle, C., Navas, M.L., Vile, D., Kazakou, E., Fortunel, C., Hummel, I. & Garnier, E. (2007) Let the concept of trait be functional! *Oikos*, **116**, 882-892. doi: 10.1111/j.2007.0030-1299.15559.x.
- Wakefield, E.D., Cleasby, I.R., Bearhop, S., Bodey, T.W., Davies, R.D., Miller, P.I., Newton, J., Votier, S.C. & Hamer, K.C. (2015) Long-term individual foraging site fidelity: why some gannets don't change their spots. *Ecology*, **96**, 3058-3074. doi: 10.1890/14-1300.1.
- Walker, B.H. (1992) Biodiversity and ecological redundancy. *Conservation Biology*, **6**, 18-23. doi: 10.1046/j.1523-1739.1992.610018.x.
- Weimerskirch, H., Pinaud, D., Pawlowski, F. & Bost, C.A. (2007) Does prey capture induce area-restricted search? A fine-scale study using GPS in a marine predator, the wandering albatross. *American Naturalist*, **170**, 734-743. doi: 10.1086/522059.
- Wellnitz, T. & Poff, N.L. (2001) Functional redundancy in heterogeneous environments: implications for conservation. *Ecology Letters*, **4**, 177-179. doi: 10.1046/j.1461-0248.2001.00221.x.
- Welsh, J.Q. & Bellwood, D.R. (2012) Spatial ecology of the steephead parrotfish (*Chlorurus microrhinos*): an evaluation using acoustic telemetry. *Coral Reefs*, **31**, 55-65. doi: 10.1007/s00338-011-0813-8.
- White, J., Simpfendorfer, C.A., Tobin, A.J. & Heupel, M.R. (2014) Spatial ecology of shark-like batoids in a large coastal embayment. *Environmental Biology of Fishes*, **97**, 773-786. doi: 10.1007/s10641-013-0178-7.
- Wickham, H. (2016) *ggplot2: elegant graphics for data analysis*. Springer.

- Wilga, C.D., Maia, A., Nauwelaerts, S. & Lauder, G.V. (2012) Prey handling using whole-body fluid dynamics in batoids. *Zoology*, **115**, 47-57. doi: 10.1016/j.zool.2011.09.002.
- Wright, J.P. & Jones, C.G. (2006) The concept of organisms as ecosystem engineers ten years on: Progress, limitations, and challenges. *Bioscience*, **56**, 203-209. doi: 10.1641/0006-3568(2006)056[0203:Tcooae]2.0.Co;2.
- Wurtsbaugh, W.A. & Neverman, D. (1988) Post-feeding thermotaxis and daily vertical migration in a larval fish. *Nature*, **333**, 846-848. doi: 10.1038/333846a0.
- Yachi, S. & Loreau, M. (1999) Biodiversity and ecosystem productivity in a fluctuating environment: the insurance hypothesis. *Proceedings of the National Academy of Sciences of the United States of America*, **96**, 1463-1468. doi: 10.1073/pnas.96.4.1463.
- Yager, P.L., Nowell, A.R.M. & Jumars, P.A. (1993) Enhanced deposition to pits - a local food source for benthos. *Journal of Marine Research*, **51**, 209-236. doi: 10.1357/0022240933223819.
- Yick, J.L., Tracey, S.R. & White, R.W.G. (2011) Niche overlap and trophic resource partitioning of two sympatric batoids co-inhabiting an estuarine system in southeast Australia. *Journal of Applied Ichthyology*, **27**, 1272-1277. doi: 10.1111/j.1439-0426.2011.01819.x.
- Yurkowski, D.J., Ferguson, S., Choy, E.S., Loseto, L.L., Brown, T.M., Muir, D.C.G., Semeniuk, C.A.D. & Fisk, A.T. (2016) Latitudinal variation in ecological opportunity and intraspecific competition indicates differences in niche variability and diet specialization of Arctic marine predators. *Ecology and Evolution*, **6**, 1666-1678. doi: 10.1002/ece3.1980.
- Yurkowski, D.J., Hussey, N.E., Semeniuk, C., Ferguson, S.H. & Fisk, A.T. (2015) Effects of lipid extraction and the utility of lipid normalization models on $\delta^{13}\text{C}$ and $\delta^{15}\text{N}$ values in Arctic marine mammal tissues. *Polar Biology*, **38**, 131-143. doi: 10.1007/s00300-014-1571-1.
- Zhao, T., Villeger, S., Lek, S. & Cucherousset, J. (2014) High intraspecific variability in the functional niche of a predator is associated with ontogenetic shift and individual specialization. *Ecology and Evolution*, **4**, 4649-4657. doi: 10.1002/ece3.1260.
- Zuur, A., Ieno, E.N., Walker, N., Saveliev, A.A. & Smith, G.M. (2009) *Mixed effects models and extensions in ecology with R*. Springer Science & Business Media.

Appendix A

Table A1 Correlations among continuous variables for active tracking data. * indicates a significant correlation at $\alpha=0.05$. KUD: 50 and 95 % kernel utilisation distributions, DW: ray disc width.

Correlation	Method	Coefficient (95 % CI)	Test Statistic	p-value
KUD 95 – DW	Pearson	0.755 (0.284,0.933)	t=3.457	0.007*
KUD 50 – DW	Pearson	0.693 (0.159,0.913)	t=2.884	0.018*
KUD 95 – Time Tracked	Pearson	-0.064 (-0.639,0.557)	t=-0.192	0.852
KUD 50 – Time Tracked	Pearson	0.233 (-0.426,0.731)	t=0.722	0.489
KUD 95 – Tidal Range	Pearson	0.142 (-0.190,0.446)	t=0.853	0.340
KUD 50 – Tidal Range	Pearson	-0.007 (-0.330,0.318)	t=-0.041	0.968
ROM – Tidal Range	Spearman	0.210	S=7220	0.206
ROM – DW	Spearman	0.084	S=8367	0.614

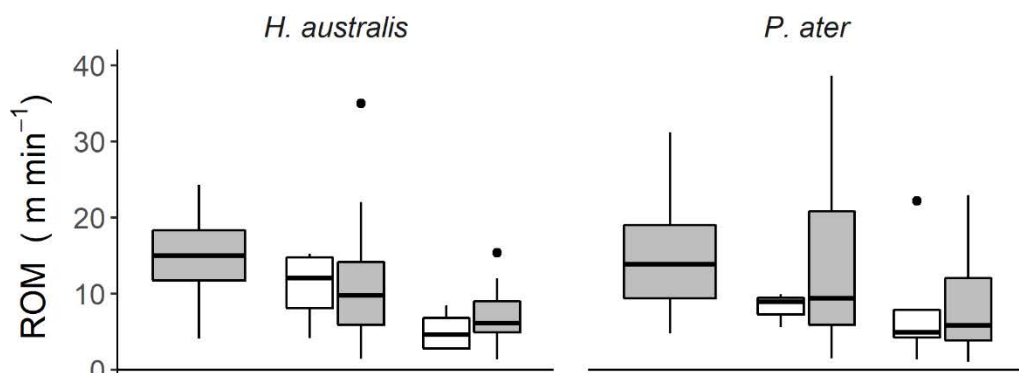
Table A2. Statistical comparisons of rates of movement (ROM) for rays at Lucinda. Kruskal-Wallis tests were used to compare among all tidal phases with post-hoc Dunn tests to evaluate pairwise differences. * represents a significant difference at $\alpha=0.05$. Dunn-test p-values were corrected for multiple comparisons using the Benjamini- Hochberg method.

Comparison	<i>Himantura australis</i>			<i>Pastinachus ater</i>		
	Test Statistic	p-value		Test Statistic	p-value	
All	$\chi^2_3=$ 11.02	0.012*		$\chi^2_3=$ 18.36	<0.001*	
Ebb – Flood	Z= -0.27	0.789		Z= -0.54	0.590	
Ebb – High	Z= 0.64	0.625		Z= 2.21	0.041*	
Flood – High	Z= 0.91	0.545		Z= 2.86	0.008*	
Ebb – Low	Z= 2.73	0.019*		Z= 2.99	0.008*	
Flood – Low	Z= 2.99	0.017*		Z= 3.67	0.001*	
High – Low	Z= 2.09	0.074		Z= 0.81	0.503	

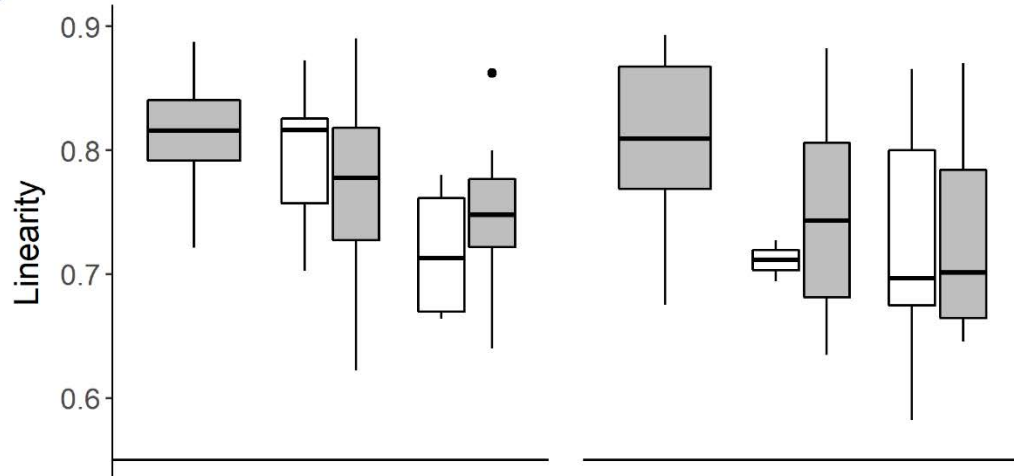
Figure A3. Boxplots of a) rate of movement (ROM), b) linearity, and c) feeding rate for both short and long drone tracks of *Pastinachus ater* and *Himantura australis* at Lucinda. Boxes represent the first and third quartiles with whiskers extending to data points within 1.5 times the inter-quartile range. Horizontal black lines represent the median and individual points represent outliers.

a

LongTrack ShortTrack



b



c

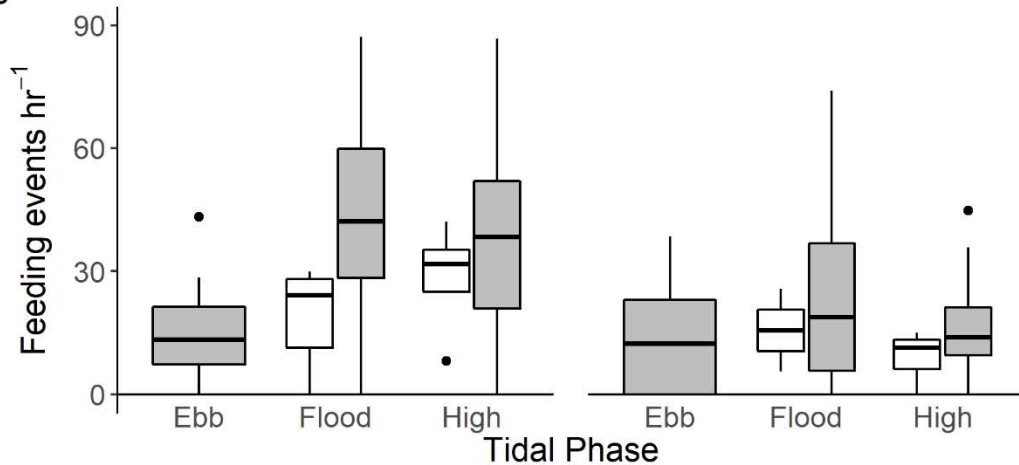


Table A4. Rate of movement (ROM) and feeding rate comparisons among tidal phases for combined short and long drone tracks of *Pastinachus ater* and *Himantura australis*. Kruskal-Wallis tests were used to compare among all tidal phases with post-hoc Dunn tests to evaluate pairwise differences. * represents a significant difference at $\alpha=0.05$. P values were corrected for multiple comparisons using the Benjamini- Hochberg method for Dunn tests.

Species	Comparison	ROM (m min^{-1})		Feeding Rate (pits hr^{-1})	
		Test Statistic	p-value	Test Statistic	p-value
<i>P. ater</i>	All	$\chi^2_2 = 11.914$	0.003*	$\chi^2_2 = 2.205$	0.332
	Flood – High	Z = 1.933	0.080	-	-
	Ebb – Flood	Z = 1.689	0.091	-	-
	Ebb – High	Z = 3.445	0.002*	-	-
<i>H. australis</i>	All	$\chi^2_2 = 22.74$	<0.001*	$\chi^2_2 = 13.864$	<0.001*
	Flood – High	Z = 2.674	0.011*	Z = 0.293	0.770
	Ebb – Flood	Z = 2.343	0.019*	Z = -3.453	0.002*
	Ebb – High	Z = 4.743	<0.001*	Z = -3.131	0.003*

Figure A5. Feeding rates of *Himantura australis* and *Pastinachus ater* at Lucinda in a) the cold (May–October) and warm seasons (November–April) and b) in long and short drone tracks.

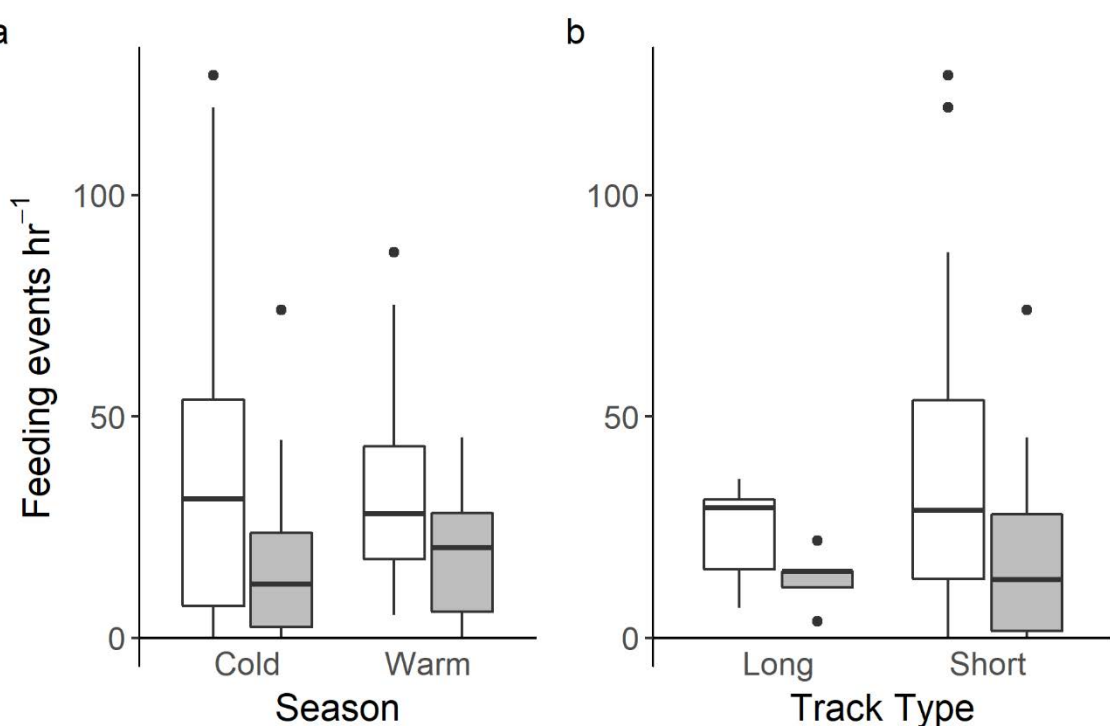
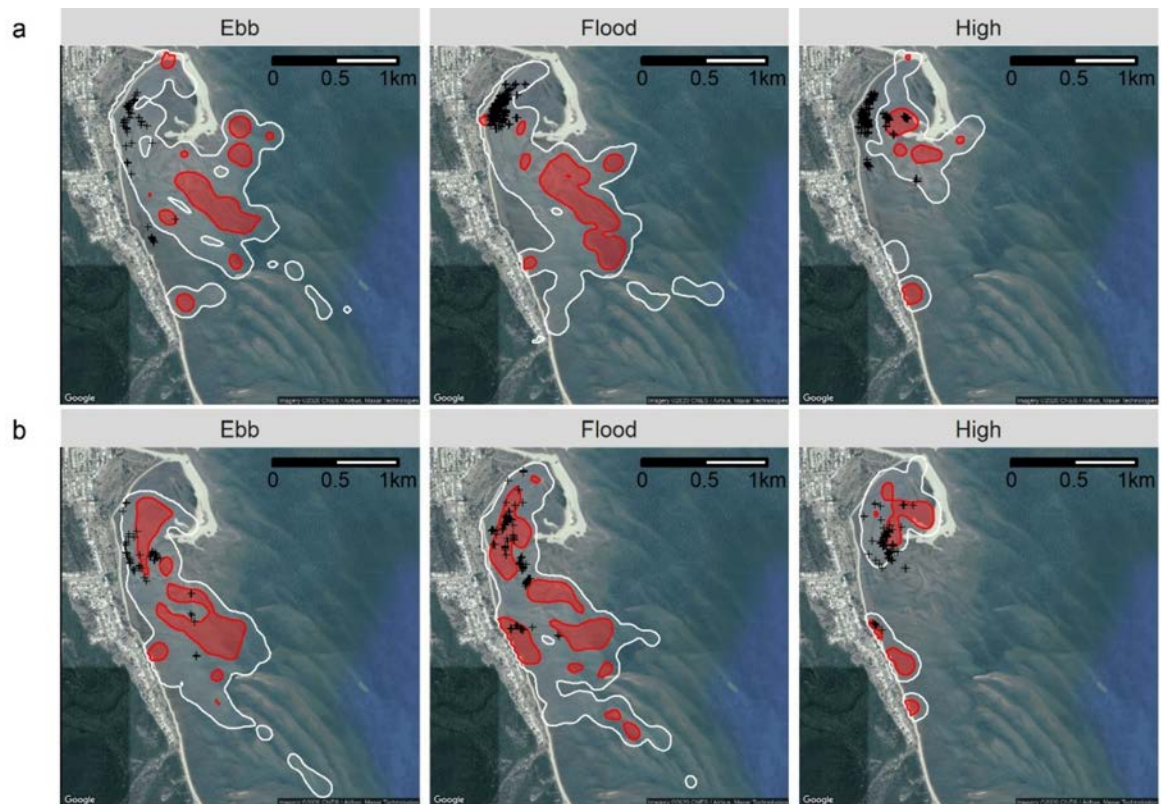


Figure A6. 95 % (white) and 50 % (red) kernel utilisation distributions by tidal phase for all a) *Pastinachus ater* and b) *Himantura australis* individuals acoustically tracked at Lucinda. Feeding locations from drone tracks in each tidal phase are indicated with + symbols.



Appendix B

Figure B1. Linear relationship between drone height and image resolution.

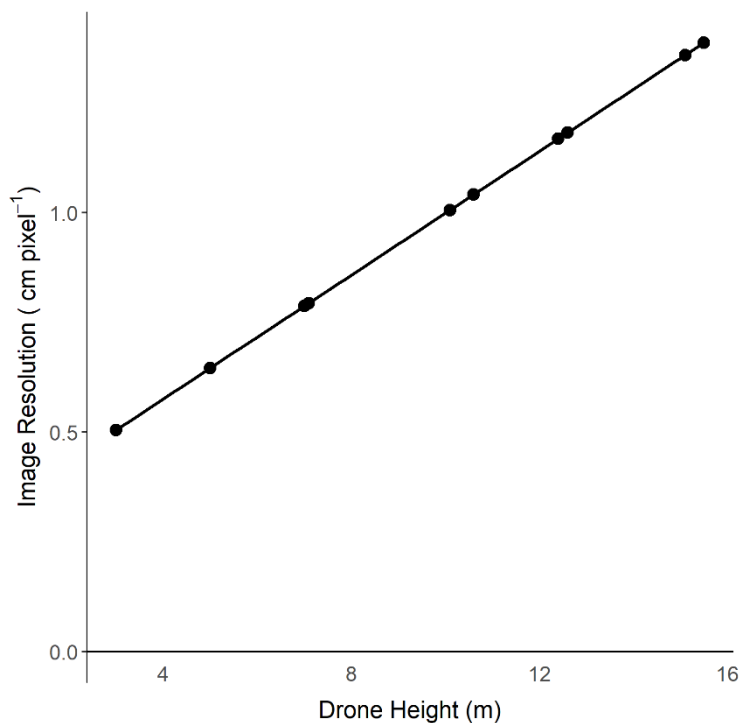


Table B2. General linear mixed-effects model results examining the influence of feeding time, feeding type, and disc width (DW) on feeding pit area. Primary feeding types (Pft) are represented as water jetting (WJ), and suction (SU) with excavation feeding as the reference category. Secondary feeding type codes are the same with “NA” indicating events with no secondary feeding type was observed.

Predictor	Estimate	Standard Error	t-value	p-value
Intercept	2.9825	0.3172	9.4025	<0.0001
In(feeding time)	0.5463	0.0401	13.6044	<0.0001
DW	0.0359	0.0047	7.5834	<0.0001
Pft – WJ	-0.8428	0.0887	-9.5005	<0.0001
Pft – SU	-0.9011	0.1299	-6.9339	<0.0001
Sft – WJ	-0.6471	0.1271	-5.0883	<0.0001
Sft – NA	-0.4415	0.0896	-4.9276	<0.0001
Sft – SU	-0.4577	0.1477	-3.0979	0.0021

Table B3. General linear mixed-effects model results examining the influence of feeding time, feeding type, disc width (DW), and species on feeding pit area. Primary feeding types (Pft) are represented as water jetting (WJ), and suction (SU) with excavation feeding as the reference category. Secondary feeding types (Sft) are coded the same and with “NA” indicating events with no secondary feeding.

Predictor	Estimate	Standard Error	t-value	p-value
Intercept	2.9551	0.3164	9.3398	<0.0001
In(feeding time)	0.5570	0.0408	13.6361	<0.0001
DW	0.0332	0.0050	6.5471	<0.0001
Pft – WJ	-0.8393	0.0886	-9.4632	<0.0001
Pft – SU	-0.9165	0.1301	-7.0443	<0.0001
Sft – WJ	-0.6487	0.1270	-5.1077	<0.0001
Sft – NA	-0.4320	0.0897	-4.8112	<0.0001
Sft – SU	-0.4812	0.1481	-3.2489	0.0013
Species - Whipray	0.2006	0.1399	1.4340	0.1560

Figure B4. Linear relationship between the actual and predicted pit areas from the general linear mixed model (solid line). The dashed line represents a perfect 1:1 relationship between actual and predicted areas.

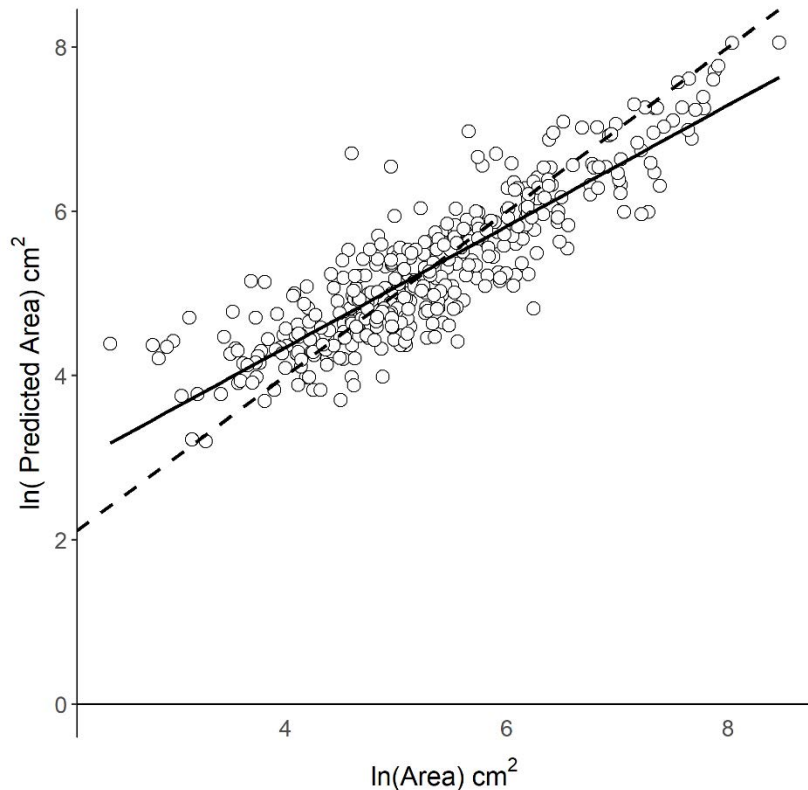


Figure B5. Distribution of feeding pit sizes for *Pastinachus ater* and *Himantura australis*. Feeding pit sizes are grouped into 100 cm^2 bins.

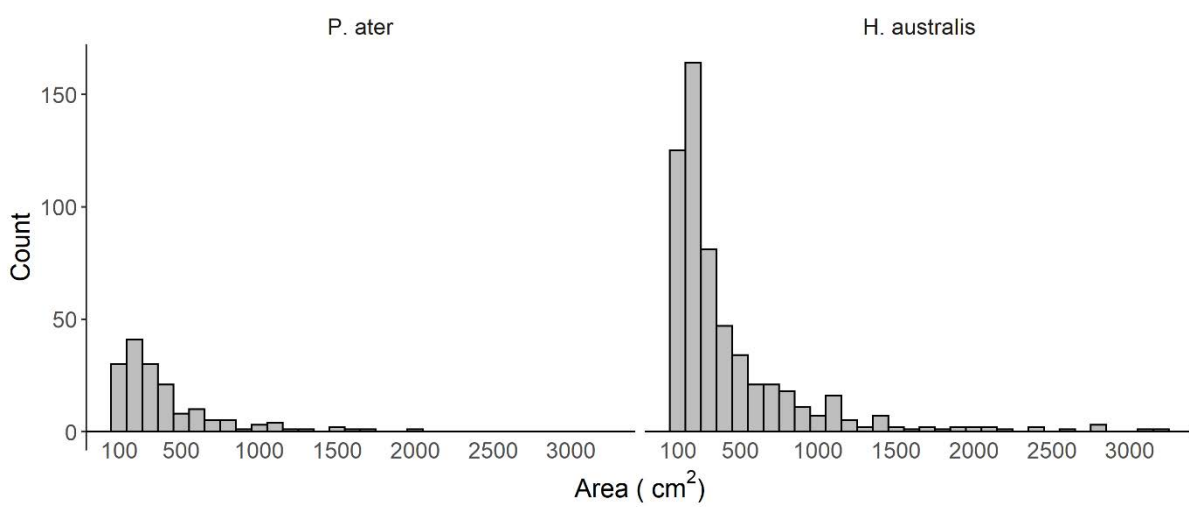


Figure B6. a) Logistic relationship between feeding pit volume and area and b) linear relationship between the predicted and actual pit volumes. Dashed line represents a perfect 1:1 relationship between actual and predicted volumes.

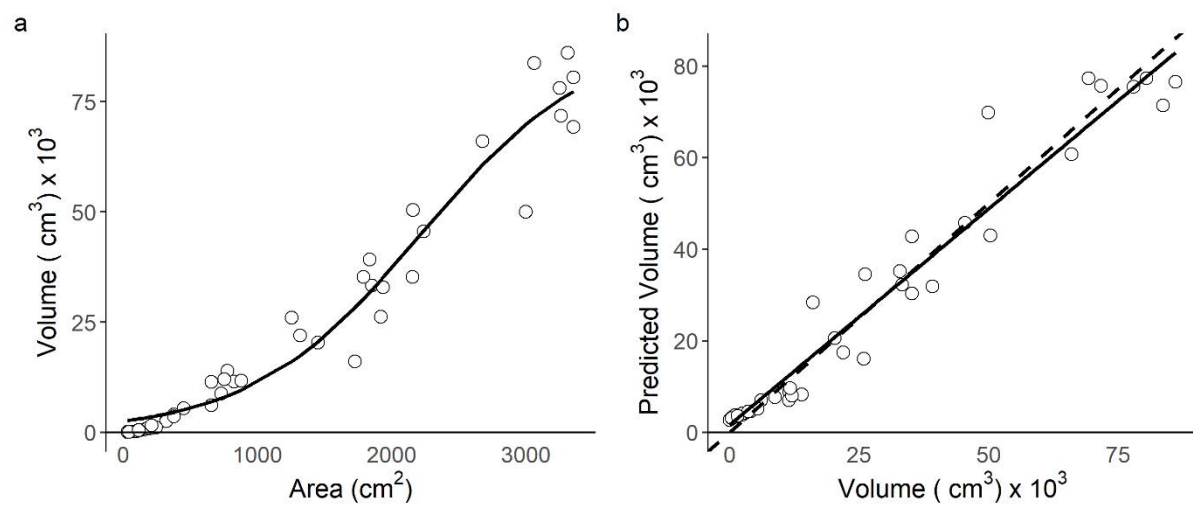
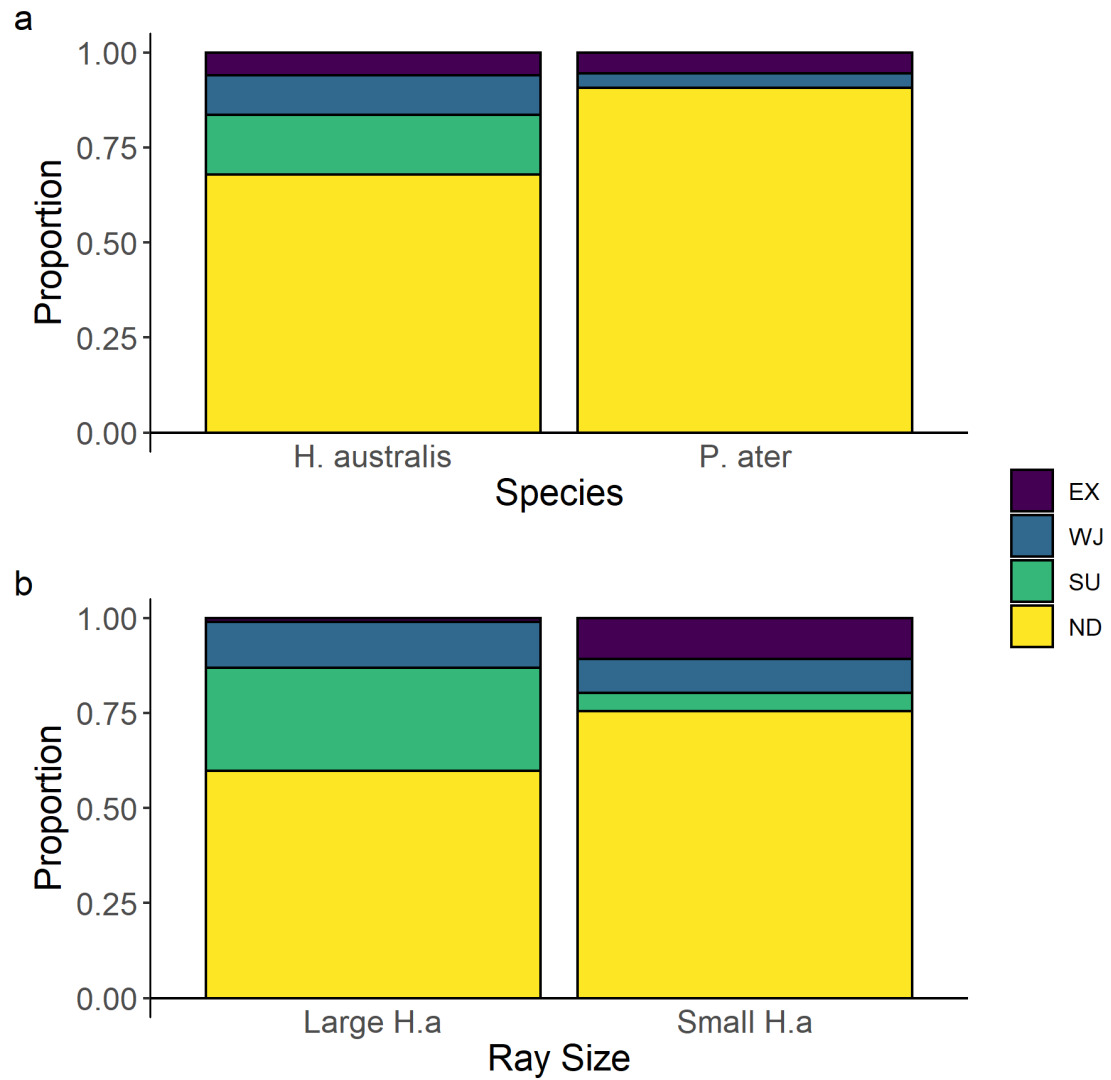


Table B7. Results from Pearson's correlation tests among feeding rates (events hr^{-1} , pits hr^{-1}), bioturbation rates (BioT) ($\text{cm}^3 \text{ hr}^{-1}$), and ray disc width (DW) among all drone tracks for *Himantura australis* and *Pastinachus ater*. * indicates a significant correlation at $\alpha=0.05$.

Species	Correlation	Coefficient (95 % CI)	t-value	p-value
<i>H. australis</i>	$\ln(\text{events hr}^{-1}) - \text{DW}$	0.062 (-0.195,0.311)	0.477	0.635
	$\ln(\text{pits hr}^{-1}) - \text{DW}$	0.217 (-0.044,0.454)	1.664	0.102
	$\ln(\text{BioT}) - \text{DW}$	0.414 (0.172,0.609)	3.373	0.001 *
	$\ln(\text{BioT}) - \ln(\text{pits hr}^{-1})$	0.790 (0.667,0.871)	9.553	<0.001 *
<i>P. ater</i>	$\ln(\text{Events}) - \text{DW}$	-0.186 (-0.437,0.092)	-1.337	0.187
	$\ln(\text{pits hr}^{-1}) - \text{DW}$	0.141 (-0.149,0.409)	0.967	0.339
	$\ln(\text{BioT}) - \text{DW}$	0.388 (0.116,0.605)	2.853	0.006 *
	$\ln(\text{BioT}) - \ln(\text{pits hr}^{-1})$	0.886 (0.805,0.935)	12.968	<0.001 *

Figure B8. Proportion of feeding events with excavation (EX), water jetting (WJ), suction (SU) as secondary feeding types for a) *Himantura australis* and *Pastinachus ater* and b) large (≥ 54 cm DW) and small (< 54 cm DW) *H. australis* (H.a). “NA” indicates feeding events with no secondary feeding type.



Appendix C

Table C1. $\delta^{13}\text{C}$ (‰), $\delta^{15}\text{N}$ (‰), and C:N ratios of bulk (BK) muscle tissue for individual *Pastinachus ater* (*P.a*) and *Himantura australis* (*H.a*) and the change in each value after lipid extraction (ΔLE), urea extraction (ΔUE), and both urea and lipid extraction (ΔULE) relative to bulk (BK) samples (i.e Treatment – Bulk sample). N/A indicates there was insufficient material to process samples in the treatment. Disc width (DW) for each individual is given in mm.

Species	DW	$\delta^{13}\text{C}$				$\delta^{15}\text{N}$				C:N			
		BK	ΔLE	ΔUE	ΔULE	BK	ΔLE	ΔUE	ΔULE	BK	ΔLE	ΔUE	ΔULE
<i>P.a</i>	425	-13.1	0.0	-0.5	-0.2	9.0	-0.1	+1.0	+1.2	2.6	0.0	+0.6	+0.5
	480	-12.5	0.0	0.0	-0.3	8.4	+0.2	+1.1	+1.3	2.6	0.0	+0.6	+0.6
	432	-11.7	-0.7	-1.3	-1.0	10.4	-0.3	+0.8	+1.1	2.4	+0.1	+0.8	+0.6
	460	-12.3	-0.1	-0.6	-0.2	8.7	-0.6	+0.9	+1.4	2.4	0.0	+0.8	+0.6
	450	-7.9	-0.8	+0.1	+1.3	7.8	+0.4	+0.5	+0.1	2.5	0.0	+0.5	+0.4
	428	-13.2	+0.3	-1.3	-0.5	8.1	-0.1	+0.7	+0.8	2.5	-0.1	+1.0	+0.7
	440	-14.3	+0.6	-0.1	+0.5	9.8	-0.2	+0.5	+0.6	2.6	-0.2	+0.7	+0.5
	410	-13.2	-0.2	-0.4	-0.1	9.0	-0.3	+0.9	+0.9	2.6	0.0	+0.6	+0.5
	456	-14.4	+1.2	+1.3	+0.7	9.4	-0.3	+0.9	+1.0	2.5	-0.2	+0.5	+0.6
	442	-14.3	+0.7	+0.6	+0.4	11.9	0.0	+1.2	+1.2	2.7	-0.1	+0.5	+0.5
<i>H.a</i>	350	-10.8	+0.1	+0.6	N/A	8.3	-0.2	+0.6	N/A	2.7	-0.1	+0.6	N/A
	396	-14.0	+0.1	0.0	+0.2	9.3	-0.4	+1.4	+1.4	2.5	-0.1	+0.8	+0.6
	388	-13.2	+0.4	+0.6	+0.4	9.2	+0.3	+1.5	+1.6	2.4	-0.1	+0.8	+0.7
	370	-13.3	+0.4	0.0	+0.1	8.8	-0.1	+1.5	+1.4	2.5	-0.1	+0.8	+0.7
	360	-13.5	0.0	+0.1	+0.7	9.9	+0.1	+0.9	+0.9	2.7	0.0	+0.7	+0.5
	434	-13.4	-0.1	-0.3	0.0	8.3	0.0	+0.7	+1.1	2.7	0.0	+0.5	+0.5
	362	-14.0	+0.4	+0.5	+0.2	9.9	0.0	+1.2	+1.4	2.5	0.0	+0.8	+0.8
	356	-13.0	-0.3	-0.2	+0.4	8.6	+0.1	+0.9	+0.7	2.5	0.0	+0.7	+0.6
	374	-14.2	0.0	+0.1	+0.1	8.6	-0.4	+0.9	+0.9	2.7	-0.2	+0.7	+0.5
	362	-14.5	+0.3	0.0	+0.6	8.3	+0.4	+1.3	+1.6	2.4	0.0	+0.8	+0.7

Table C2. $\delta^{13}\text{C}$ (‰), $\delta^{15}\text{N}$ (‰), and C:N ratios of bulk (BK) plasma tissue for individual *Pastinachus ater* (*P.a*) and *Himantura australis* (*H.a*) and the change in each value after lipid extraction (ΔLE), urea extraction (ΔUE), and both urea and lipid extraction (ΔULE) relative to bulk (BK) samples (i.e Treatment - Bulk). N/A indicates there was insufficient material to process samples in the treatment. Disc width (DW) for each individual is given in mm.

Species	DW	$\delta^{13}\text{C}$				$\delta^{15}\text{N}$				C:N			
		BK	ΔLE	ΔUE	ΔULE	BK	ΔLE	ΔUE	ΔULE	BK	ΔLE	ΔUE	ΔULE
<i>P.a</i>	425	-12.1	-0.1	-1.8	-1.9	6.6	0.0	-0.3	-0.4	1.5	0.0	+2.3	+2.2
	480	-11.9	-0.1	-1.7	-1.6	6.3	-0.1	-0.3	-0.3	1.6	0.0	+2.3	+2.4
	432	-11.2	-0.4	-2.1	-1.9	5.6	+0.1	+0.1	+0.1	1.5	+0.1	+2.4	+2.6
	460	-11.2	-0.1	-1.9	-1.8	6.2	+0.1	-0.2	-0.3	1.6	0.0	+2.1	+2.1
	420	-12.3	-0.1	-1.6	-1.8	6.7	0.0	-0.2	-0.2	1.6	0.0	+2.3	+2.3
	450	-10.7	-0.3	-2.0	-2.0	7.0	-0.1	-0.8	-0.8	1.4	0.0	+2.5	+2.5
	428	-13.1	0.0	-1.4	-1.6	5.7	+0.1	-0.2	-0.2	1.6	0.0	+2.3	+2.4
	470	-12.6	-0.1	-1.9	-1.8	7.0	-0.1	-0.5	-0.4	1.6	0.0	+2.2	+2.2
	410	-13.6	-0.1	-2.3	-2.4	5.5	-0.1	-0.4	-0.4	1.4	0.0	+2.3	+2.3
	440	-11.7	-0.2	-2.0	-1.9	8.1	-0.2	-1.0	-0.8	1.4	0.0	+2.3	+2.3
<i>H.a</i>	410	-12.5	-0.6	-2.0	-2.3	5.9	+0.1	-0.3	-0.3	1.5	+0.2	+2.6	+2.6
	442	-11.9	+0.1	-2.0	N/A	9.2	+0.1	-1.4	N/A	1.4	0.0	+2.6	N/A
	350	-12.0	+0.1	-1.5	-1.5	6.3	0.0	+0.2	+0.2	1.5	-0.1	+2.8	+2.8
	396	-12.2	0.0	-1.4	N/A	7.1	0.0	-0.1	N/A	1.6	0.0	+2.5	N/A
	388	-12.3	-0.1	-1.5	-1.3	7.3	-0.1	-0.3	-0.3	1.6	-0.1	+2.5	+2.5
	370	-12.5	-0.1	-1.3	-1.0	6.8	-0.1	-0.1	-0.1	1.6	0.0	+2.7	+2.7
	360	-11.6	+0.1	-0.9	-0.9	8.0	0.0	-0.6	-0.6	1.4	-0.1	+2.2	+2.1
	362	-12.0	-0.1	-1.3	-1.3	7.9	-0.1	-0.5	-0.5	1.6	0.0	+2.4	+2.4
	356	-12.4	-0.1	-1.5	-1.5	7.5	-0.1	-0.3	-0.3	1.7	0.0	+2.5	+2.5
	374	-12.1	+0.1	-1.6	-1.6	7.2	0.0	-0.4	-0.4	1.5	-0.1	+2.6	+2.7
	320	-11.4	-0.5	-1.1	-1.1	8.3	-0.1	-0.4	-0.4	1.4	+0.3	+2.3	+2.3

Table C3. Statistical results for pairwise comparisons of $\delta^{13}\text{C}$, $\delta^{15}\text{N}$, and C:N ratios for all treatment combinations for *Pastinachus ater* (*P.a*) and *Himantura australis* (*H.a*). Asterisks (*) indicate significant differences at $\alpha=0.05$ with sequential Bonferroni adjustments. $\delta^{13}\text{C}$ and $\delta^{15}\text{N}$ were compared using paired Wilcoxon signed-rank tests (V statistic and p-values given) and C:N ratios were compared using paired t-tests (t-statistic, df and p-values given).

Species	Tissue	Comparison	$\delta^{13}\text{C}$		$\delta^{15}\text{N}$		C:N		
			V	p-value	V	p-value	t	df	P-value
<i>P.a</i>	Muscle	BK – LE	27	1.000	42	0.160	1.49	9	0.170
		BK – UE	36	0.432	0	0.002*	-13.60	9	<0.001*
		BK – ULE	26	0.922	0	0.002*	-18.56	9	<0.001*
		LE – UE	42	0.160	0	0.002*	-12.76	9	<0.001*
		LE – ULE	43.5	0.114	1	0.008*	-12.75	9	<0.001*
		UE – ULE	13	0.160	10	0.084	3.42	9	0.008*
	Plasma	BK – LE	70.5	0.015*	37	0.906	-1.38	11	0.195
		BK – UE	78	0.002*	77	0.003*	-53.13	11	<0.001*
		BK – ULE	66	0.004*	65	0.005*	-54.81	10	<0.001*
		LE – UE	78	0.001*	78	0.001*	-63.13	11	<0.001*
<i>H.a</i>	Muscle	BK – LE	8.5	0.109	29	0.919	3.36	9	0.008*
		BK – UE	19	0.432	0	0.002*	-20.49	9	<0.001*
		BK – ULE	0	0.004*	0	0.004*	-19.57	8	<0.001*
		LE – UE	29	0.922	0	0.006*	-21.44	9	<0.001*
		LE – ULE	12	0.236	0	0.004*	-22.50	8	<0.001*
		UE – ULE	9	0.129	15	0.426	6.41	8	0.002*
	Plasma	BK – LE	35	0.155	42.5	0.021	-0.085	8	0.935
		BK – UE	45	0.009*	42	0.0243	-41.03	8	<0.001*
		BK – ULE	36	0.008*	34	0.0234	-30.93	7	<0.001*
		LE – UE	45	0.0091*	40	0.0391	-30.53	8	<0.001*
		LE – ULE	36	0.0142*	32	0.0547	-24.46	7	<0.001*
		UE – ULE	10.5	0.6115	12.5	0.8653	-0.92	7	0.389

Treatment codes: Bulk (BK), Lipid Extracted (LE), Urea Extraction (UE), Urea and Lipid Extraction (ULE)

Appendix D

Table D1. Species, sample sizes (n), mean $\delta^{13}\text{C}$, and mean $\delta^{15}\text{N}$ stable isotope values of all non-ray organisms collected at Lucinda. Size ranges are given for fish. Sample sizes in brackets indicate the number of individuals included in each sample for invertebrates.

Species	n	Size (mm)	$\delta^{13}\text{C} \pm \text{SE}\text{\%}$	$\delta^{15}\text{N} \pm \text{SE}\text{\%}$
Primary Producers				
Mangroves				
<i>Rhizophora</i> sp.	3	-	-28.5 ± 0.1	4.5 ± 0.1
<i>Sonneratia</i> sp.	3	-	-28.6 ± 0.2	5.0 ± 0.2
<i>Avicennia</i> sp.	3	-	-28.4 ± 0.6	4.6 ± 0.7
Macroalgae				
<i>Caulerpa taxifolia</i>	5	-	-15.4 ± 0.2	4.7 ± 0.3
Invertebrates				
Bivalves				
Tellinidae	3	-	-15.6 ± 0.3	5.8 ± 0.3
Decapod crustaceans				
<i>Fenneropenaeus indicus</i>	5	-	-18.2 ± 0.2	7.3 ± 0.1
<i>Mictyris longicarpus</i>	5(3)	-	-13.8 ± 0.2	6.3 ± 0.1
<i>Trypaea australiensis</i>	5(3)	-	-16.9 ± 0.8	7.5 ± 0.1
Gastropods				
<i>Nassarius</i> sp.	5	-	-14.9 ± 0.1	8.3 ± 0.1
Neritidae	3	-	-15.0 ± 0.2	7.5 ± 0.1
Fish				
Carnivores				
<i>Caranx</i> sp.	4	166-312	-16.4 ± 0.4	10.7 ± 0.4
<i>Drepane punctata</i>	4	260-330	-17.5 ± 0.7	10.4 ± 0.1
<i>Gerres filamentosus</i>	3	76-84	-13.8 ± 0.1	9.4 ± 0.1
<i>Lates calcarifer</i>	1	538	-19.3	10.9
<i>Platycephalus endrachtensis</i>	2	169-260	-15.0 ± 0.7	9.8 ± 0.2
<i>Scomberoides commersonianus</i>	4	147-380	-16.6 ± 0.3	10.5 ± 0.3
<i>Sillago analis</i>	3	231-242	-14.5 ± 0.5	9.8 ± 0.1
<i>Strongylura leiura</i>	2	-	-16.3 ± 0.3	10.0 ± 0.1

<i>Trachinotus blochii</i>	1	136	-16.7	9.2
Detritivores				
<i>Liza vaigiensis</i>	1	151	-13.9	9.1
<i>Nematalosa come</i>	3	102-105	-19.3 ± 2.6	7.0 ± 0.5
<i>Valamugil buchanani</i>	1	108	-20.2	6.7
Herbivores				
<i>Arrhamphus sclerolepis</i>	3	179-212	-13.3 ± 1.5	7.2 ± 0.7
Planktivores				
<i>Ambassis nalua</i>	3	96-113	-16.5 ± 0.6	10.5 ± 0.2
<i>Atherinomorus</i> sp.	3	63-66	-17.8 ± 0.8	9.5 ± 0.4